

# Defining the role of mRNA localisation in cell migration.

*A thesis submitted to The University of Manchester  
for the degree of Doctor of Philosophy  
in the Faculty of Biology, Medicine, and Health.*

2021

Joshua J. Bradbury

*School of Medical Sciences  
Division of Developmental Biology and Medicine*

# Table Of Contents.

<b>List of figures.....</b>	<b>6</b>
<b>List of tables.....</b>	<b>9</b>
<b>Abstract.....</b>	<b>10</b>
<b>Declaration.....</b>	<b>11</b>
<b>Copyright statement .....</b>	<b>12</b>
<b>Acknowledgements .....</b>	<b>13</b>
<b>CHAPTER 1. INTRODUCTION.....</b>	<b>14</b>
1.1 HOW ARE CELLS ORGANISED.....	14
1.2 HOW ARE PROTEINS TARGETED TO THEIR SITE OF FUNCTION.....	14
1.3 INTRODUCTION TO mRNA LOCALISATION .....	16
1.3.1 <i>General Mechanism of mRNA Localisation</i> .....	16
1.3.2 <i>Advantages of mRNA Localisation</i> .....	19
1.4 MECHANISM OF mRNA LOCALISATION.....	22
1.4.1 <i>Zipcodes and RNA Binding Proteins</i> .....	22
1.4.2 <i>RNA Transport Granules</i> .....	26
1.4.3 <i>Liquid-Liquid Phase Separation</i> .....	27
1.4.4 <i>Localised RNA Motile Behaviour</i> .....	28
1.4.5 <i>Do RNAs travel together or separately?</i> .....	30
1.5 TRANSLATION .....	31
1.6 EXTRINSIC SIGNALS CONTROL TARGETING AND TRANSLATION .....	34
1.7 mRNA LOCALISATION AND LOCAL TRANSLATION IN CELL MIGRATION .....	35
1.7.1 <i>Mechanism of ZBP1-mediated mRNA transport in cell migration</i> .....	35
1.7.2 <i>Mechanism of APC-dependent mRNA transport in cell migration</i> .....	37
1.7.3 <i>Local translation in protrusions of migrating cells.</i> .....	38
1.7.4 <i>The broader protrusion transcriptome.</i> .....	40
1.7.5 <i>Functional roles of mRNA localisation in cell migration.</i> .....	40
1.8 ANGIOGENESIS AS A MODEL OF CELL MIGRATION.....	41
1.9 EXPERIMENTAL AIMS.....	45

**CHAPTER 2. *RAB13* mRNA COMPARTMENTALISATION SPATIALLY ORIENTS TISSUE MORPHOGENESIS..... 46**

**CHAPTER 3. *TRAK2* mRNA LOCALISATION REGULATES SPATIAL MITOCHONDRIA DISTRIBUTION AND CELL MIGRATION..... 72**

3.1 ABSTRACT.....	73
3.2 INTRODUCTION.....	73
3.3 RESULTS.....	76
3.3.1 <i>Cell-Derived Matrix modifies endothelial cell motile behaviour</i> .....	76
3.3.2 <i>Polarised mRNAs are enriched in the leading edge during matrix migration</i> .....	77
3.3.3 <i>G-rich motifs drive KIF1C and TRAK2 mRNA localisation</i> .....	80
3.3.4 <i>CRISPR-Cas9 scheme for deletion of endogenous 3'UTR localisation elements</i> .....	83
3.3.5 <i>Genomic excision of G-Motifs impairs mRNA distribution without altering protein expression</i> .....	85
3.3.6 <i>Genomic excision of G-motifs impairs mRNA localisation in CDM migration</i> .....	87
3.3.7 <i>TRAK2 mRNA depolarisation causes mitochondria accumulation in leading edge</i> .....	90
3.3.8 <i>mRNA localisation is essential for regulated cellular motility</i> .....	94
3.4 DISCUSSION.....	98
3.4.1 <i>Mechanism of Polarised mRNA Targeting</i> .....	98
3.4.2 <i>mRNA localisation regulates retrograde mitochondria transport</i> .....	99
3.4.3 <i>Mitochondria positioning controls cell motility</i> .....	101
3.5 MATERIALS AND METHODS .....	103
3.5.1 <i>Cell Culture, Transfections, and Cell-Derived Matrix Production</i> .....	103
3.5.2 <i>Generation of CRISPR-Cas9 mutant cell lines</i> .....	104
3.5.3 <i>smFISH and Immunofluorescence</i> .....	104
3.5.4 <i>Antibodies</i> .....	105
3.5.5 <i>Plasmid Construction</i> .....	105
3.5.6 <i>Microscopy</i> .....	105
3.5.7 <i>Western Blotting</i> .....	106
3.5.8 <i>Image Analysis</i> .....	106
3.5.9 <i>Statistics</i> .....	107
3.6 REFERENCES.....	108

**CHAPTER 4. *MICROTUBULE-DEPENDENT LOCALISATION OF mRNAs ENCODING CCN FAMILY PROTEINS TO PERI-GOLGI SITES* ..... 118**

4.1 ABSTRACT.....	119
4.2 INTRODUCTION.....	111
4.3 RESULTS.....	123
4.3.1 <i>CYR61, CTGF, and EDN1 display mRNA polarisation along cell long axis</i> .....	125
4.3.2 <i>Comparing CYR61 localisation to secretory pathway components</i> .....	125

4.3.3	<i>CYR61 mRNA is enriched adjacent to the cis-Golgi.</i>	127
4.3.4	<i>CYR61 mRNA is not physically attached to the Golgi.</i>	119
4.3.5	<i>CYR61 mRNA localisation is dependent on microtubules.</i>	129
4.4	DISCUSSION	131
4.4.1	<i>Entry to the secretory pathway via specialised ER compartments</i>	131
4.4.2	<i>RNA localisation can direct secretory protein translation and function in Drosophila.</i>	133
4.4.3	<i>Why localise CCN family mRNAs?</i>	135
4.5	MATERIALS AND METHODS	138
4.5.1	<i>Cell Culture.</i>	138
4.5.2	<i>smFISH and Immunofluorescence.</i>	138
4.5.3	<i>Antibodies.</i>	138
4.5.4	<i>Microscopy.</i>	139
4.5.5	<i>Image Analysis.</i>	139
4.5.6	<i>Inhibitor Treatment.</i>	139
4.6	REFERENCES	140

**CHAPTER 5 – APPENDIX. THE MOLECULAR MECHANISM OF POLARISED RNA LOCALISATION IN ENDOTHELIAL CELLS. .... 148**

5.1	INTRODUCTION	149
5.1.2	<i>Are polarised mRNAs transported together as part of the same granule?</i>	149
5.1.3	<i>Is the use of G-rich motifs specific to the k5 mRNAs?</i>	150
5.1.4	<i>Which trans-acting factors drive mRNA polarisation?</i>	150
5.2	RESULTS	151
5.2.1	<i>Polarised mRNAs colocalise with each other.</i>	151
5.2.2	<i>The use of G-rich motifs is context specific as only k5 3'UTRs drive mRNA polarisation.</i>	154
5.2.3	<i>Characterisation of RBPs necessary for k5 localisation.</i>	157
5.3	DISCUSSION	159
5.3.1	<i>K5 mRNAs are found in close proximity to each other.</i>	159
5.3.2	<i>G-rich motifs specifically drive polarisation of the k5 mRNAs, and other polarized mRNAs must use alternative mechanisms.</i>	162
5.3.3	<i>Neither APC nor hnRNPA2 drive RAB13 localisation in endothelial cells.</i>	162
5.4	MATERIALS AND METHODS	164
5.4.1	<i>Cell Culture</i>	164
5.4.2	<i>siRNA Knockdown.</i>	164
5.4.3	<i>qPCR.</i>	164
5.4.4	<i>Western Blot.</i>	155
5.4.5	<i>smFISH.</i>	165
5.4.6	<i>RNA-Protein Pull Down.</i>	165
5.4.7	<i>MS2-MCP System.</i>	166
5.5	REFERENCES	167

<b>CHAPTER 6 – DISCUSSION.....</b>	<b>169</b>
6.1 SUMMARY.....	169
6.2 IDENTIFICATION OF COMMON LOCALISATION ELEMENTS.....	169
6.3 NECESSARY AND SUFFICIENT LOCALISATION ELEMENTS .....	170
6.4 MOLECULAR FUNCTIONS OF LOCALISED mRNAs.....	171
6.5 CELLULAR FUNCTIONS OF LOCALISED mRNAs .....	172
6.6 ANGIOGENESIS AS A MODEL TO UNDERSTAND THE ROLE OF mRNA LOCALISATION IN CELL MIGRATION.....	172
<b>CHAPTER 7 – FUTURE WORK. ....</b>	<b>173</b>
7.1 MOLECULAR FUNCTIONS OF MANY LOCALISED mRNAs REMAIN UNKNOWN .....	173
7.2 MOLECULAR DETERMINANTS OF POLARISED mRNA LOCALISATION REMAIN UNKNOWN .....	174
7.3 ROLE OF THE EXTRACELLULAR ENVIRONMENT IN CONTROLLING mRNA LOCALISATION.....	176
7.4 TRANSLATION OF POLARISED RNAs .....	177
<b>CHAPTER 8 – CONCLUSION. ....</b>	<b>178</b>
<b>CHAPTER 9 – REFERENCES. ....</b>	<b>180</b>

## List of Figures:

### Chapter 1:

Figure 1.1: General Mechanism of mRNA Localisation

Figure 1.2: Why localise mRNA?

Figure 1.3: Experimental Models of Angiogenesis.

### Chapter 2:

Figure 1. Clustering of RNAseq datasets identifies mRNAs exhibiting universal targeting to protrusions in diverse cell types.

Figure 2: Clustering of RNAseq datasets defines an RNA motif enriched in 3'UTR sequences that target k 5 mRNAs to protrusions.

Figure 3: CRISPR-Cas9 excision of the 3'UTR localisation element of *RAB13* disrupts mRNA targeting

Figure 4: *RAB13* mRNA polarisation spatially orients filopodia dynamics.

Figure 5: mRNA polarisation achieves spatial compartmentalisation of RAB13 translation and protein function.

Figure 6: The 3'UTR of *rab13* targets mRNA to endothelial cell protrusions in vivo.

Figure 7: CRISPR-Cas9 editing of the zebrafish *rab13* 3'UTR perturbs mRNA polarisation.

Figure 8: *rab13* mRNA polarisation orients blood vessel morphogenesis

Figure EV1: Clustering of RNAseq datasets defines unexpected cell type-specific diversity to mRNA polarisation.

Figure EV2: CRISPR-Cas9 editing of the *RAB13* 3'UTR in vitro and in vivo does not generate off-target mutations.

Figure EV3: Induction of endothelial cell collective migration drives RAB13 mRNA polarisation in leader cells.

Figure EV4: Protein translation in endothelial cell protrusions.

Figure EV5: The 3'UTR of *rab13* shows low conservation across species whilst retaining mRNA localisation potential.

### Chapter 3

Figure 3.1: Cell-Derived Matrix modifies endothelial cell motile behaviour.

Figure 3.2: Polarised mRNAs are enriched in the leading edge during matrix migration.

Figure 3.3: G-rich motifs drive *KIF1C* and *TRAK2* mRNA localisation.

Figure 3.4: CRISPR-Cas9 scheme for deletion of endogenous 3'UTR localisation elements.

Figure 3.5: Genomic excision of G-Motifs impairs mRNA distribution without altering protein expression.

Figure 3.6: Genomic excision of G-motifs impairs mRNA localisation in CDM migration.

Figure 3.7: *TRAK2* mRNA depolarisation causes mitochondria oversupply in leading edge.

Figure 3.8: mRNA Localisation is essential for regulated cellular motility.

Figure 3.9: Model for the control of leading edge mitochondria distribution and cell migration speed by *TRAK2* mRNA polarisation.

Supp. Figure 3.1: Genomic localisation element excision specifically alters host mRNA distribution.

Supp. Figure 2: *TRAK2* mRNA depolarisation causes altered mitochondria distribution.

### Chapter 4

Figure 4.1: *CYR61*, *CTGF*, and *EDN1* display mRNA polarisation along cell long axis.

Figure 4.2: Comparison of *CYR61* mRNA distribution with secretory pathway organelles.

Figure 4.3: *CYR61* mRNA displays unique peri-Golgi localisation.

Figure 4.5: *CYR61* mRNA is not physically connected to the Golgi.

Figure 4.6: *CYR61* mRNA co-distributes with microtubules.

Figure 4.7: Potential molecular functions of *k7* mRNA peri-Golgi localisation.

## **Chapter 5**

Figure 5.1: Polarised mRNAs colocalise with each other.

Figure 5.2: Identification of additional polarised mRNAs.

Figure 5.3: Additional polarised mRNA 3'UTRs do not contain localisation sequences.

Figure 5.4: Characterising RNA-Binding Proteins involved in polarised mRNA transport.

## **Chapter 6**

Figure 6: Defining the role of mRNA localisation in cell migration



## **List of Tables**

Table 1: Zipcodes and RBPs

Table 3.1: Table of Oligonucleotides.

Table 3.2: Table of smFISH probe sequences.

Table 4.1: Table of smFISH probe sequences.

Table 5.1: Table of smFISH probe sequences.

Table 5.2: Table of Oligonucleotides.

## Abstract

Cells are organised so that specific functions are carried out in specific regions. The necessary components for these functions, including proteins, cytoskeleton, and organelles, must therefore be non-uniformly distributed in subcellular space. One way this can be achieved is by actively targeting messenger RNAs to, and locally translating them within, sites where the encoded protein is required. However, the diversity of mRNA subcellular localisations, the mechanisms by which they reach their destination, and the function that mRNA localisation confers on translated proteins, particularly in the context of cell migration, is not well understood.

Here, using RNA-seq coupled with a cell fractionation scheme, the cell-type diversity of mRNA enrichment in migratory protrusions has been revealed. In doing so, groups of mRNAs that display shared mRNA localisation patterns were identified, including distally-located highly-polarised mRNAs, and distinct peri-Golgi associated mRNAs. Then, using motif-enrichment analysis in combination with the MS2-MCP reporter system for RNA visualisation, G-rich 3'UTR sequence motifs were shown to be the driving force behind mRNA polarisation. Next, endogenous mRNA localisation could be disrupted by genomic excision of G-rich sequence motifs using CRISPR-Cas9 editing tools, to provide novel insights into the roles of localised mRNAs. *RAB13* mRNA localisation was revealed to define a zone of active filopodia production in the leading front of migratory endothelial cells, and this was essential for directional pathfinding during *in vivo* angiogenesis. Finally, polarised *TRAK2* mRNA was then shown to be required to maintain normal mitochondria distribution in the leading edge, and for regulating endothelial cell motile speed during matrix migration.

Together, this thesis has characterised the cell-type diversity of mRNA localisation patterns in motile cells, shed light on the mechanism behind polarised mRNA localisation, and greatly expanded the realm of known molecular functions of localised mRNAs. Therefore, the evidence presented within contributes significantly to our understanding of how mRNA localisation spatiotemporally regulates protein activity. Moreover, this work will have implications for future research concerning the molecular control of cell motility during development.

## **Declaration**

Work included in the Appendix of this thesis has previously been submitted as part of an MSci dissertation (Yuting Feng), where I supervised the project. I declare that no other portion of the work referred to in the thesis has been submitted in support of an application for another degree or qualification of this or any other university or other institute of learning.

## Copyright Statement

- i. The author of this thesis (including any appendices and/or schedules to this thesis) owns certain copyright or related rights in it (the “Copyright”) and s/he has given The University of Manchester certain rights to use such Copyright, including for administrative purposes.
- ii. Copies of this thesis, either in full or in extracts and whether in hard or electronic copy, may be made only in accordance with the Copyright, Designs and Patents Act 1988 (as amended) and regulations issued under it or, where appropriate, in accordance with licensing agreements which the University has from time to time. This page must form part of any such copies made.
- iii. The ownership of certain Copyright, patents, designs, trademarks and other intellectual property (the “Intellectual Property”) and any reproductions of copyright works in the thesis, for example graphs and tables (“Reproductions”), which may be described in this thesis, may not be owned by the author and may be owned by third parties. Such Intellectual Property and Reproductions cannot and must not be made available for use without the prior written permission of the owner(s) of the relevant Intellectual Property and/or Reproductions.
- iv. Further information on the conditions under which disclosure, publication and commercialisation of this thesis, the Copyright and any Intellectual Property University IP Policy (see: <http://documents.manchester.ac.uk/display.aspx?DocID=24420>, in any relevant Thesis restriction declarations deposited in the University Library, The University Library’s regulations (see <http://www.library.manchester.ac.uk/about/regulations/>) and in The University’s policy on Presentation of Theses.

## **Acknowledgements**

They say it takes a village to raise a child, well it takes a lab to raise a PhD student. So, I have to start by thanking them for doing such a great job. Firstly, my supervisor Shane, your enthusiasm for science is infectious. It has been a pleasure working with you. Thanks for everything, throughout the almost 6 years we have known each other – time flies! Next, my mentor Guilherme, without whom none of this would have been possible. You taught me everything I know with the patience of a saint. We'll always have Krakow. Holly, thank you for the plants and the allotment chats. Sabrina and George, my lab siblings, we've made it through together. Georgia, if it was easy everyone would do it. Now your mantra is in two theses. Finally, Rapha, you have distracted me with music and films and books when I most needed it. Your influence has been great.

Thank you to the entirety of D-wing of the Michael Smith building which, somehow, I have occupied for so long. Especially thank you to the Papalopulu, Das, and Dorey labs for advice throughout.

Thank you to the institutions that have created me. The University of Manchester for hosting me for one third of my life. And HOME cinema, where I invested my stipend, and you repaid me with wonder and joy.

To my parents, I hope you are proud of your very own developmental biology project. You gave all three of us the greatest gift – you gave us the chance.

Finally, my companion, my cycle-to-work pal, my allotment labourer, my western blot queen, Anya. Thank you for being a miracle in my life, every day. Onto the next adventure, together.

## **1 Introduction**

### **1.1 How are cells organised?**

Cells are complex machines that carry out many different activities simultaneously. To achieve this, cells are organised so that specific functions take place in specific regions. The molecular building blocks required for each function must therefore be placed in the correct location at the correct time. This challenge is particularly evident in polarised cells. For example, the extreme morphology of neurons requires that their extended distal processes act as semiautonomous administrative regions, hundreds or thousands of microns away from the cell body. Divisions of labour are also used in mesenchymal-like migrating cells. The front of the cell is characterised by the extension of dynamic filopodia sensing the environment (Mayor & Etienne-Manneville, 2016), by the polarisation of membrane trafficking (Orlando & Guo, 2009), and by focal adhesions linking the cell to the extracellular matrix. In contrast, the rear of the cell is highly contractile and retracts as the cell moves (Ridley, 2015). These specialised local functions at cellular poles are dependent on the partitioning of cytoskeletal architecture (Li & Gundersen, 2008), organelles (Kupfer et al., 1982), receptors (Rodriguez-Boulan & Macara, 2014), and biochemical reactions (Etienne-Manneville, 2004). Active localisation of products of gene expression with precise spatiotemporal fidelity is essential for the creation and maintenance of these specialised compartments, yet remains poorly understood.

### **1.2 How are proteins targeted to their site of function?**

One of the ways in which cells compartmentalise specific functions is to physically segregate those functions in membrane-bound organelles. Proteins that are required inside organelles like the endoplasmic reticulum (ER), the nucleus, and peroxisomes are targeted to those places via short amino acid sequences in the protein itself. Upon translation of these signal sequences, transportive protein complexes bind the sequences and target the protein co- or post-translationally to the required organelle membrane (Weis et al., 2013).

The mechanisms described above for directing proteins to discrete locations are relatively well defined. However, it is not as clear how cytoplasmic proteins reach their fluid, non-membrane bound sites of function. The cytoplasm in most cells displays some subfunctionalisation where different cohorts of proteins are required in different regions. This is no more evident than in polarised cells where front/rear or apical/basal zones perform

different roles. Maintaining these specialised cytoplasmic regions is a challenge that cells have evolved different mechanisms to overcome.

One example comes from the establishment of apical-basal polarity by the conserved partitioning-defective (PAR) proteins and their partners. PAR proteins are cytoplasmic regulators that develop asymmetric cortical distributions via feedback loops and mutual exclusion. In epithelia, the apically-located atypical protein kinase C (aPKC) phosphorylates PAR3 and PAR1, excluding them from the apical cortex (Hurov et al., 2004; Izumi et al., 1998). Concurrently, basolaterally-located PAR1 phosphorylates and excludes apical PAR3 from the basolateral cortex (Goldstein & Macara, 2007). Spatial cues from the apically-located transmembrane protein Crumbs are key for both initiating and maintaining the apical localisation of aPKC (Rodriguez-Boulán & Macara, 2014).

Signals from the extracellular environment are also important for organising protein localisation and polarity in the cytoplasm of migrating cells. Receptor activation by chemotactic ligands activates the phosphoinositide 3-kinase (PI 3-K) pathway in the front of migrating cells. This results in activation of Cdc42 and Rac and organisation of cytoskeletal changes that allow the cell to extend protrusions in the direction of migration. Positive feedback is important here, as active Rac can also induce PI3K pathway activation. In contrast, the rear of the cell is dominated by high Rho activity, and consequently high actomyosin contractility (Ridley et al., 2003). Mutually exclusive domains of active Cdc42/Rac at the front and active Rho at the rear are reinforced through unidirectional inactivation of Rho by Rac at the leading edge (Raftopoulou & Hall, 2004).

Taken together, these two examples from epithelial cells and migrating cells describe how reciprocal interactions and positive feedback can allow protein localisation to become restricted to specific cellular compartments in the cytoplasm. But there are some limitations to this process. For example, it is hypothesised that some proteins may only function correctly in a newly-synthesised, free from post-translational modifications state (Herbert & Costa, 2019; N. Y. Kim et al., 2020; Saha et al., 2010). The passive process of protein localisation using positive feedback and mutual exclusion described above does not allow for the requirement of these “new” proteins. Since the PAR protein mechanism relies on countless transient and chance interactions to function correctly, cells have also adopted more direct mechanisms to increase the efficiency of generating spatially restricted protein networks (Weatheritt et al., 2014).

## 1.3 Introduction to mRNA Localisation.

### 1.3.1 General Mechanism of mRNA Localisation.

One way that cells circumvent the challenges of cytoplasmic protein localisation is to actively localise then locally translate messenger RNAs at specific subcellular sites (Ryder & Lerit, 2018). Initially, active localisation of mRNAs and subsequent local translation was considered a niche process used only by a handful of proteins. Because of this, most of our understanding of mRNA localisation comes from studying mRNAs that display particularly striking localisation patterns. These mRNAs encode proteins that can have critical functions in fate determination, embryonic patterning, and generating cellular polarity (Medioni et al., 2012). For example, a collection of mRNAs are transported to the bud tip in *Saccharomyces cerevisiae*, where they encode proteins that ensure that the daughter cell adopts a different mating type to the mother (Shepard et al., 2003). The most well characterised of these is *ASH1* mRNA, which encodes a transcriptional repressor (Bertrand et al., 1998; Niedner et al., 2014). Multiple mRNAs including *oskar*, *gurken*, and *nanos* are localised during early *Drosophila* development (Johnstone & Lasko, 2001). Translation of these mRNAs then creates morphogen gradients that control embryonic axis formation. Finally, *ACTB* mRNA is asymmetrically distributed in neurons and migrating cells, where it plays an essential role in cytoskeletal organisation (Herbert & Costa, 2019; Holt & Schuman, 2013). Therefore, mRNA localisation is an essential, evolutionarily conserved process across phyla (Buxbaum et al., 2014).

The mechanisms by which mRNAs reach their destination follows a stereotypical process in many different cell types. The subcellular destination of localised mRNA is controlled by *cis*-acting regulatory sequence elements in the transcript. These sequence elements are bound by *trans*-acting mRNA binding proteins (RBPs). The binding of RBPs is thought to allow formation of large ribonucleoprotein (RNP) transport complexes, consisting of multiple proteins and mRNAs, each playing an integral part during the localisation process. Most commonly, RNP complexes are transported via linkage to molecular motors and active transport via the cytoskeleton. When mRNAs reach their destination, they are often anchored in place, RBPs are shed, and localised translation takes place (Fig. 1.1).

Alternatively, some mRNAs are not actively transported but reach their destination via diffusion and entrapment. *nanos* mRNAs can still accumulate in the posterior *Drosophila* oocyte in the absence of microtubules, a phenomenon attributed to the role that diffusion and



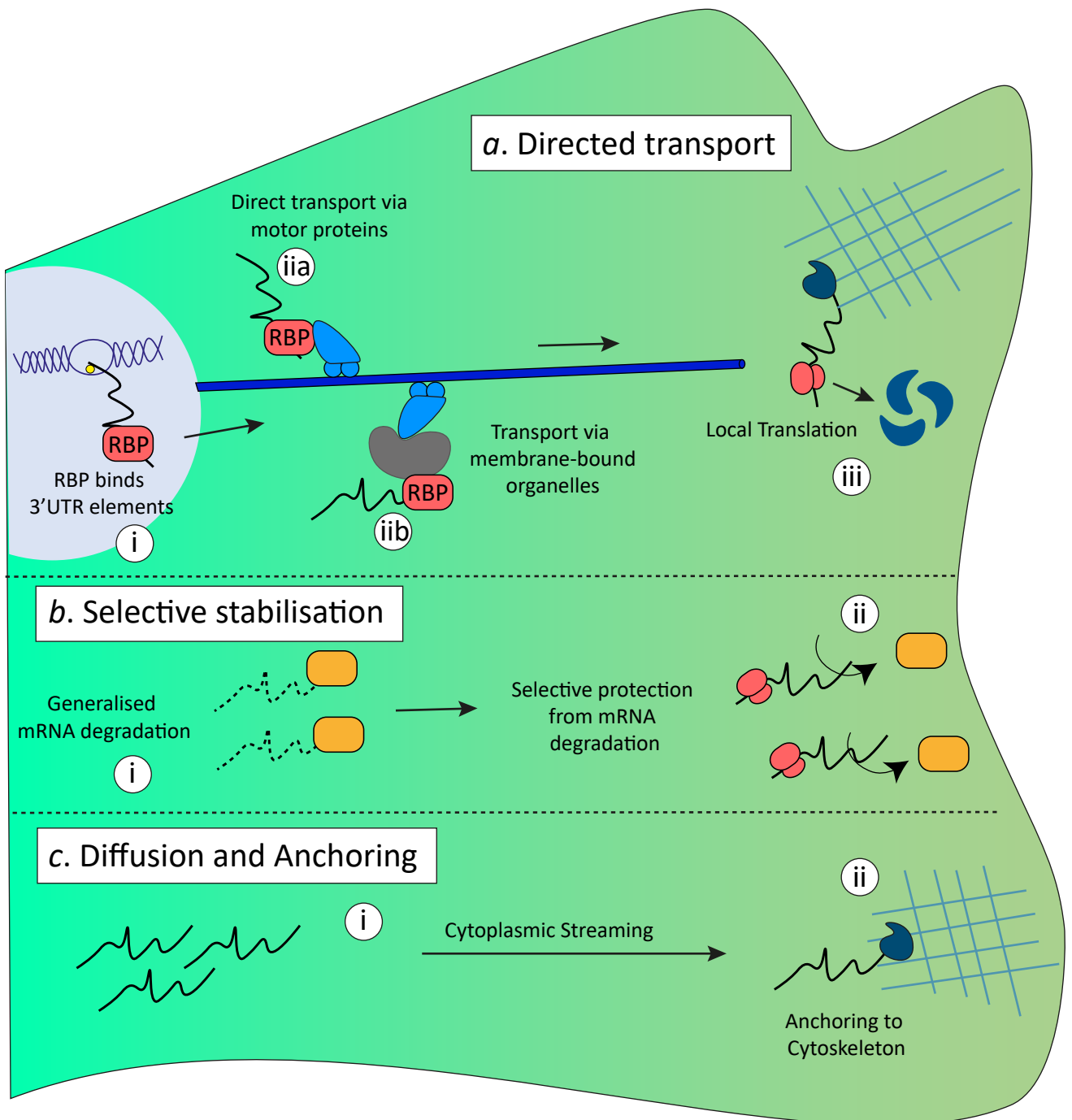


**Figure 1.1: Mechanisms of mRNA localisation.**

- a.* mRNAs localised via directed transport often contain 3'UTR elements that are bound by RBPs inside the nucleus (i). After nuclear export, mRNAs can be transported either by direct binding of molecular motors to RBPs (ia), or via piggybacking on membrane-bound organelles (iib) as they are moved via the cytoskeleton. Once an mRNA reaches its destination, RBPs are shed from the RNA, and local translation begin.
- b.* Some mRNAs are generally degraded throughout the cytoplasm (i), but specifically protected from degradation (ii) in sites where the resulting protein is required.
- c.* Rather than directed transport via molecular motors, some mRNAs can be moved via cytoplasmic flows (i) and diffusion to reach their destination. Once there, anchoring to the cytoskeleton (ii) helps to maintain the distribution.

strong cytoplasmic flow plays in the localisation. Subsequently, *nanos* mRNAs are anchored to the actin cytoskeleton to maintain their posterior distribution (Forrest & Gavis, 2003). Some mRNAs are also transported by an entirely different mechanism. *hsp83* transcripts are degraded in a generalised fashion throughout the *Drosophila* embryo, except for within a local posterior region where they are protected from degradation (Ding et al., 1993; Tadros et al., 2007).

Recently, various mRNA species have been reported to hitch-hike to their destination by utilising organelle transport mechanisms. For example, in the filamentous fungi *Ustilago maydis*, the RBP Rrm4 connects *Cdc3* mRNAs via the protein Upa1 to endosomes (Baumann et al., 2014). Endosome-mRNA complexes are then transported bi-directionally in hyphae (cellular protrusions) by kinesin-3 and dynein (Baumann et al., 2012). Another key protein is Upa2, which binds to the PolyA tail of transported mRNAs and carries out a scaffolding function (Jankowski et al., 2019). Also present at transporting endosomes are various aspects of the translation machinery, including ribosomal proteins (Baumann et al., 2014). This is also the case for Rab7a-positive late endosomes in axons of mammalian neurons, which are associated with mRNAs, ribosomes, and RBPs (Cioni et al., 2019). Endosomal transport and translation of mRNAs is essential for normal neuronal maintenance, since in its absence mitochondria are dysfunctional and axons degenerate. Indeed, it seems endosomes are not the only organelle on which mRNAs hitch a ride. The RBP ANXA11 has been shown to tether mRNAs to lysosomes in mammalian neurons to facilitate their transport (Y. C. Liao et al., 2019). Hence, piggybacking on organelles appears to be a key mechanism by which mRNAs can be transported in diverse biological systems.

### **1.3.2 Advantages of mRNA Localisation**

mRNA localisation and local translation has numerous advantages compared to the mutual exclusion mechanism described previously, and over the directed transport of proteins themselves (Fig. 1.2). Firstly, the repeated translation of multiple proteins from a single mRNA at the site of protein function is hypothesised to be more thermodynamically efficient than the transport of multiple individual proteins, since multiple proteins can be produced from a single mRNA (Martin & Ephrussi, 2009). Secondly, mRNA targeting of protein subunits may help to assemble macromolecular complexes by ensuring that members are in the right place at the right time, in proximity to necessary cofactors (Mingle et al., 2005a). Co-distribution of mRNAs is necessary for production of protein complexes since protein complexes assemble co-

# Why Localise RNA?

A. Efficiency of protein synthesis

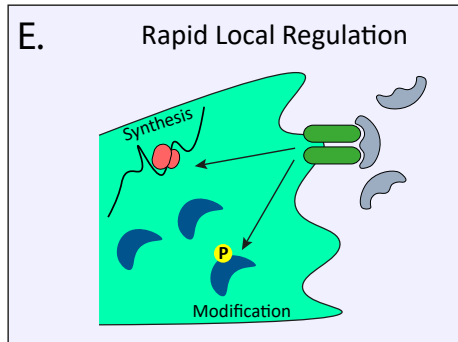
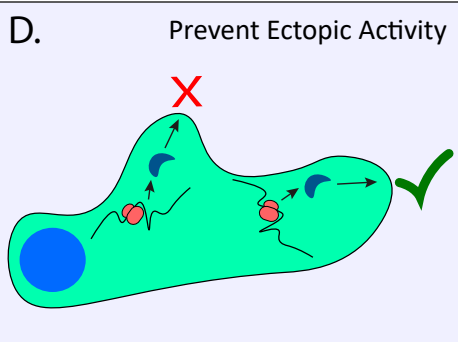
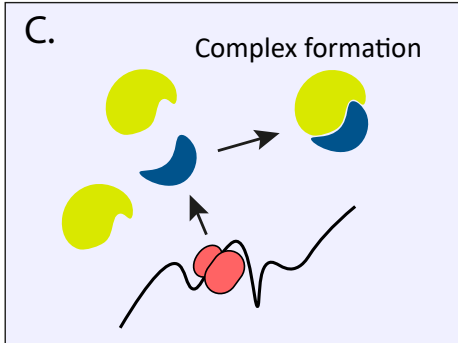
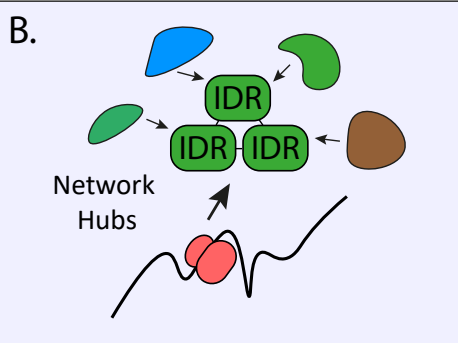
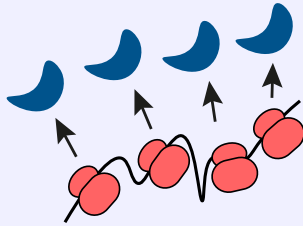


## Figure 1.2 Why localise RNA?

RNA localisation and local translation has numerous advantages over simply transporting proteins to where they are required:

- A. Multiple proteins can be produced from repeated translation of a single RNA, so RNA localisation is thought to increase efficiency.
- B. Localised RNAs have been shown to be more likely encode proteins that contain intrinsically-disordered repeats (IDRs), which are protein domains that can readily participate in promiscuous interactions. Therefore, RNA localisation is thought to produce translated proteins that can act as network hubs.
- C. Similarly, RNA localisation is thought to be used to allow placement of translated protein in close proximity to specific interactors, therefore facilitating the building of protein complexes.
- D. Localised RNA in specific subcellular regions is known to enact specific local downstream functions, and conversely keeping these RNAs away from regions where they are not required can prevent ectopic activity.
- E. Finally, RNA localisation is thought to enable rapid responses to extracellular signalling events. Extrinsic cues are thought to be able to drive local signal transduction resulting in regulation of proximal localised RNAs, either through regulation of ribosomes and protein synthesis, or through modification of the locally-translated protein itself. This is thought to be advantageous to the cell because slow transcriptional changes and alteration of protein activity level through the changes to gene expression can be avoided.

translationally. For example, in yeast 9 out of 12 tested protein complexes including the eukaryotic initiation factor eIF2 co-translationally assemble (Shiber et al., 2018). Moreover, it has been suggested that proteins synthesised at distal locations from asymmetrically localised mRNAs frequently contain intrinsically-disordered regions (IDRs) (Weatheritt et al., 2014). IDRs are structural protein domains that act as scaffolds and enable protein-binding promiscuity. Therefore, localised mRNAs frequently encode proteins that act as hubs in protein interaction networks (Cumberworth et al., 2013). Thirdly, targeting of transcripts to a specific locale could prevent the accumulation of proteins in areas where they may have deleterious effects (Ainger et al., 1997). Indeed, various diseases are caused by toxicity due to inappropriate protein localisation (Babu et al., 2011). Finally, transport of localised mRNAs or translation rate could be directly regulated at specific sites by proximal extrinsic signals. This could enable cells to control protein expression in subcellular space without relying on slow transcriptional changes (Jung et al., 2014). Whilst much of the conclusions presented here are implied from indirect evidence, numerous functional experiments have confirmed the vital role that mRNA localisation plays in diverse biological systems (G. Liao et al., 2011; Long et al., 1997; Shestakova et al., 2001). It is now clear that mRNA localisation may be more prevalent than previously thought, since transcriptomes are asymmetrically distributed in a wide variety of systems (Lécuyer et al., 2007; Mardakheh et al., 2015; Mili et al., 2008; Zappulo et al., 2017).

## **1.4 Mechanism of mRNA Localisation.**

### **1.4.1 Zipcodes and mRNA Binding Proteins.**

The subcellular destination of a localised mRNA is usually encoded in its sequence through *cis*-acting localisation elements (LEs), sometimes called zipcodes (Jambhekar & Derisi, 2007). LEs interact with mRNA-binding proteins (RBPs), which in turn bind the machinery that transports mRNAs to their destination. LEs display large variability in size, ranging from less than ten to hundreds of nucleotides in length (Chabanon et al., 2004). LEs are also variable in position in the transcript; although they are most often found in 3'UTRs they are occasionally found in the 5'UTR (Meer et al., 2012), coding regions (Long et al., 1997), and introns (Buckley et al., 2011; Chaudhuri et al., 2020). Interplay between mRNA structure and mRNA sequence in LEs is also crucial. A variety of stem-loops, bulges, hairpins, helices, and G-quadruplexes are predicted to be formed by different LEs (Table 1). G-quadruplexes especially have gained prominence in recent times, with evidence suggesting

RBPs	mRNAs	LE Location and Description	LE Characteristics	Function	Refs.
Y14/Tsunagi, Mago nashi	oskar (Drosophila)	CDS 1st exon splice site 28-nt stem loop	S	Germ line differentiation	(Ghosh et al., 2012; Johnstone & Lasko, 2001; Micklem et al., 2000; Simon et al., 2015)
Bruno	oskar (Drosophila)	3'UTR	R, S	Germ line differentiation	(Kim-Ha et al., 1995)
Staufen	oskar (Drosophila)	3'UTR	R, M, S	Germ line differentiation	(Ghosh et al., 2012; Johnstone & Lasko, 2001; Micklem et al., 2000; Simon et al., 2015)
	bicoid (Drosophila)	3' UTR; 625-nt, multiple long stems + helical region	R, M	Embryonic patterning	(Ferrandon et al., 1994; Macdonald & Kerr, 1998; Macdonald & Struhl, 1988)
mStau2	αCaMKII (mouse)	Intronic Loop		Memory formation	(Ortiz et al., 2017)
	vg1 and vegT (Xenopus)	3' UTR (366nt)		Embryonic patterning	(Mowry & Melton, 1992; Yoon & Mowry, 2004)
ZBP1, VERA, IMP1	ActB (mammalian)	3' UTR 5'-UCGGACU--GCACACCC-3'		Fibroblast movement and axon guidance	(Chao et al., 2010; Nicastro et al., 2017; Patel et al., 2012)
	vg1 and vegT (Xenopus)	3' UTR 5'-UUCAC-3'	R	Embryonic Patterning	(Bubunencko et al., 2002)
HuD	Tau (rat)	3'UTR U-rich sequence		Axonal polarity maintenance	(Aranda-Abreu et al., 1999; Atlas et al., 2004; Cuadrado et al., 2002)
hnRNPA/B, Squid	MBP (mammalian)	3' UTR; 21nt A2-Response Element (A2RE)	R, M	Myelin sheath formation	(Ainger et al., 1993, 1997; Hoek et al., 1998; Munro et al., 1999)
	αCaMKII, NRG1, ARC (mammalian)	3'UTR; A2RE-like sequences	R, M	Memory formation	(Gao et al., 2008)
	gurken (Drosophila)	3' UTR		Embryonic development	(Norvell et al., 1999)
	oskar (Drosophila)	3'UTR		Germ line differentiation	(Huynh et al., 2004)
CPEB	MAP2 (rat)	3' UTR Cytoplasmic Polyadenylation Element (CPE)		Microtubule assembly	(Huang et al., 2003)
	ZO-1 (mouse)	3' UTR (5 conserved CPEs)	R	Epithelial tight junction assembly and polarity	(Nagaoka et al., 2012)
	cyclinB1 and Xbub3 (Xenopus)	3' UTR CPE		Spindle in Cell Division	(Groisman et al., 2000)
Rumpelstiltskin	nanos (Drosophila)	3' UTR; 4 redundant elements	R	Embryonic polarity	(Jain & Gavis, 2008)
ARC1	Arc1 (mammal + Drosophila)	3' UTR		Synaptic plasticity	(Ashley et al., 2018)
She2/She3	ASH1 (yeast)	ORFs and 3' UTR	R	Mate type switching	(Bertrand et al., 1998; Long et al., 2000; Olivier et al., 2005)
Sec27	OXA1 (yeast)	3' UTR and ORF		Mitochondrial inner membrane biogenesis	(Sylvestre et al., 2003)
Puf3p	COX17 (yeast)	3' UTR (UGUR motif)		Mitochondrial biogenesis and motility	(García-Rodríguez et al., 2007; Saint-Georges et al., 2008)
RBP-L/RBP-P	glutelin (rice)	ORF (repeated motifs) and 3' UTR (U-rich)		Grain development	(Tian et al., 2019)
	prolamine (rice)	ORF (repeated motifs) and 3' UTR (U-rich)		Grain development	(Tian et al., 2019)
FMRP	MAP1b and CamKIIα (mammalian)	G-quadruplex	R	Neurogenesis and memory formation	(Dictenberg et al., 2008; Goering et al., 2019; Menon et al., 2008)
SMAUG	hsp83 (Drosophila)	3' UTR		Development; maternal transcript elimination	(Ding et al., 1993; Tadros et al., 2007)
LARP6	ribosomal protein mRNAs (mammalian)	5' TOP sequence		Fibroblast protrusion formation	(Dermitt et al., 2020)
TDP-43	NEFL and RAC1 (mammalian)	3' UTR UG-rich sequences		Neuronal development and plasticity	(Chu et al., 2019)
NOVA	girk2 (mouse)	Intronic and 3' UTR YCAY		Spinal motor neuron dendrite activity	(Racca et al., 2010)
She2/She3	NIP1 (yeast)	unknown		Daughter inheritance of translation granules	(Pizzinga et al., 2019)

**TABLE 1.1 Localisation Element and RNA Binding Protein partners.**

**Abbreviations: S = Synergistic; R = Repeated; M = Modular**

that the number of G-quadruplexes within mRNA 3'UTRs can promote mRNA localisation to neurites (Goering et al., 2020; Subramanian et al., 2011). Within these structural LEs, functionality is often triangulated to a handful of key nucleotides, whilst the rest of the sequence may be superfluous provided the overall LE structure is maintained.

Localisation is often dependent on multiple LEs repeated throughout the 3'UTR or coding sequence. These LEs can act synergistically, redundantly, or as modular components in complex stepwise pathways (Johnstone & Lasko, 2001). Nevertheless, there are also some mRNAs whose localisation is solely attributed to a single LE composed of a short nucleotide sequence (Hoek et al., 1998; Torvund-Jensen et al., 2018). Therefore, one key theme of LEs is their variability. Experimental strategies to identify LEs most often involve using laborious sequence truncations with reporter constructs and mRNA live imaging, in combination with predictive bioinformatics. These experiments have allowed the elucidation of some general principles of LEs which also, in part, help to explain why identification of functional LEs has been so challenging in the past.

Firstly, LEs are often repeated multiple times within mRNAs. For example, the vegetally-localised *vg1* mRNA in *Xenopus* oocytes contains 4 sequences (named E1-E4) that are each repeated multiple times within a 340 nucleotide (nt) LE (Deshler et al., 1997; Mowry & Melton, 1992). The highly conserved mRNA-targeting RBP Vera has been shown to be necessary for driving the localisation of *vg1* by binding to the E2 repeat (Deshler et al., 1997). Deletion experiments in *vg1* have shown that each of these repeated redundant regions, as small as 6nt, influence localisation, with E2 elements appearing to be the driving force (Gautreau et al., 1997). Despite this, it has been difficult to ascertain an exact threshold number of repeats required and although these repeats appear to be necessary, they are not sufficient. Similarly, the localisation of *nanos* mRNA in the *Drosophila* oocyte is dependent on two repeats of a CGUU motif in the 3'UTR, both of which have been shown to be necessary (Jain & Gavis, 2008). These motifs are bound by the RPB Rumpelstiltskin. Interestingly, the CGUU repeats are also not sufficient to direct localisation suggesting that the wider sequence/structure context that these CGUU repeats are situated in plays a role. To conclude, multiple LEs are often repeated throughout 3'UTRs, each with varying degrees of necessity to the localisation process.

Potential reasons for the repetition of LEs include facilitating either i). synergistic or ii). redundant binding of multiple RBPs (Engel et al., 2020). Firstly, synergistic binding of



multiple RBPs may allow a threshold level of binding events to be reached and facilitate formation of a cloud of RBP-LE interactions within a competent mRNA transport granule (Arn et al., 2003). Secondly, redundancy in LEs may be part of a mechanism to overcome the promiscuity and transience of RBP interactions, as presentation of multiple RBP binding sites may increase the probability that an RBP will bind to the mRNA (Macdonald & Kerr, 1997).

Another important characteristic of LEs is that multiple modular LEs sometimes act in concert to regulate separate steps of the localisation process. To return to *vg1* mRNA in the *Xenopus* oocyte, the E1-E4 repeats in combination with Vera are not sufficient to direct localisation alone. Instead, an additional repeated VM1 motif is required (Bubunencko et al., 2002; Lewis et al., 2004). VM1 motifs are bound by the protein VgRBP60/hnRNP I. To make the situation more complex, a third RBP XStau is also shown to interact with the broader *vg1* localisation element and is also essential for vegetal localisation (Yoon & Mowry, 2004).

The localisation of *oskar* to the posterior pole of the *Drosophila* oocyte demonstrates how multiple concurrent mRNA processing events can be essential during transport. *oskar* 3'UTR contains a large stem loop structure with multiple Staufen recognition sequences. Staufen is essential for targeting of *oskar* transcripts (Kim-Ha et al., 1991; St Johnston et al., 1991). Alongside Staufen, homologs of the exon junction complex including Y14 (Hachet & Ephrussi, 2001) and mago nashi (Micklem et al., 1997) are also essential. Both proteins are deposited to *oskar* mRNA at the first exon-exon junction, binding to a specific LE that forms a stem loop called the SOLE (Ghosh et al., 2012; Simon et al., 2015). These proteins are important in splicing, and inhibition of splicing has been shown to impair *oskar* posterior localisation (Hachet & Ephrussi, 2004). Another, layer of complexity is added to *oskar* by the binding of RBP Bruno to the 3'UTR (Kim-Ha et al., 1995). Bruno is thought to repress the translation of *oskar* mRNA during transit to the posterior pole by two potential mechanisms. Firstly, Bruno can bind to Cup, a protein which in turn binds to eIF4E. This then prevents association between eIF4E and eIF4G, hence inhibiting translation initiation (Nakamura et al., 2004). In the second mechanism, Bruno binding to response elements in the 3'UTR of *oskar* causes mRNA oligomerisation and the formation of large, translationally silenced particles (Chekulaeva et al., 2006). Inhibition of Bruno by phosphorylation allows translation to take place at the posterior pole (G. Kim et al., 2015). One final protein involved is Hrp48, which has been shown to interact with both the 5' and 3' UTRs of *oskar* (Huynh et al., 2004). *hrp48* mutants present with an alternative mislocalisation phenotype, at distinct stages of

*Drosophila* oogenesis to *staufen* mutants, suggesting an alternative regulatory role in localisation. These examples show how multiple levels of mRNA regulation must be coordinated to safely transport an mRNA to its destination.

The repetitive use of LEs, and the use of step-wise and modular localisation mechanisms has made full characterisation of the mechanisms of mRNA localisation exceedingly challenging. Inhibition of LEs by genetic manipulation or steric blocking can be compensated for by redundant regions. Deletion of LEs and mutation of RBPs often results in observation of partial mislocalisation phenotypes. Even for mRNAs where we have a relatively good understanding of the variety of LEs and their associated RBPs, the exact co-operative action and sequence of binding events required for their localisation have not been fully characterised. Due to these challenges, it is therefore likely that the total cohort and stoichiometry of proteins required for the transport of an mRNA is yet to be realised.

#### **1.4.2 mRNA Transport Granules.**

Simplified models of the mechanism of mRNA localisation often describe the process as a linear interaction series between LEs, RBPs, and molecular motors. However, the examples above have shown that an orchestra of RBPs and adaptor proteins are in fact required within complexes called mRNA transport granules for the localisation of mRNAs. Each protein member of the orchestra can play a specific role in mRNA processing during the transport process. Understanding the specific role that each protein member plays in a transport granule, and the dynamics of their interaction with the granule, is particularly challenging.

The assembly of the transport granules that enable localisation of Asymmetric Synthesis of HO 1 (*ASH1*) mRNA to the bud tip in yeast is perhaps the most well characterised. A collection of different RBPs and interactors perform different functions throughout the *ASH1* transport process (Niedner et al., 2014). Assembly of transport complexes begins co-transcriptionally, with the binding of RBP Swi5p-dependent HO expression Protein 2 (She2p) to *ASH1* zipcodes. Surprisingly, initial interaction of She2p with an mRNA Polymerase II-associated complex consisting of Spt4/5, is necessary before binding of She2p to *ASH1* (Shen et al., 2010). Further studies have also shown that She2p binds chromatin and nascent mRNA non-specifically (Müller et al., 2011). Therefore, building of the mRNA transport process begins early in the life of the mRNA, whilst it is still in the nucleus.

Stability of the She2p/*ASH1* interaction within the nucleus is provided by binding of Localization of *ASH1* mRNA Protein 1 (Loc1p) to both She2p and *ASH1* mRNA

simultaneously. Without Loc1p, She2p interaction with *ASH1* is more transient. Loc1p also contains several nucleolar localisation signals which help to move the transport granules to the nucleolus from the nucleoplasm (Niedner et al., 2013).

Once inside the nucleolus, translational repressor Puf6b is thought to be incorporated into the mRNA transport granule, since it appears in She2p pull down experiments and also shows strong nucleolar enrichment (Niedner et al., 2013). An additional RBP translational regulator called Khd1p is also essential for the localisation of *ASH1*, although it is not clear at which stage of the localisation it is required, and it does not appear in She2p pull down assays (Irie et al., 2002). Khd1p represses translation through binding to the C-terminal domain of eIF4G1 (Paquin et al., 2007). Both Puf6b and Khd1p bind to separate LEs in the *ASH1* mRNA (Gu et al., 2004; Irie et al., 2002; Paquin et al., 2007). Puf6b is maintained in the transport granule until the mRNA is ready to be translated at the end of its journey in the bud tip (Deng et al., 2008). In contrast, Loc1p is strictly nuclear (Long et al., 2001). The role that Loc1p plays in ensuring stability of the transport granule is therefore passed to another protein when the granule is exported to the cytoplasm. Here, She2p instead binds to another adaptor protein, She3p. She3p is constitutively bound to Myo4p, which is a type V myosin (Bohl et al., 2000; Kruse et al., 2002). Myo4p drives the targeting of the complex to the bud tip via actin filaments (Long et al., 2000; Müller et al., 2011). This multi-stage process shows how the specific composition of proteins in transport granules is modulated throughout the mRNA journey.

### **1.4.3 Liquid-Liquid Phase Separation.**

Complexes of mRNA and protein are used in all aspects of the mRNA life cycle from transcription to storage, translation, and degradation (Moujaber & Stochaj, 2018). In some cases, self-assembly of proteins and mRNAs can induce phase separation. Phase separation is a biophysical process that allows RBPs and mRNAs to become concentrated in membraneless compartments that display similar properties to liquid droplets (Shin & Brangwynne, 2017). This allows cells to spatiotemporally regulate mRNA processing events by physically segregating them from other cellular processes. Two key examples of phase separated granules are stress granules (SGs) and P-Bodies (PBs), which are both involved in translational regulation. Classically, SGs are thought to harbour proteins involved in translation initiation, whereas mRNA decay is thought to occur more preferentially in PBs, although some proteins are shared between both (Riggs et al., 2020). Formation of both types

of granule is linked to cellular stress, although PBs have also been observed constitutively (Kedersha & Anderson, 2007).

Although phase separated droplets have been reported to play an important role in the subcellular organisation of many different aspects of translational control (Guo et al., 2021), their role in the mRNA localisation process is not so clear. Some RBPs implicated in the regulation of mRNA transport and translation have been observed to participate in phase-separation. For example, the RBP TDP-43 is a crucial component of some anterograde mRNA transport granules in neurons (Alami et al., 2014). TDP-43 containing granules display many of the biophysical properties of liquid droplets including the ability to fuse with other droplets, to change trajectory, deformability by shear stress, and sensitivity to disruption by hydrophobic manipulation (Gopal et al., 2017). Another neuronal RBP purported to be involved in the localisation of hundreds of mRNAs, FMRP, has also been shown to form spherical membraneless foci *in vitro* (Goering et al., 2020; Tsang et al., 2019). However, most of our knowledge of the role of phase separation in mRNA transport comes primarily from neurodegenerative disease research. Mutations to many different RBPs including FMRP, TDP-43, Tia1 (Mackenzie et al., 2017) and FUS (Murthy et al., 2019), have been shown to promote phase separation of mRNA in patients with Amyotrophic Lateral Sclerosis (Murakami et al., 2015). These phase-separated granules impair mRNA transport and translation. It therefore seems likely that phase separation may play an inhibitory role in mRNA transport in neurons. However, the physiological role of these RBPs in mRNA transport is not as well understood as their pathological role. Whether phase separation plays a role in physiological mRNA transport, and the identities of mRNAs regulated within phase separated granules, therefore remains to be seen. Hence, whilst phase separation has great potential to explain the biophysical characteristics of mRNA transport granules, more research is required to fully understand the extent of their role, particularly in mammalian cells other than neurons.

#### **1.4.4 Localised mRNA Motile Behaviour.**

The directed transport of mRNA granules to their destination is generally mediated by cytoskeletal trafficking. The cytoskeleton in polarised cells is also polarised (Raman et al., 2018). G-actin and  $\alpha/\beta$  tubulin monomers are arranged from head to tail in filaments so that one end of the filament is different to the other. The two ends are not just structurally different, also functionally. Plus/barbed ends of microtubules and actin respectively have a

faster rate of monomer association than the minus/pointed (Li & Gundersen, 2008). mRNA transport granules in combination with directional molecular motors can use this inherent polarity to navigate through the cytoplasm.

mRNA localisation has been reported to occur using both actin and microtubule networks, using myosins, kinesins and dyneins (Buxbaum et al., 2014). However, the interaction between localisation elements, RBPs, and molecular motors is complex and varies between localised mRNAs. mRNAs with multiple localisation elements can bind multiple RBPs and multiple motor proteins. This can increase the distance that mRNAs can travel in a single run on a cytoskeletal filament (processivity) (Amrute-Nayak & Bullock, 2012). In concurrence, removal of localisation elements sometimes only reduces processivity, and does not completely abrogate mRNA transport (Fusco et al., 2003; Sladewski et al., 2013). This suggests that mRNAs are intrinsically capable of being moved by motors, and that LEs interacting with RBPs may only bias or increase the rate of that movement (Gagnon & Mowry, 2011).

Recently, live imaging of endogenous mRNA in neurons has provided great insight into the mechanism by which mRNAs reach their destinations. Most *Actb* and *Arc* mRNAs in mouse neurons move in a diffusive or corralled (locally restricted) manner (Das et al., 2018; Park et al., 2014). Similarly, in mouse fibroblasts, the majority of *Actb* transcripts displayed diffusive movements (Park et al., 2014). In both fibroblasts and neurons, only a small proportion of *Actb* transcripts are directed, processive movement, although slight cell-type differences exist (1% in fibroblasts, 10% in neurons). This is much lower than previously reported values for exogenous mRNA (22%), highlighting the differences between endogenous and reporter mRNA (Fusco et al., 2003). It is surprising that such a low proportion of endogenous transcripts are processively being transported at any moment. It therefore seems that the model of mRNA localisation as a rapid, active process is perhaps an oversimplification, and raises the question of how mRNAs are able to efficiently reach their destinations. Moreover, rapid and directed movements of mRNA seem to occur in both anterograde and retrograde directions (Das et al., 2018; Park et al., 2014). So how is mRNA polarisation achieved? Evidence suggests that *Actb* transcripts move in an anterograde direction 1.1-1.5x more frequently than retrograde. Similarly, in rat hippocampal neurons, *Actb*, *Camk2a*, and *Psd95* directed movements are slightly anterograde biased (Donlin-Asp et al., 2021). In contrast, anterograde/retrograde directional frequency for *Arc* transcripts is equal, but the run distance of anterograde mRNA particles is slightly longer (Das et al., 2018). These results

show transport dynamics may vary between mRNAs, but in general mRNAs are localised by low-frequency processive transport events which are slightly biased to occur in an anterograde direction.

Detailed analysis of the time frame of *Actb* transcript dynamics through the mRNA lifetime has shown that mRNA movements cycle between mobile and stationary phases. Mobile phases last for just a few seconds, followed by longer, minute-scale stationary phases (Yoon et al., 2016). These movement events are repeated stochastically until an mRNA reaches its final destination and translation takes place (M. S. Song et al., 2018). By this method, *Actb* transcripts are thought to be searching for active dendritic spines to be translated in. mRNA motility in dendrites is therefore coupled tightly to translation status. Confirmation of this has come from experiments where displacement of ribosomes has been shown to cause enhanced motility of transcripts, and freezing of ribosomes to mRNAs led to the opposite effect (Donlin-Asp et al., 2021). Therefore, the transport dynamics of localised mRNAs in neurons are inherently dependent on the translation status of the mRNA, and these two processes must be precisely integrated to synthesise protein within the correct locale.

#### **1.4.5 Do mRNAs travel together or separately?**

One unresolved question is whether multiple mRNAs can be transported together. The nature of mRNA transport granules, with their cloud of interactors, would suggest that multiplicity is possible and perhaps even favourable. Transporting collections of mRNAs together could improve efficiency by reducing the number of energetically demanding individual transport events. Functionally related mRNAs could also be deposited at the same time, thereby enabling coordination of protein interaction at the destination. Imaging of endogenous mRNA has recently allowed testing of this hypothesis.

In neuronal dendrites the copy number of mRNAs within individual granules is variable from mRNA to mRNA. The majority of *Actb*, *Camk2a*, and *Psd95* transcripts exist as single copies (Donlin-Asp et al., 2021). However, a significant minority of each population apparently exist as higher order complexes containing multiple transcripts of the same gene, with slightly fewer of these multi-mRNA complexes for *Actb*. Fusion events when mRNA particles encounter one another have also been observed (Donlin-Asp et al., 2021). These live cell experiments imaging endogenous mRNA revealed new insights that contradicted previous evidence from fixed cells. Previously, pairwise single-molecule imaging of 8 different transcripts (*Arc*, *Actb*, *CamkIIa*, *Efla*, *Map2*, *Nrgn*, *Prkcz*, and *Ube3*) in fixed

dendrites of hippocampal neurons found that no two mRNA molecules assembled into the same structure. Even mRNAs expected to use the same localisation machinery did not colocalise (Batish et al., 2012). Interestingly, *Actb* mRNAs in fibroblasts are not found as multimeric complexes, suggesting cell-type differences in localisation mechanism for the same transcript may exist (Park et al., 2014).

In contrast, in budding yeast, live cell dual-colour imaging has shown that different localised mRNAs including *ASH1* and *IST2* are packaged into common granules to enable transport to the bud tip (Lange et al., 2008). mRNAs that are not localised to the bud tip, or that do not contain a specific localisation sequence are excluded from these granules. Specificity of localisation can therefore be achieved by regulating access to transport granules. The results presented here highlight how the exact transport granule composition, whether alone or together, varies between transcript and even cell type.

## 1.5 Translation

The regulation of local protein production via mRNA localisation is only possible when coupled to the control of translation. Here we will now discuss the general mechanism by which translation takes place, followed by the mechanisms by which the translation machinery is distributed in the cell.

Translation requires orchestration of a wide variety of components including ribosomes, proteins, transfer mRNAs (tRNAs), and energy in the form of nucleoside triphosphates (Hershey et al., 2019). The principal machines that conduct the translation process by catalysing peptide bond formation between adjacent amino acids are the ribosomes.

Ribosomes in eukaryotes are large macromolecular systems which are subdivided into 40S and 60S subunits. The 40S subunit consists of 1 mRNA and 33 proteins, whereas the 60S consists of 3 mRNAs and 46 proteins. The process of translation can be divided into three key phases: initiation, elongation, and termination. In eukaryotes, translation initiation results in the formation of a complex between the ribosome, the mRNA to be translated, and an initiator methionyl-transfer mRNA (Met-tRNA), in which Met-tRNA interacts with the initiating AUG base sequence in the mRNA via codon-anticodon base-pairing (Merrick & Pavitt, 2018). Eukaryotic cells use a collection of at least 12 proteins called initiation factors (eIFs) to bring about translation initiation, each of which play distinct yet vital roles. The second phase of translation is elongation, where repetitive cycles of aminoacyl-tRNA codon-anticodon binding to the mRNA, peptide bond formation between adjacent amino acids, and

translocation through the ribosome occurs (Dever et al., 2018). This yields the production of chain of amino acids connected via peptide bonds. The third phase of translation is termination, which begins when the ribosome reaches a stop codon in the mRNA. No aminoacyl-tRNA recognises the stop codon, and instead release factors eRF1 and eRF3 catalyse the hydrolysis of the peptidyl-tRNA (Hellen, 2018). Then, additional proteins cause ejection of mRNA and tRNA from the ribosome, and the ribosome is recycled for reuse by dissociation into its subunits.

Local protein synthesis requires that the entire translation machinery including ribosomes, tRNAs, and protein factors, are located at the specific subcellular location that the translation is to take place. Classically, ribosomes are described to exist in two broad locations, either free in the cytoplasm or bound to the surface of the ER. However, ribosomes are also known to be enriched in specific locales like focal adhesions (Willett et al., 2010) and at the surface of mitochondria (Gold et al., 2017). The spatial distribution of ribosomes in the cytoplasm is known to be regulated by Kinesin-1 in combination with microtubules in a number of different cell systems including *C. elegans* neurons (Noma et al., 2017) and human cardiomyocytes (Scarborough et al., 2021). One common theme linking the biogenesis of both ribosomes and tRNAs is the requirement for distinct nuclear and cytoplasmic steps in the process. Ribosome assembly occurs primarily in the nucleolus, but prior to this, ribosomal mRNAs go through a complicated journey. They are first transcribed in the nucleus before export to the cytoplasm where translation takes place, before ribosomal proteins are then imported into the nucleus where accessory proteins and small nucleolar RNAs help to assemble the ribosomal proteins with the ribosomal RNA (Baßler & Hurt, 2019) The assembled 40S and 60S ribosomal subunits are then exported to the cytoplasm where they unite to carry out translation. Similarly, yeast tRNAs are first transcribed in the nucleus, before export to the cytoplasm and splicing on the surface of mitochondria. Charging of tRNAs with amino acids is then catalysed by cytoplasmic aminoacyl tRNA synthetases (Chatterjee et al., 2018). Retrograde transport of tRNAs back into the nucleus is also used as a quality control mechanism to ensure the tRNAs are correctly spliced and modified (Kramer & Hopper, 2013). Hence, dynamic intracellular movements of both ribosomes and tRNAs need to be tightly regulated to control protein synthesis.

Much of our knowledge of local translation comes from studies conducted in neurons. As described previously, the unique architecture of neurons necessitates that proteins are synthesised locally in dendrites, axons, and synapses, which can be situated at great distance



from the cell body and nucleus. Consequently, numerous aspects of the protein synthetic pathway have been identified in neuronal processes including mRNAs (Zappulo et al., 2017) and polyribosomes (Bodian, 1965).

Transcriptome profiling has shown that hundreds of mRNAs are localised to neurites, and that the mRNA repertoire can vary between neuron types (Gumy et al., 2011; Minis et al., 2014; Zappulo et al., 2017). These high throughput techniques, combined with single molecule imaging and biochemical analysis of translation, have greatly expanded our knowledge of the spatiotemporal control of local protein synthesis (Dieck et al., 2015; Yan et al., 2016). For example, *Bdnf* transcripts are localised to dendrites using a spatial code in their 5'UTRs, where they are synthesised throughout the dendritic arbor in response to extracellular signals (An et al., 2008; Baj et al., 2011). This process is required for BDNF to carry out its essential function as a growth factor supporting growth, survival, and plasticity (Bathina & Das, 2015). *Camk2a* transcripts are also localised and locally translated in dendrites (Mayford, Bach, et al., 1996; Mayford, Baranes, et al., 1996). CAMK2A is a calcium-activated kinase, specifically and highly expressed in the brain, with important roles in memory formation (Zalcman et al., 2018). Association of *Camk2a* transcripts with polysomes and local translation has been observed in neuronal process extracts (Bagni et al., 2000; Néant-Fery et al., 2012). *Camk2a* translation appears to also play an important role in axons and synapses. Synapse formation in rat and *Aplysia* neurons is dependent on local CAMK2A synthesis, (Lyles et al., 2006; Sebeo et al., 2009). Similarly,  $\beta$ -Catenin transcripts are enriched in axon boutons along with ribosomes (Kundel et al., 2009). Locally translated  $\beta$ -Catenin then regulates synaptic vesicle release (Taylor et al., 2013). Together, this evidence shows how local protein synthesis of specific proteins is required to enable neuron processes to independently carry out specific functions a long way from the cell body.

Recently, techniques like ribosome profiling, which involves sequencing of mRNAs undergoing active translation, have enabled the characterisation of the “translatome” of certain subcellular compartments. These experiments have highlighted how there is significant heterogeneity in translation signature between protrusions of different neuronal cell types (Glock et al., 2021; Ludwik et al., 2019; Ouwenga et al., 2018; Zappulo et al., 2017). In the future, combining these datasets with mRNA sequencing datasets could help to reveal the relative contributions that mRNA localisation and local translation make to the neurite proteome in specific neuron types. Moreover, future work should aim to correlate

translation events with neuron physiological events to understand exactly how proteome remodelling contributes to cell behaviour.

## **1.6 Extrinsic signals control targeting and translation.**

Cells are continually interpreting cues from the environment. Responding to these stimuli requires tight spatiotemporal control of protein production. mRNA localisation can help cells to achieve this via two possible methods: *i*). actively localise mRNAs from surrounding subcellular regions to the site where the extracellular signal was received, or *ii*) actively translate mRNAs that are already in the vicinity of the received signal. Evidence suggests that both are possible in different scenarios.

Most evidence for direct targeting of mRNA to sites of active signalling comes from neuronal growth cones. Growth cones are highly motile protrusive structures that seek out synaptic targets during neuronal development or regeneration. During directional steering the cytoskeleton must be dynamically remodelled in response to attractive and repulsive cues, and local protein synthesis is essential to provide the building blocks that mediate this process. Studies using neurotrophin-coated beads have shown that attractive cues can direct *Actb* transcripts to accumulate in the side of the growth cone proximal to the cue (Leung et al., 2018; Willis et al., 2007; Yao et al., 2006). *Rgs4* transcripts are also dynamically enriched in dendrites in response to specific cues. Induction of local glutamate signalling was found to stimulate transcripts to become enriched in dendrites via biasing transcript motile behaviour to anterograde (Bauer et al., 2019). Similarly, activation of glutamate signalling at specific dendrites in hippocampal neurons stimulated the transport of *Actb* transcripts into those dendrites. This process was specifically dependent on N-methyl-D-aspartate (NMDA) receptor activity. Therefore, this work builds on previous evidence that dendrite stimulation causes “capture” of dynamically moving mRNAs, and that activity at spines is essential for informing an mRNA that it has reached its destination (Bauer et al., 2019; Yoon et al., 2016).

Interestingly, cue-induced mRNA localisation appears to be evolutionarily conserved. A similar process occurs in simpler eukaryotes. In mating yeast, pheromone signals induce the localisation of mRNAs to cellular mating protrusions. Signal transduction activates Scp160, an RBP that then drives mRNA localisation to these mating protrusions via myosin-dependent transport (Gelin-Licht et al., 2012).

Studies in *Aplysia* (sea slug) synapses have shown how extracellular signals can cause an increase in both mRNA transport and local translation. *sensorin* mRNA is rapidly localised to

and translated in *Aplysia* synapses in response to serotonin. This process was specific to long-term potentiation, and did not occur during long-term depression, indicating that specific stimuli can result in specific translation outcomes (D. O. Wang et al., 2009). Building on this evidence, it was then shown that *sensorin* mRNA does not get directly targeted out of the nucleus into the neuronal arbour in response to signals, but re-distribution of constituent mRNA within dendrites does occur. This is coordinated with a concomitant upregulation of translation at specifically stimulated dendrites (S. Kim & Martin, 2015).

A wide variety of stimulations and ligands have been shown to influence local translation in neurons including BDNF (Kang & Schuman, 1996), metabotropic glutamate receptor signalling (Huber et al., 2000), activity deprivation and subsequent homeostatic plasticity (Sutton et al., 2006), and cannabinoid receptor activation (Younts et al., 2016). It has not been clear until recently how the local proteome is remodelled in different neuronal compartments in response to different forms of neuronal plasticity and signalling. In particular, most evidence for local translation in neurons has come from research in post-synaptic dendrites. By combining high resolution imaging and translomics, it has been shown recently that different forms of neuronal stimulation induce different translation signatures in different synaptic compartments, including in presynapses (Hafner et al., 2019). Importantly, this shows how different signals can induce unique proteome remodelling events, and therefore provides evidence for how subfunctionalisation of neuron compartments can be achieved,

## **1.7 mRNA localisation and local translation in cell migration**

Local protein synthesis is a fundamental characteristic of polarised cells. Although much of the evidence presented previously was identified in neurons, the principles are likely to apply across all polarised cells. In migrating cells for example, dynamic processes in the front and rear of cells must be co-ordinated to allow efficient migration through the environment. At the rear, contractile forces are dominant, allowing retraction and assisting with directional steering. At the front, adhesion to the substrate enables traction, and protrusions explore and sense the extracellular space (Ridley et al., 2003). Polarised mRNA localisation helps cells set up these distinct compartments, with particular importance at focal adhesions (de Hoog et al., 2004).

### **1.7.1 Mechanism of ZBP1-mediated mRNA transport in cell migration.**

A particularly well-studied example is the targeting of polarised *ACTB* mRNA to the lamellipodia of migrating fibroblasts, endothelial cells, and cancer cells (Hooock et al., 1991; Lawrence & Singer, 1986; Shestakova et al., 1999). Localisation of *ACTB* mRNA is primarily driven by a short 54nt LE in its 3'UTR which contains an essential 5' CGGAC and variable 3' C/A-CA-C/U sequences. The spacing of these two sequences is vital, and a gap of less than 10 nucleotides results in reduction in binding affinity of ZBP1 (Chao et al., 2010; Ross et al., 1997). Multiple different mRNA-binding domains are present in ZBP1, including two K Homology (KH3 and KH4) domains which are necessary for binding to the LE (Farina et al., 2003). Recently, the binding interaction between these domains and the LE has been refined to a few key bases. The KH3 domain recognises the 3' CA binucleotide sequence with low specificity, whereas KH4 recognises the 5' GGA trinucleotide sequence with high specificity (Nicastro et al., 2017). Remarkably, the spatial arrangement of these two important sequences can be reversed within transcripts, without a concomitant reduction in mRNA localisation (Patel et al., 2012).

ZBP1 appears to be conserved in targeting mRNAs that encode cytoskeletal modulators. mRNAs encoding all seven subunits of the ARP2/3 complex are reported to be enriched in fibroblast protrusions (Mingle et al., 2005b). ARP2/3 is a critical actin nucleator, responsible for branching of actin networks. Putative ZBP1 binding sites have been identified in their 3'UTRs, and importantly, ZBP1 knockdown causes ARP2/3 mislocalisation (Gu et al., 2012). Similarly, *Cofilin-1* (*CFL1*) mRNA is enriched in the leading edge (Maizels et al., 2015). CFL1 plays an important role in actin depolymerisation, thereby reorganising cytoskeletal networks and modulating protrusion formation. Localisation is thought to be dependent on a similar ZBP1-related mechanism. So, ZBP1-mediated transport is a shared mechanism of mRNA localisation for numerous mRNAs encoding cytoskeletal modulators to the protrusions of migratory cells.

The targeting mechanism used by ZBP1-RNP complexes to reach the leading edge has been interrogated extensively. Firstly, early studies showed that stimulation with lysophosphatidic acid (LPA) induced polarisation of *Actb* (V. M. Latham et al., 2001; V. M. J. Latham et al., 1994). Similarly, LPA was required to induce polarisation of *Arp2/3* and *Cfl1* (Maizels et al., 2015; Mingle et al., 2009). LPA-induced localisation of *Actb* and *Arp2/3* is dependent on RhoA/Rho Kinase signalling and subsequent Myosin IIB activation (V. M. J. Latham et al., 1994; Mingle et al., 2009). Importantly, *Actb* mRNA is mislocalised in Myosin IIB knockout mice (V. M. Latham et al., 2001). Therefore, transport via actin filaments appears to be

important for ZBP1-mediated mRNA localisation. However, more recent work has also identified a role for microtubules. ZBP1 has been found to physically associate with kinesin-like molecular motor KIF11 (T. Song et al., 2015). KIF11 also colocalises with *Actb* mRNA granules, and KIF11 knockdown reduced *Actb* localisation to migratory protrusions. Therefore, both microtubule and actin molecular motors are required for ZBP1-mediated mRNA transport during cell migration. Exactly how these motors are coordinated is not yet clear. Once *Actb* mRNA transport complexes reach their destination in the leading edge, the translation elongation factor EF1A binds to both the mRNA and the dense cortical actin network, thereby forming a scaffold and anchoring the mRNA in place (Liu et al., 2002). Anchoring is thought to be essential for overcoming random diffusion and maintaining a precise spatial distribution of mRNA. Together, this evidence describes the transport process for mRNAs that encode cytoskeletal modulators via ZBP1-mediated localisation to migratory protrusions.

### **1.7.2 Mechanism of APC-dependent mRNA transport in cell migration.**

One further *trans*-acting factor shown to have a critical role in targeting mRNAs in migrating cells is adenomatous polyposis coli (APC). APC is a multifunctional tumour-suppressor protein that has long been implicated in cell migration and is known to play diverse roles in microtubule biology (Aoki & Taketo, 2007; Näthke et al., 1996). Importantly, APC is known to interact with various microtubule plus-end trafficking motors, and it also accumulates at growing tips where it regulates microtubule stability (Kroboth et al., 2007; Mimori-Kiyosue et al., 2000; Wen et al., 2004). APC has an intrinsically disordered basic region which facilitates promiscuous binding to protein partners (Deka et al., 1999; Minde et al., 2011), and has also been shown to bind to mRNA (Preitner et al., 2014). The first evidence for a role in mRNA localisation for APC came from its protein localisation in cell protrusions, specifically in RNP complexes at the plus-end of detyrosinated microtubules (Mili et al., 2008). Subsequent results showed that knockdown of APC reduces the protrusion-enrichment of a cohort of mRNAs in migrating fibroblasts. Cellular contractility and extracellular matrix stiffness has been shown to regulate APC-mediated mRNA localisation, via activation of Rho signalling and promoting the formation of a detyrosinated microtubule network (T. Wang et al., 2017). Therefore, APC is a critical RBP regulator of a well-defined cohort of polarised mRNAs in migratory fibroblasts.

The essential components and stoichiometry of APC RNP granules have recently been tested using an *in vitro* reconstitution assay (Baumann et al., 2020). In these experiments, APC was shown to form stable complexes containing *Actb* or *Tubb2b* mRNA in combination with kinesin-2 family molecular motor KIF3A via adaptor protein KAP3 (Baumann et al., 2020). This competent RNP complex is thought to drive localisation via G-rich sequences in the 3'UTRs of target mRNAs, although fully-characterised LE sequences for APC have remained elusive (Baumann et al., 2020; Preitner et al., 2014). Recently, an alternative molecular motor, the kinesin-1 family member KIF1C, has also been identified as an essential factor during the localisation of APC-transported mRNAs. APC-transported mRNAs were found to colocalise with KIF1C in motile particles in migrating cells in a 3'UTR dependent manner (Pichon et al., 2021). It remains to be seen exactly how the actions of KIF3A and KIF1C are coordinated in targeting APC-dependent mRNAs to motile protrusions.

### **1.7.3 Local translation in protrusions of migrating cells.**

Recent work has been undertaken to characterise the relative contributions of mRNA targeting, local translation and protein targeting to the protrusion proteome. Using a scheme to specifically inhibit translation in protrusions, in combination with transcriptomics and proteomics, local translation was shown to be a key regulator of protein localisation (Mardakheh et al., 2015). Inhibiting local translation also caused reduced protrusion formation and poor invasiveness. Therefore, local translation appears to be broadly important in migratory protrusions.

Understanding of the role that local translation plays in the regulation of specific mRNAs comes mostly from research on ZBP1- and APC-dependent localised mRNAs. One key question is whether localised mRNAs are able to be translated during the transport process, or conversely whether they are translationally repressed. During transport of *Actb* mRNA to the leading edge, ZBP1 represses translation (Hüttelmaier et al., 2005). This is thought to ensure that premature protein synthesis does not take place during the mRNA journey, which would perhaps result in the aberrant protein activity at inappropriate locations. In the protrusion, translational repression is released by phosphorylation of key ZBP1 tyrosine residues by Src kinase. This causes ZBP1 to be released from *Actb* transcripts and translation to begin (Hüttelmaier et al., 2005). Src kinase activity is mostly restricted to the cell periphery, so *Actb* translation only begins once mRNAs have reached the distal parts of the cell (Hüttelmaier et al., 2005). Therefore, translation of localised *Actb* transcripts is precisely

controlled in subcellular space, so that translated Actb monomers are deposited in the correct peripheral locale.

The translational regulation of APC-dependent mRNAs has also been characterised, and there are key differences to the ZBP1-dependent mechanism of *Actb* mRNA localisation. In contrast to *Actb* translation, which is inhibited by ZBP1 during the *Actb* transport process, live imaging studies suggest translation of APC-dependent mRNAs can in fact occur in proximal subcellular positions just as frequently as in distal regions. This suggests that APC-dependent mRNA translation is not inhibited during transit. However, local translation of APC-dependent mRNAs was indeed found to be inhibited specifically in protrusions during retraction, and enhanced at extending protrusions. Therefore, translation of APC-dependent localised mRNAs appears to be under tight spatial control during cell migration, although in this case the molecular mechanism has not yet been defined. Nevertheless, this evidence is the first to show that translation of localised mRNAs is inherently linked to dynamic migratory cell movements (Moissoglu et al., 2019).

Translation of APC-dependent localised mRNAs is also known to be regulated by additional protein factors present in mRNA granules. Fused in Sarcoma (FUS), which coprecipitates with APC-dependent mRNAs, has been shown to positively regulate APC-dependent mRNA translation (Yasuda et al., 2013). Surprisingly, overexpression of FUS promotes the formation of large, translationally-active cytoplasmic mRNA granules. Protrusion-localised mRNAs are sequestered and translated within these granules at ectopic subcellular sites (Yasuda et al., 2017). These granules are remarkably similar to neuronal granules that contribute to the pathogenesis of Amyotrophic Lateral Sclerosis, which is known to be caused by mutations to FUS (Murakami et al., 2015). Pathogenesis of neurodegenerative diseases like ALS might therefore be caused by the aberrant translation of normally protrusion-localised mRNAs at incorrect sites. It remains to be seen how additional regulatory factors like FUS may perhaps control the transition from translationally-repressed to translationally-active for localised mRNAs in physiological scenarios. It is enticing to think that the dynamic spatial control of localised mRNA translation via cell protrusive movements described above may perhaps be enacted by proteins like FUS, although further research is required to understand this. Together this evidence shows that the translational regulation of localised mRNAs in migratory protrusions appears to vary depending on the mechanism of mRNA transport and localised mRNA identity.

#### **1.7.4 The broader protrusion transcriptome.**

Cell fractionation using the Boyden Chamber (Boyden, 1962), in combination with next-generation sequencing technologies, has revealed that specific groups of mRNAs are consistently protrusion-enriched irrespective of cell type. This is suggestive of shared mRNA localisation pathways that migratory cells depend on. For example, mRNAs encoding for ribosomal proteins are consistently enriched and translated in the leading edge of invasive cells (Mardakheh et al., 2015; Mili et al., 2008). Localisation of the entire cohort of ribosomal protein mRNAs is predicted to be enabled by the RBP LA-related protein 6 (LARP6), which is also enriched in protrusions (Dermit et al., 2020). It is hypothesised that localisation of ribosomal protein mRNAs to protrusions could be used to enable on-site ribosome biogenesis. Moreover, the potential for tailoring of constituent ribosomal components via local remodelling, and therefore creating spatially distinct and functionally specialised ribosome pools has been hypothesised in the past (Cioni et al., 2018; Shi et al., 2017). This evidence adds another layer of complexity to the regulation of local mRNA translation, by hinting that mRNA localisation and translation of ribosomal protein mRNAs could produce specialised ribosome pools in protrusions, which in turn could regulate the translation of specific cohorts of localised mRNAs.

#### **1.7.5 Functional roles of mRNA localisation in cell migration**

Identification of minimal LEs responsible for mRNA targeting has been constrained by their complex nature described previously. This has impeded our ability to interrogate the functional consequences of endogenous mRNA localisation in cell migration, since the most certain way to impede localisation is by genetic ablation or steric blocking of LEs. Perhaps this partially explains why the function of mRNA localisation has only been characterised for a handful of mRNAs in migrating cells (Shestakova et al., 2001), despite evidence that hundreds of mRNAs display asymmetric distributions (Jakobsen et al., 2013; Mardakheh et al., 2015; Mili et al., 2008; Shankar et al., 2010; Stuart et al., 2008).

Inhibition of targeting of *Actb* mRNA using antisense oligonucleotides that prevent ZBP1 binding to the LE has been shown to disrupt the morphology of the leading edge and impede directional migration (Kislauskis et al., 1994, 1997; Shestakova et al., 2001). This evidence is supported by the fact that a highly polarised distribution of mRNA is correlated with persistent directional migration (Park et al., 2012). Manipulation of *Actb* mRNA localisation has also provided evidence for molecular function. For example, tethering of mRNA to focal



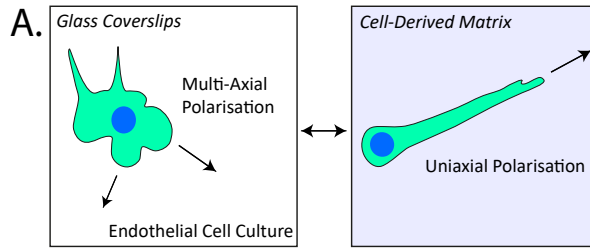
adhesions alters cell motility, and is suggestive of a key role for localised mRNA in cell adhesion (Katz et al., 2012). Indeed, ACTB produced from localised mRNA is thought to incorporate in actin filaments that functionally link focal adhesions to the cytoskeleton. Therefore, one important question faced by the field over previous decades is how ACTB protein synthesised from localised *ACTB* transcripts may differ from ACTB synthesised at other cellular locations. This question is particularly relevant for ACTB, since it is one of the most abundant proteins in the cell and its region of expression is not restricted to the protrusion. It has been hypothesised that restricting the distribution of newly synthesised ACTB proteins to a tightly defined space could locally increase the concentration of protein, and this could influence actin filament polymerisation (Condeelis & Singer, 2005). Alternatively, the importance of mRNA localisation for ACTB function in protrusions could perhaps be explained by newly synthesised ACTB possessing distinct molecular characteristics to “old” ACTB. For example, new ACTB monomers could have a faster rate of polymerisation (Solomon & Rubenstein, 1987) and less affinity for capping and severing proteins (Saha et al., 2010). Moreover, sequestration of *ACTB* transcripts away from protrusions in proximal subcellular regions significantly impairs the ability of ACTB proteins to incorporate in F-actin, therefore showing that newly synthesised ACTB in protrusions has distinct properties to ACTB produced elsewhere (N. Y. Kim et al., 2020). Therefore, it seems that mRNA localisation may function to control “new protein” functionality in specific subcellular locales, generating distinct pools of protein with varying molecular abilities, and this can determine a cells migratory ability.

A competition assay has recently been used to impede localisation of a cohort of APC-dependent protrusion-localised mRNAs (T. Wang et al., 2017). By overexpressing the 3'UTR from a localised mRNA (*RAB13*), and purportedly sequestering the pool of available localisation machinery, the localisation of APC-dependent mRNAs was shown to reduce the efficiency of cell migration. Despite this work, the molecular functions of APC-dependent localised mRNAs are still not clear.

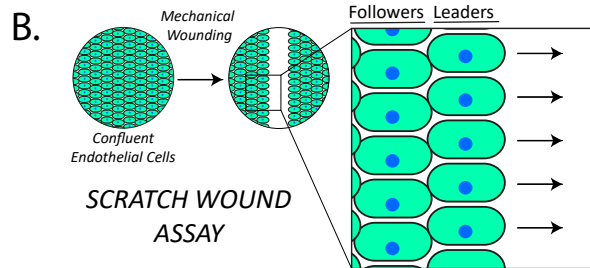
## **1.8 Angiogenesis as a model of cell migration**

Despite the vital advances described previously, our understanding of the mechanisms and functions of mRNA localisation is far from complete. The role that mRNA localisation plays during complex physiological and pathological cell migration is still not known. Much of our previous knowledge comes from *in vitro* studies that may not faithfully recapitulate *in vivo*

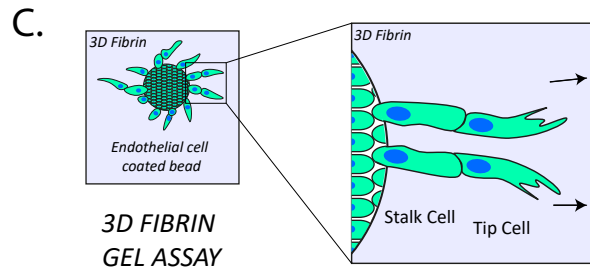
Complexity



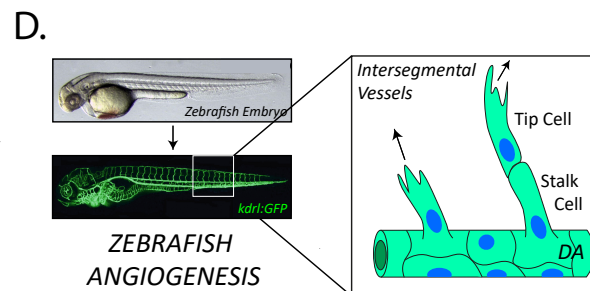
- ADVANTAGES**
- Simple, Easy to Use
  - High Throughput
  - Thin Samples for Imaging
  - CDM Induces *in vivo* migration style
- DISADVANTAGES**
- No collective behaviour
  - On glass, migration style is not as physiologically relevant



- ADVANTAGES**
- Simple, Easy to Use
  - High Throughput
  - Thin Samples for Imaging
  - Some collective behaviour and cell-cell junctions.
- DISADVANTAGES**
- Migration style is not physiologically relevant
  - Mechanical wounding damages cells



- ADVANTAGES**
- Reproduces Tip/Stalk hierarchy
  - 3D invasive migration
  - Cells migrate collectively
- DISADVANTAGES**
- Low Throughput
  - Fibrin does not entirely reproduce *in vivo* characteristics.



- ADVANTAGES**
- Gold standard for physiological relevance
  - Stereotyped morphogenesis
  - Later stages of lumen formation and anastomosis can be studied
- DISADVANTAGES**
- Some human-specific genes cannot be studied
  - Lower throughput than *in vitro*
  - Complex environment makes imaging more challenging

### Figure 1.3    Angiogenesis as a model of cell migration.

Numerous *in vitro* and *in vivo* models exist for the investigation of cell migration during angiogenesis, with carrying degrees of physiological relevance and complexity.

- A. The simplest and most user-friendly are *in vitro* cell cultures. Endothelial cells adopt different migratory characteristics when grown on glass or in cell-derived matrix. This can be used to test simple single-cell motile properties, but in these conditions, cells do not display collective migration of *in vivo* angiogenesis.
- B. A form of collective behaviour can be induced by the use of the scratch-wound assay, in which endothelial cells are grown to confluency before mechanical wounding, and hence induction of wound closure by sheet migration. However, the migration mode of cells along a flat substrate does not recapitulate fully the invasive movement of *in vivo* endothelial cells.
- C. Achieving 3-dimensionality in *in vitro* cell culture can be challenging, but this is provided by the Fibrin Gel Assay. Here, microcarrier beads are coated with endothelial cells and implanted into fibrin gel. Endothelial cells then sprout into the fibrin, reproducing the tip-stalk hierarchy of *in vivo* angiogenesis. One drawback of this assay is that an extracellular matrix composed solely of fibrin is not entirely physiologically-relevant.
- D. Finally, the gold standard for cell migration research in the context of angiogenesis is *in vivo* growth of blood vessels during embryonic development. One model of this is the formation of the intersegmental vessels in the zebrafish embryo. Zebrafish are highly amenable to genetic manipulation, including the fluorescent-labelling of vascular tissue (*kdrl:GFP*), enabling confocal imaging of the cellular mechanisms of angiogenesis. The growth of the intersegmental vessels begins with sprouting of cells from the dorsal aorta (DA), collective migration of cells dorsally, and organisation into a tip:stalk cell hierarchy.

motile cell behaviours. Utilising suitable models for investigation of mRNA localisation is therefore critical.

One suitable model is the collective migration of cells during the formation of new blood vessels (Fig. 1.3). During development new blood vessels grow by sprouting from existing ones in a process called angiogenesis (Herbert & R Stainier, 2011). Angiogenesis is also co-opted during disease, as cancer cells stimulate the vascularisation of tumours (Lugano et al., 2019). The cellular mechanism of angiogenesis is conserved and stereotyped across phyla. Hence, in recent times, the zebrafish intersegmental vessels have come to the fore as a suitable model for the characterisation of angiogenesis. The principal regulator of angiogenesis is vascular endothelial growth factor A (VEGFA), which is received by quiescent endothelial cells in the dorsal aorta, causing the adoption of a motile phenotype (Gerhardt et al., 2003). The activated cells then migrate dorsally, away from the parent vessel, creating a new branch. A hierarchy of cell identities is quickly established in the nascent vessel. Highly motile “tip” cells lead the sprout, extend numerous filopodia (Franco et al., 2015), and sense and respond to chemotactic cues. In contrast, trailing “stalk” cells are less migratory, maintain the connection to the existing vessel, and establish a vascular lumen as the vessel matures (Kamei et al., 2006). Nascent sprouts continue to collectively migrate between the somites until the tip cells make contact with adjacent vessels in the dorsal region of the embryo. Cells then anastomose to create the dorso-longitudinal anastomotic vessel (Childs et al., 2002).

In situations where higher throughput is required, or when human-specific genes are investigated, it is also possible to turn to *in vitro* models of angiogenesis. The main challenge when optimising *in vitro* models is in reproducing as much of the surrounding physiology from *in vivo* situations as possible. Various *in vitro* models of angiogenesis have been developed, each with their own specific advantages (Staton et al., 2009). The simplest *in vitro* models are cell migration assays that allow for testing of classical cell motility phenotypes in a rapid and reproducible manner. For example, the scratch wound assay is commonly used. In this assay, confluent endothelial cells are induced to migrate to fill an area of low cell density. Using a thin, 2D sample such as the scratch wound can be beneficial for fluorescent imaging with high signal:noise. However, the mode of migration that cells adopt is not entirely physiologically relevant, since 3D cell migration is morphologically distinct to 2D (Yamada et al., 2019). Numerous assays have been developed that add physiological relevance including tube formation assays (Arnaoutova et al., 2009) and co-cultures

(Hetheridge et al., 2011). However, three-dimensionality was finally added via development of the fibrin gel bead assay (Nakatsu et al., 2007). Here, endothelial cell-coated microcarrier beads are embedded in a 3D fibrin matrix and fibroblasts are seeded on top, where they provide the secreted components that stimulate angiogenesis. Fibrin gel bead assays mimic all aspects of angiogenesis including sprouting, migration, tube formation and anastomosis, as well as the hierarchical organisation of cells during sprouting. Finally, versatile cell-derived matrix assays can be used. In these assays, fibroblasts are used to produce a 3D matrix which mimics the extracellular matrix *in vivo* (Cukierman et al., 2001; Franco-Barraza et al., 2016). When migratory cells are applied to the matrix, they migrate individually. With the complexities of collective cell movement excluded, cell-derived matrixes can be used to model the physiology of cell migration at the single cell level. In practise, combining rapid and multiplexed *in vitro* assays with the situational complexity of 3D *in vitro* and *in vivo* assays is often the most effective method for investigations. The importance of angiogenesis in health and disease, and the various well-established *in vitro* and *in vivo* models, make angiogenesis the ideal system for studying how mRNA localisation contributes to physiologically relevant cell migration.

## **1.9 Experimental Aims**

Cell migration requires the simultaneous coordination of multiple processes. To achieve this, specific cellular functions are compartmentalised in specific subcellular regions. The enrichment of proteins in specific subcellular zones, and conversely the depletion of proteins from other areas, is a prerequisite for this division of labour.

One purported mechanism by which cells create these local pools of protein is by actively localising and locally translating mRNAs. A plethora of evidence has been produced describing the vital role that mRNA localisation plays in diverse biological scenarios, from embryo patterning to yeast fate determination. In contrast, our knowledge of the role of mRNA localisation during physiological cell migration has trailed behind.

Therefore, the aim of this thesis is to characterise the mechanisms and functions of mRNA localisation in cell migration during angiogenesis. Specifically, the aims are to:

1. Characterise the diversity of mRNA localisation patterns in migrating endothelial cells.
2. Identify the molecular components that drive those localisations.
3. Test the functionality of localised mRNAs during cell migration in angiogenesis.

# ***RAB13* mRNA compartmentalisation spatially orients tissue morphogenesis.**

Guilherme Costa<sup>1\*</sup>, Joshua J. Bradbury<sup>1</sup>, Nawseen Tarannum<sup>1</sup>, and Shane P. Herbert<sup>1\*</sup>

1 = Faculty of Biology, Medicine and Health, University of Manchester, Manchester, UK.

\* = Corresponding Authors.



Journal Publication – The EMBO Journal.

## **Author Contributions**

This manuscript is representative of collaborative work conducted during my PhD. The experiments I conducted include Figure 1d-e, g-i; Figure EV1b-d; Figure 2d-f. Author NT contributed to part of the 3'UTR cloning in Figure 2e. This work would not have been possible without first author GC, who conducted the majority of the experimental work and analysis presented within. I contributed to conceptualisation, methodology, and direction of research throughout the research project alongside GC, and supervisor SPH. I assisted drafting of the manuscript alongside GC and SPH.

SOURCE  
DATATRANSPARENT  
PROCESSOPEN  
ACCESS

# RAB13 mRNA compartmentalisation spatially orients tissue morphogenesis

Guilherme Costa<sup>1,2,\*</sup> , Joshua J Bradbury<sup>1</sup>, Nawseen Tarannum<sup>1</sup> & Shane P Herbert<sup>1,\*\*</sup> 

## Abstract

**Polarised targeting of diverse mRNAs to cellular protrusions is a hallmark of cell migration. Although a widespread phenomenon, definitive functions for endogenous targeted mRNAs and their relevance to modulation of *in vivo* tissue dynamics remain elusive. Here, using single-molecule analysis, gene editing and zebrafish live-cell imaging, we report that mRNA polarisation acts as a molecular compass that orients motile cell polarity and spatially directs tissue movement. Clustering of protrusion-derived RNAseq datasets defined a core 192-nt localisation element underpinning precise mRNA targeting to sites of filopodia formation. Such targeting of the small GTPase RAB13 generated tight spatial coupling of mRNA localisation, translation and protein activity, achieving precise subcellular compartmentalisation of RAB13 protein function to create a polarised domain of filopodia extension. Consequently, genomic excision of this localisation element and perturbation of RAB13 mRNA targeting—but not translation—depolarised filopodia dynamics in motile endothelial cells and induced mispatterning of blood vessels in zebrafish. Hence, mRNA polarisation, not expression, is the primary determinant of the site of RAB13 action, preventing ectopic functionality at inappropriate subcellular loci and orienting tissue morphogenesis.**

**Keywords** angiogenesis; endothelial cell; filopodia; mRNA targeting; zebrafish

**Subject Categories** Development; Membranes & Trafficking; Translation & Protein Quality

**DOI** 10.15252/embo.2020106003 | Received 22 June 2020 | Revised 8 August 2020 | Accepted 14 August 2020 | Published online 18 September 2020

**The EMBO Journal (2020) 39: e106003**

## Introduction

Dynamic subcellular polarisation of a myriad of proteins fundamentally shapes the front-rear orientation and directed movement of motile cells during tissue formation (reviewed in Mayor & Etienne-Manneville, 2016). In parallel, cell migration is associated with subcellular polarisation of numerous mRNAs (reviewed in Herbert & Costa, 2019), but whether this phenomenon is also relevant to the

modulation of tissue dynamics remains an open question. However, in many other biological contexts, mRNA localisation and local translation are well-established as key determinants of cell polarity (Buxbaum *et al*, 2015). This mode of spatial control of gene expression contributes to polarised cellular responses in broad contexts, ranging from axon growth (Leung *et al*, 2006; Yao *et al*, 2006) and synaptic function (e.g. Kang & Schuman, 1996; Lyles *et al*, 2006; Younts *et al*, 2016) to epithelial polarity (Nagaoka *et al*, 2012; Moor *et al*, 2017). Moreover, there is a wealth of data in diverse cell types demonstrating that large numbers of mRNAs are co-distributed together at distinct subcellular sites, which has led to the idea that such mRNA polarisation functions to generate local transcriptomes (reviewed in Engel *et al*, 2020). This suggests that clusters of mRNAs encoding proteins belonging to common complexes and biological pathways co-localise to participate in local processes (e.g. Mingle *et al*, 2005; Hotz & Nelson, 2017). Indeed, it has been proposed that such co-distribution of mRNAs also ensures the fidelity of interactions between locally produced proteins in rapidly changing cell environments (Weatheritt *et al*, 2014). Nevertheless, during cell migration, the impact of mRNA polarisation on the control of translated protein function, local assembly of the migratory machinery and motile cell polarity remain poorly understood, as does the *in vivo* relevance of this phenomenon.

The polarised localisation of mRNAs is driven by *cis*-localisation elements (LEs) that are commonly found in 3' untranslated regions (UTRs) (Andreassi & Riccio, 2009; Mayr, 2016). Indeed, alternative 3'UTRs have been shown to control the spatial localisation of mRNAs (Taliaferro *et al*, 2016; Tushev *et al*, 2018) and modulate protein distribution (An *et al*, 2008; Ciolli Mattioli *et al*, 2019), suggesting that tight control of LE usage may underpin spatial regulation of gene expression. Although the complex sequence and structural composition of LEs render the identification of conserved RNA motifs within large groups of co-localised mRNAs a challenging task, several individual LEs have been characterised in detail using diverse model organisms (reviewed in Jambhekar & Derisi, 2007). In vertebrate cells, LEs ranging from just a few to hundreds of nucleotides in length have been identified within 3'UTRs (e.g. Mowry & Melton, 1992; Kislauskis *et al*, 1994; Ainger *et al*, 1997). However, considering the difficulties in manipulating endogenous transcripts, our understanding of LE function during complex tissue formation in vertebrate organisms remains relatively poor.

<sup>1</sup> Faculty of Biology, Medicine and Health, University of Manchester, Manchester, UK

<sup>2</sup> Wellcome-Wolfson Institute for Experimental Medicine, Queen's University of Belfast, Belfast, UK

\*Corresponding author. Tel: +44 0289 097 6020; E-mail: g.costa@qub.ac.uk

\*\*Corresponding author. Tel: +44 0161 275 1140; E-mail: shane.herbert@manchester.ac.uk

Here, using novel reporter transgenics in zebrafish embryos and targeted gene editing, we shed light on the function of LE-mediated mRNA polarisation in the control of tissue formation *in vivo*. Following clustering analysis of transcriptome-wide data, we define a core group of 5 mRNAs that are universally targeted to the leading edge of migratory cells *in vitro*. Moreover, we identify a conserved RNA motif within the 3'UTRs of these genes and a 192-nt LE containing four of these motifs that is sufficient to target transcripts to polarised sites of filopodia remodelling. Excision of this LE in transcripts encoding the small GTPase RAB13 perturbs mRNA localisation (but not translation) and was sufficient to depolarise RAB13-mediated filopodia dynamics in motile endothelial cells *in vitro*. Hence, *RAB13* mRNA polarisation achieves precise spatial compartmentalisation of RAB13 protein activity to the front of migrating cells and blocks ectopic protein action at inappropriate subcellular loci. Consequently, excision of the *rab13* LE in zebrafish embryos also perturbed mRNA polarisation and induced mispatterning of nascent blood vessels. Altogether, our findings show that mRNA polarisation spatially restricts protein activity to precisely orient motile cell polarity and tissue movement *in vivo*.

## Results

### Clustering of RNAseq datasets identifies mRNAs exhibiting universal targeting to protrusions

To explore the ability of targeted mRNAs to direct tissue formation, we first aimed to define mRNA localisation motifs driving transcript polarisation in motile endothelial cells (ECs), as an initial step towards probing their function in coordinating blood vessel morphogenesis *in vivo*. As a starting point, we identified 233 transcripts enriched in fractionated cellular protrusions of migrating primary human umbilical vein ECs (HUVECs) *in vitro* (Fig 1A and B; Table EV1). ECs were seeded on Transwells in low serum and induced to migrate upon addition of VEGF-A to the lower chamber (Fig 1A). Consequently, the motile protrusions and trailing cell bodies of ECs were separated and protrusion-enriched transcripts identified by RNAseq (Fig 1B; Table EV1). *k*-means clustering analysis of these data alongside RNAseq datasets from unrelated cell types (NIH/3T3 fibroblasts (Wang *et al*, 2017), MDA-MB231

metastatic breast cancer cells (Mardakheh *et al*, 2015), induced neuronal cells (Zappulo *et al*, 2017)) revealed unexpected cell type-specific diversity to transcript polarisation, with only five mRNAs exhibiting universal targeting to protrusions in all cell types tested (cluster *k* 5; *RAB13*, *TRAK2*, *RASSF3*, *NET1*, *KIF1C*; Figs 1B and C, and EV1A). Strikingly, cluster *k* 5 mRNAs shared near-identical spatial distributions by single-molecule FISH (smFISH) (Raj *et al*, 2008; Tsanov *et al*, 2016), being highly polarised to cellular protrusions relative to a control transcript, *GAPDH* (Fig 1D–G). Indeed, all cluster *k* 5 mRNAs exhibited a significantly higher Polarisation Index (PI) than *GAPDH* when co-detected in migrating ECs (Fig 1E) and the ratio of *k* 5 mRNA PI to *GAPDH* PI was consistently greater than one in individual cells (Fig 1F). Moreover, *k* 5 transcripts were highly spatially distinct from other clusters, such as mRNAs of cluster *k* 7 that exhibited less-polarised perinuclear targeting (Figs 1G and H, and EV1B and D). Likewise, protrusion localisation of the well-established polarised mRNA *ACTB* (Condeelis & Singer, 2005) was significantly more diffuse than *k* 5 mRNAs, as were other cluster *k* 2 members such as *PPDPF* (Figs 1G and I, and EV1B and C). Finally, protrusion-enriched mRNAs were also tightly clustered according to protein function (Table EV2), with *k* 5 transcripts specifically encoding cell periphery-associated modulators of vesicle trafficking and membrane remodelling (Tommasi *et al*, 2002; Brickley *et al*, 2005; Kopp *et al*, 2006; Srougi & Burrige, 2011; Wu *et al*, 2011). Hence, tight coupling of distinct mRNA spatial distributions with discrete protein functionalities likely indicates that the universal polarisation of *k* 5 mRNAs is a key functional requirement in processes common to all motile cells.

### Clustering of RNAseq datasets defines an RNA motif enriched in 3'UTR sequences that target *k* 5 mRNAs to protrusions

Considering that the polarisation of cluster *k* 5 mRNAs was particularly acute, highly stereotyped and uniquely conserved amongst cell types (Fig 1C–G), we hypothesised that these transcripts employed common targeting mechanisms. Indeed, using the MEME Suite (Bailey & Elkan, 1994) we detected consistent repeat use of a conserved sequence motif in the 3'UTRs of all *k* 5 transcripts (Fig 2A and B, and Table EV3). This motif distinguished the *k* 5 mRNAs from other identified mRNA clusters, which contained the motif at much lower frequency (Fig 2C). Moreover, this motif was

**Figure 1. Clustering of RNAseq datasets identifies mRNAs exhibiting universal targeting to protrusions in diverse cell types.**

- A Strategy used to screen for mRNAs enriched in motile protrusions of HUVECs migrating through Transwell membranes.
- B RNAseq data are plotted in  $\log_2$  fold change (FC) levels of protrusions over cell bodies against adjusted  $-\log_{10}$  false discovery rate (FDR) ( $n = 2$  replicates, average FC values are represented). The horizontal dashed line marks the FDR ( $q$ ) = 0.05 threshold; vertical dashed lines mark the FC = 0.625 (left) or FC = 1.6 (right) thresholds.
- C Heat map represents the *k*-means clustering of transcript  $\log_2$  FC levels (protrusions over cell bodies) extracted from RNAseq datasets published elsewhere. The corresponding HUVEC FC levels are shown in parallel.
- D smFISH co-detection of *k* 5 mRNAs and *GAPDH* in subconfluent motile HUVECs.
- E Polarisation Index (PI) of *k* 5 mRNAs and *GAPDH* in co-detected in HUVECs ( $n \geq 28$  cells;  $**P < 0.01$ ,  $***P < 0.001$ ,  $****P < 0.0001$ ; Wilcoxon test).
- F *k* 5 mRNA PIs plotted against respective *GAPDH* PIs. The slope of the coloured lines represents the average *k* 5 mRNA/*GAPDH* PI ratio; the dashed grey line represents a 1:1 ratio ( $n \geq 28$  cells).
- G Top: distribution pattern of mRNAs clustered in *k* 2, *k* 5, *k* 7 and *GAPDH*. Bottom: smFISH co-detection of exemplar *k* 7/*k* 2 mRNAs and *GAPDH* in subconfluent motile HUVECs.
- H PIs of *k* 7 mRNAs and *GAPDH* co-detected in HUVECs ( $n \geq 25$  cells;  $*P < 0.05$ ,  $**P < 0.01$ ,  $***P < 0.001$ ; paired *t* test).
- I PIs of *k* 2 mRNAs and *GAPDH* co-detected in HUVECs ( $n \geq 19$  cells;  $*P < 0.05$ ; Wilcoxon test).

Data information: arrows indicate orientation of RNA localisation; yellow dashed lines outline cell borders; red circles highlight smFISH spots; scale bars = 20  $\mu\text{m}$  (D, G). Bar charts are presented as means  $\pm$  s.d.



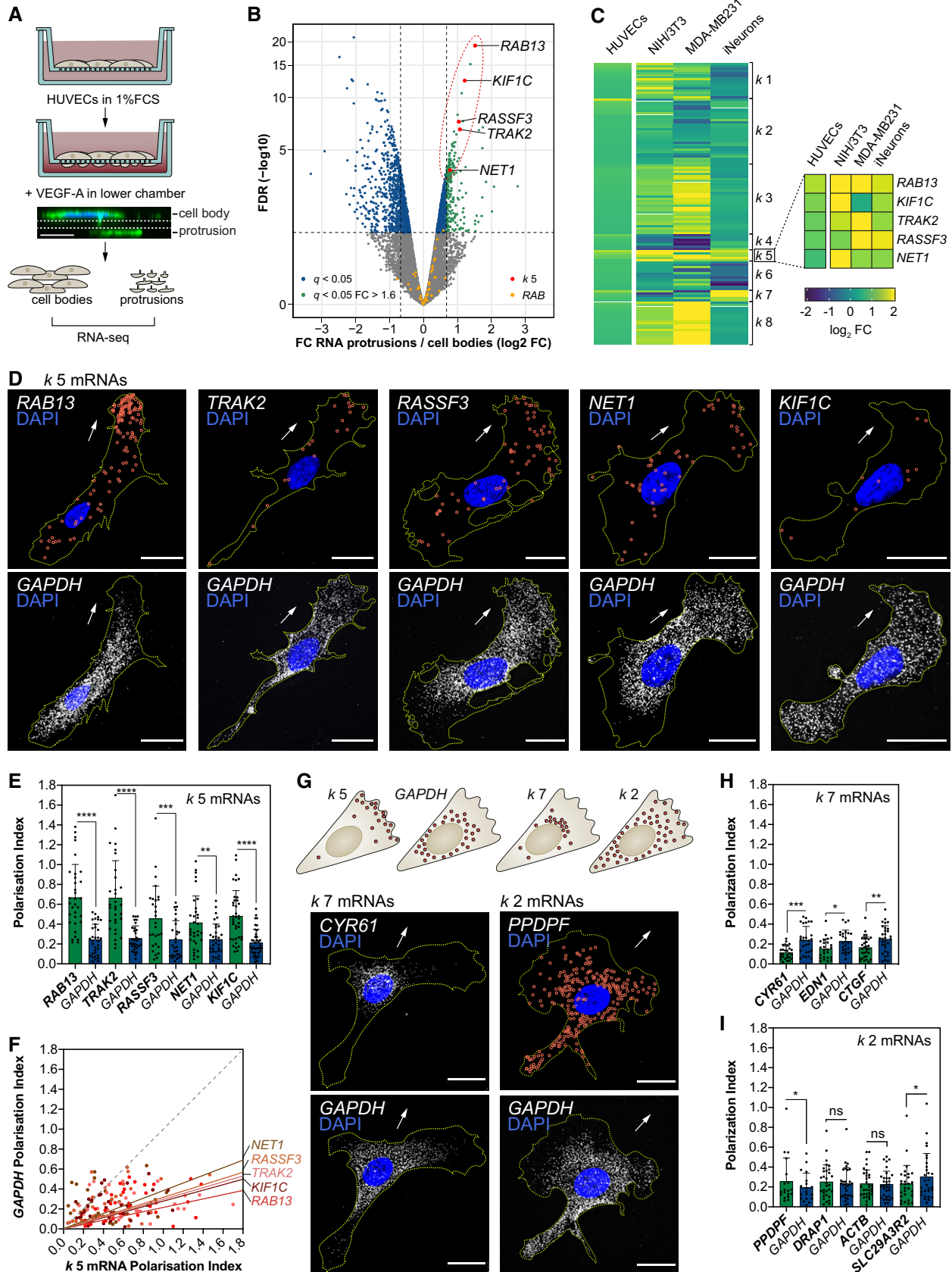


Figure 1.

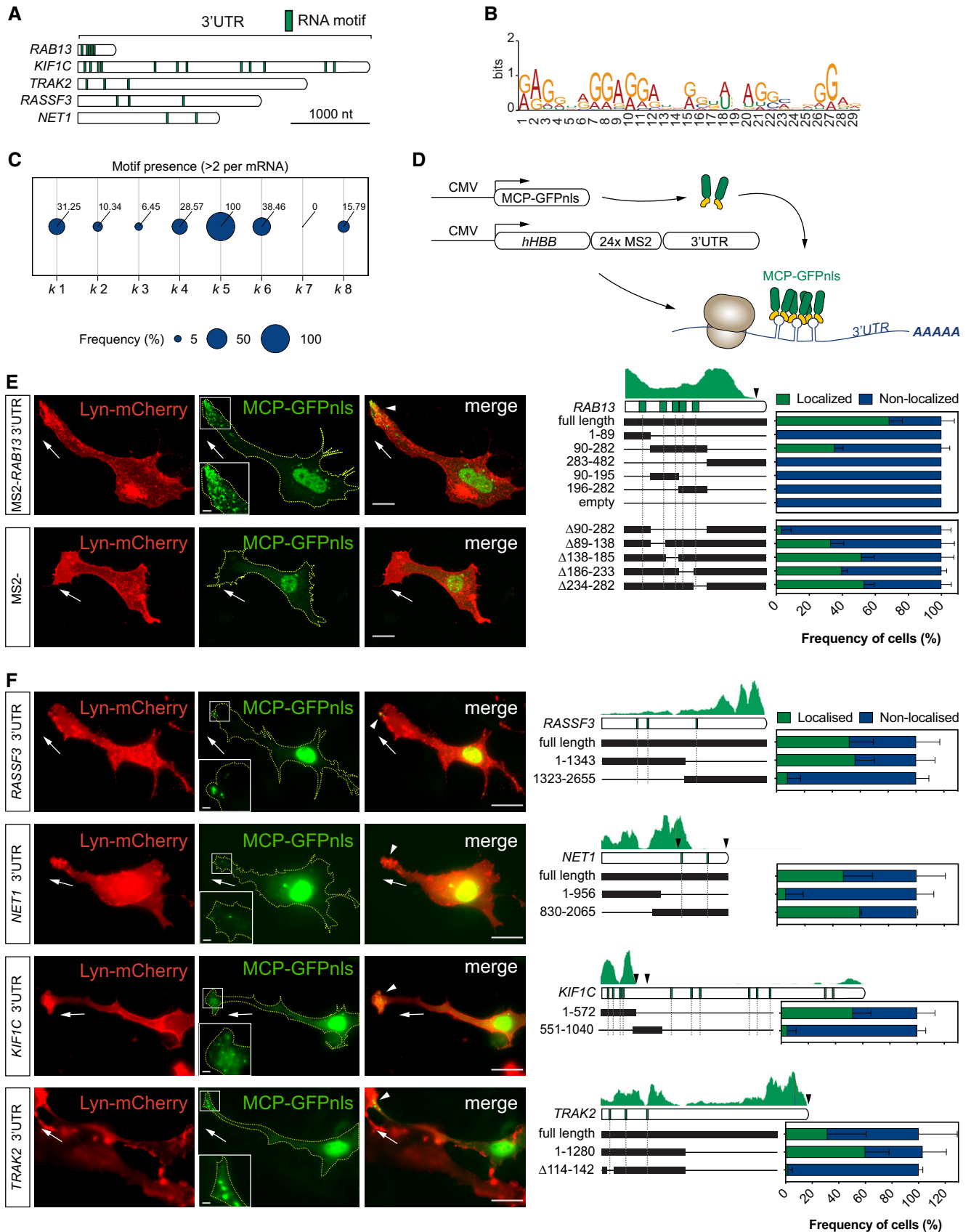


Figure 2.

**Figure 2. Clustering of RNAseq datasets defines an RNA motif enriched in 3'UTR sequences that target *k* 5 mRNAs to protrusions.**

- A Diagram of *k* 5 mRNA 3'UTRs and relative positions of the RNA motif shared between transcripts.  
 B RNA motif over-represented in *k* 5 mRNA 3'UTRs.  
 C Frequency of mRNAs within each *k*-means cluster containing at least 2 of the RNA motif over-represented in *k* 5 mRNAs.  
 D Scheme depicts the *in vitro* MS2 system strategy. CMV promoter-driven expression of MCP-GFPnls and *hHBB*-24xMS2-tagged *RAB13* 3'UTR. The visualisation of MCP-GFPnls bound to 24xMS2 allows the identification of the minimal region in the 3'UTR of *RAB13* necessary for its localisation.  
 E Left: representative subconfluent motile cells co-transfected with plasmids expressing Lyn-mCherry, MCP-GFPnls and 24xMS2-*RAB13* 3'UTR or 24xMS2. Right: percentage of cells with MCP-GFPnls localised to protrusions when co-transfected with full length or deletion versions of *RAB13* 3'UTR ( $n \geq 3$  experiments).  
 F Left: representative cells co-transfected with plasmids expressing Lyn-mCherry, MCP-GFPnls and 24xMS2-*k* 5 3'UTRs. Right: percentage of cells with MCP-GFPnls localised to protrusions when co-transfected with full length or deletion versions of *k* 5 3'UTR ( $n \geq 3$  experiments).

Data information: white arrowheads indicate non-nuclear localisation of MCP-GFPnls; arrows indicate the orientation of RNA localisation; yellow dashed lines outline cell borders; scale bars = 20  $\mu$ m (E, F); scale bars in insets = 5  $\mu$ m (E) and 2  $\mu$ m (F). For each *k* 5 mRNA 3'UTR, a diagram of the full-length 3'UTR and the positions of the RNA motif is shown together with the respective RNAseq mapped reads from HUVEC protrusions; black arrowheads indicate predicted polyadenylation sites (E, F). Bar charts are presented as means  $\pm$  s.d.

striking in its clustering as five repeats within a short 3'UTR region of *RAB13*, a known polarised mRNA (Mili *et al*, 2008; Jakobsen *et al*, 2013; Moissoglu *et al*, 2019) (Fig 2A). To interrogate its function, we tagged the non-localising human *HBB* coding sequence with both the *RAB13* 3'UTR and the reporter MS2 hairpin repeats (Bertrand *et al*, 1998; Mili *et al*, 2008; Fig 2D). Following co-expression with the MS2 capping protein (MCP)-GFPnls that is usually confined to the nucleus (Fusco *et al*, 2003), the localisation of MS2-tagged mRNAs can be monitored through changes to the spatial distribution of the GFP signal (Fig 2D). Potential localisation properties of the motif-containing *RAB13* 3'UTR were confirmed upon expression of the MS2 reporter system in ECs (Fig 2E). Using this approach in combination with truncations or deletions of the *RAB13* 3'UTR, we identified a minimal 192-nt LE encompassing four motif repeats that was both necessary and sufficient to exclusively polarise mRNA at motile EC protrusions (region 90–282 in Fig 2E). Furthermore, similar truncation and deletion analysis of the remaining *k* 5 mRNAs confirmed that these transcripts employ common *cis*-regulatory mechanisms, as mRNA targeting ability was consistently reliant on motif-containing 3'UTR regions (Fig 2F). Indeed, precise deletion of a single motif in *TRAK2* was sufficient to entirely block mRNA targeting (Fig 2F). Of note, unlike *TRAK2*, more than two functional motifs were required to drive *RAB13* polarisation, as deletions of individual motifs were tolerated and constructs containing two motifs were insufficient to

drive *RAB13* mRNA localisation (Fig 2E). Hence, distinct cluster *k* 5 mRNAs may exhibit different minimal requirements for the number of motifs needed to drive targeting.

**CRISPR-Cas9 excision of the 3'UTR localisation element of *RAB13* disrupts mRNA targeting**

As *RAB13* was the only identified RAB small GTPase to exhibit such mRNA polarisation (Fig 1B), we hypothesised that the identified LE and targeting of the transcript were critical for *RAB13* protein function in motile cells. However, studies probing the precise function of endogenous polarised mRNAs in motile cells are currently lacking, predominantly due to difficulties identifying targeting motifs and the potential propensity for genomic manipulation to perturb transcript stability and/or translation. However, precise genomic excision of the *RAB13* minimal LE in ECs using CRISPR-Cas9 tools did not perturb *RAB13* mRNA or protein expression (Fig 3A–G). ECs were transfected with both a GFP-expressing plasmid and CRISPR-Cas9 ribonucleoprotein complexes targeting the 90–282-nt LE in exon 8 of *RAB13*, prior to expansion of GFP-expressing clones (Fig 3A). Clones were then selected for either biallelic deletion of the LE ( $\Delta$ LE) or presence of the full-length *RAB13* 3'UTR (Wt) (Fig 3B) and were sequenced to confirm specific deletion of the LE in mutated clones (Figs 3C and EV2A). Moreover, RNAseq analysis verified that overall splicing of *RAB13*

**Figure 3. CRISPR-Cas9 excision of the 3'UTR localisation element of *RAB13* disrupts mRNA targeting.**

- A CRISPR-Cas9 strategy to derive HUVECs with an excision of the LE in the *RAB13* 3'UTR ( $\Delta$ LE) and parallel generation of wild-type (Wt) control cells. The Wt *RAB13* exon 8 is represented with its coding sequence in dark and the 3'UTR in clear boxes. The 5' and 3' gRNA-targeted regions are represented with green lines. Arrows: relative positions of the forward (*f*) and reverse (*r*) PCR primers used to identify HUVECs with CRISPR-Cas9-mediated excision of the LE.  
 B Representative genotyping PCR demonstrates the band size shift in  $\Delta$ LE HUVECs.  
 C Detailed DNA sequence depicting nucleotide positions within the *RAB13* 3'UTR of Wt and  $\Delta$ LE HUVECs.  
 D Wt and  $\Delta$ LE HUVEC RNAseq mapped reads depicting *RAB13* exon usage.  
 E Quantification of *RAB13* mRNA smFISH spot number in Wt and  $\Delta$ LE HUVECs ( $n = 3$  experiments; ns: not significant; unpaired *t* test).  
 F Number of *RAB13* mRNA smFISH spots plotted against the respective Polarisation Index (PI) ( $n = 29$  cells; ns: not significant; linear regression).  
 G Left: representative Western blotting (WB) of Wt and  $\Delta$ LE HUVECs. Right: densitometry analysis of WB data ( $n = 3$  samples; ns: not significant; unpaired *t* test).  
 H smFISH co-detection of *RAB13* and control *GAPDH* in Wt and  $\Delta$ LE motile HUVECs cultured under subconfluent conditions.  
 I PI of *RAB13* and *GAPDH* co-detected in Wt and  $\Delta$ LE HUVECs ( $n = 29$  cells; \*\*\* $P < 0.001$ , ns: not significant; Mann–Whitney test).  
 J *RAB13* PI plotted against respective *GAPDH* PI. The slope of the coloured lines represents the average *RAB13*/*GAPDH* PI ratio; the dashed grey line represents a 1:1 ratio ( $n = 29$  cells).

Data information: 3 Wt and 3  $\Delta$ LE HUVECs independent clones were used to collect data (E–J). Arrows indicate orientation of RNA localisation; yellow dashed lines outline cell borders; red circles highlight smFISH spots; scale bars = 20  $\mu$ m (H). Bar charts are presented as means  $\pm$  s.d. Source data are available online for this figure.

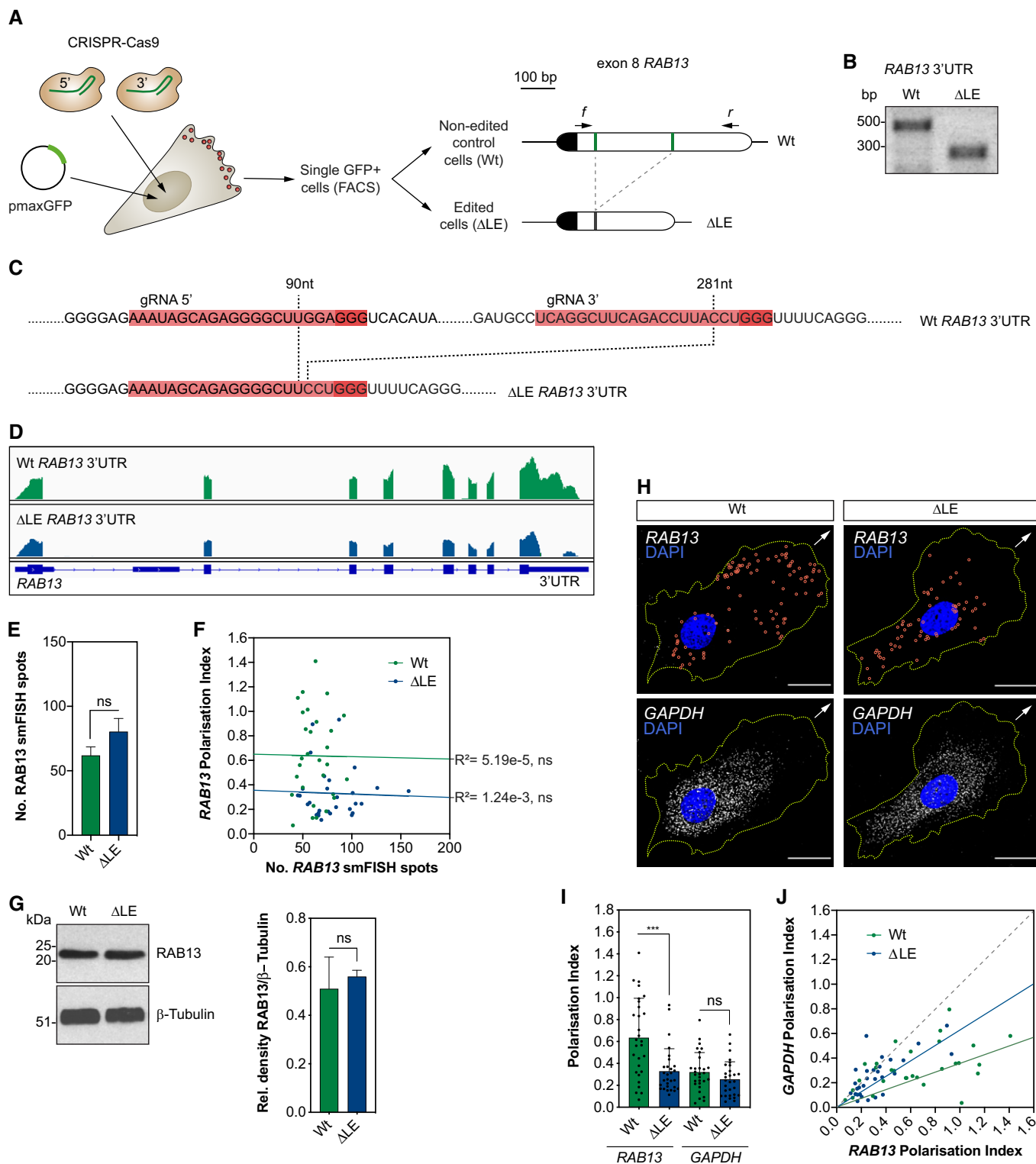
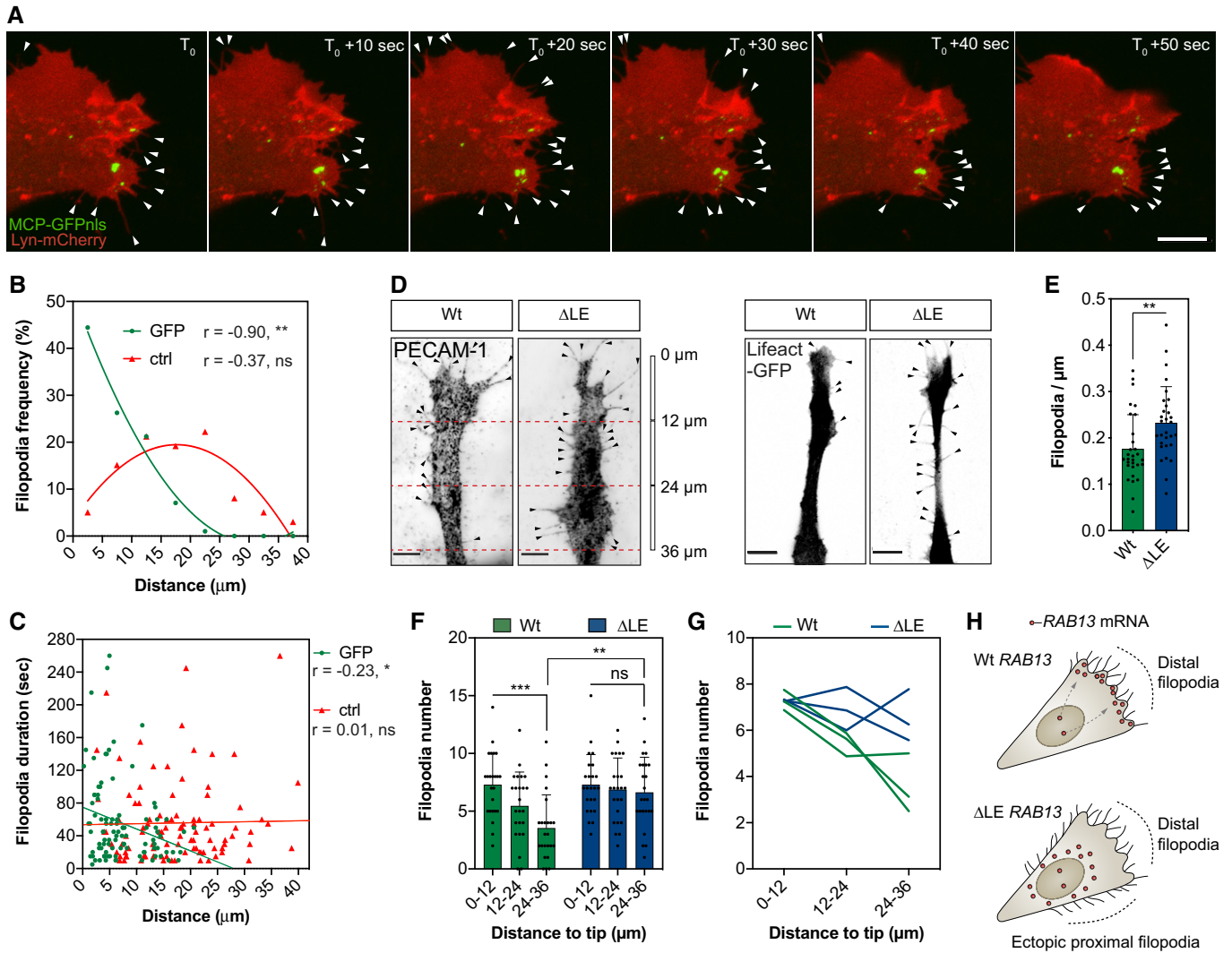


Figure 3.

mRNA was unaffected by genomic excision of the LE (Fig 3D) and confirmed the high specificity of these CRISPR-Cas9 tools, as no nucleotide mismatches were observed at any putative low-frequency off-target sites (Fig EV2B). Importantly, excision of the LE did not perturb *RAB13* mRNA levels or protein expression

(Fig 3E–G), but did eradicate the polarised spatial pattern of *RAB13* localisation, such that the transcript became diffusely distributed in ECs similar to *GAPDH* (Fig 3H). In particular, quantification of the PI of co-detected *RAB13* and *GAPDH* mRNAs revealed that loss of the LE consistently reduced *RAB13*



**Figure 4. RAB13 mRNA polarisation spatially orients filopodia dynamics.**

A Representative time-lapse microscopy of a bEnd.3 cell co-transfected with plasmids expressing Lyn-mCherry, MCP-GFPnls and 24xMS2-RAB13 3'UTR.  
 B Frequency of newly formed filopodia formed within 5-µm intervals relative to the nearest MCP-GFPnls particle or a randomised (ctrl) position ( $n = 99$  filopodia;  $**P < 0.01$ , ns: not significant; Pearson's  $r$  correlation).  
 C Distance of newly formed filopodia to MCP-GFPnls or a ctrl position plotted against filopodia duration ( $n = 99$  filopodia;  $*P < 0.05$ , ns: not significant; Spearman's  $r$  correlation).  
 D Wt and  $\Delta$ LE HUVECs co-cultured on fibroblast monolayers. Endothelial cells were identified either with an antibody against the endothelial cell marker PECAM-1 (left) or through expression of a nucleofected plasmid encoding the cytoskeletal marker Lifeact-GFP (right).  
 E Number of filopodia detected in co-cultured HUVECs ( $n = 30$  cells;  $**P < 0.01$ ; unpaired  $t$  test).  
 F Number of filopodia detected in co-cultured HUVECs within 12-µm intervals relative to cell distal tip ( $n = 30$  cells;  $**P < 0.01$ ,  $***P < 0.001$ , ns: not significant; one-way ANOVA with Bonferroni's correction).  
 G Number of filopodia detected in individual clones of co-cultured HUVECs within 12-µm intervals relative to cell distal tip.  
 H Illustration of the spatial relationship between RAB13 mRNA localisation and sites of filopodia production.

Data information: 3 Wt and 3  $\Delta$ LE HUVECs independent clones were used to collect data (D–G). Arrowheads indicate filopodia (A, D); scale bars = 10 µm (A) and 6 µm (D). Bar charts are presented as means  $\pm$  s.d.

polarisation to levels equivalent to GAPDH controls (Fig 3I and J). Finally, correlation of RAB13 mRNA spot count versus RAB13 mRNA PI revealed that mRNA polarisation is actually independent of total mRNA levels and further confirmed that it is perturbed upon excision of the LE (Fig 3F). Hence, genomic excision of the 3'UTR LE specifically perturbs RAB13 mRNA polarisation.

**RAB13 mRNA polarisation spatially orients filopodia dynamics**

RAB13 is an established modulator of cortical F-actin crosslinking and cytoskeletal remodelling at leading front of migrating cells, via interaction with its effector protein, MICAL-L2 (Sakane et al, 2012, 2013; Ioannou et al, 2015). Consistent with this function, live-cell

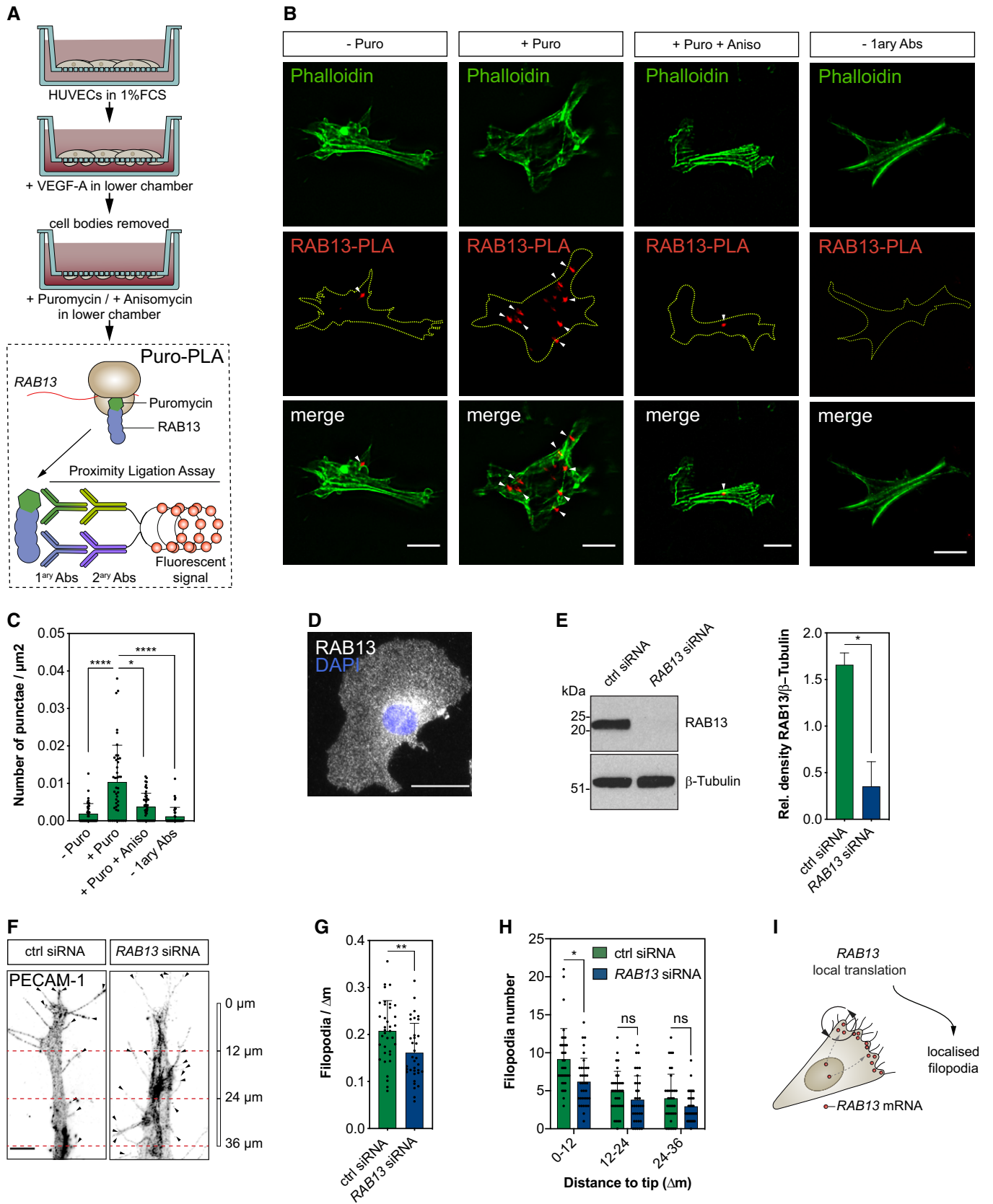


Figure 5.

**Figure 5. mRNA polarisation achieves spatial compartmentalisation of RAB13 translation and protein function.**

- A Strategy used to detect local protein synthesis in protrusions formed by HUVECs migrating through Transwell membranes.
- B Representative Puro-PLA experiments detecting newly synthesised RAB13 in HUVEC protrusions present in the lower side of Transwell membranes. Puro: puromycin; Aniso: anisomycin; 1ary Abs: primary antibodies.
- C Quantification of RAB13 Puro-PLA punctae normalised to protrusion area ( $n \geq 40$  protrusions;  $*P < 0.05$ ,  $****P < 0.0001$ ; Kruskal–Wallis test with Dunn's correction).
- D Representative RAB13 IF assay on migrating HUVECs.
- E Left: representative Western blotting (WB) of siRNA-transfected HUVECs. Right: densitometry analysis of WB data ( $n = 3$  samples;  $*P < 0.05$ ; paired t test).
- F Control (ctrl) and RAB13 siRNA-treated HUVECs co-cultured on fibroblast monolayers. Endothelial cells were identified with an antibody against the endothelial cell marker PECAM-1.
- G Number of filopodia detected in co-cultured HUVECs ( $n \geq 35$  cells;  $**P < 0.01$ ; unpaired t test).
- H Number of filopodia detected in co-cultured HUVECs within 12- $\mu\text{m}$  intervals relative to cell distal tip ( $n \geq 35$  cells;  $*P < 0.05$ , ns: not significant; Kruskal–Wallis test with Dunn's correction).
- I Illustration of the spatial relationship between the sites of RAB13 mRNA localisation, local translation and RAB13 protein-mediated filopodia distribution.

Data information: white arrowheads indicate Puro-PLA punctate; yellow dashed lines outline protrusion borders (B); black arrowheads indicate filopodia (F); scale bars = 10  $\mu\text{m}$  (B, D) and 6  $\mu\text{m}$  (F). Bar charts are presented as means  $\pm$  s.d.

Source data are available online for this figure.

imaging of RAB13 3'UTR dynamics employing MS2 reporter constructs revealed enriched targeting of mRNA to sites of incipient filopodia formation in cell protrusions, suggesting a tight spatial coupling between RAB13 mRNA localisation and RAB13 protein activity (Fig 4A–C and Movie EV1). Furthermore, quantification revealed that filopodia preferentially emerged in close proximity to GFP particles transported by the RAB13 3'UTR reporter, but not with random cytoplasmic spot positions (Fig 4B). In addition, there was a putative causal relationship between RAB13 mRNA proximity and increased filopodia stability (Fig 4C). Likewise, induction of cell migration drove a significant increase in the levels and polarisation of RAB13 mRNA *in vitro* (Fig EV3), further indicating a dynamic involvement in leading-edge remodelling and establishment of cell polarity. Hence, these data revealed that polarisation of RAB13 mRNA may spatially compartmentalise RAB13-mediated F-actin remodelling to orient motile cell polarity. Consistent with this hypothesis, loss of RAB13 mRNA polarisation—but not loss of expression—was indeed sufficient to depolarise filopodia dynamics in motile ECs (Fig 4D–G). When co-cultured with fibroblasts to mimic polarised blood vessel sprouting (Hetheridge *et al*, 2011), Wt ECs exhibited highly polarised filopodia extensions biased towards the leading edge of motile cells (Fig 4D and F). In contrast, filopodia in ECs lacking the RAB13 LE ( $\Delta\text{LE}$ ) were no longer spatially compartmentalised and became ectopically homogeneously distributed along the distal–proximal cell axis (Fig 4D and F). Importantly, these observations were consistent between individual Wt and  $\Delta\text{LE}$  CRISPR-Cas9 clones (Fig 4G). Consequently, mutant ECs exhibited a significant increase in overall filopodia frequency (Fig 4E). Hence, these data indicate that tight control of RAB13 mRNA localisation spatially specifies a polarised domain of filopodia extension in motile cells (Fig 4H).

### mRNA polarisation achieves spatial compartmentalisation of RAB13 translation and protein function

These striking observations suggested that RAB13 mRNA polarisation acts to exclusively spatially compartmentalise RAB13-mediated filopodia extension at distal sites. As such, targeting of RAB13 mRNA and local translation could effectively block ectopic protein function at inappropriate subcellular loci to orient motile cells. However, this could only be achieved if the sites of RAB13 mRNA localisation, translation and protein function were all

tightly spatially coupled. Indeed, such coupling may be consistent with long-standing proposals that newly translated RABs form a discrete protein pool from mature RABs, potentially with distinct interaction partners (e.g. specific RAB escorting proteins and GDP dissociation inhibitors) and separate biological functions (Pfeffer *et al*, 1995; Shen & Seabra, 1996; Seabra *et al*, 2002). Hence, local translation of polarised RAB13 transcript may generate nascent protein with distinct functional roles to mature RAB13 at specific subcellular sites, thus achieving tight spatial compartmentalisation of RAB13-mediated membrane remodelling. As predicted, such coupling of polarised RAB13 mRNA localisation with local translation was confirmed in EC protrusions upon detection of nascent protein using puromycinilation-proximity ligation assays (Puro-PLA) (tom Dieck *et al*, 2015). ECs were cultured on Transwells and cell bodies removed prior to pulse labelling with puromycin to exclude detection of nascent proteins transported from the cell body to protrusions (Fig 5A). Isolated EC protrusions readily incorporated puromycin, which could be blocked upon pre-incubation with the translation inhibitor anisomycin (Fig EV4), indicating active protein translation at the leading edge of migrating ECs. Importantly, Puro-PLA on isolated EC protrusions using antibodies recognising puromycin and RAB13 revealed numerous distinct punctae corresponding to newly synthesised RAB13, unlike anisomycin pre-treated and antibody-free controls (Fig 5B and C). Hence, polarised targeting of RAB13 mRNA to motile cell protrusions drives local RAB13 translation. Moreover, spatial control of mRNA polarisation and local translation was coupled to regional compartmentalisation of RAB13 protein function, as loss of endogenous RAB13 specifically disrupted filopodia dynamics only at distal sites of mRNA targeting (Fig 5E–H). The siRNA-mediated knockdown of RAB13 expression (Fig 5E) did not perturb RAB13-independent filopodia at proximal regions in ECs (Fig 5H), but significantly depleted filopodia numbers at distal sites, as is particularly obvious in Fig 5F. Consequently, ECs exhibited overall reduced numbers of filopodia upon RAB13 knockdown (Fig 5G). This was not simply a consequence of spatial targeting of protein to the leading edge, as immunofluorescence assays revealed that RAB13 was homogeneously distributed throughout migrating cells (Fig 5D), indicating that in contrast to the mRNA encoding it, RAB13 steady-state protein is not polarised. Alternatively, it was the location of RAB13 mRNA itself that defined the domain of RAB13-dependent filopodia dynamics, as excision of the LE and

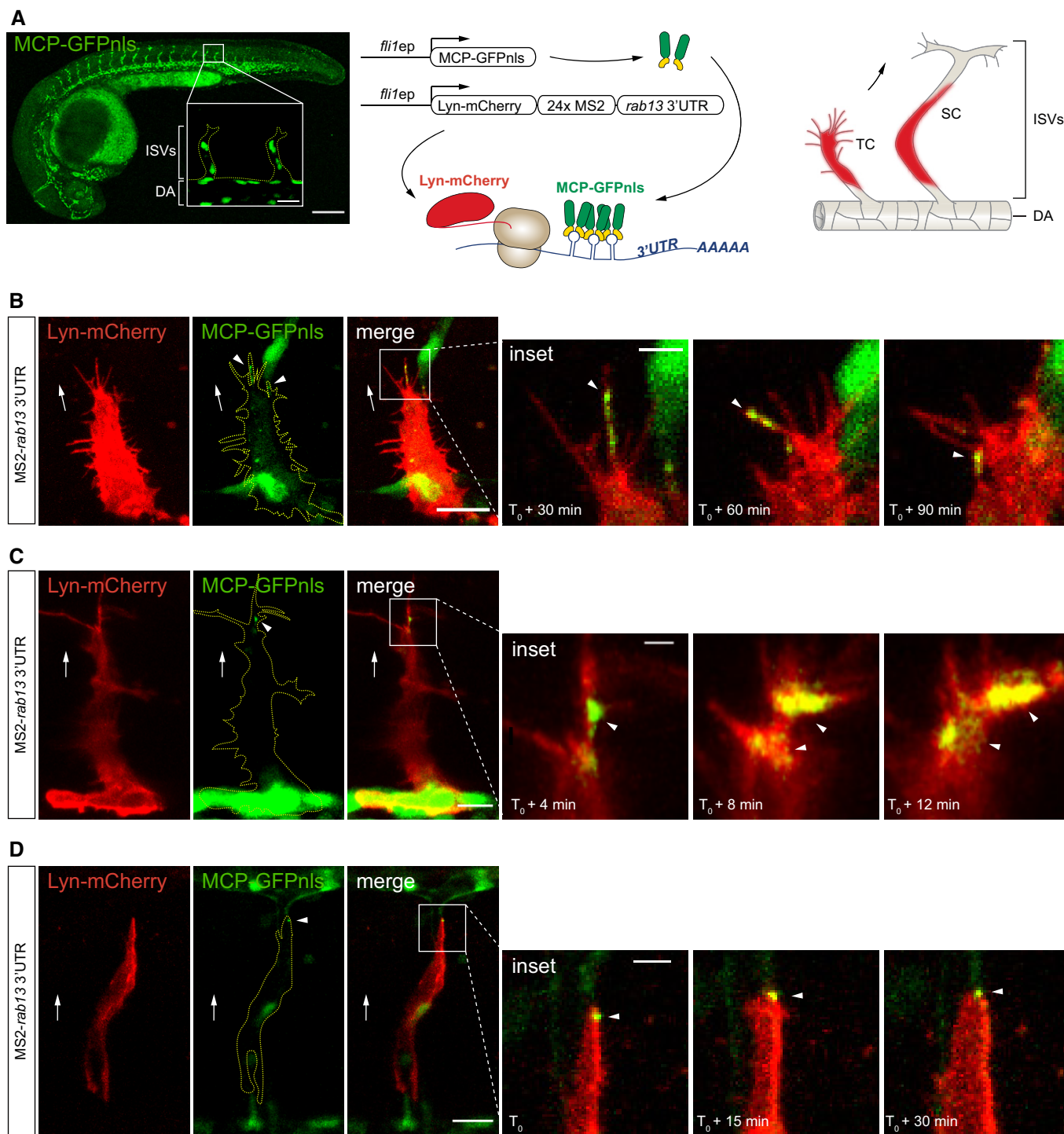


**Figure 6. The 3'UTR of *rab13* targets mRNA to endothelial cell protrusions *in vivo*.**

**A** Left: *Tg(fli1ep:MCP-GFPnls)* zebrafish embryo at 26 h post-fertilisation (hpf) displaying vascular-specific expression of MCP-GFPnls. Inset shows the nuclear expression of MCP-GFPnls in the intersomitic vessels (ISVs) sprouting from the dorsal aorta (DA). Middle: scheme depicts the *in vivo* MS2 system strategy with *fli1* enhancer/promoter (*fli1ep*)-driven expression of reporter constructs, simultaneous translation of Lyn-mCherry reporter and binding of MCP-GFPnls to 24xMS2-*rab13* 3'UTR. Right: scheme illustrates ISV cells expressing Lyn-mCherry imaged in panels B–D. TC: tip cell; SC: stalk cell.

**B–D** Time-lapse microscopy of *Tg(fli1ep:MCP-GFPnls)* tip and stalk cells displaying mosaic expression of Lyn-mCherry-24xMS2-*rab13* 3'UTR in ISV cells.

Data information:  $T_0 = 24$  hpf (C), 28 hpf (B), 48 hpf (D). Arrowheads indicate non-nuclear localisation of MCP-GFPnls; arrows indicate direction of ISV sprouting; yellow dashed lines outline ISV (A) or ISV cell (B–D) borders; scale bars = 200  $\mu$ m (A), 20  $\mu$ m (B, D) and 10  $\mu$ m (C); scale bars in insets = 20  $\mu$ m (A), 5  $\mu$ m (B, D) and 2  $\mu$ m (C).



diffuse mislocalisation of *RAB13* mRNA was sufficient to drive ectopic depolarised filopodia (Fig 4D–G). Hence, the site of *RAB13* mRNA localisation, translation and protein function appears to be tightly spatially coupled in migrating cells. Consequently,

polarisation of *RAB13* transcript forms a molecular compass that achieves precise subcellular compartmentalisation of protein function, defines a polarised domain of filopodia extension and ultimately orients motile cell polarity (Fig 5I).

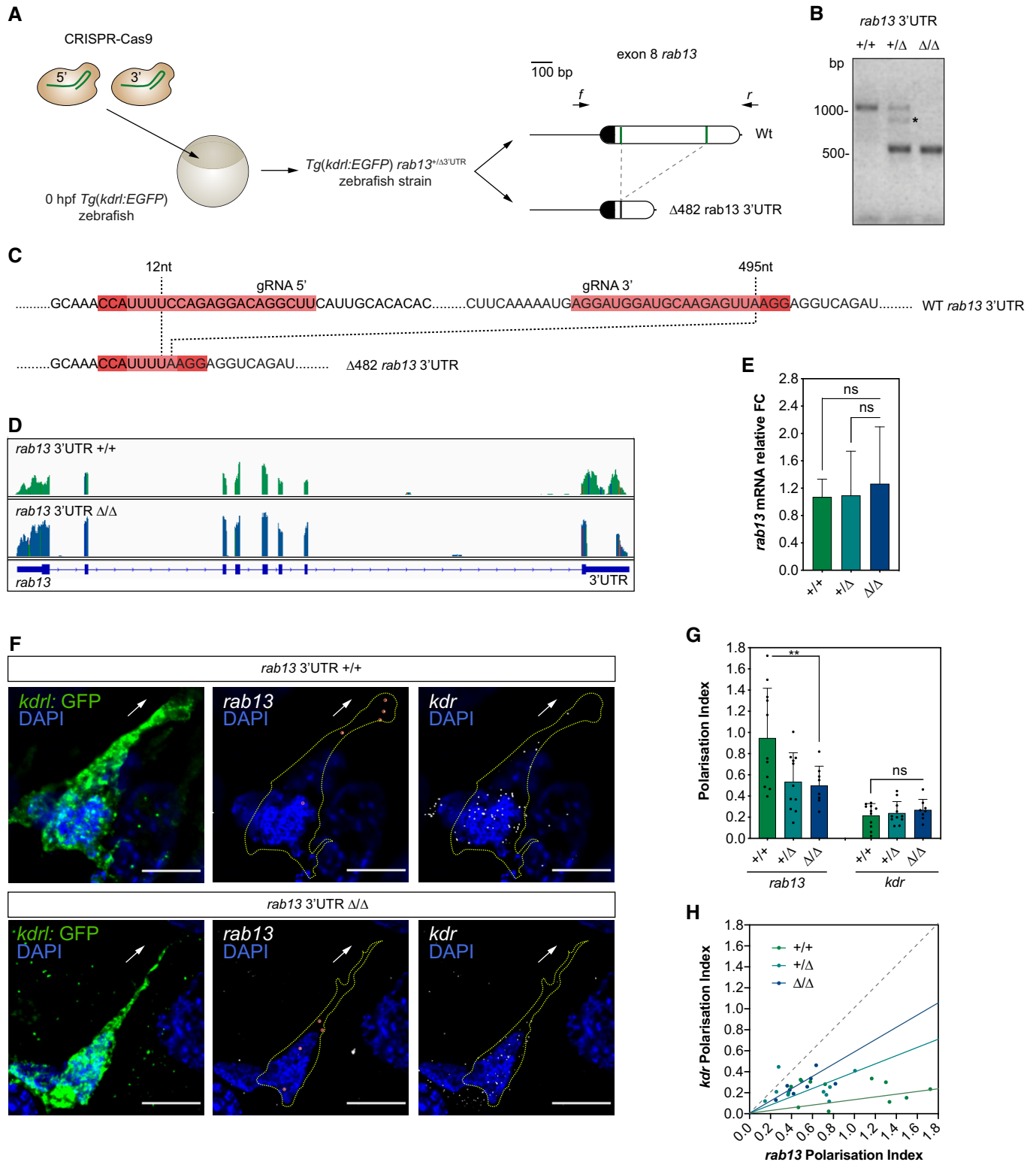


Figure 7.

**Figure 7. CRISPR-Cas9 editing of the zebrafish *rab13* 3'UTR perturbs mRNA polarisation.**

- A CRISPR-Cas9 strategy to generate the *Tg(kdrl:EGFP) rab13<sup>+/ $\Delta$ 3'UTR</sup>* zebrafish strain. The wild-type (Wt) *rab13* exon 8 is represented with its coding sequence in dark and the 3'UTR in clear boxes; the 5' and 3' gRNA-targeted regions are represented with green lines. Arrows: relative positions of the forward (f) and reverse (r) PCR primers used to identify animals with CRISPR-Cas9-mediated deletions ( $\Delta$ ) in the *rab13* 3'UTR.
- B Representative genotyping PCR demonstrates the band size shift in zebrafish harbouring a  $\Delta$ 482 *rab13* 3'UTR. Asterisk marks a heteroduplex formed between Wt and  $\Delta$ 482 *rab13* 3'UTR PCR amplicons.
- C Detailed DNA sequence depicting nucleotide positions within the Wt and  $\Delta$ 482 *rab13* 3'UTR.
- D RNAseq mapped reads depicting *rab13* exon usage in *Tg(kdrl:EGFP) rab13<sup>+/ $\Delta$ 3'UTR</sup>* and *rab13 <sup>$\Delta$ 3'UTR/ $\Delta$ 3'UTR</sup>* zebrafish embryos. Coloured lines indicate SNPs.
- E qPCR analysis of *rab13* mRNA levels in individual 26–28 hpf clutch-matched sibling embryos ( $n \geq 9$  embryos; ns: not significant; Kruskal–Wallis test with Dunn's correction).
- F smFISH detection of *rab13* and *kdrl* mRNA in cultured GFP-expressing endothelial cells extracted from 48 hpf *Tg(kdrl:EGFP) rab13<sup>+/ $\Delta$ 3'UTR</sup>* and *rab13 <sup>$\Delta$ 3'UTR/ $\Delta$ 3'UTR</sup>* zebrafish embryos.
- G Polarisation Index (PI) of *rab13* and *kdrl* detected by smFISH in individual zebrafish cells ( $n \geq 8$  cells; \*\* $P < 0.01$ , ns: not significant; one-way ANOVA with Bonferroni's correction).
- H *rab13* PI plotted against respective *kdrl* PI. The slope of the coloured lines represents the average *rab13/kdrl* PI ratio; the dashed grey line represents a 1:1 ratio ( $n \geq 8$  cells).
- Data information: +/+, +/ $\Delta$  and  $\Delta/\Delta$  represent *Tg(kdrl:EGFP) rab13<sup>+/ $\Delta$ 3'UTR</sup>*, *rab13<sup>+/ $\Delta$ 3'UTR</sup>* and *rab13 <sup>$\Delta$ 3'UTR/ $\Delta$ 3'UTR</sup>* embryos, respectively (E, G, H). Arrows indicate orientation of RNA localisation; yellow dashed lines outline cell borders; red circles highlight smFISH spots; scale bars = 10  $\mu$ m (F). Bar charts are presented as means  $\pm$  s.d.

**The 3'UTR of *rab13* targets mRNA to endothelial cell protrusions *in vivo***

Although a widespread phenomenon, the functional role for localised mRNAs in tissue migration and vertebrate morphogenesis remains unexplored. Hence, having defined a key role for mRNA polarisation in the spatial control of EC behaviour *in vitro*, we then sought to define the broader relevance of this phenomenon to modulation of tissue dynamics *in vivo*. The production of polarised filopodia protrusions is a characteristic hallmark of motile endothelial tip cells, which lead new blood vessel branches during angiogenesis (Gerhardt *et al*, 2003; Isogai *et al*, 2003). As such, using live-cell imaging approaches in the zebrafish model system, we probed the function of *rab13* mRNA polarisation in the control of tip cell behaviour and angiogenesis *in vivo*. Firstly, we generated a novel vascular-specific MCP-GFPnls transgenic strain, *Tg(fli1ep:MCP-GFPnls)*, and monitored the targeting dynamics of a MS2-tagged *rab13* 3'UTR reporter during intersegmental vessel (ISV) angiogenesis (Isogai *et al*, 2003; Fig 6A). Dynamic accumulation of MCP-GFPnls adjacent to or within filopodia at the leading edge of ISV tip cells revealed that *rab13* mRNA localisation *in vivo* closely mirrored the 3'UTR-driven polarisation of human *RAB13* mRNA *in vitro* (Fig 6B and C; Movies EV2 and EV3). Thus, the targeting function of the *RAB13/rab13* 3'UTR is highly conserved, despite rather low sequence conservation (Fig EV5B and C). Importantly, polarised localisation of MCP-GFPnls was not observed in the absence of the MS2-tagged *rab13* 3'UTR (Fig EV5A), confirming the presence of LEs within this region. Moreover, the polarised targeting of *rab13* mRNA was retained in less-motile ISV stalk cells, which trail tip cells, although at less dynamic and more discrete foci (Fig 6D; Movie EV4). Hence, the polarised targeting of *RAB13/rab13* mRNA in motile cells is highly conserved between species and in tissues.

**CRISPR-Cas9 editing of the zebrafish *rab13* 3'UTR perturbs mRNA polarisation**

Next, we sought to determine whether *rab13* mRNA localisation *in vivo* is functionally implicated in blood vessel spouting. Similar to *in vitro* experiments, we performed CRISPR-Cas9-mediated

excision of a fragment within the *rab13* 3'UTR locus ( $\Delta$ 3'UTR) to further confirm the presence of LEs and their potential role in *rab13* mRNA polarisation *in vivo*. Microinjection of zebrafish embryos with CRISPR-Cas9 ribonucleoprotein complexes targeting exon 8 of *rab13* was sufficient to generate germline *rab13 <sup>$\Delta$ 3'UTR/ $\Delta$ 3'UTR</sup>* mutants lacking 482-nt of the *rab13* 3'UTR, as confirmed by sequencing (Figs 7A–C and EV2C). Additional RNAseq analysis of mutant embryos verified that overall splicing of *rab13* mRNA was unaffected by genomic excision of the LE (Fig 7D) and confirmed the high specificity of CRISPR-mediated excision, as no nucleotide mismatches were observed at any putative low-frequency off-target sites (Fig EV2D). Moreover, genomic excision of the *rab13* LE had no effect on mRNA levels (Fig 7E), although protein levels could not be tested due to a lack of good antibodies against zebrafish Rab13. Importantly, smFISH applied to explanted endothelial cells from dissociated *rab13 <sup>$\Delta$ 3'UTR/ $\Delta$ 3'UTR</sup>* mutant embryos confirmed that *rab13* mRNAs lacking these LEs were more diffusely distributed (Fig 7F–H), similar to observations in human ECs (Fig 3H–J). In contrast, control *kdrl* mRNAs displayed unperturbed PI measurements in *rab13* mutant versus Wt ECs (Fig 7F and G). Hence, we reveal a previously unappreciated and conserved role for 3'UTR LEs in the dynamic polarisation of *rab13* mRNA during cell migration.

***rab13* mRNA polarisation orients blood vessel morphogenesis**

During ISV branching, migrating tip cells must make key directional decisions, particularly when negotiating the multi-tissue junction of the horizontal myoseptum (Lu *et al*, 2004; Torres-Vazquez *et al*, 2004; Lamont *et al*, 2009) (HM; Fig EV5D). Hence, we hypothesised that mRNA localisation-mediated orientation of EC filopodia may indeed generate spatial cues that direct vascular tissue movement. Consistent with a key role for mRNA polarisation in the spatial coordination of vascular morphogenesis, live-cell imaging of ISVs branching in Wt and *rab13 <sup>$\Delta$ 3'UTR/ $\Delta$ 3'UTR</sup>* embryos revealed that loss of *rab13* polarisation severely perturbed tip cell path-finding decisions (Fig 8A and B). Unlike ISVs in Wt and *rab13<sup>+/ $\Delta$ 3'UTR</sup>* embryos that efficiently negotiated their way past the HM position, ISVs in *rab13 <sup>$\Delta$ 3'UTR/ $\Delta$ 3'UTR</sup>* mutants struggled with this directional decision,

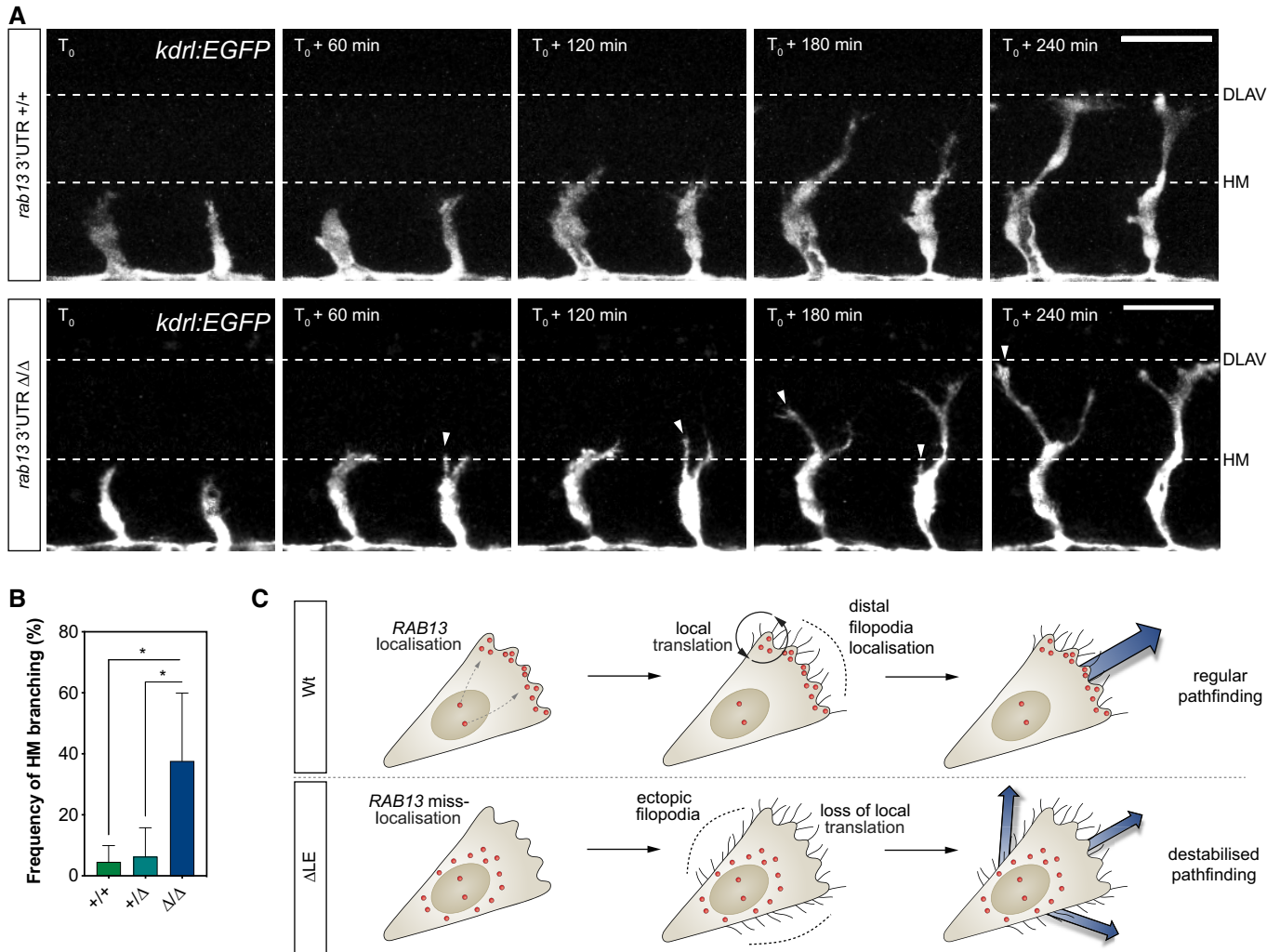


**Figure 8. *rab13* mRNA polarisation orients blood vessel morphogenesis.**

**A** Time-lapse confocal microscopy of representative *Tg(kdrl:EGFP) rab13<sup>+/+</sup>* and *rab13<sup>Δ3'UTR/Δ3'UTR</sup>* embryos. DLAV: dorsal longitudinal anastomotic vessel; HM: horizontal myoseptum.

**B** Frequency of ISV ectopic branching occurring at the HM ( $n = 4$  experiments;  $*P < 0.05$ ; one-way ANOVA with Bonferroni's correction).

**C** Illustration of the role for *RAB13* mRNA localisation, local translation and compartmentalisation of *RAB13* function in defining the orientation of EC filopodia dynamics, motile EC polarity and blood vessel pathfinding.

Data information:  $T_0 = 25$  hpf; arrowheads indicate extra branches emerging from the main ISVs at the HM position; scale bars = 50  $\mu$ m (A).  $+/+$ ,  $+/\Delta$  and  $\Delta/\Delta$  represent *Tg(kdrl:EGFP) rab13<sup>+/+</sup>*, *rab13<sup>+/\Delta3'UTR</sup>* and *rab13<sup>Δ3'UTR/Δ3'UTR</sup>* embryos, respectively (B). Bar chart is presented as means  $\pm$  s.d.

resulting in a sevenfold increase in tip cells exhibiting ectopic misdirected branches (Fig 8A and B). Of interest, *rab13<sup>Δ3'UTR/Δ3'UTR</sup>* mutants were viable with no detectable gross defects in other embryonic or vascular tissues, indicating a highly specific ISV phenotype. More importantly, *rab13* mRNA stability was unperturbed in *rab13<sup>Δ3'UTR/Δ3'UTR</sup>* mutant embryos (Fig 7E), indicating that observed defects were not due to decreased *rab13* expression but a consequence of perturbed mRNA localisation. Thus, we provide the first *in vivo* evidence that spatial targeting of mRNAs and precise compartmentalisation of protein function generate key directional cues that orient motile cells during vertebrate tissue morphogenesis (Fig 8C).

## Discussion

Whilst it is well established that numerous transcripts are targeted to the leading protrusions of motile cells (Herbert & Costa, 2019), how this regulates translated protein function, its importance for cell migration and the *in vivo* relevance of this phenomenon are poorly understood. Here, using gene editing to modulate subcellular mRNA targeting, we reveal that tight spatial coupling of mRNA localisation, translation and protein function achieves precise subcellular compartmentalisation of protein action and prevents ectopic protein functionality at inappropriate subcellular loci. We find that such mRNA-mediated spatial compartmentalisation of *RAB13* activity

serves to define a polarised domain of filopodia remodelling that orients motile cells. Moreover, using unique tissue-specific reporters of mRNA localisation in intact vertebrates, alongside gene editing, we uncover a key role for *rab13* mRNA localisation in the coordination of cell pathfinding during tissue morphogenesis. Hence, we define mRNA polarisation as a novel paradigm for the spatial control of motile cell polarity and oriented tissue movement *in vivo*.

Moreover, our findings lend weight to recent observations that newly synthesised protein can have a distinct functionality to pre-existing protein (Kim *et al*, 2020). Considering that steady-state RAB13 protein is homogeneously distributed in migrating ECs, our work indicates that nascent protein must have distinct functional properties to the mature protein pool that enables tight spatial coupling of *RAB13* translation and local filopodia remodelling. Indeed, in a parallel study published back-to-back with our work, Moissoglu *et al* (2020) show that nascent RAB13 co-translationally interacts with its exchange factor, RABIF, to drive local activation of newly synthesised protein in MDA-MB-231 cells. In their report, Moissoglu *et al* (2020) demonstrate that modulation of mRNA localisation using antisense oligonucleotides did not disrupt *RAB13* expression, translation or steady-state protein localisation, but shifted the site and levels of co-translational RAB13 activation. Consequently, spatial manipulation of *RAB13* mRNA targeting fundamentally defined the location of RAB13 protein action and perturbed cell protrusion in migration. Hence, the work by Moissoglu *et al* (2020) provides a convincing mechanistic basis for how *RAB13* localisation ultimately orients motile cell polarity and tissue movement *in vivo*, via precise spatial control of co-translational interactions with exchange factors that define the site of GTPase activation.

Considering that *RAB13* is one of only five mRNAs exhibiting conserved polarisation in all cell types tested, the function of *RAB13* mRNA targeting may be a universally conserved mechanism for spatial coordination of complex morphogenetic events. Moreover, it is striking that all five-cluster *k* 5 mRNAs encode highly dynamic membrane trafficking and/or small GTPase-regulating proteins, all known to modulate cell motility. Hence, for classes of proteins normally constant in motion, mRNA polarisation may be essential to spatially compartmentalise and precisely fix their site of function. It is tempting to speculate that cluster *k* 5 mRNA co-targeting and localised translation may participate in a coordinated effort to modulate actin dynamics and/or membrane protrusion at the leading edge. As such, perturbation of the localisation mechanisms that transport *RAB13* and other cluster *k* 5 mRNAs may be expected to generate a more acute phenotype than perturbation of *RAB13* targeting alone. Indeed, other studies have provided evidence that mRNAs sharing subcellular compartments can encode subunits of common protein complexes involved in actin remodelling (Mingle *et al*, 2005) or components of related chemotaxis pathways (Hotz & Nelson, 2017). Nevertheless, the functional role of mRNA co-localisation in the context of cell migration remains largely elusive. As ever-increasing technological advances continue to unveil the nature of compartmentalised transcriptomes, this will shed further light on the patterns of co-localised mRNAs (Eng *et al*, 2019; Xia *et al*, 2019) and protein synthesis (Chouaib *et al*, 2020) that likely underpin key events directing cell migration.

Whilst it is well established that polarised trafficking of *RAB13* and other cluster *k* 5 mRNAs are attributed to their interaction with APC, a microtubule plus-end associated protein that escorts mRNAs

to the leading edge of motile cells (Mili *et al*, 2008; Wang *et al*, 2017), the function of APC itself in cell migration is unclear. Despite reports on the importance of APC for EC migration (Harris & Nelson, 2010), knockdown of APC does not impact protrusion formation during migration in all cell types (Mili *et al*, 2008). Yet, from our work and that of Moissoglu *et al* (2020), it is clear that the function of *RAB13* mRNA polarisation in the coordination of cell movement is itself conserved between distinct cell types and organisms. As such, a full explanation for the context dependency of APC function has yet to be defined, but may indicate differences in the mode of motility employed by distinct cell types, the types of dynamic protrusions employed (be they RAB13-dependent or not) or even hint at the use of currently unknown APC-independent mRNA transport mechanisms in cell migration.

Finally, this work reveals an unexpected spatial diversity to identified clusters of polarised mRNAs. Considering our observations that the sites of mRNA targeting and protein function are tightly coupled, this raises the exciting possibility that other distinct mRNA distributions, such as the perinuclear localisation of cluster *k* 7, reflect even broader functionalities for compartmentalised gene expression/function in the coordination of diverse aspects of tissue development, health and disease.

## Materials and Methods

### Zebrafish husbandry

Zebrafish were grown and maintained according to UK Home Office regulation guidelines, and all studies were approved by the University of Manchester Ethical Review Board.

### Embryo micro-injections and generation of zebrafish strains

To generate the transgenic zebrafish strain *Tg(fli1ep:MCP-GFPnls)* using Tol2 transposon transgenesis, 32 pg of Cerulean-H2B:bas*fli1ep:MCP-GFPnls* Tol2-based plasmid was co-injected with 32 pg Tol2 mRNA into one-cell stage AB zebrafish embryos. The next day, embryos with mosaic GFP expression were selected, raised to adulthood and then outbred to AB zebrafish to identify founders with germline transmission of the transgene. Adult *Tg(fli1ep:MCP-GFPnls)* were inbred, and one-cell stage embryos were co-injected with 32 pg of Cerulean-H2B:bas*fli1ep:Lyn-mCherry-24xMS2-rab13-3'UTR* Tol2-based plasmid and 32 pg Tol2 mRNA for mosaic expression analysis.

The mutant *rab13*  $\Delta 3'$ UTR strain was generated with CRISPR-Cas9 tools. One-cell stage *Tg(kdrl:EGFP)<sup>s843</sup>* embryos (Jin *et al*, 2005) were injected with 150 pg of each *in vitro* transcribed gRNA and co-injected with 150 pg Cas9 NLS nuclease (New England Biolabs). Embryos were raised to adulthood and outbred to AB zebrafish to identify founders with germline transmission deletions in the *rab13* 3'UTR. Heterozygous animals harbouring a 482-nucleotide deletion in the *rab13* 3'UTR (*Tg(kdrl:EGFP)<sup>s843</sup> rab13<sup>+/Δ3'UTR</sup>*) were in-crossed, and the resulting embryos were used for live-cell imaging analysis.

### gRNA generation and *in vitro* transcription

The online CRISPRscan tool (Moreno-Mateos *et al*, 2015) was used to design gRNAs targeting the zebrafish 3'UTR region in the

*rab13* locus (Table EV4) and to determine off-target loci. Next, 0.3  $\mu$ M oligonucleotides comprising the target sequences (flanked by the T7 promoter and the Tail annealing sequence) were mixed with 0.45  $\mu$ M Tail primer (Table EV4) and PCR-amplified with Platinum Pfx DNA Polymerase (Thermo Fisher Scientific) in a T100 thermal cycler (Bio-Rad). The following cycling conditions were used: 1 cycle of initial denaturation at 94°C for 10 min, 30 cycles of denaturation at 94°C for 30 s, annealing at 45°C for 30 s, extension at 68°C for 30 s and a final extension cycle at 68°C for 7 min. Subsequently, 200 ng of PCR-amplified templates was used to transcribe gRNAs using a MEGAshortscript T7 Transcription Kit (Thermo Fisher Scientific), following the manufacturer's recommendations.

To synthesise Tol2 mRNA, 1  $\mu$ g NotI-linearised pCS2-TP plasmid was transcribed using a SP6 mMMESSAGE mMACHINE kit (Thermo Fisher Scientific) according to the manufacturer's protocol.

### Embryo genotyping

Genomic DNA was extracted by incubating either whole embryos or embryo heads in lysis buffer (10 mM Tris-HCl pH 8, 1 mM EDTA, 80 mM KCl, 0.3% NP40, 0.3% Tween) containing 0.5  $\mu$ g/ $\mu$ l Proteinase K (Promega) at 55°C for 1–2 h, followed by a denaturation step at 95°C for 15 min in a T100 thermal cycler. Genotyping PCR was performed using 2  $\mu$ l genomic DNA, 0.4  $\mu$ M zebrafish genotyping primers (Fig 7A and Table EV4) and 1 $\times$  MyTaq Red DNA Polymerase (Bioline) according to the manufacturer's protocol in a T100 thermal cycler. PCRs were resolved in 1% agarose (Bioline) gels containing 0.5  $\mu$ g/ml ethidium bromide (Sigma) for analysis. PCR products were cloned into TOPO-TA vectors (Thermo Fisher Scientific) according to the manufacturer's protocol and analysed via Sanger sequencing on an ABI 3730 device.

### Cell culture, scratch wound and co-culture angiogenesis assays

Trunks of 26–48 hpf embryos were incubated in trypsin-EDTA solution (Sigma) at 28°C for 15 min. Trypsinisation was quenched with complete L-15 medium (Sigma) containing 10% foetal bovine serum (FBS, Sigma) and 10 U/ml–100  $\mu$ g/ml penicillin-streptomycin (Sigma). Cells were pelleted at 376 g for 5 min at room temperature (RT), resuspended in complete ECGM2 (PromoCell) and cultured on fibroblast-coated coverslips. Zebrafish cells were cultured in 24-well plates and maintained at 28°C for 18 h.

HUVECs (PromoCell) were cultured in complete ECGM2 (PromoCell) in gelatin-coated (Millipore) dishes. Human pulmonary fibroblasts (HPF; PromoCell) were cultured in M199 (Thermo Fisher Scientific) containing 10% FBS, 50  $\mu$ g/ml gentamycin (Sigma) and 50 ng/ml amphotericin (Sigma). Brain endothelial cells (bEnd.3 and bEnd.5) were cultured in DMEM (Sigma) supplemented with 10% FBS, 10 ng/ml recombinant human VEGF-A (PeproTech) and 10 U/ml–100  $\mu$ g/ml penicillin-streptomycin.

For scratch wound assays, HUVECs cultured on gelatin-coated coverslips were grown to confluence and used in scratch wound assays as described elsewhere (Liang *et al*, 2007).

Co-cultures of HUVEC and HPF and the corresponding siRNA-mediated knockdown experiments were performed as previously described by Hetheridge *et al* (2011).

### CRISPR-Cas9 cell editing and cell transfections

The online Alt-R CRISPR-Cas9 design tool (<https://eu.idtdna.com>) was used to design crRNAs targeting the RAB13 3'UTR locus and to determine off-target loci. HUVECs were transfected with Alt-R CRISPR-Cas9 ribonucleoprotein complexes (Integrated DNA Technologies) targeting the 90–282-nt localisation element within the 3'UTR. Briefly, each sequence-specific crRNA (Table EV4) was mixed with tracrRNA at 1:1 50  $\mu$ M, incubated at 95°C for 5 min in a T100 thermal cycler and allowed to cool to RT for 60 min. Next, 12  $\mu$ M each crRNA:tracrRNA (gRNA) was incubated with 20  $\mu$ M Alt-R Cas9 nuclease in PBS (Sigma) at RT for 20 min to form ribonucleoprotein complexes and mixed with 500  $\times$  10<sup>3</sup> HUVECs. Additionally, 2  $\mu$ g pmaxGFP Vector (Lonza) was included in the HUVEC-ribonucleoprotein mix to identify transfected cells. Transfections were performed in a Nucleofector 2b Device (Lonza), using a HUVEC Nucleofector Kit (Lonza) according to the manufacturer's instructions, and the cells were further cultured for 72 h. Afterwards, single GFP-expressing cells were isolated in a FACSria Fusion cell sorter (BD Biosciences) into gelatin-coated 96-well plates to grow individual clones. Genomic DNA was extracted from expanded HUVEC clones and PCR-analysed with sequence-specific primers (Fig 3A and Table EV4) as described for zebrafish embryo genotyping. Clones with either biallelic deletion of the localisation element ( $\Delta$ LE) or with the full-length RAB13 3'UTR (Wt) were maintained until passage 6, and three clones from each genotype were used for analysis.

Knockdown experiments were performed with ON-TARGETplus Non-targeting Control or RAB13 siRNAs (Horizon) using GeneFECTOR (VennNova) as previously described (Hetheridge *et al*, 2011).

For *in vitro* MS2 experiments, bEnd.3 or bEnd.5 cells were transfected with pcDNA3-Lyn-mCherry, pCS2-MCP-GFPnls and different versions of pcDNA3-HBB-24XMS2SL-RAB13 3'UTR. Briefly, 100  $\times$  10<sup>3</sup> cells/well cultured in 6-well plates were transfected with 0.5–1  $\mu$ g each plasmid DNA using Lipofectamine 2000 or Lipofectamine 3000 following the manufacturer's protocol (Thermo Fisher Scientific) and analysed 48 h later.

### Transwell assays and cell body/protrusion fractionation

Transwell experiments to segregate cell bodies and protrusions were performed as described elsewhere (Mili *et al*, 2008), with the following modifications: 1.5  $\times$  10<sup>6</sup> HUVECs were cultured for 2 h in 24-mm Transwells (Costar), containing 3- $\mu$ m-pore polycarbonate membranes, in M199 (Thermo Fisher Scientific) supplemented with 1% FBS. Subsequently, 25 ng/ml VEGF-A was added to the lower chambers to promote cell migration over the next hour. Whilst only 1 Transwell was used for the cell body fraction, 2 Transwells were used to harvest each HUVEC protrusion sample.

### RNA isolation, qPCR and RNAseq

Embryo and cell-derived RNA was isolated using a RNAqueous-Micro Kit (Thermo Fisher Scientific) according to the manufacturer's protocol. For gene expression analysis, cDNA was synthesised with a High-Capacity RNA-to-cDNA Kit (Thermo Fisher Scientific) following the manufacturer's protocol.

qPCR experiments were performed with 1–2  $\mu$ l cDNA, 0.25  $\mu$ M gene-specific primers (Table EV4) and 1 $\times$  Power SYBR Green Master

Mix (Thermo Fisher Scientific) in a StepOne Real-Time PCR System (Applied Biosystems). *GAPDH* expression was used to normalise gene expression levels, and the relative mRNA levels were analysed with the  $2^{-\Delta\Delta CT}$  method.

For RNAseq, quality and integrity of RNA samples obtained from HUVEC cell bodies and protrusions were assessed using a 2200 TapeStation (Agilent Technologies). Next, RNAseq libraries were generated using the TruSeq Stranded mRNA assay (Illumina) according to the manufacturer's protocol. Adapter indices were used to multiplex libraries, which were pooled prior to cluster generation using a cBot instrument. The loaded flow cell was then paired-end-sequenced (76 + 76 cycles, plus indices) on an Illumina HiSeq 4000 instrument, and the output data were demultiplexed (allowing one mismatch) and BCL-to-Fastq conversion performed using Illumina's bcl2fastq software, v2.17.1.14. Sequence adapters were removed, and reads were quality trimmed using Trimmomatic v0.36 (Bolger *et al*, 2014) (Transwell samples) or BBDuk (part of the BBDuk suite; v36.32) (HUVEC and zebrafish CRISPR-Cas9 experiments). Processed reads from the human-derived samples were mapped against the reference human genome (hg38) using STAR v2.5.3/2.7.2b (Dobin *et al*, 2013), and counts per gene were calculated using annotation from GENCODE v30/32 (<http://www.genecodegenes.org/>). Zebrafish-derived samples were mapped against the reference assembly GRCz11 and gene annotation from Ensembl v99. Normalisation and differential expression was calculated with Bioconductor package DESeq2 v1.24 (Transwell samples), and RNAseq mapped reads were visualised with Jalview v2.11.0 (Waterhouse *et al*, 2009) (HUVEC and zebrafish CRISPR-Cas9 experiments).

### smFISH

Zebrafish cells and HUVECs were fixed in methanol-free 4% formaldehyde (Thermo Fisher Scientific) and used in smFISH assays. Briefly, cells were permeabilised with 70% ethanol at RT for 1 h or 4°C overnight, washed with smFISH wash buffer (2× SSC, 10% formamide) and incubated with smFISH probes (Table EV5) in smFISH hybridisation buffer (10% dextran sulphate, 2× SSC, 10% formamide) at 37°C overnight. Afterwards, cells were washed with smFISH wash buffer twice at 37°C for 30 min, washed once with 2× SSC for 10 min, counterstaining with 1 µg/ml DAPI (Sigma) and washed twice with PBS for 5 min at RT. Coverslips were air-dried and mounted on microscope slides with ProLong Gold Antifade Mountant (Thermo Fisher Scientific). All probes targeting protrusion-enriched mRNAs were designed with Stellaris Probe Designer (LGC Biosearch Technologies), synthesised and labelled with Quasar 570 or Quasar 670 (LGC Biosearch Technologies). Alternatively, probes were synthesised with an upstream FLAP sequence (CCTCCTAAGTTTCGAGCTGGACTCAGTG) (Tsanov *et al*, 2016) and annealed to a complementary FLAP probe labelled with Alexa 594 (Integrated DNA Technologies). Co-hybridisation experiments were carried out with predesigned *GAPDH* probes labelled with Quasar 670 (HUVECs) or *kdr* probes labelled with Quasar 570 (zebrafish cells) (LGC Biosearch Technologies).

### Puro-PLA and immunofluorescence (IF)

For Puro-PLA, cell bodies of HUVECs cultured in Transwells were scraped off and remaining protrusions were exposed to 3 µM

puromycin (Sigma) added to lower chambers for 6 min. In translation inhibition experiments, 40 µM anisomycin (Sigma) was added to the lower Transwell chamber 30 min before cell body removal and 6 min after cell body removal together with 3 µM puromycin. Subsequently, HUVEC protrusions grown in Transwell membranes were fixed in methanol-free 4% formaldehyde, removed from the Transwell inserts and used in Puro-PLA experiments as described elsewhere (tom Dieck *et al*, 2015). Following the Puro-PLA protocol, Transwell membranes were incubated for 20 min with 1:40 Alexa Fluor 488 Phalloidin (Thermo Fisher Scientific) in PBS, washed in Duolink wash buffer B (Sigma) and mounted on microscope slides with Duolink *In Situ* Mounting Medium containing DAPI (Sigma).

For IF experiments, cells and Transwell membranes containing protrusions were permeabilised in PBS containing 0.2–0.5% Triton X-100 (Sigma), blocked in 4% goat serum (Sigma) for 15 min and incubated with primary antibodies in blocking solution at 4°C overnight. Next, cells were washed in PBS containing 0.2% Tween, incubated with secondary antibodies at RT for 1 h, counterstaining with 1 µg/ml DAPI and washed again. Transwell membranes were further incubated with 1:40 Phalloidin Alexa Fluor 488 (Thermo Fisher Scientific) in PBS at RT for 20 min before washing. Cells and Transwell membranes were mounted with ProLong Gold Antifade Mountant (Thermo Fisher Scientific).

### Western blotting

Proteins were extracted with RIPA buffer (25 mM Tris-HCl pH 7.6, 150 mM NaCl, 1% NP-40, 1% sodium deoxycholate and 0.1% SDS) and quantified with Pierce BCA Protein Assay Kit (Thermo Fisher Scientific) following the supplier's recommendations. Samples were denatured with Laemmli buffer (250 mM Tris-HCl pH 6.8, 2% SDS, 10% glycerol, 0.0025% bromophenol blue, 2.5% β-mercaptoethanol) at 95°C for 5 min, loaded on 10% Mini-PROTEAN TGX precast protein gels (Bio-Rad) and separated in a Mini-PROTEAN Electrophoresis System (Bio-Rad). Proteins were transferred onto nitrocellulose membranes using a Trans-Blot Turbo Transfer System RTA Kit following the manufacturer's protocols (Bio-Rad). Subsequently, membranes were blocked in 5% milk (Sigma) or 5% BSA (Sigma) in TBS containing 0.1% Tween at RT for 1 h and incubated with primary antibodies at 4°C overnight. The next day, membranes were washed with TBS containing 0.1% Tween, incubated with secondary antibodies at RT for 1 h and washed again. Signal detection was carried out with SuperSignal West Dura Extended Duration Substrate (Thermo Fisher Scientific) according to the supplier's recommendations.

### Antibodies

Primary and secondary antibodies were used at the following concentrations: 1:1,600 mouse PECAM-1 89C2 (Cell Signaling Technology), 1:100 rabbit RAB13 (Puro-PLA, Millipore), 1:1,000 rabbit RAB13 (Western blotting and IF, Cambridge Bioscience), 1:3,500 mouse puromycin (Kerafast), 1:1,000 rabbit β-tubulin 9F3 (Cell Signaling Technology), 1:200 mouse ZO-1 1A12 (Thermo Fisher Scientific), 1:500 goat anti-mouse Alexa Fluor 488 or Alexa Fluor 568 (Thermo Fisher Scientific), 1:500 goat anti-rabbit Alexa Fluor 568 (Thermo Fisher Scientific), 1:5,000 goat anti-mouse HRP-linked

(Cell Signaling Technology) and 1:5,000 goat anti-rabbit HRP-linked antibody (Cell Signaling Technology).

### Plasmid construction

The pCS2-MCP-GFPnls plasmid used in *in vitro* MS2 system assays was generated excising a MCP-GFPnls fragment with SpeI and KpnI from pMS2-GFP, a gift from Robert Singer (Addgene plasmid # 27121) (Fusco *et al*, 2003), and subcloning it into a pCS2 + vector using the XbaI and KpnI sites.

To construct the Cerulean-H2B:*basfli1ep*:MCP-GFPnls Tol2-based plasmid for *in vivo* studies, MCP-GFPnls was amplified from pMS2-GFP with sequence 0.3  $\mu$ M specific primers (Table EV4) and Platinum Pfx DNA Polymerase in a T100 thermal cycler. Subsequently, the PCR product was cloned into a pDONR221 P3-P2 using Gateway Technology (Thermo Fisher Scientific) according to the manufacturer's manual. The final Tol2-based construct was assembled into the pTol2Dest(R1R2) (Addgene plasmid # 73484) (Villefranc *et al*, 2007) using Gateway 3-fragment recombination with pE(L1L4)Cerulean-H2B in the first position, pE(R4R3)*basfli1ep* (De Bock *et al*, 2013) in the second position and pE(L3L2)MCP-GFPnls in the third position.

For *in vitro* MS2 system experiments, 3'UTRs were PCR-amplified from human genomic DNA with 0.3  $\mu$ M sequence-specific primers (Table EV4) using Platinum Pfx DNA Polymerase or MyTaq Red DNA Polymerase (Bioline) in a T100 thermal cycler and the resulting PCR product was cloned using either Zero Blunt PCR or TOPO TA Cloning Kits (Thermo Fisher Scientific), following the manufacturer's manual. Next, the human *HBB* gene was PCR-amplified using 0.3  $\mu$ M sequence-specific primers (Table EV4) and Platinum Pfx DNA Polymerase in a T100 thermal cycler and cloned into the NotI and BamHI sites of the pCR4-24XMS2SL-stable plasmid, a gift from Robert Singer (Addgene plasmid # 31865) (Bertrand *et al*, 1998). Subsequently, a multiple cloning site (MCS; Table EV4) was introduced into the BglII and SpeI sites of pCR4-*HBB*-24XMS2SL and the recombinant *HBB*-24XMS2SL-MCS sequence was subcloned into the pcDNA3 mammalian expression vector (Thermo Fisher Scientific) using the NotI and XbaI sites. Full length 3'UTRs were then subcloned into pcDNA3-*HBB*-24XMS2SL-MCS using NheI and XhoI/ApaI sites. Alternatively, truncated and deletion versions of the 3'UTRs were generated by PCR using 0.3  $\mu$ M sequence-specific primers (Table EV4) and Platinum Pfx DNA Polymerase, Phusion High-Fidelity polymerase (NEB) or using QuikChange II Site-Directed Mutagenesis Kit (Agilent Technologies) following the manufacturer's instructions and introduced into the pcDNA3-*HBB*-24XMS2SL-MCS using the NheI and XhoI sites.

In order to generate the zebrafish MS2 system reporter construct, the 24XMS2SL cassette was firstly subcloned from pCR4-24XMS2SL-stable into a *kdrl*:Lyn-mCherry Tol2-based plasmid (Costa *et al*, 2016) using a BamHI site. Next, the zebrafish *rab13* 3'UTR was PCR-amplified with 0.4  $\mu$ M sequence-specific primers (Table EV4) and MyTaq Red DNA Polymerase from zebrafish genomic DNA in a T100 thermal cycler and then subcloned into the Tol2 *kdrl*:Lyn-mCherry-24XMS2SL plasmid using NheI and BglII sites. The resulting Lyn-mCherry-24XMS2SL-*rab13* 3'UTR recombinant sequence was amplified with 0.3  $\mu$ M sequence-specific primers (Table EV4) and Platinum Pfx DNA Polymerase in a T100 thermal cycler and

subcloned into a pDONR221 P3-P2 using Gateway Technology. Lastly, the final Tol2-based construct was assembled into the pTol2Dest(R1R2) using Gateway 3-fragment recombination with pE(L1L4)Cerulean-H2B in the first position, pE(R4R3)*basfli1ep* in the second position and Lyn-mCherry-24XMS2SL-*rab13* 3'UTR in the third position.

All plasmid maps and details are available upon request.

### Microscopy

Confocal time-lapse imaging of zebrafish embryos was carried out as previously described (Costa *et al*, 2016). MS2 system-transfected cells were live-imaged every 5 s in a Nikon A1R-inverted confocal microscope equipped with an Okolab incubation chamber, using a 60 $\times$  objective. Fixed images of cultured cells and Transwell membranes were acquired on an Olympus IX83-inverted microscope using Lumencor LED excitation, either a 60 $\times$ /1.42 PlanApo or a 100 $\times$ /1.35 UplanApo objective and a Sedat QUAD (DAPI/FITC/TRITC/Cy5) filter set (Chroma 89000). The images were collected using a R6 (Qimaging) CCD camera with a Z optical spacing of 0.2  $\mu$ m. Raw images were then deconvolved using the Huygens Pro software (SVI), and maximum intensity projections of these images were used for analysis.

### smFISH spot quantification, Polarisation Index and filopodia analysis

Processed smFISH images were used to calculate mRNA polarisation with the PI metric developed by Park *et al* (2012) and to assess mRNA spot number with FISH-quant (Mueller *et al*, 2013).

For the studies of filopodia distance to GFP signal in MS2 system movies, filopodia parameters (position, duration and frequency) of MS2 system-transfected cells were determined using Filopodyan plugin for FIJI (Urbancic *et al*, 2017). Only filopodia that emerged and retracted through the duration of the movies were analysed. Subsequently, the coordinates of GFP particles were extracted with the TrackMate plugin for FIJI (Tinevez *et al*, 2017). In order to generate control coordinates in each movie, the Lyn-mCherry channel was thresholded to generate regions of interest (ROI) and the FIJI built-in macro function "random" was used within the ROI at each frame. The Euclidean distances between the base of newly formed filopodia and both the nearest GFP particle and the control randomised coordinate were calculated.

### RNA motif enrichment analysis and Gene Ontology

Discovery of recurring motifs across the *k* 5 mRNA 3'UTRs was carried out using MEME (Bailey & Elkan, 1994) (settings set to: mode - anr; nmotifs: 5; minw: 6; maxw: 50; objfun classic; markov\_order 0). The only motif present in all 3'UTR was selected for downstream studies. In order to quantify the frequency mRNA within the remaining *k*-means clusters containing at least two repeats of the studied RNA motif, 3'UTR sequences were scanned in FIMO (Grant *et al*, 2011) using the position-specific probability matrix obtained in MEME (settings set to: match *P*-value < 1E-5).

Gene Ontology studies were performed using DAVID using the HUVEC-enriched mRNAs as background (Huang da *et al*, 2009a,b).

## Statistics and *k*-means clustering

All data are represented as means  $\pm$  standard deviation. Statistical analysis of the data was carried out using GraphPad Prism software and RStudio. D'Agostino–Pearson or Shapiro–Wilk normality tests were applied to smFISH, Puro-PLA, filopodia, ISV branching data and RNA, protein levels to determine the appropriate statistical test. Statistical significance is reported for  $P < 0.05$ .

*k*-means clustering was performed in RStudio. Briefly, mRNA fold changes (FC) between cell bodies and protrusions of the cell types mentioned in the main text were obtained from the respective publications—NIH/3T3 fibroblasts (Wang *et al*, 2017), MDA-MB231 metastatic breast cancer cells (Mardakheh *et al*, 2015) and induced neuronal cells (Zappulo *et al*, 2017). mRNAs were included in the clustering analysis if they were enriched in HUVEC protrusions (FC > 1.6, FDR < 0.05) and expressed in all three cell types. The  $\log_2$  FC values between cell fractions were extracted, scaled and centred, followed by *k*-means clustering ( $k = 8$ ). The number of clusters was defined by the number of cell types and by the possible transcript statuses (enriched or depleted in each of the three cell types) –  $2^3 = 8$ . The output is represented in heat maps using the  $\log_2$  FC data prior to scaling and centring.

## Data availability

The RNAseq datasets presented in this study have been deposited to the Gene Expression Omnibus repository (<https://www.ncbi.nlm.nih.gov/geo/>) with the accession numbers GSE133055 and GSE155449.

RStudio scripts are available upon request.

**Expanded View** for this article is available online.

## Acknowledgements

We are grateful to E. Schuman and S. tom Dieck at the MPI for Brain Research, Frankfurt, Germany, for help and guidance setting up Puro-PLA assays. Moreover, we thank Rob Wilkinson at the University of Nottingham, UK, for access to his preliminary results for CRISPRi-mediated *rab13* knockdown in zebrafish. We also thank N. Papalopulu and group members at the University of Manchester, UK, for critical feedback, reagents and materials. We wish to thank members of the University of Manchester Biological Services, Genomic Technologies, Bioimaging Facilities and Flow Cytometry Facilities, for technical support. This work was funded by the Wellcome Trust (095718/Z/11/Z and 219500/Z/19/Z to S.P.H.), Wellcome Institutional Strategic Support Fund (204796/Z/16/Z to G.C.) and the British Heart Foundation (PG/16/2/31863 to S.P.H.).

## Author contributions

GC and SPH conceptualised the study. GC contributed to methodology. GC involved in formal analysis. GC, JB and NT investigated the study. GC and SPH wrote the original draft of the manuscript. GC and SPH wrote, reviewed and edited the manuscript. GC and SPH supervised the study. GC and SPH acquired the funding.

## Conflict of interest

The authors declare that they have no conflict of interest.

## References

- Ainger K, Avossa D, Diana AS, Barry C, Barbarese E, Carson JH (1997) Transport and localization elements in myelin basic protein mRNA. *J Cell Biol* 138: 1077–1087
- An JJ, Gharami K, Liao GY, Woo NH, Lau AG, Vanevski F, Torre ER, Jones KR, Feng Y, Lu B *et al* (2008) Distinct role of long 3' UTR BDNF mRNA in spine morphology and synaptic plasticity in hippocampal neurons. *Cell* 134: 175–187
- Andreassi C, Riccio A (2009) To localize or not to localize: mRNA fate is in 3'UTR ends. *Trends Cell Biol* 19: 465–474
- Bailey TL, Elkan C (1994) Fitting a mixture model by expectation maximization to discover motifs in biopolymers. *Proc Int Conf Intell Syst Mol Biol* 2: 28–36
- Bertrand E, Chartrand P, Schaefer M, Shenoy SM, Singer RH, Long RM (1998) Localization of ASH1 mRNA particles in living yeast. *Mol Cell* 2: 437–445
- Bolger AM, Lohse M, Usadel B (2014) Trimmomatic: a flexible trimmer for Illumina sequence data. *Bioinformatics* 30: 2114–2120
- Brickley K, Smith MJ, Beck M, Stephenson FA (2005) GRIF-1 and OIP106, members of a novel gene family of coiled-coil domain proteins: association *in vivo* and *in vitro* with kinesin. *J Biol Chem* 280: 14723–14732
- Buxbaum AR, Haimovich G, Singer RH (2015) In the right place at the right time: visualizing and understanding mRNA localization. *Nat Rev Mol Cell Biol* 16: 95–109
- Chouaib R, Safieddine A, Pichon X, Imbert A, Kwon OS, Samacoits A, Traboulsi A-M, Robert M-C, Tsanov N, Coleno E *et al* (2020) A dual protein-mrna localization screen reveals compartmentalized translation and widespread co-translational RNA targeting. *Dev Cell* S1534-5807(20)30584-0
- Ciulli Mattioli C, Rom A, Franke V, Imami K, Arrey G, Terne M, Woehler A, Akalin A, Ulitsky I, Chekulaeva M (2019) Alternative 3' UTRs direct localization of functionally diverse protein isoforms in neuronal compartments. *Nucleic Acids Res* 47: 2560–2573
- Condeelis J, Singer RH (2005) How and why does beta-actin mRNA target? *Biol Cell* 97: 97–110
- Costa G, Harrington KI, Lovegrove HE, Page DJ, Chakravartula S, Bentley K, Herbert SP (2016) Asymmetric division coordinates collective cell migration in angiogenesis. *Nat Cell Biol* 18: 1292–1301
- De Bock K, Georgiadou M, Schoors S, Kuchnio A, Wong BW, Cantelmo AR, Quaegebeur A, Chesquiere B, Cauwenberghs S, Eelen G *et al* (2013) Role of PFKFB3-driven glycolysis in vessel sprouting. *Cell* 154: 651–663
- tom Dieck S, Kochen L, Hanus C, Heumuller M, Bartnik I, Nassim-Assir B, Merk K, Mosler T, Garg S, Bunse S *et al* (2015) Direct visualization of newly synthesized target proteins *in situ*. *Nat Methods* 12: 411–414
- Dobin A, Davis CA, Schlesinger F, Drenkow J, Zaleski C, Jha S, Batut P, Chaisson M, Gingeras TR (2013) STAR: ultrafast universal RNA-seq aligner. *Bioinformatics* 29: 15–21
- Eng CL, Lawson M, Zhu Q, Dries R, Koulina N, Takei Y, Yun J, Cronin C, Karp C, Yuan GC *et al* (2019) Transcriptome-scale super-resolved imaging in tissues by RNA seqFISH. *Nature* 568: 235–239
- Engel KL, Arora A, Goering R, Lo HG, Taliaferro JM (2020) Mechanisms and consequences of subcellular RNA localization across diverse cell types. *Traffic* 21: 404–418
- Fusco D, Accornero N, Lavoie B, Shenoy SM, Blanchard JM, Singer RH, Bertrand E (2003) Single mRNA molecules demonstrate probabilistic movement in living mammalian cells. *Curr Biol* 13: 161–167



- Gerhardt H, Golding M, Fruttiger M, Ruhrberg C, Lundkvist A, Abramsson A, Jeltsch M, Mitchell C, Alitalo K, Shima D et al (2003) VEGF guides angiogenic sprouting utilizing endothelial tip cell filopodia. *J Cell Biol* 161: 1163–1177
- Grant CE, Bailey TL, Noble WS (2011) FIMO: scanning for occurrences of a given motif. *Bioinformatics* 27: 1017–1018
- Harris ES, Nelson WJ (2010) Adenomatous polyposis coli regulates endothelial cell migration independent of roles in beta-catenin signaling and cell-cell adhesion. *Molecular Biology of the Cell* 21: 2611–2623
- Herbert SP, Costa G (2019) Sending messages in moving cells: mRNA localization and the regulation of cell migration. *Essays Biochem* 63: 595–606
- Hetheridge C, Mavria G, Mellor H (2011) Uses of the *in vitro* endothelial-fibroblast organotypic co-culture assay in angiogenesis research. *Biochem Soc Trans* 39: 1597–1600
- Hotz M, Nelson WJ (2017) Pumilio-dependent localization of mRNAs at the cell front coordinates multiple pathways required for chemotaxis. *Nat Commun* 8: 1366
- Huang da W, Sherman BT, Lempicki RA (2009a) Bioinformatics enrichment tools: paths toward the comprehensive functional analysis of large gene lists. *Nucleic Acids Res* 37: 1–13
- Huang da W, Sherman BT, Lempicki RA (2009b) Systematic and integrative analysis of large gene lists using DAVID bioinformatics resources. *Nat Protoc* 4: 44–57
- Ioannou MS, Bell ES, Girard M, Chaineau M, Hamlin JN, Daubaras M, Monast A, Park M, Hodgson L, McPherson PS (2015) DENND2B activates Rab13 at the leading edge of migrating cells and promotes metastatic behavior. *J Cell Biol* 208: 629–648
- Isogai S, Lawson ND, Torrealday S, Horiguchi M, Weinstein BM (2003) Angiogenic network formation in the developing vertebrate trunk. *Development* 130: 5281–5290
- Jakobsen KR, Sorensen E, Brondum KK, Daugaard TF, Thomsen R, Nielsen AL (2013) Direct RNA sequencing mediated identification of mRNA localized in protrusions of human MDA-MB-231 metastatic breast cancer cells. *J Mol Signaling* 8: 9
- Jambhekar A, Derisi JL (2007) Cis-acting determinants of asymmetric, cytoplasmic RNA transport. *RNA* 13: 625–642
- Jin SW, Beis D, Mitchell T, Chen JN, Stainier DY (2005) Cellular and molecular analyses of vascular tube and lumen formation in zebrafish. *Development* 132: 5199–5209
- Kang H, Schuman EM (1996) A requirement for local protein synthesis in neurotrophin-induced hippocampal synaptic plasticity. *Science* 273: 1402–1406
- Kim NY, Lee S, Yu J, Kim N, Won SS, Park H, Heo WD (2020) Optogenetic control of mRNA localization and translation in live cells. *Nat Cell Biol* 22: 341–352
- Kislauskis EH, Zhu X, Singer RH (1994) Sequences responsible for intracellular localization of beta-actin messenger RNA also affect cell phenotype. *J Cell Biol* 127: 441–451
- Kopp P, Lammers R, Aepfelbacher M, Woehlke G, Rudel T, Machuy N, Steffen W, Linder S (2006) The kinesin KIF1C and microtubule plus ends regulate podosome dynamics in macrophages. *Mol Biol Cell* 17: 2811–2823
- Lamont RE, Lamont EJ, Childs SJ (2009) Antagonistic interactions among Plexins regulate the timing of intersegmental vessel formation. *Dev Biol* 331: 199–209
- Leung KM, van Horck FP, Lin AC, Allison R, Standart N, Holt CE (2006) Asymmetrical beta-actin mRNA translation in growth cones mediates attractive turning to netrin-1. *Nat Neurosci* 9: 1247–1256
- Liang CC, Park AY, Guan JL (2007) *In vitro* scratch assay: a convenient and inexpensive method for analysis of cell migration *in vitro*. *Nat Protoc* 2: 329–333
- Lu X, Le Noble F, Yuan L, Jiang Q, De Lafarge B, Sugiyama D, Breant C, Claes F, De Smet F, Thomas JL et al (2004) The netrin receptor UNC5B mediates guidance events controlling morphogenesis of the vascular system. *Nature* 432: 179–186
- Lyles V, Zhao Y, Martin KC (2006) Synapse formation and mRNA localization in cultured Aplysia neurons. *Neuron* 49: 349–356
- Mardakheh FK, Paul A, Kumper S, Sadok A, Paterson H, McCarthy A, Yuan Y, Marshall CJ (2015) Global analysis of mRNA, translation, and protein localization: local translation is a key regulator of cell protrusions. *Dev Cell* 35: 344–357
- Mayor R, Etienne-Manneville S (2016) The front and rear of collective cell migration. *Nat Rev Mol Cell Biol* 17: 97–109
- Mayr C (2016) Evolution and biological roles of alternative 3'UTRs. *Trends Cell Biol* 26: 227–237
- Mili S, Moissoglu K, Macara IG (2008) Genome-wide screen reveals APC-associated RNAs enriched in cell protrusions. *Nature* 453: 115–119
- Mingle LA, Okuhama NN, Shi J, Singer RH, Condeelis JS, Liu G (2005) Localization of all seven messenger RNAs for the actin-polymerization nucleator Arp2/3 complex in the protrusions of fibroblasts. *J Cell Sci* 118: 2425–2433
- Moissoglu K, Yasuda K, Wang T, Chrisafis G, Mili S (2019) Translational regulation of protrusion-localized RNAs involves silencing and clustering after transport. *Elife* 8: e44752
- Moissoglu K, Stueland M, Gasparski AN, Wang T, Jenkins LM, Hastings ML, Mili S (2020) RNA localization and co-translational interactions control RAB13 GTPase function and cell migration. *EMBO J* 39: e104958
- Moor AE, Golan M, Massasa EE, Lemze D, Weizman T, Shenhav R, Baydatch S, Mizrahi O, Winkler R, Golani O et al (2017) Global mRNA polarization regulates translation efficiency in the intestinal epithelium. *Science* 357: 1299–1303
- Moreno-Mateos MA, Vejnar CE, Beaudoin JD, Fernandez JP, Mis EK, Khokha MK, Giraldez AJ (2015) CRISPRscan: designing highly efficient sgRNAs for CRISPR-Cas9 targeting *in vivo*. *Nat Methods* 12: 982–988
- Mowry KL, Melton DA (1992) Vegetal messenger RNA localization directed by a 340-nt RNA sequence element in *Xenopus* oocytes. *Science* 255: 991–994
- Mueller F, Senecal A, Tantale K, Marie-Nelly H, Ly N, Collin O, Basyuk E, Bertrand E, Darzacq X, Zimmer C (2013) FISH-quant: automatic counting of transcripts in 3D FISH images. *Nat Methods* 10: 277–278
- Nagaoka K, Udagawa T, Richter JD (2012) CPEB-mediated ZO-1 mRNA localization is required for epithelial tight-junction assembly and cell polarity. *Nat Commun* 3: 675
- Park HY, Trcek T, Wells AL, Chao JA, Singer RH (2012) An unbiased analysis method to quantify mRNA localization reveals its correlation with cell motility. *Cell Rep* 1: 179–184
- Pfeffer SR, Dirac-Svejstrup AB, Soldati T (1995) Rab GDP dissociation inhibitor: putting rab GTPases in the right place. *J Biol Chem* 270: 17057–17059
- Raj A, van den Bogaard P, Rifkin SA, van Oudenaarden A, Tyagi S (2008) Imaging individual mRNA molecules using multiple singly labeled probes. *Nat Methods* 5: 877–879
- Sakane A, Abdallah AA, Nakano K, Honda K, Ikeda W, Nishikawa Y, Matsumoto M, Matsushita N, Kitamura T, Sasaki T (2012) Rab13 small G protein and junctional Rab13-binding protein (JRAB) orchestrate actin cytoskeletal organization during epithelial junctional development. *J Biol Chem* 287: 42455–42468

- Sakane A, Alamir Mahmoud Abdallah A, Nakano K, Honda K, Kitamura T, Imoto I, Matsushita N, Sasaki T (2013) Junctional Rab13-binding protein (JRAB) regulates cell spreading via filamins. *Genes Cells* 18: 810–822
- Seabra MC, Mules EH, Hume AN (2002) Rab GTPases, intracellular traffic and disease. *Trends Mol Med* 8: 23–30
- Shen F, Seabra MC (1996) Mechanism of digeranylgeranylation of Rab proteins. Formation of a complex between monogerynylgeranyl-Rab and Rab escort protein. *J Biol Chem* 271: 3692–3698
- Srougi MC, Burrige K (2011) The nuclear guanine nucleotide exchange factors Ect2 and Net1 regulate RhoB-mediated cell death after DNA damage. *PLoS ONE* 6: e17108
- Taliaferro JM, Vidaki M, Oliveira R, Olson S, Zhan L, Saxena T, Wang ET, Graveley BR, Gertler FB, Swanson MS et al (2016) Distal alternative last exons localize mRNAs to neural projections. *Mol Cell* 61: 821–833
- Tinevez JY, Perry N, Schindelin J, Hoopes GM, Reynolds GD, Laplantine E, Bednarek SY, Shorte SL, Eliceiri KW (2017) TrackMate: an open and extensible platform for single-particle tracking. *Methods* 115: 80–90
- Tommasi S, Dammann R, Jin SG, Zhang XF, Avruch J, Pfeifer GP (2002) RASSF3 and NORE1: identification and cloning of two human homologues of the putative tumor suppressor gene RASSF1. *Oncogene* 21: 2713–2720
- Torres-Vazquez J, Gitler AD, Fraser SD, Berk JD, Van NP, Fishman MC, Childs S, Epstein JA, Weinstein BM (2004) Semaphorin-plexin signaling guides patterning of the developing vasculature. *Dev Cell* 7: 117–123
- Tsanov N, Samacoits A, Chouaib R, Traboulsi AM, Gostan T, Weber C, Zimmer C, Zibara K, Walter T, Peter M et al (2016) smiFISH and FISH-quant – a flexible single RNA detection approach with super-resolution capability. *Nucleic Acids Res* 44: e165
- Tushev G, Glock C, Heumuller M, Biever A, Jovanovic M, Schuman EM (2018) Alternative 3' UTRs modify the localization, regulatory potential, stability, and plasticity of mRNAs in neuronal compartments. *Neuron* 98: 495–511 e496
- Urbancic V, Butler R, Richier B, Peter M, Mason J, Livesey FJ, Holt CE, Gallop JL (2017) Filopodyan: an open-source pipeline for the analysis of filopodia. *J Cell Biol* 216: 3405–3422
- Villefranc JA, Amigo J, Lawson ND (2007) Gateway compatible vectors for analysis of gene function in the zebrafish. *Dev Dyn* 236: 3077–3087
- Wang T, Hamilla S, Cam M, Aranda-Espinoza H, Mili S (2017) Extracellular matrix stiffness and cell contractility control RNA localization to promote cell migration. *Nat Commun* 8: 896
- Waterhouse AM, Procter JB, Martin DM, Clamp M, Barton GJ (2009) Jalview Version 2—a multiple sequence alignment editor and analysis workbench. *Bioinformatics* 25: 1189–1191
- Weatheritt RJ, Gibson TJ, Babu MM (2014) Asymmetric mRNA localization contributes to fidelity and sensitivity of spatially localized systems. *Nat Struct Mol Biol* 21: 833–839
- Wu C, Agrawal S, Vasanthi A, Drazba J, Sarkaria S, Xie J, Welch CM, Liu M, Anand-Apte B, Horowitz A (2011) Rab13-dependent trafficking of RhoA is required for directional migration and angiogenesis. *J Biol Chem* 286: 23511–23520
- Xia C, Fan J, Emanuel G, Hao J, Zhuang X (2019) Spatial transcriptome profiling by MERFISH reveals subcellular RNA compartmentalization and cell cycle-dependent gene expression. *Proc Natl Acad Sci USA* 116: 19490–19499
- Yao J, Sasaki Y, Wen Z, Bassell GJ, Zheng JQ (2006) An essential role for beta-actin mRNA localization and translation in Ca<sup>2+</sup>-dependent growth cone guidance. *Nat Neurosci* 9: 1265–1273
- Younts TJ, Monday HR, Dudok B, Klein ME, Jordan BA, Katona I, Castillo PE (2016) Presynaptic protein synthesis is required for long-term plasticity of GABA release. *Neuron* 92: 479–492
- Zappulo A, van den Bruck D, Ciolli Mattioli C, Franke V, Imami K, McShane E, Moreno-Estelles M, Calviello L, Filipchuk A, Peguero-Sanchez E et al (2017) RNA localization is a key determinant of neurite-enriched proteome. *Nat Commun* 8: 583



**License:** This is an open access article under the terms of the Creative Commons Attribution 4.0 License, which permits use, distribution and reproduction in any medium, provided the original work is properly cited.

## Expanded View Figures

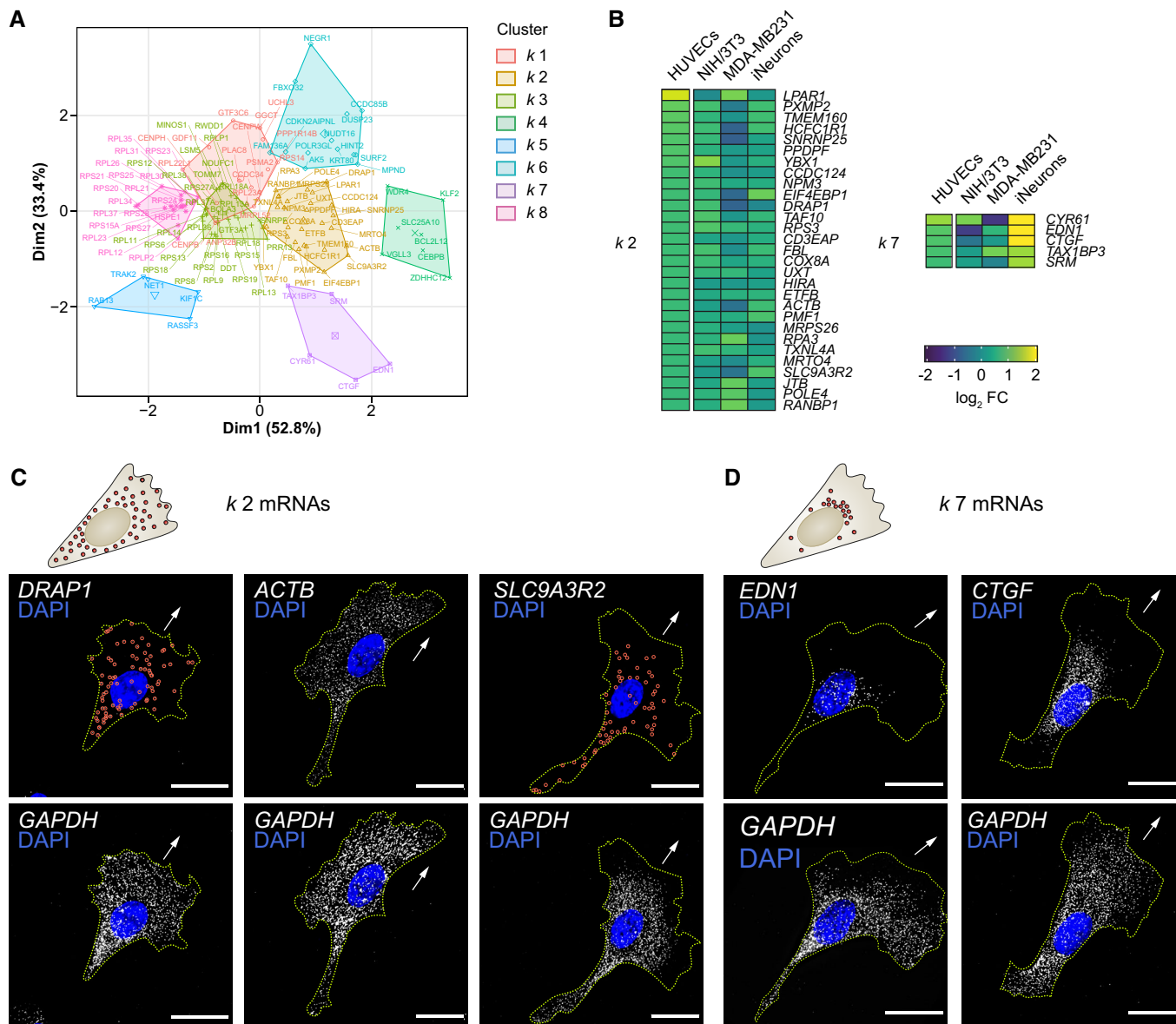


**Figure EV1. Clustering of RNAseq datasets defines unexpected cell type-specific diversity to mRNA polarisation.**

A Principal component plot depicting the *k*-means clustering analysis of mRNAs enriched across cell protrusion types.  
 B Detail of the heat map shown in Fig 1C representing log<sub>2</sub> fold change (FC) levels (protrusions over cell bodies) of mRNAs present in clusters *k* 2 and *k* 7. The corresponding HUVEC log<sub>2</sub> FC levels are shown in parallel.  
 C Top: distribution pattern of mRNAs clustered in *k* 2. Bottom: smFISH co-detection of *k* 2 mRNAs and *GAPDH* in HUVECs.  
 D Top: distribution pattern of mRNAs clustered in *k* 7. Bottom: smFISH co-detection of *k* 7 mRNAs and *GAPDH* in HUVECs.

Data information: arrows indicate the orientation of RNA localisation; yellow dashed lines outline cell borders; red circles highlight smFISH spots; scale bars = 20 μm (C, D).

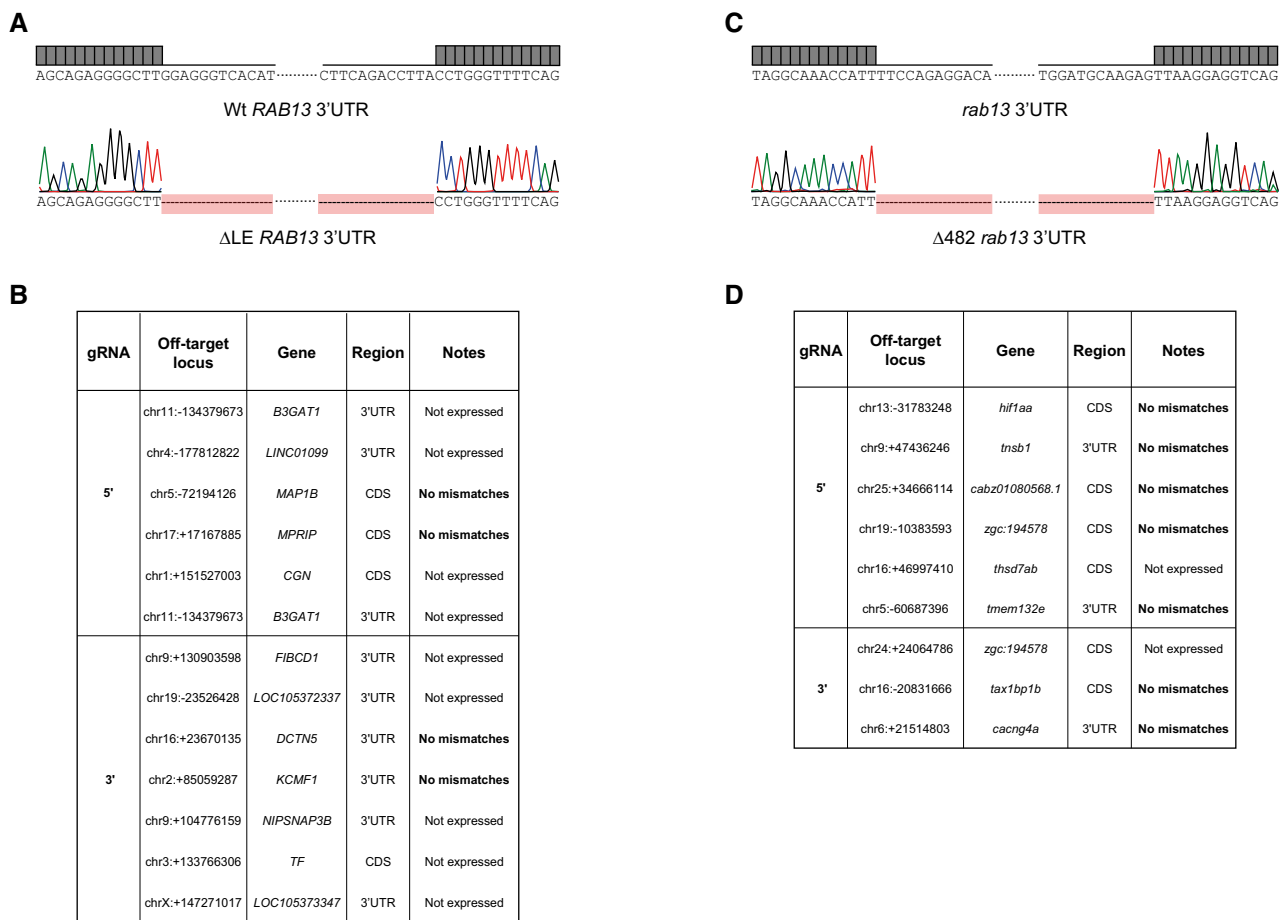


**Figure EV2. CRISPR-Cas9 editing of the RAB 3'UTR *in vitro* and *in vivo* does not generate off-target mutations.**

- A Chromatogram confirming the excision of the LE within *RAB13* 3'UTR in HUVECs.
- B List of predicted CRISPR-Cas9 off-target genes and RNAseq mismatch detection in CRISPR-Cas9-derived HUVEC clones (*n* = 1 each genotype).
- C Chromatogram confirming the CRISPR-Cas9-mediated excision of 482-nt within the *rab13* 3'UTR in zebrafish embryos.
- D List of predicted CRISPR-Cas9 off-target genes and RNAseq mismatch detection in *Tg(kdrl:EGFP) rab13<sup>+/+</sup>* and *rab13<sup>Δ3'UTR/Δ3'UTR</sup>* embryos (*n* = 2 each genotype).

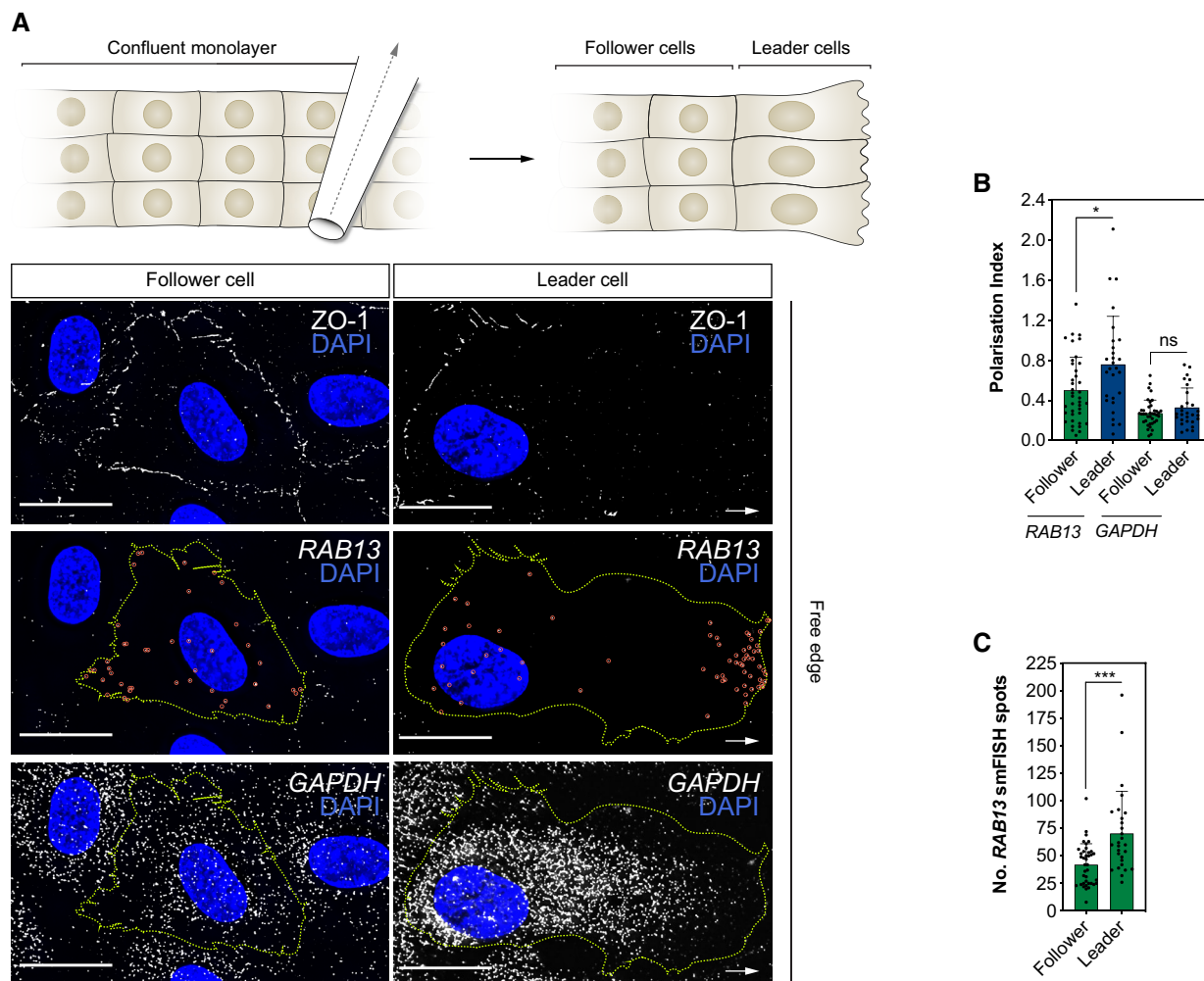


**Figure EV3. Induction of endothelial cell collective migration drives *RAB13* mRNA polarisation in leader cells.**

**A** Top: scratch wound assay generates a free edge on a confluent monolayer of HUVECs and encourages cell migration. Bottom: smFISH co-detection of *RAB13* mRNA and *GAPDH* mRNA in representative HUVECs migrating in a scratch wound assay. ZO-1 immunolabelling defines cell boundaries.

**B** Polarisation Index of *RAB13* and *GAPDH* co-detected in HUVECs cultured in scratch wound assays ( $n \geq 28$  cells;  $*P < 0.05$ ; ns: not significant; Mann–Whitney test).

**C** Quantification of the number of *RAB13* mRNA smFISH spots per cell ( $n \geq 28$  cells;  $***P < 0.001$ ; Mann–Whitney test). Leader: cells identified at the edge of the scratch; follower: cells identified in confluent regions adjacent to leader cells.

Data information: arrows indicate orientation of RNA localisation; yellow dashed lines outline cell borders; red circles highlight smFISH spots; scale bars = 20  $\mu\text{m}$  (A). Bar charts are presented as means  $\pm$  s.d.

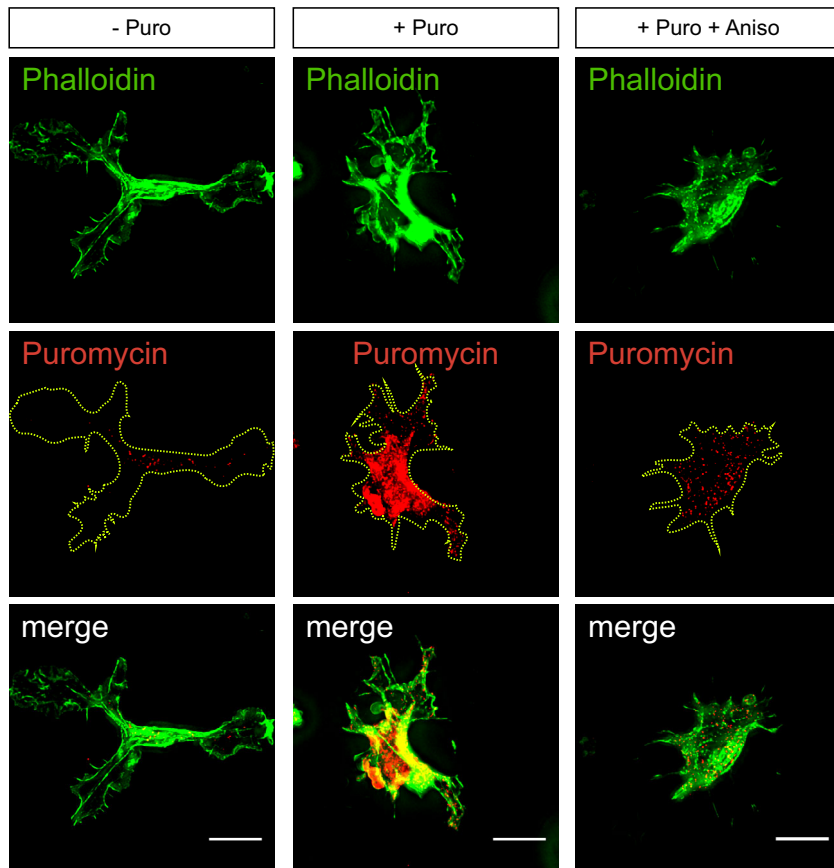


**Figure EV4. Protein translation in endothelial cell protrusions.**

Immunofluorescence analysis of HUVEC protrusions generated on the underside of Transwell membranes and exposed to puromycin after cell body removal. Yellow dashed lines outline protrusion borders; scale bars = 10  $\mu$ m.

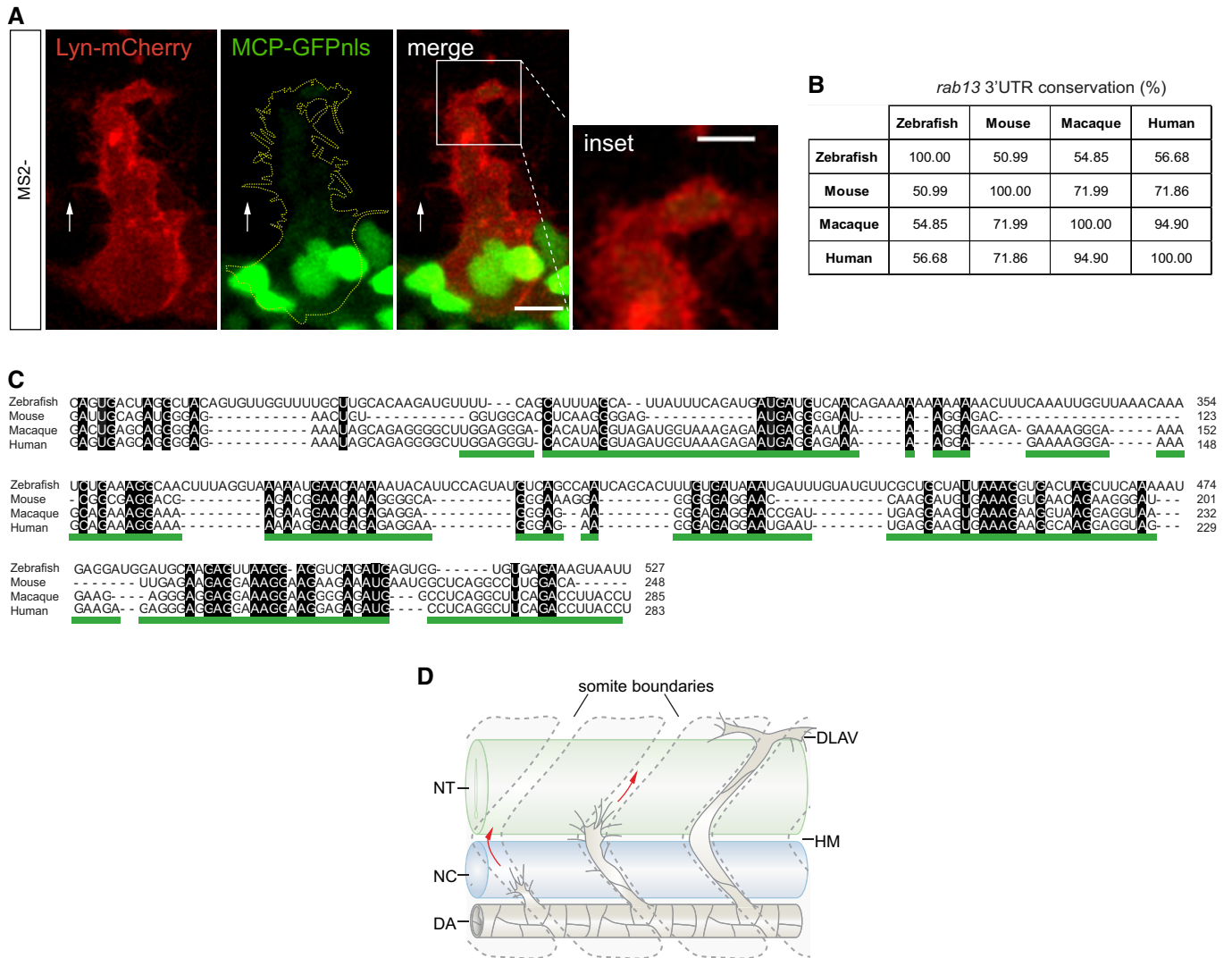


**Figure EV5. The 3'UTR of *rab13* shows low conservation across species whilst retaining mRNA localisation potential.**

A *Tg(fli1ep:MCP-GFPnl3)* tip cell expressing a control Lyn-mCherry-24xMS2 construct.

B Percentage identity matrix of *rab13* 3'UTR orthologue sequences.

C Multiple sequence alignment between *rab13* 3'UTR orthologues. Black boxes indicate absolute nucleotide similarity. The human *RAB13* 3'UTR localisation element is underlined in green.

D Scheme depicts stages of zebrafish ISV sprouting. DA: dorsal aorta; DLAV: dorsal longitudinal anastomotic vessel; HM: horizontal myoseptum; NC: notochord; NT: neural tube.

Data information: white arrows indicate direction of ISV sprouting; yellow dashed line outlines ISV cell borders; scale bars = 10  $\mu$ m; scale bar in inset = 5  $\mu$ m (A).

# ***TRAK2* mRNA localisation controls cell migration through mitochondria distribution.**

Joshua J. Bradbury<sup>1</sup> and Shane P. Herbert<sup>1,\*</sup>

1. Faculty of Biology, Medicine and Health, University of Manchester, Manchester, UK.

\* = Corresponding Authors.

Intended Journal – eLife.

## **Contribution**

JJB and SPH conceptualised the study. JJB conducted the experimental work and data analysis. JJB designed the figures and wrote the manuscript.



### 3.1 Abstract

Enrichment of specific mRNAs in protrusions of migratory cells is a well-established phenomenon. Despite this knowledge, definitive understanding of the mechanistic and functional role of localised mRNAs, especially during complex physiological cell migration, has been elusive. Here, using single-molecule mRNA imaging, endogenous gene editing, and *in vitro* cell culture models, we reveal that *TRAK2* mRNA polarisation acts as a brake on motile cell speed by maintaining subcellular mitochondria distribution in the leading edge. First, we show that specific mRNAs adopt a striking distribution in the leading edge during uniaxial, highly polarised, endothelial cell migration within cell-derived matrix. Necessary localisation elements were then interrogated using the MS2-MCP reporter system, to reveal gene-specific requirements in the spacing and number of G-rich sequence motifs to enable mRNA targeting. Genomic excision of necessary localisation motifs caused depolarisation of endogenous mRNA distribution, without impairing translated protein expression. Molecular functionality of localised mRNA was then tested to show that *TRAK2* mRNA depolarisation caused excess mitochondria to amass in distal endothelial protrusions, phenocopying observations when *TRAK2* protein expression is reduced. Adoption of a modified cell behaviour in which motile speed is enhanced was also stimulated by *TRAK2* mRNA mislocalisation. Hence, *TRAK2* mRNA localisation enables precise spatial control of *TRAK2* protein activity in distal protrusions, maintains mitochondria distribution, and controls endothelial cell migratory behaviour.

### 3.2 Introduction

Targeted localisation of messenger mRNA is a conserved and prevalent phenomenon throughout biology (Medioni et al., 2012). Transcriptome-wide analysis has revealed that many thousands of different mRNAs are enriched in diverse subcellular regions in a wide variety of organisms (Costa et al., 2020; Lécuyer et al., 2007; Shepard et al., 2003; Zappulo et al., 2017), including the protrusions of migratory cells (Costa et al., 2020; Jakobsen et al., 2013; Mili et al., 2008; Shankar et al., 2010; Stuart et al., 2008). However, the molecular and cellular functions of localised mRNAs are not well understood.

The destination of a localised mRNA is encoded within its sequence via localisation elements (LEs) often found in their 3'UTRs. LE's interact with mRNA binding proteins (RBPs), which in turn drive the mRNA transport process (Andreassi & Riccio, 2009; Chabanon et al., 2004). LEs vary widely in sequence composition and structural conformation. Using computational

motif identification tools, we have recently identified a conserved LE repeated throughout the 3'UTRs of a cohort of protrusion-enriched mRNAs (Costa et al., 2020). The relative contribution of these repeated LEs to mRNA transport, and the function of the localised mRNAs themselves, remains incompletely understood.

The complex nature of LEs, and the challenges associated with endogenous gene manipulation, means that the molecular function of localised mRNAs in migratory cells has only been tested in a few instances, namely *RAB13* and  *$\beta$ -actin*. Localisation of *RAB13* mRNA defines a zone of active filopodia production in the distal reaches of motile cell protrusions. This is achieved through co-translational association of RAB13 with a GEF, RABIF, which activates locally translated RAB13. Polarised RAB13 activity then preferentially activates downstream effector MICAL-L2. This process is essential for cell pathfinding during *in vivo* endothelial migration (Costa et al., 2020; Moissoglu et al., 2020). Similarly, localisation of  *$\beta$ -actin* mRNA to migratory protrusions also controls directed cell motility.  *$\beta$ -actin* mRNA is localised to focal adhesions of fibroblasts via a LE in its 3'UTR in conjunction with RBP ZBP1 (Kislauskis et al., 1994, 1997; Ross et al., 1997). Specific enrichment and subsequent translation of  *$\beta$ -actin* mRNA is thought to provide local  $\beta$ -actin monomers needed to integrate with the local actin network and functionally link the cytoskeleton with focal adhesions (Katz et al., 2012). Therefore, localised mRNAs in cell migration have so far only been attributed functions in cytoskeletal reorganisation and membrane remodelling. Conversely, the contribution that localised mRNAs may make to other essential cellular processes remains unexplored. This includes the function of highly conserved polarised mRNA *TRAK2* (Costa et al., 2020; Moissoglu et al., 2020; Pichon et al., 2021).

*TRAK2* is an adaptor that physically connects motor proteins to the mitochondrial outer membrane protein Miro (MacAskill et al., 2009; van Spronsen et al., 2013). Both *TRAK2* and Miro have been shown to be necessary to enable the correct distribution of mitochondria in cells (Glater et al., 2006; López-Doménech et al., 2016; Stowers et al., 2002). Most evidence suggests that *TRAK2* preferentially mediates minus-end directed microtubule transport, since overexpression of *TRAK2* causes mitochondria to accumulate in perinuclear regions (López-Doménech et al., 2018; van Spronsen et al., 2013). However, *TRAK2* has recently been suggested to be capable of driving both plus- and minus-end directed movement (Fenton et al., 2021). In an *in vitro* reconstitution assay, *TRAK2* participates in competent transport particles that contain both kinesin-1 and dynein-dynactin, but minus-end

transport via TRAK2 is only viable when dynein-binding protein LIS1 is present. This evidence suggests TRAK2 coordinates both plus- and minus-end directed transport of mitochondria *in vitro* (Fenton et al., 2021), but may preferentially drive minus-end directed movement in cells. The directionality of TRAK2-mediated mitochondria distribution, and how the localisation of *TRAK2* mRNA contributes to this, is therefore still not completely understood.

Here we reveal a novel function for mRNA localisation in the control of organelle distribution. First, we define necessary LEs that drive the localisation of mRNAs to the protrusions of motile endothelial cells using the MS2-MCP system. The leading-edge localisation of endogenous polarised mRNA was then disrupted by genomic excision of the LEs. In doing so, we caused the mislocalisation of polarised mRNAs without altering the level of their protein expression. We then reveal that *TRAK2* mRNA mislocalisation is sufficient to drive abnormal mitochondria accumulation in the leading edge, which phenocopies the loss of the protein through siRNA knockdown. Hence, *TRAK2* mRNA localisation is critical for TRAK2 protein function, and for maintaining the correct mitochondria distribution in cells.

### 3.3 Results

#### 3.3.1 Cell-Derived Matrix modifies endothelial cell motile behaviour

To assess the functional consequences of mRNA localisation in cell migration, we first optimised suitable *in vitro* cell culture models. Great insight into the function of localised mRNA has been provided by experiments conducted in simple 2D cell culture with cells grown as a monolayer (Katz et al., 2012; Shestakova et al., 2001). However, 2D systems fail to reproduce all the complex aspects of *in vivo* cell migration. Cells migrating in 2D encounter a simple, single surface, which they translocate along via repeated cycles of protrusion, adhesion, and retraction. This is facilitated by a wide, flat lamellipodia containing transient focal adhesions which provide an interface between cell and surface (Ridley et al., 2003). In contrast, cells migrating *in vivo* encounter a much more complex terrain, with variations in topology and mechanical properties. Hence, migrating cells *in vivo* can adopt a variety of different morphologies and migratory modes to achieve the specific migratory task at hand (Caswell & Zech, 2018). For cells that migrate in a mesenchymal manner, this often involves becoming uniaxially polarised in the direction of migration, protrusion of an extended leading front, and positioning of the nucleus towards the rear (Petrie et al., 2012). Perhaps the most important factor in driving the adoption of these different migratory modes is the extracellular matrix (ECM) (reviewed in Yamada & Sixt, 2019). Endothelial migration *in vivo* is particularly dependent on correct ECM conformation (Astrof & Hynes, 2009). We therefore aimed to identify a physiologically relevant model of cell migration, incorporating aspects of *in vivo* ECM, to test the function of localised mRNAs in endothelial cell migration.

We settled on the use of cell-derived decellularized ECM (CDM). In this system, confluent fibroblasts secrete and organise an ECM consisting mainly of fibronectin fibrillar lattices (Cukierman et al., 2001; Franco-Barraza et al., 2016). Secreted *in vitro* CDM is therefore likely to mimic the required characteristics of *in vivo* endothelial ECM, since fibronectin activation of  $\alpha 5\beta 1$  integrin is essential for angiogenesis (George et al., 1997; Zovein et al., 2010). When hCMEC/d3 cells were grown in CDM, we immediately noticed striking differences in cell behaviour when compared to cells grown in 2D. Cells grown in 2D on glass adopted a lamellipodial style of migration, with multiple lamellipodia per cell (Fig. 3.1a, white arrowheads). In contrast, endothelial cells in matrix adopted a uniaxial morphology resembling the migration of other mesenchymal cells in 3D environments (Figure 3.1b, green arrowheads) (Petrie et al., 2012). Since we observed such an acute

alteration of morphology (Fig. 3.1c, d), we quantified these observed differences using established measures of cell geometry. Aspect ratio (length/width) was significantly larger in endothelial cells in matrix, and circularity was lower (Fig. 3.1e, f). We also observed a decrease in total cell area (Fig. 3.1g). Together this evidence indicates that endothelial cells in matrix adopt a smaller, more elongated, and less round geometry when compared to cells on glass. This type of morphology was reminiscent of migrating cells *in vivo* (Costa et al., 2016). Morphological changes were accompanied by changes to migration dynamics. Endothelial cells in CDM migrated with greater directional persistence and velocity (Fig. 3.1h-k). Together, this analysis indicates that endothelial cells in CDM adopt a more polarised mode of migration, similar to observations of endothelial motility *in vivo*.

### **3.3.2 Polarised mRNAs are enriched in the leading edge during matrix migration.**

We next aimed to assess the role of mRNA localisation during this more physiologically relevant mode of endothelial cell migration. Functional roles for localised mRNA in cell migration have only been identified for *RAB13* and *ACTB* ( $\beta$ -actin) mRNA, which are known to be enriched in the protrusions of multiple cell types including fibroblasts and cancer cells (Lawrence & Singer, 1986; Shestakova et al., 1999). Therefore, we first characterised their localisation as classical examples of polarised mRNAs in our model of CDM migration.

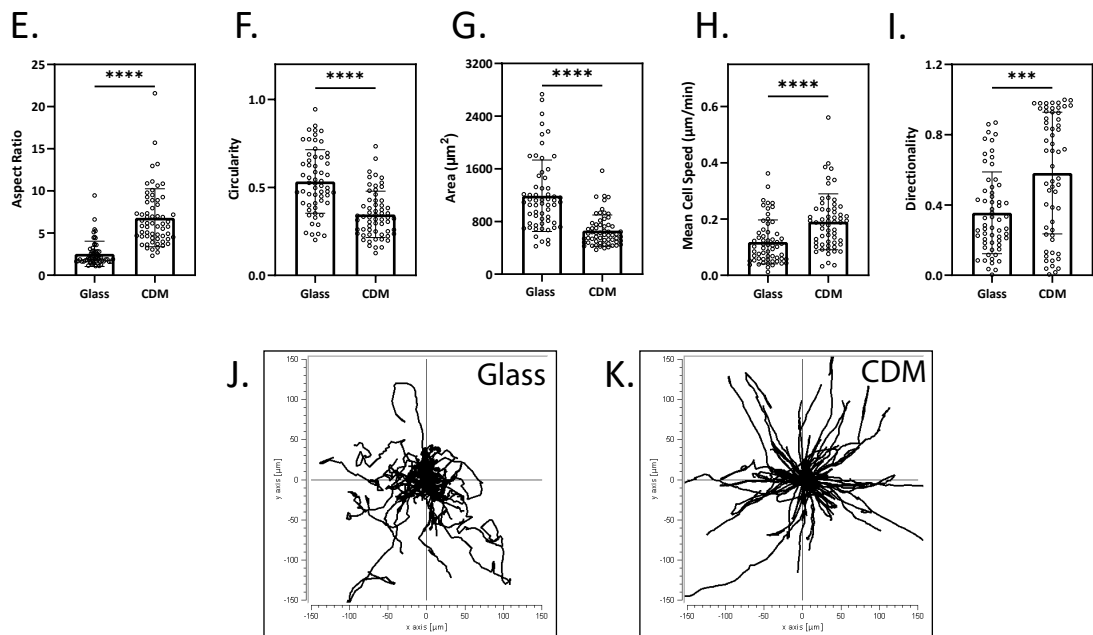
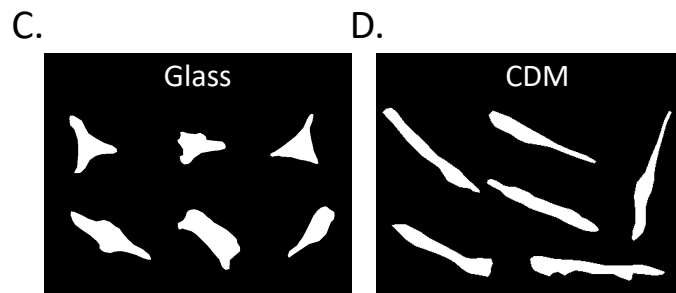
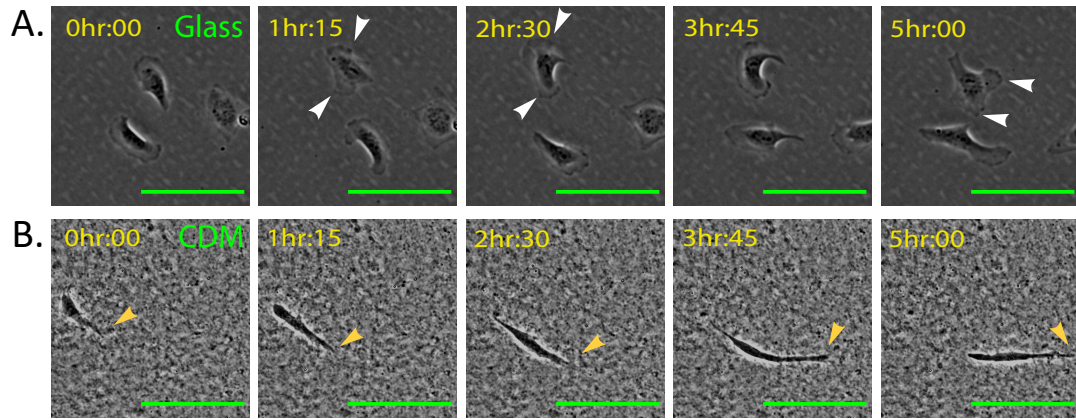


### Figure 3.1: Cell-Derived Matrix Modifies Endothelial Cell Motile Behaviour

- A. Time-lapse imaging of hCMEC/d3 migration on glass. White arrows indicate presence of multiple lamellipodia structures.
- B. Time-lapse imaging of hCMEC/d3 migration in cell-derived matrix. Green arrows indicate clearly defined leading edge.
- C. Representative hCMEC/d3 shapes when cultured on glass.
- D. Representative hCMEC/d3 shapes when cultured in cell-derived matrix.
- E. Aspect ratio of hCMEC/d3 ( $n \geq 50$  cells, Mann-Whitney  $U$ -test).
- F. Circularity of hCMEC/d3 ( $n \geq 50$  cells, unpaired  $t$ -test).
- G. Area of hCMEC/d3 ( $n \geq 50$  cells, Mann-Whitney  $U$ -test).
- H. Mean migratory speed of hCMEC/d3 ( $n \geq 50$  cells, unpaired  $t$ -test).
- I. Directional persistence of hCMEC/d3 ( $n \geq 50$  cells, Mann-Whitney  $U$ -Test).
- J. Rose plots of accumulated migratory distance of hCMEC/d3 migration on glass and in cell-derived matrix.

Data Information: Error bars = SD; Scale bars = 100 $\mu$ m; \* $P < 0.05$ , \*\* $P < 0.01$ , \*\*\* $P < 0.001$ , \*\*\*\* $P < 0.0001$ .

Interestingly, we observed that the classic localised mRNA *ACTB* was not significantly enriched in the leading edge when compared to a control mRNA, *GAPDH*, which is used here as it is diffusely distributed throughout the cell (Fig. 3.2a, f). This is suggestive of previously undescribed motile cell-type diversity in *ACTB* localisation. In contrast, *RAB13* mRNA was strongly enriched in the leading edge when compared to *GAPDH*, which is indicative of its essential role in endothelial cell polarisation (Fig. 3.2b, f) (Costa et al., 2020). We also observed that *RAB13* mRNA polarisation appeared more acute during CDM migration than in cells on glass (Costa et al., 2020).

*KIF1C* and *TRAK2* mRNA are known to be enriched in protrusions of various cell types, yet how this localisation influences cell migration and translated protein function has not been tested (Arora et al., 2021; Samacoits et al., 2018). We found *KIF1C* and *TRAK2* to be also strongly enriched in the leading edge of endothelial cells during matrix migration (Fig. 3.2c, d, g), again exhibiting much more acute polarisation than in cells plated on glass (Costa et al., 2020). This prompted us to investigate the role that *KIF1C* and *TRAK2* mRNA targeting plays during endothelial migration.

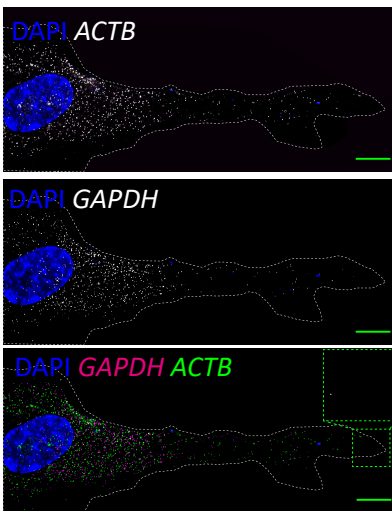
### **3.3.3 G-rich motifs drive *KIF1C* and *TRAK2* mRNA localisation.**

The subcellular destination of a localised mRNA is often defined via 3'UTR sequence elements. In our previous work we identified a uniquely conserved 29bp G-rich sequence element responsible for driving localisation of a group of mRNAs including *KIF1C* and *TRAK2* to motile protrusions (Costa et al., 2020). In all of these localised mRNAs, G-motifs were repeated multiple times within the 3'UTRs, as is often the case for mRNA localisation elements (Chabanon et al., 2004), but the number and distribution of repeats varied greatly between mRNAs. Precise characterisation of the minimal requirement for each of these G-motifs has not been conducted on an mRNA-specific basis. Hence, we first tested the specific requirements for individual G-motifs in targeting *KIF1C* and *TRAK2* mRNA to motile cell protrusions.

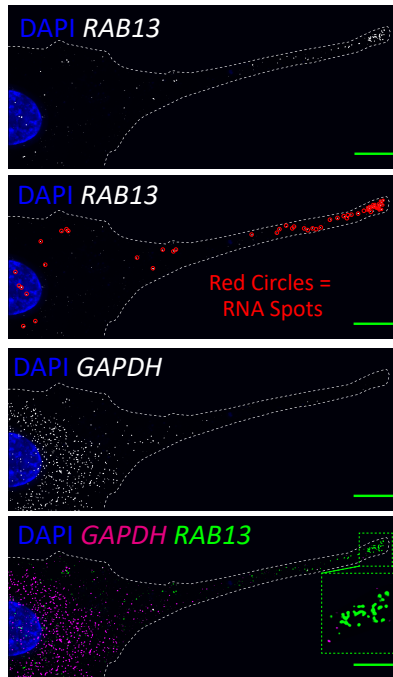
To achieve this, we utilised the MS2-MCP reporter construct system. With this tool, mRNAs are tagged with repeats of the bacteriophage-derived MS2 hairpin, which is a high-affinity binding site for the MS2-capping protein (MCP). Expression of MCP fused to GFP (MCP-GFP) can then be used to visualise the subcellular localisation of mRNA (Bertrand et al., 1998). We generated a construct in which the non-targeted *HBB* coding sequence is tagged



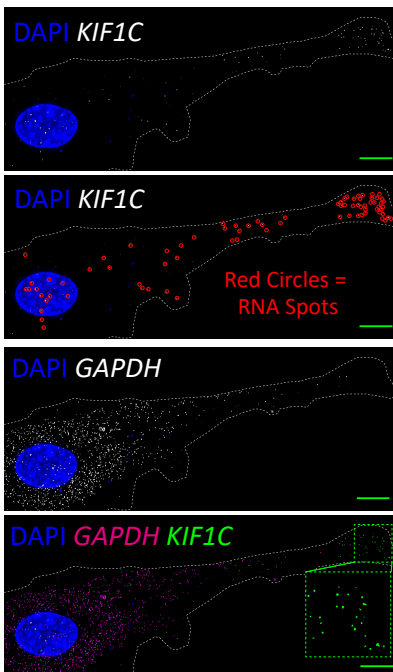
A.



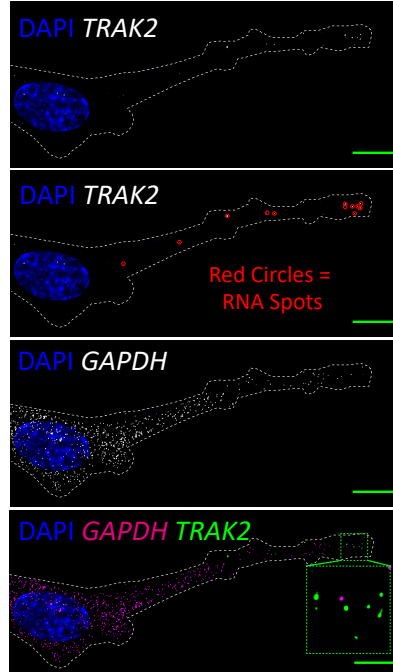
B.



C.



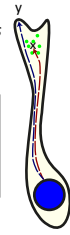
D.



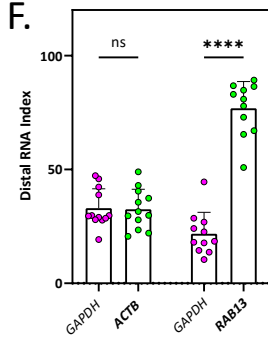
E.

$x = \text{RNA Centre of Mass}$   
 $y = \text{Leading Edge}$

$$\text{Distal RNA Index} = \frac{\text{Length X}}{\text{Length Y}} \times 100$$



F.



G.

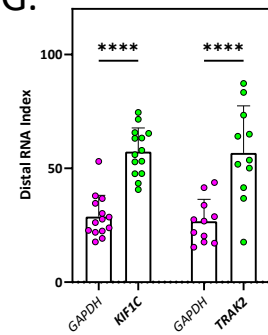


**Figure 3.2: Polarised mRNAs are Enriched in the Leading Edge during Matrix Migration.**

- A. smFISH co-detection of *ACTB* and *GAPDH* mRNA in the leading front of motile hCMEC/d3 cells during cell-derived matrix migration.
- B. smFISH co-detection of *RAB13* and *GAPDH* mRNA in the leading front motile hCMEC/d3 cells during cell-derived matrix migration.
- C. smFISH co-detection of *KIF1C* and *GAPDH* mRNA in the leading front motile hCMEC/d3 cells during cell-derived matrix migration.
- D. smFISH co-detection of *TRAK2* and *GAPDH* mRNA in the leading front motile hCMEC/d3 cells during cell-derived matrix migration.
- E. Schematic showing method for calculation of Distal mRNA Index.
- F. Distal mRNA Index comparing *ACTB* vs. *GAPDH* and *RAB13* vs. *GAPDH* ( $n \geq 11$  cells, one-way ANOVA with Šidák's multiple comparisons test).
- G. Distal mRNA Index comparing *KIF1C* vs. *GAPDH* and *TRAK2* vs. *GAPDH* ( $n \geq 11$  cells, one-way ANOVA with Šidák's multiple comparisons test).

Data Information: Red circles highlight single smFISH mRNA spots; Error bars = SD; Scale bars = 10 $\mu$ m; \*P < 0.05, \*\*P < 0.01, \*\*\*P < 0.001, \*\*\*\*P < 0.0001.

with 24x MS2 loops and 3'UTR sequence elements. We then tested the ability of 3'UTR G-motifs to drive *HBB* mRNA localisation and hence, GFP accumulation in endothelial protrusions by co-expressing the MS2 construct with a nuclear tagged version of MCP-GFP (Fig. 3.3a). In control transfections, GFP accumulation was restricted to the nucleus by the nuclear localisation sequence tagged MCP. However, regions of the *KIF1C* and *TRAK2* 3'UTRs were both observed to drive GFP accumulation to the tips of cellular protrusions (Fig. 3.3b).

We then aimed to identify minimal necessary *TRAK2* and *KIF1C* localisation sequences by sequential truncation and deletions of their 3'UTRs (Fig. 3.3c). The full length *TRAK2* 3'UTR was capable of driving mRNA enrichment, but a shorter 1280bp region at the 5' end of the 3'UTR encompassing three G-motifs had a slightly greater localising capacity. Deletion of a single G-motif from 374-403bp within the 3'UTR had no discernible effect on mRNA localisation. In contrast, when we deleted this central G-motif in combination with a more 5' G-motif from 114-143bp, we found a significant reduction in localising capacity. We then confirmed the necessity of the motif 114-143bp G-motif by deleting it individually, and we observed a similar abrogation in mRNA polarisation. Hence, a single 29bp G-motif in the *TRAK2* 3'UTR is necessary for driving mRNA localisation.

In contrast, for *KIF1C*, we found a distal 3'UTR region from 1106-1600bp containing three G-motifs had no localising capacity, but a proximal region from 1-572bp containing four tightly clustered had strong localisation capacity. However, we found that the region surrounding these proximal four motifs was highly sensitive to deletion, since removal of sequence at either side of the G-motif cluster abrogated localisation. This suggests that the wide sequence surrounding the G-motif cluster may be responsible for driving *KIF1C* localisation, and it is possible that *KIF1C* localisation is G-motif independent. Hence, necessary 3'UTR elements for *TRAK2* and *KIF1C* localisation were tested here, revealing mRNA-specific requirements in spacing, number, and conformation of G-motifs to enable localisation.

### **3.3.4 CRISPR-Cas9 scheme for deletion of endogenous 3'UTR localisation elements.**

Despite studies of exogenous mRNA targeting abilities, as shown in Figure 3.3, our understanding of the role that endogenous sequence elements play in driving mRNA localisation is lacking. To assess the function of *KIF1C* and *TRAK2* localisation, we used the CRISPR-Cas9 system to excise the necessary G-motifs identified in Figure 3.3 from their

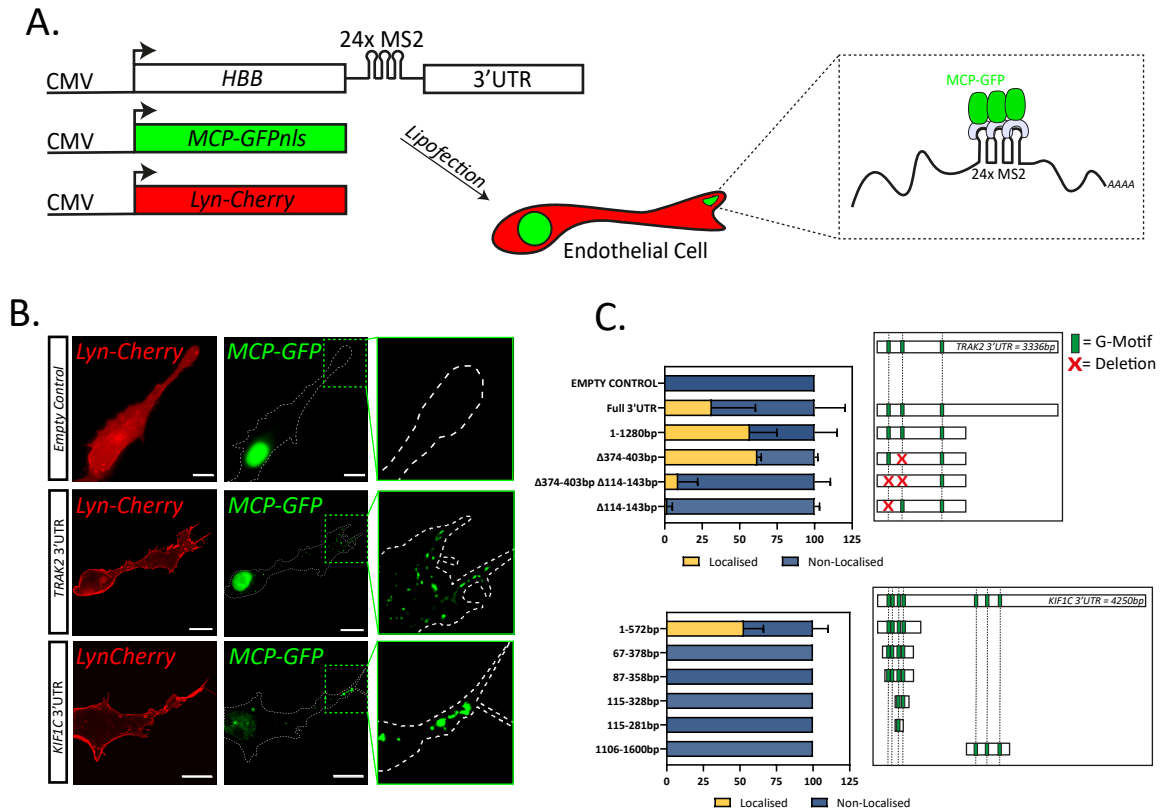


**Figure 3: G-rich motifs drive *KIF1C* and *TRAK2* RNA localisation.**

- A. Schematic showing the *in vitro* MS2 system strategy to identify minimal necessary localisation elements. CMV promoter-driven expression of lyn-Cherry, MCP-GFPnls, and hHBB-24xMS2-tagged 3'UTRs. 24xMS2 binding by MCP-GFPnls allows visualisation of RNA localisation.
- B. Representative bEND5 cells co-expressing lyn-Cherry, MCP-GFPnls, and either 24xMS2, 24xMS2-*TRAK2* 3'UTR, or 24xMS2-*KIF1C* 3'UTR.
- C. Left: Percentage of bEND5 cells with MCP-GFPnls located in protrusions when transfected with truncations or deletions of *TRAK2* and *KIF1C* 3'UTRs. Cells were counted manually. Cells were defined as containing localised mRNA when GFP signal was observed in both the protrusions and the nucleus. In contrast, cells were defined as containing non-localised mRNA when GFP was only present in the nucleus. ( $n \geq 3$  experiments). Right: Scheme showing distribution of G-rich motifs within *TRAK2* and *KIF1C* 3'UTRs.

Data Information: Error bars = SD; Scale bars = 10 $\mu$ m.

respective genomic loci. CRISPR Ribonucleoprotein (RNP) Complexes were introduced to endothelial cells via nucleofection along with a vector expressing GFP. Single endothelial cells were then isolated using fluorescence-activated cell sorting (FACS) to generate clonal populations (Fig. 3.4a). Guide mRNAs were designed to encompass the crucial G-motifs identified as necessary for localisation in the MS2 system (Fig. 3.4b, c). Clones containing homozygous deletions of the G-motifs in their 3'UTRs ( $\Delta$ KIF1C and  $\Delta$ TRAK2) were identified by PCR and sequencing before selection for further analysis (Fig. 3.4d).

Comparisons were made to wild-type (wt) cells, which were created by nucleofection of CRISPR RNP complexes containing no guide mRNA.

### **3.3.5 Genomic excision of G-Motifs impairs mRNA distribution without altering protein expression.**

We tested the functional consequences of motif excision on mRNA localisation by single molecule imaging. When cells were cultured on glass, *TRAK2* and *KIF1C* mRNA was robustly mislocalised upon removal of the functional G-motifs (Fig. 3.5a, b). We quantified mRNA mislocalisation here using well-established unbiased analysis methods for cells in 2D (Park et al., 2012). The polarised spatial pattern of *TRAK2* mRNA was found to be significantly impaired in  $\Delta$ TRAK2 cells, with *TRAK2* mRNA adopting a diffuse distribution similar to *GAPDH* (Fig. 3.5c). *TRAK2* mRNA was also significantly less dispersed, which is indicative of mRNA accumulation in central regions (Fig. 3.5d). In contrast, *KIF1C* mRNA polarisation was not affected in  $\Delta$ KIF1C cells (Fig. 3.5e). This is perhaps due to the highly variable polarisation of *KIF1C* mRNA when cells are in non-physiological 2D scenarios, or the low number of cells analysed in this particular experiment. Nevertheless, *KIF1C* mRNA was significantly less dispersed in  $\Delta$ KIF1C cells, indicating some impairment of normal mRNA localisation (Fig. 3.5f).

Studies probing the function of endogenous mRNA localisation via manipulation of endogenous sequence elements are rare. One of the reasons for this is the challenging requirement of altering mRNA localisation without altering mRNA and protein expression. This challenge is amplified by the fact that 3'UTRs perform many critical regulatory functions aside from mRNA localisation which could be affected by 3'UTR manipulation (Mayr, 2018). Despite this, we observed that G-motif deletion in  $\Delta$ TRAK2 cells did not affect the number of *TRAK2* mRNA spots per cell (Fig. 3.5g). However, *KIF1C* spot number was significantly reduced in  $\Delta$ KIF1C cells (Fig. 3.5h), indicating that removal of the G-rich elements in *KIF1C* may have affected other aspects of mRNA processing. We also performed

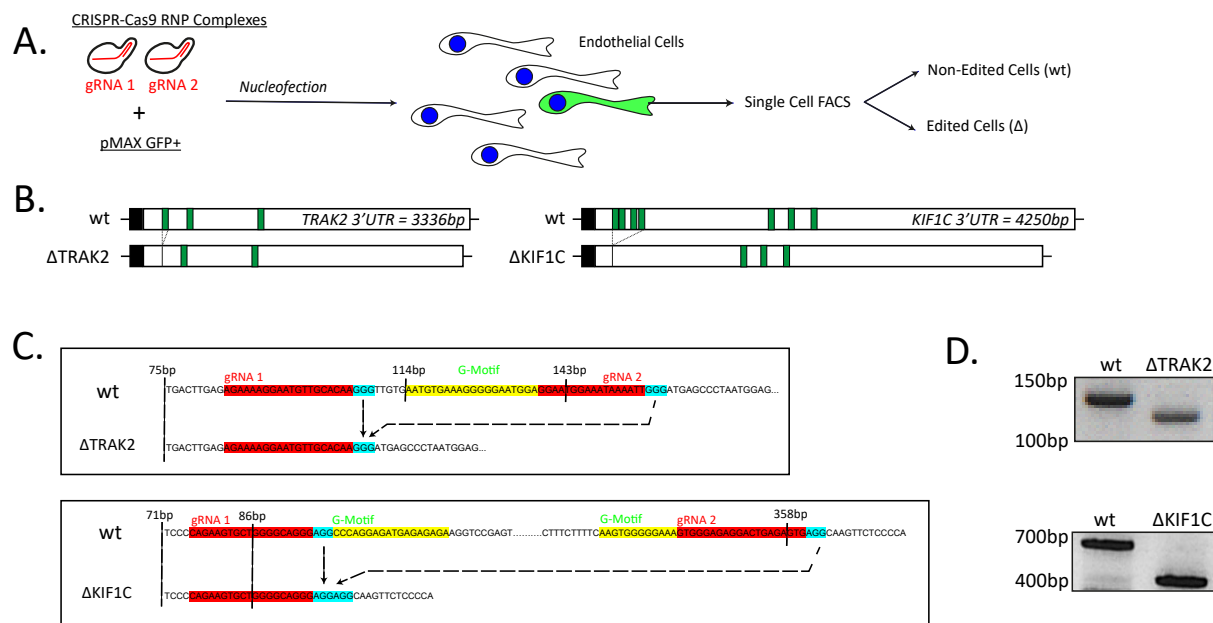


**Figure 3.4: CRISPR-Cas9 scheme for deletion of endogenous 3'UTR localisation elements.**

- Strategy to generate endothelial cell lines with excised 3'UTR localisation elements ( $\Delta$ ) and a non-edited control cell line (wt).
- Scheme showing strategy for endogenous removal of necessary G-motifs from *TRAK2* and *KIF1C* 3'UTRs to generate  $\Delta$ TRAK2 and  $\Delta$ KIF1C cell lines, respectively. Black regions indicate final exons of both RNAs, and clear regions indicate 3'UTRs. Green boxes represent G-motifs.
- Detailed depiction of DNA sequence showing locations of gRNAs target (red highlighted text), NGG PAM sequences (grey highlighted text), and G-motifs (green highlighted text) within *TRAK2* and *KIF1C* 3'UTRs of wt and  $\Delta$ TRAK2/ $\Delta$ KIF1C cell lines.
- Representative genotyping PCR showing band shift in  $\Delta$ TRAK2/ $\Delta$ KIF1C cells.

Western Blots to test whether G-motif deletion affected mRNA translation and protein expression. As expected, deletion of *TRAK2* G-motifs did not disrupt *TRAK2* protein expression in whole cell extracts (Fig. 3.5i, j). To our surprise, *KIF1C* expression in  $\Delta$ *KIF1C* cells was also not affected, despite the reduction in mRNA expression (Fig. 3.5k, l). This illustrates how G-motifs can be precisely excised from 3'UTRs, causing significant mRNA mislocalisation, with no impact on expressed protein levels.

### **3.3.6 Genomic excision of G-motifs impairs mRNA localisation in CDM migration.**

Much of the previous research on mRNA localisation in migrating cells has been conducted in cells in 2D. This means that cells are often multipolar and simultaneously produce multiple protrusions (see Fig. 3.1). This contrasts with motility *in vivo*, where cells produce a clearly defined front and rear. We therefore aimed to understand how G-motif excision affected mRNA localisation in the more physiological context of CDM migration.

Focusing on the leading front of endothelial cells during migration in CDM, we found that *TRAK2* mRNA was depolarised to more proximal regions upon localisation element deletion (Fig 3.6a). Using the Distal mRNA Index quantification method, we found that average *TRAK2* spot localisation was significantly depolarised to a level similar to control mRNA *GAPDH*. In contrast *GAPDH* polarisation remained unchanged (Fig. 3.6b). We also focused on the leading edge to obtain a more detailed understanding of the phenotype. By taking sequential 10 $\mu$ m regions back from the tip of leading edge, we found that the relative frequency of *TRAK2* mRNA position was altered in  $\Delta$ *TRAK2* cells. A significantly reduced proportion of mRNA spots were found in distal reaches of the protrusion, and a significantly larger proportion proximally (Fig. 3.6c). In mutant cells, *TRAK2* then displays a similar distribution to *GAPDH*, the localisation of which is unaffected and remains proximally biased (Fig. 3.6d).

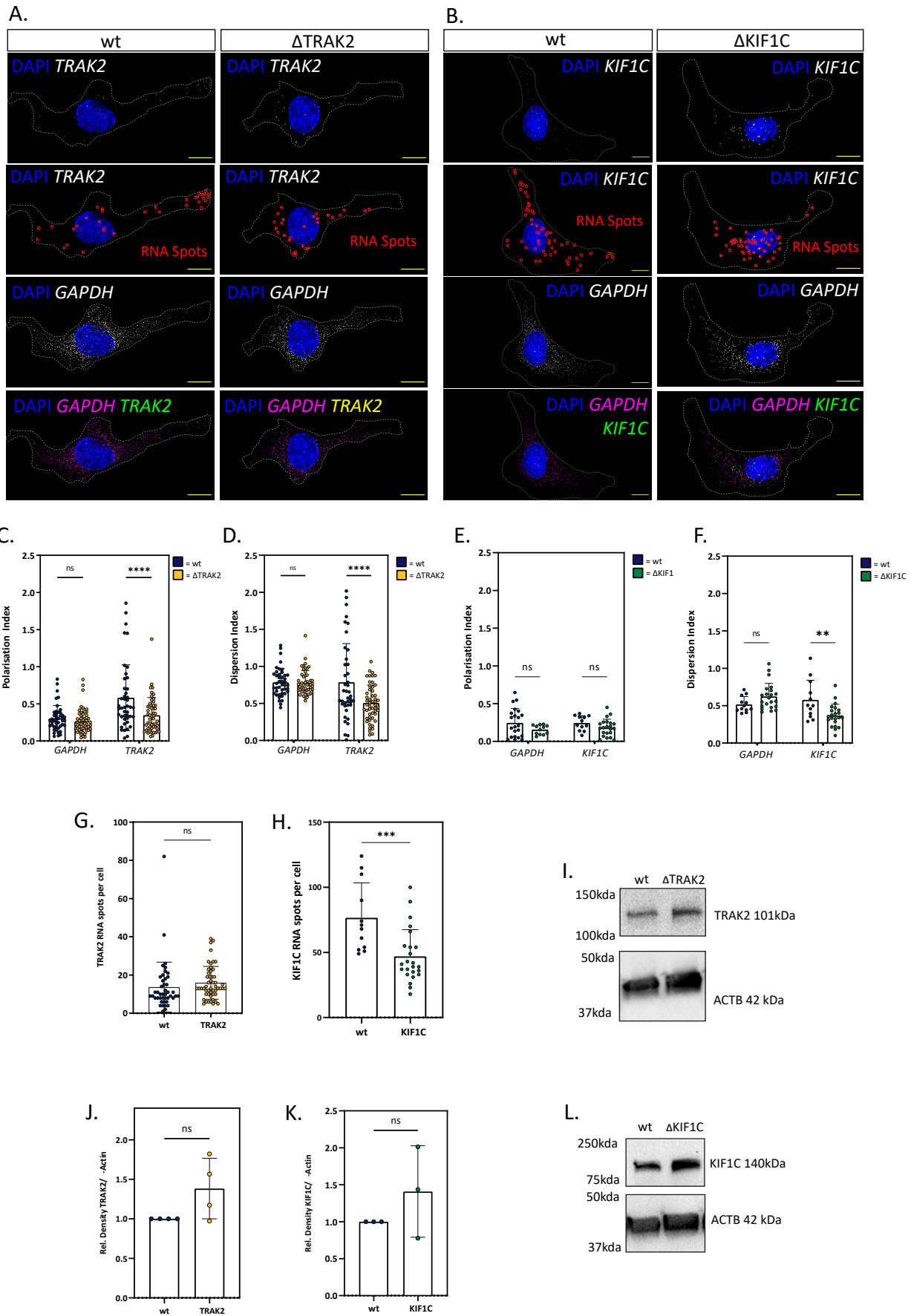




**Figure 3.5: Genomic excision of G-Motifs impairs mRNA distribution without altering protein expression.**

- A. smFISH co-detection of *TRAK2* and *GAPDH* in *wt* and  $\Delta$ TRAK2 cell lines.
- B. smFISH co-detection of *KIF1C* and *GAPDH* in *wt* and  $\Delta$ KIF1C cell lines.
- C. Polarisation Index of *TRAK2* and *GAPDH* mRNA in *wt* and  $\Delta$ TRAK2 cell lines ( $n \geq 40$  cells, one-way ANOVA with Šídák's multiple comparisons test).
- D. Dispersion Index of *TRAK2* and *GAPDH* mRNA in *wt* and  $\Delta$ TRAK2 cell lines ( $n \geq 40$  cells, one-way ANOVA with Šídák's multiple comparisons test).
- E. Polarisation Index of *KIF1C* and *GAPDH* mRNA in *wt* and  $\Delta$ KIF1C cell lines ( $n \geq 12$  cells, one-way ANOVA with Šídák's multiple comparisons test).
- F. Dispersion Index of *KIF1C* and *GAPDH* mRNA in *wt* and  $\Delta$ KIF1C cell lines ( $n \geq 12$  cells, one-way ANOVA with Šídák's multiple comparisons test).
- G. Number of *TRAK2* smFISH spots per *wt* and  $\Delta$ TRAK2 cell ( $n \geq 40$  cells, unpaired *t*-test).
- H. Number of *KIF1C* smFISH spots per *wt* and  $\Delta$ KIF1C cell ( $n \geq 12$  cells, unpaired *t*-test).
- I. Representative Western Blotting of *wt* and  $\Delta$ TRAK2 cells.
- J. Densitometric analysis of  $\Delta$ TRAK2 Western Blot data ( $n = 4$  samples, unpaired *t*-test).
- K. Representative Western Blotting of *wt* and  $\Delta$ KIF1C cells.
- L. Densitometric analysis of  $\Delta$ KIF1C Western Blot data ( $n = 3$  samples, unpaired *t*-test).

Data Information: Red circles highlight single smFISH mRNA spots; Error bars = SD; Scale bars = 10 $\mu$ m; Ns = Not Significant, \*P < 0.05, \*\*P < 0.01, \*\*\*P < 0.001, \*\*\*\*P < 0.0001.

Having previously observed no significant difference in the polarisation of *KIF1C* in  $\Delta$ *KIF1C* cells in 2D (Fig. 3.5e), we next tested whether mislocalisation could be observed in a more physiological context. Deletion of G-motifs caused *KIF1C* to significantly depolarise (Fig. 6e), and Distal mRNA Index was significantly reduced (Fig. 3.6f). In the most distal 0-10 $\mu$ m region of the leading edge in  $\Delta$ *KIF1C* cells, *KIF1C* spot proportion was significantly reduced (Fig. 3.6g). As was also the case for *TRAK2* G-motif deletion, *GAPDH* mRNA distribution remained unchanged after *KIF1C* depolarisation, and *KIF1C* appeared to display a similar proximally skewed localisation in  $\Delta$ *KIF1C* cells. Finally, as a key control, we found *RAB13* to remain highly polarised in our mutant cells. As *RAB13* targeting to cellular protrusions is driven by similar G-motifs to *KIF1C* and *TRAK2*, this confirms the specificity of observed mislocalisation phenotypes (Supp. Fig. 3.1a, b). Together this evidence shows how genomic G-motif excision specifically impairs endogenous *KIF1C* and *TRAK2* mRNA localisation during 3D endothelial migration.

### **3.3.7 *TRAK2* mRNA depolarisation causes mitochondria accumulation in leading edge.**

*TRAK2* is an adaptor protein responsible for the linking of mitochondria to the cytoskeletal network, enabling the trafficking of mitochondria through the cytoplasm. As a route to understanding how *TRAK2* mRNA localisation may contribute to this function, we first confirmed the role of *TRAK2* protein in mitochondria transport in our system. Using siRNAs to significantly reduce *TRAK2* expression (Fig. 3.7a, b) we observed a specific mitochondria distribution phenotype (Fig. 3.7c, d). Focussing on the distal regions of the endothelial protrusions, we observed a significantly larger proportion of mitochondria occupying the most distal 0-10 $\mu$ m region of the leading edge in si*TRAK2* cells (Fig. 3.7e). This is demonstrated by three examples (Fig. 3.7d). We also found that the distance between the most distal mitochondria particle and the leading edge in si*TRAK2* cells was reduced, which suggests that *TRAK2* knockdown expands the range that mitochondria can occupy in the cell (Fig. 3.7f).

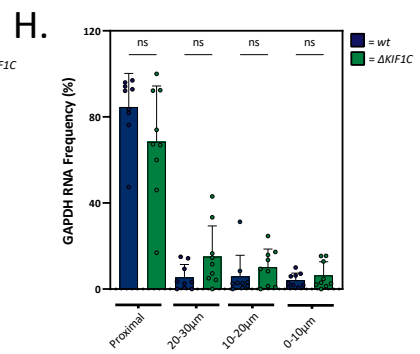
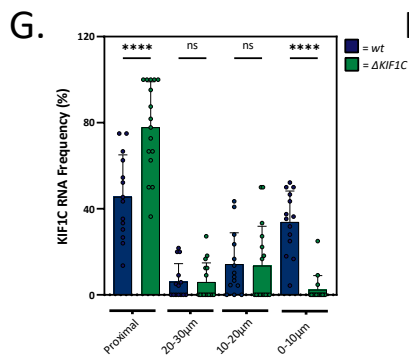
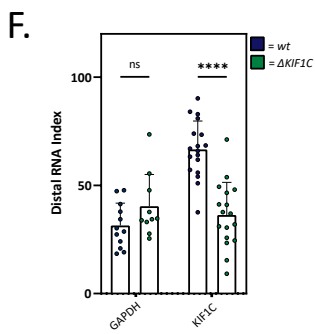
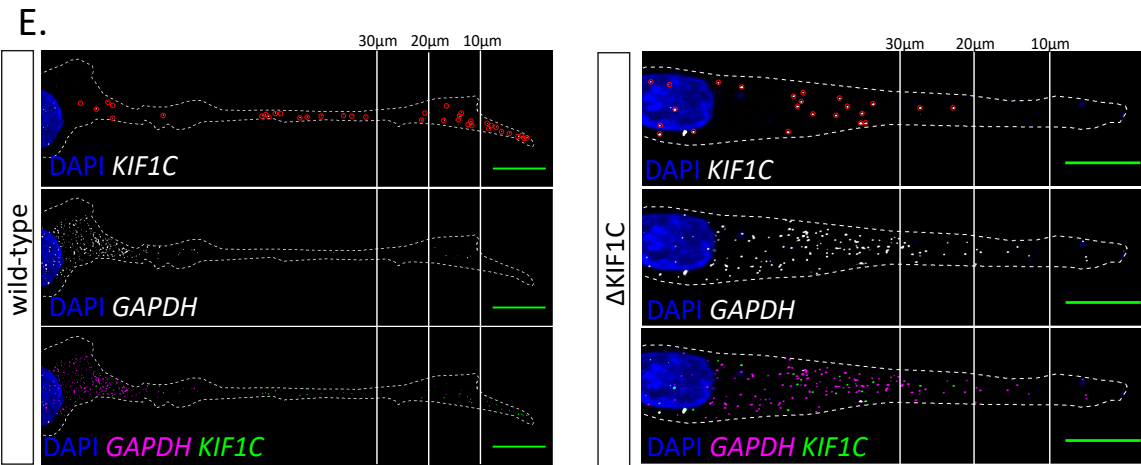
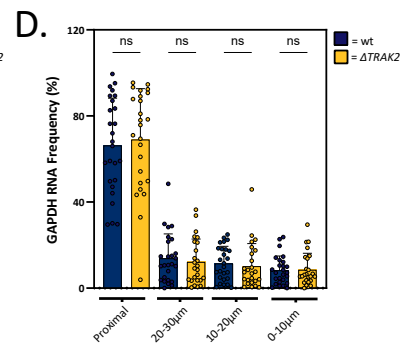
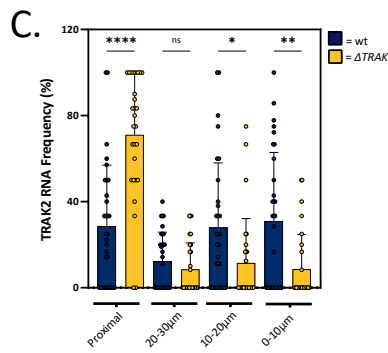
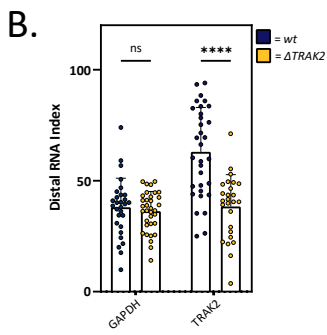
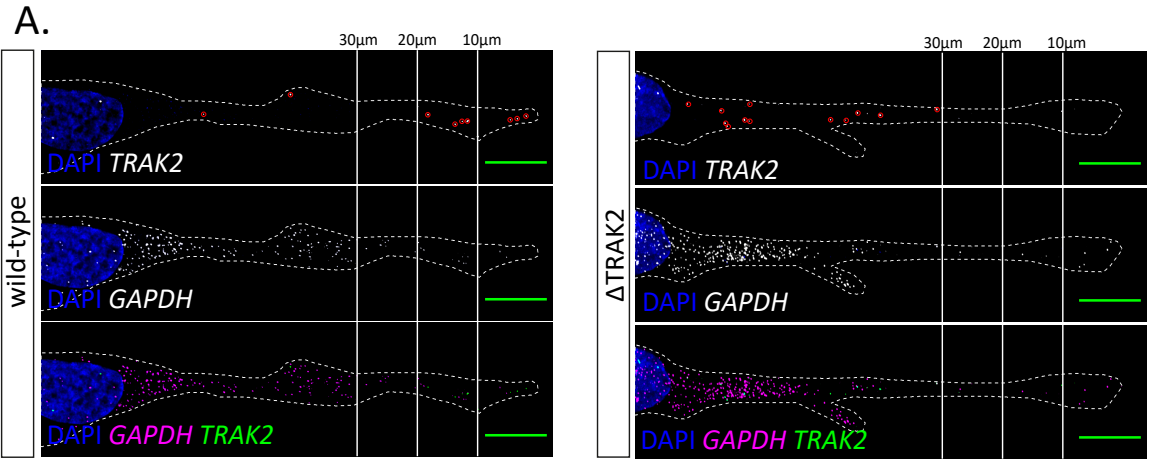


**Figure 3.6: Genomic excision of G-motifs impairs mRNA localisation in CDM migration.**

- A. smFISH co-detection of *TRAK2* and *GAPDH* mRNA in *wt* and  $\Delta$ *TRAK2* cells during cell-derived matrix migration.
- B. Distal mRNA Index quantification of *TRAK2* and *GAPDH* mRNA polarisation in *wt* and  $\Delta$ *TRAK2* cells during cell-derived matrix migration ( $n \geq 28$  cells, one-way ANOVA with Šídák's multiple comparisons test).
- C. Regionalised analysis of *TRAK2* and *GAPDH* mRNA spot proportions in *wt* and  $\Delta$ *TRAK2* cells during cell-derived matrix migration ( $n \geq 28$  cells, one-way ANOVA with Šídák's multiple comparisons test).
- D. smFISH co-detection of *KIF1C* and *GAPDH* in *wt* and  $\Delta$ *KIF1C* cell lines.
- E. Distal mRNA Index quantification of *KIF1C* and *GAPDH* mRNA polarisation in *wt* and  $\Delta$ *KIF1C* cells during cell-derived matrix migration ( $n \geq 14$  cells, one-way ANOVA with Šídák's multiple comparisons test).
- F. Regionalised analysis of *TRAK2* and *GAPDH* mRNA spot proportions in *wt* and  $\Delta$ *TRAK2* cells during cell-derived matrix migration ( $n \geq 14$  cells, one-way ANOVA with Šídák's multiple comparisons test).

Data Information: Red circles highlight single smFISH mRNA spots; Error bars = SD; Scale bars = 10 $\mu$ m; Ns = Not Significant, \*P < 0.05, \*\*P < 0.01, \*\*\*P < 0.001, \*\*\*\*P < 0.0001.

We also quantified mitochondria distribution in an unbiased manner throughout the protrusions (Supp. Fig. 3.2). Using line plots from the nucleus to the tip of the leading edge we measured mitochondria fluorescence intensity. Following normalisation and scaling (see Methods), we plotted the averaged mitochondria intensity according to position along the length of cellular protrusions. We then fitted a third order polynomial to the averaged data to obtain a model for mitochondria distribution. In both control (siCTRL) and TRAK2 knockdown (siTRAK2) samples we observed greater mitochondria intensity in proximal regions, which gradually decreased into distal regions (see fire intensity plot). However, this distribution was significantly altered in siTRAK2 cells, as shown by the deviation of the siTRAK2 polynomial curve from siCTRL. Upon TRAK2 knockdown mitochondria distribution therefore became biased to distal regions (Supp. Fig. 3.2a). Together these results suggest that TRAK2 might be required for retrograde mitochondria trafficking, since reduction of TRAK2 expression causes mitochondria to accumulate distally. This corroborates previous reports documenting TRAK2 function (Onodera et al., 2018; van Spronsen et al., 2013), and contextualises TRAK2 function in physiological cell migration, to reveal a key role in the spatial control of mitochondria distribution.

Despite previous observations of the acute polarisation of *TRAK2* mRNA (Costa et al., 2020; Moissoglu et al., 2020; Pichon et al., 2021), the functional role that polarisation of *TRAK2* mRNA confers on translated protein, and hence mitochondria distribution, has not been tested. Therefore, we tested whether *TRAK2* mRNA mislocalisation affected mitochondria distribution (Fig. 3.7g). Taking a regionalised approach again showed that a significantly increased proportion of mitochondria were found in the leading edge (Fig. 3.7i), and this is demonstrated by a range of example images (Fig. 3.7h). The range of mitochondria distribution was also similarly altered to siTRAK2 treated cells (Fig. 3.7j).

Finally, using the same averaged line plot quantification method described previously, we observed that mitochondria were again skewed to the distal regions when compared to *wt* cells (Supp. Fig. 3.2b). It is clear therefore that *TRAK2* mRNA mislocalisation generates a similar phenotype to the mitochondria oversupply in the leading edge observed when TRAK2 protein levels are reduced. Hence, *TRAK2* mRNA localisation regulates the spatial activity of TRAK2 protein to define the zone of mitochondria distribution during cell migration. Therefore, *TRAK2* mRNA localisation is critical for TRAK2 protein function in motile endothelial cells.

### 3.3.8 mRNA localisation is essential for regulated cellular motility.

Given that mitochondria distribution is a key determinant of cell migration (reviewed in Furnish & Caino, 2020), we next assessed the effect of *TRAK2* mislocalisation on the ability of cells to migrate, by quantifying motile characteristics during CDM migration (Fig. 3.8a). Consistent with reports of increased distal mitochondria and local ATP production,  $\Delta$ TRAK2 cells exhibited markedly increased displacement compared to *wt* cells. In contrast,  $\Delta$ KIF1C cells displayed reduced displacement compared to *wt*, demonstrating the specificity of the  $\Delta$ TRAK2 phenotype (Fig. 3.8b). We then measured mean cell speed during matrix migration and found that whilst cell speed was reduced in  $\Delta$ KIF1C cells, it was significantly increased in  $\Delta$ TRAK2 cells when compared to *wt* cells (Fig. 3.8c). We also observed that  $\Delta$ TRAK2 cells displayed increased Accumulated and Euclidean Distance compared to *wt* cells, whereas  $\Delta$ KIF1C distance was reduced (Fig. 3.8d, e). Interestingly, we found little difference in cell directionality (Fig. 3.8f). Together, this evidence suggests that  $\Delta$ TRAK2 cells migrate faster than *wt* cells and, since cell directional persistence is not affected,  $\Delta$ TRAK2 cells migrate greater distance through the CDM. Therefore, *TRAK2* mRNA mislocalisation results in the adoption of a modified motile cell behaviour. Hence, TRAK2-mediated mitochondria transport appears to function as an internal brake on cell motility, and this process is critically regulated by targeting of *TRAK2* mRNA to the leading edge.

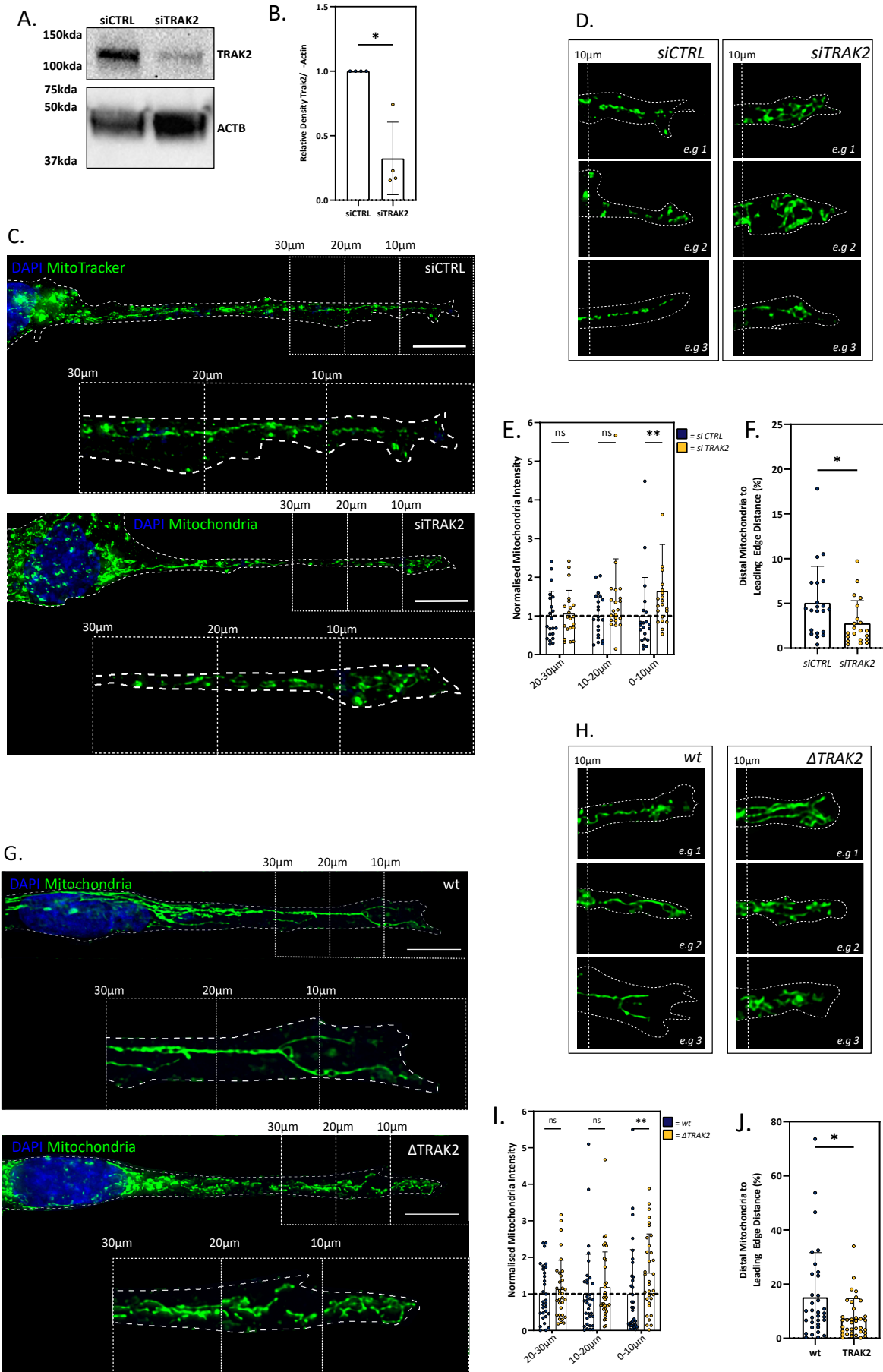


**Figure 3.7: TRAK2 mRNA depolarisation causes mitochondria oversupply in leading edge.**

- A. Representative Western Blotting of hCMEC/d3 treated with control siRNAs (siCTRL) and siRNAs specific to *TRAK2* (siTRAK2).
- B. Densitometric analysis of siRNA Western Blot data (n = 4 samples, unpaired *t*-test).
- C. Representative images of MitoTracker-treated siCTRL and siTRAK2 cells with regions marked at 10 $\mu$ m intervals from protrusion leading edge.
- D. Representative examples of distal 0-10 $\mu$ m region of the leading edge of siCTRL and siTRAK2 cells.
- E. Relative mitochondria fluorescence intensity, as a proportion of whole protrusion mitochondria fluorescence intensity, in distal regions of siCTRL and siTRAK2 cells (n  $\geq$  21 cells, Kruskal-Wallis test with Dunn's multiple comparisons test).
- F. Distance from most distal mitochondria particle to the leading edge in siCTRL and siTRAK2 cells (n  $\geq$  21 cells, Mann-Whitney *U*-test).
- G. Representative images of MitoTracker-treated *wt* and  $\Delta$ TRAK2 cells with regions marked at 10 $\mu$ m intervals from protrusion leading edge.
- H. Representative examples of distal 0-10 $\mu$ m region of the leading edge of *wt* and  $\Delta$ TRAK2 cells.
- I. Relative mitochondria fluorescence intensity, as a proportion of whole protrusion mitochondria fluorescence intensity, in distal regions of *wt* and  $\Delta$ TRAK2 cells (n  $\geq$  31 cells, Kruskal-Wallis test with Dunn's multiple comparisons test).
- J. Distance from most distal mitochondria particle to the leading edge in *wt* and  $\Delta$ TRAK2 cells (n  $\geq$  31 cells, Mann-Whitney *U*-test).

Data Information: Error bars = SD; Scale bars = 10 $\mu$ m; Ns = Not Significant, \*P < 0.05, \*\*P < 0.01, \*\*\*P < 0.001, \*\*\*\*P < 0.0001.



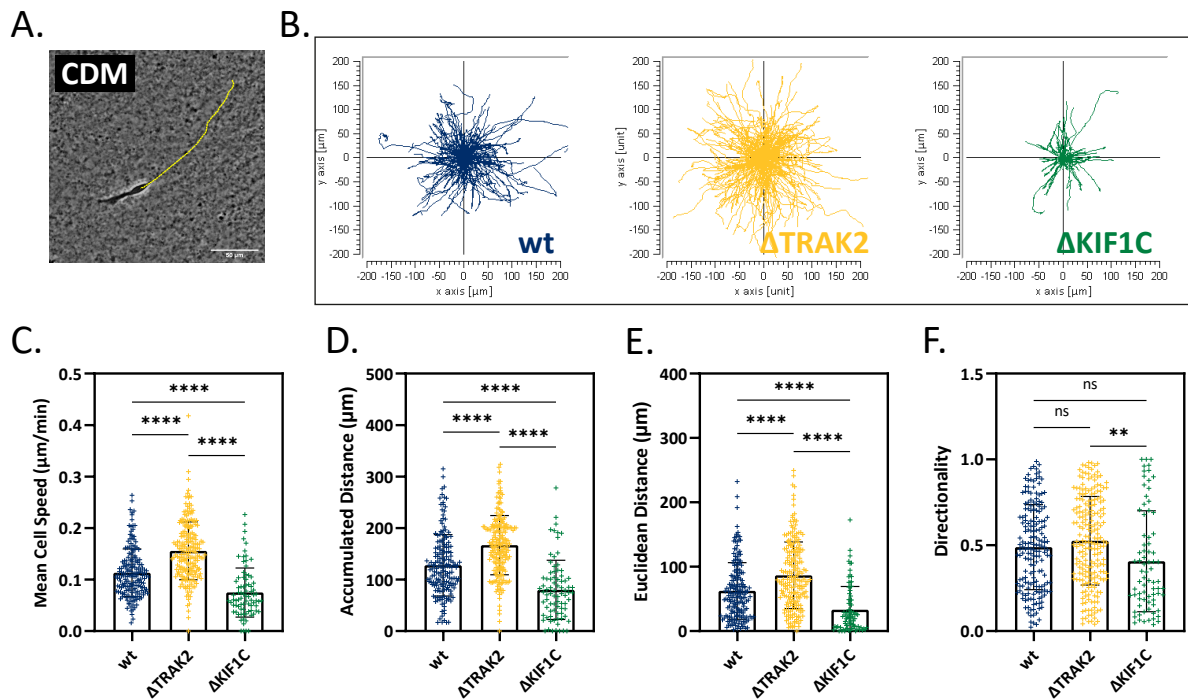


**Figure 8: RNA Localisation is essential for regulated cellular motility.**

- Individual hCMEC/d3 cells in cell-derived matrix were tracked to derived cell motility characteristics.
- Rose plots of *wt*,  $\Delta$ TRAK2, and  $\Delta$ KIF1C cells.
- Mean cell speed of *wt*,  $\Delta$ TRAK2, and  $\Delta$ KIF1C cells (one-way ANOVA with Šídák's multiple comparisons test).
- Accumulated distance travelled by *wt*,  $\Delta$ TRAK2, and  $\Delta$ KIF1C cells (one-way ANOVA with Šídák's multiple comparisons test).
- Euclidean distance travelled by *wt*,  $\Delta$ TRAK2, and  $\Delta$ KIF1C cells (one-way ANOVA with Šídák's multiple comparisons test).
- Directional persistence of *wt*,  $\Delta$ TRAK2, and  $\Delta$ KIF1C cells (one-way ANOVA with Šídák's multiple comparisons test).

Data Information: Error bars = SEM; Scale bar =  $50\mu\text{m}$ ; \*\* $P < 0.01$ , \*\*\*\* $P < 0.0001$ . *wt* = 181 cells,  $\Delta$ TRAK2 = 210 cells,  $\Delta$ KIF1C = 81 cells.

### 3.4 Discussion

Sequencing technologies have revealed that hundreds of mRNAs are enriched in migratory protrusions, but precise understanding of how mRNA distribution contributes to protein function, and the importance of this phenomenon for cell motility, is lacking. Here, we have shown how mRNA polarisation is essential for control of organelle positioning (Fig. 3.9). First, we show that despite sharing conserved G-motif sequences, polarised mRNAs require variable compositions of such sequences to enable their localisation. Excision of localisation sequences from genomic loci prohibited the targeting of endogenous polarised mRNAs to motile protrusions. We then revealed that polarised *TRAK2* mRNA is critically required for *TRAK2* protein function, and hence the correct organisation of mitochondria in the leading edge. Finally, mRNA mislocalisation modulated motile cell phenotype. Therefore, we shed light on a previously unappreciated role that mRNA polarisation plays in the subcellular distribution of mitochondria, and the contribution of this phenomenon to migratory cell behaviour.

#### 3.4.1 Mechanism of Polarised mRNA Targeting.

A variety of 3'UTR sequences and structures are known to drive mRNA localisation to almost every subcellular destination. Of particular relevance to the work here, conserved G-rich sequences are known to target a group of mRNAs to cellular protrusions of both migratory cells and neurons (Arora et al., 2021; Costa et al., 2020; Moissoglu et al., 2020). Here we have demonstrated how the configuration of necessary G-rich elements varies from mRNA to mRNA, despite shared subcellular destinations. G-rich sequences are common in 3'UTRs and perform a variety of vital roles in mRNA processing. Moreover, it has also been reported that the level of G-richness in 3'UTRs does not correlate with protrusion-enrichment of the mRNA (Arora et al., 2021). This raises an important question of how specificity of localisation is achieved, since non-localised mRNAs are also likely to contain G-rich sequences in their 3'UTRs. One possibility is that G-rich sequences play a synergistic role within mRNA structures and RBP complexes. Indeed, we have seen that regions flanking the G-rich cluster in *KIF1C* appear to be important for localisation (Fig. 3c). This indicates that localisation element function is context-dependent within the wider 3'UTR, and complex interplay between sequence and structure is likely the driving force of targeting, rather than just the presence of a G-motif alone.

Conservation of localisation element characteristics is suggestive of possible shared transport mechanisms. A variety of protein cofactors have been shown to be necessary for the localisation of polarised mRNAs including APC (Mili et al., 2008; T. Wang et al., 2017), and UNK (Arora et al., 2021). APC has been reported to anchor polarised mRNAs including *TRAK2* and *KIF1C* at the plus-ends of deetyrosinated microtubules in migratory fibroblasts (Mili et al., 2008), and APC siRNA knockdown has been suggested to reduce endogenous mRNA polarisation (T. Wang et al., 2017). However, recent evidence suggests that APC may not be the driving factor of polarised mRNA targeting in neurons, since APC siRNA knockdown actually increased the polarisation of reporter mRNA tagged with G-rich motifs (Arora et al., 2021). This study also identified a new RBP, UNK, which was shown to play a role in mRNA targeting to neuronal dendrites. Hence, cell type differences in the targeting mechanism for conserved polarised mRNAs are likely to exist.

The molecular motors that drive mRNA polarisation via interaction with RBPs are also yet to be fully characterised. APC has been reported to transport mRNA to microtubule plus-ends in *in vitro* reconstitution assays via kinesin-2 (Baumann et al., 2020). However, recent evidence suggests that KIF1C, a kinesin-1 family molecular motor, also plays a role via interaction with APC, perhaps even in the localisation of its own mRNA (Pichon et al., 2021). However, our evidence suggests that this function may be separate from the function that KIF1C performs when translated from localised *KIF1C* mRNA, since *KIF1C* mRNA mislocalisation does not impair the localisation of other polarised mRNAs (Supp. Fig. 3.1). Therefore, exactly how these different *trans*-acting factors and molecular motors are coordinated to enable mRNA transport remains to be elucidated, particularly when it appears significant cell-type differences may exist between migratory cells and neurons.

### **3.4.2 mRNA localisation regulates retrograde mitochondria transport.**

To date, proteins synthesised from localised mRNA in migratory protrusions have been attributed vital roles in cytoskeletal remodelling and membrane trafficking (Costa et al., 2020; Moissoglu et al., 2020; Shestakova et al., 2001). We present here the first evidence that mRNA localisation may also play a homeostatic role, in facilitating retrograde transport of mitochondria and hence defining the spatial range that mitochondria can occupy in the cytoplasm. Mitochondria positioning depends on a heteromeric protein complex. *TRAK2* plays a vital role in this complex, linking mitochondria to microtubules via motor proteins and the mitochondria-anchored Miro (MacAskill & Kittler, 2010). Participation in both

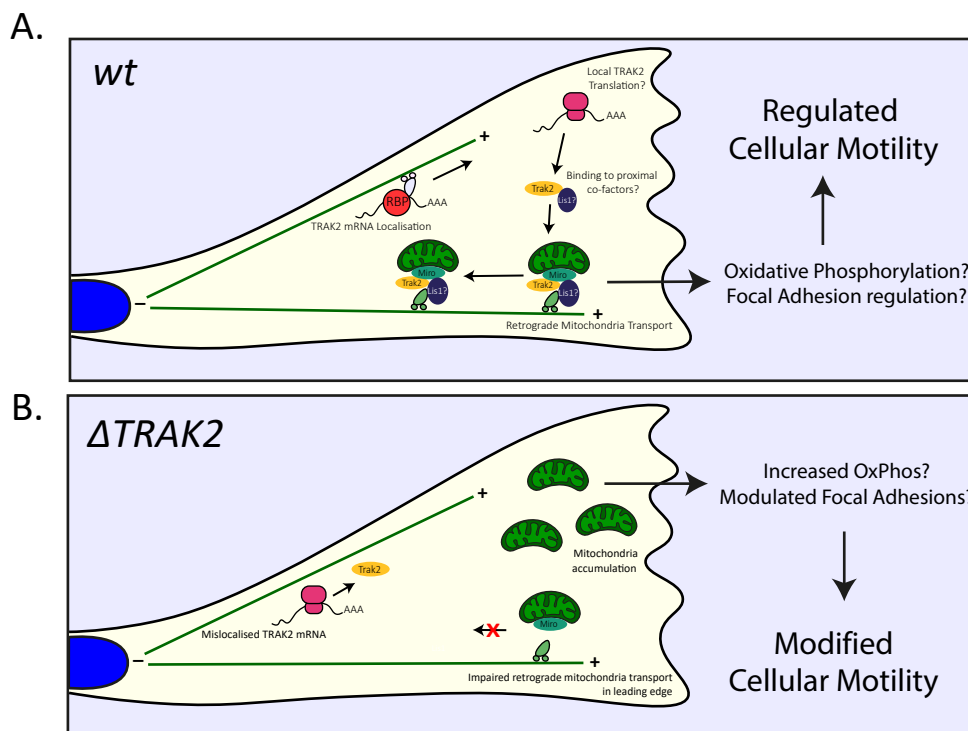


**Figure 3.9: Model for the control of leading edge mitochondria distribution and cell migration speed by *TRAK2* RNA polarisation.**

- A. In wild-type cells, *TRAK2* RNA is localised to endothelial protrusions, where local translation is likely to produce a pool of newly-translated TRAK2 protein. TRAK2 in the leading edge then incorporates into a protein complex that enables mitochondria transport containing Miro, and perhaps Lis1. Minus-end directed mitochondria trafficking is then enabled, allowing precise regulation of leading edge ATP levels and hence cell migration speed.
- B. Conversely, in  $\Delta$ TRAK2 cells, *TRAK2* RNA is mislocalised away from the leading edge, so TRAK2 protein levels in distal reaches of the protrusion are reduced. Minus-end directed trafficking of mitochondria in distal regions is therefore impaired, resulting in mitochondria accumulation. This causes dysregulated ATP levels in the leading edge, and hence modification of cell migration speed.

anterograde and retrograde transport, (and interaction with both kinesin-1 and dynein-dynactin), has been reported *in vitro* for TRAK2. In this scenario an additional co-factor Lis1 is essential to bias minus-end directed movement (Fenton et al., 2021). In our system, it seems TRAK2 functions mainly in retrograde transport, since TRAK2 siRNA knockdown causes accumulation of mitochondria in distal protrusion regions (Fig. 3.7a-f). Interestingly, other studies have shown that Lis1 appears to occupy the distal reaches of neuronal growth cones, which are structurally similar to the protrusions of migrating cells (Grabham et al., 2007). Therefore, it is plausible that *TRAK2* mRNA localisation and local translation may play a role in driving the interaction between TRAK2 and Lis1 to enable retrograde mitochondria trafficking. This is the case for other localised mRNAs, where mRNA positioning and local translation is known to influence the building of protein complexes by enabling co-translational assembly of co-factors (Moissoglu et al., 2020). Hence, *TRAK2* mRNA polarisation and local translation may serve to facilitate the formation of minus-end directed mitochondrial transport protein complexes in distal migratory protrusions.

TRAK2 function is also dependent on post-translational modifications.  $\beta$ -O-linked N-acetylglucosamine transferase (OGT) glycosylation allows TRAK2 to dynamically modulate mitochondria positioning in response to metabolic changes (Iyer et al., 2003; Pekkurnaz et al., 2014). OGT glycosylation of Milton, the *Drosophila* orthologue of TRAK2, has been reported to reduce mitochondrial motility (Pekkurnaz et al., 2014). Moreover, newly synthesised proteins are known to have different functionalities to long-lived proteins, caused by difference in their post-translational modification signatures (Kim et al., 2020). Therefore, it is conceivable that newly translated TRAK2 may have a distinct OGT glycosylation signature to “old” TRAK2. Hence, *TRAK2* mRNA localisation to the leading edge may serve to provide a local pool of newly-synthesised TRAK2 protein, that has distinct potential for driving retrograde mitochondria transport due to its specific post-translational modification signature.

### **3.4.3 Mitochondria positioning controls cell motility.**

The physiological requirement for mRNA localisation in cell migration has been tested by inhibiting the localisation of groups of mRNAs (T. Wang et al., 2017) and single mRNAs (Chrisafis et al., 2020; Costa et al., 2020; Moissoglu et al., 2020; Shestakova et al., 2001). These reports show that cell motility is often impeded upon mRNA mislocalisation. We present the first evidence that mRNA mislocalisation can increase the speed of cell migration,

rather than reduce cell migration ability (Fig. 3.8c). Variation in mitochondria distribution is a well-established hallmark of particular migratory modes. For example, cancer cell invasiveness is promoted by active enrichment of mitochondria at focal adhesions in the front of the cell (Furnish & Caino, 2020). This can shape subcellular energy gradients, biasing ATP levels proximal to lamellipodia (Cunniff et al., 2016; Schuler et al., 2017). A local supply of ATP and GTP is thought to enable cancer cells to fuel energetically demanding processes like signal transduction, protein synthesis, and focal adhesion dynamics at the leading edge. Therefore, *TRAK2* mRNA mislocalisation and mitochondria accumulation in the leading edge may enable endothelial cells to alter their mode of motility by the provision of essential biomolecules for protrusive activity. Plausibly, in the absence of *TRAK2* mRNA localisation, cellular energy could be wasted by migrating at excessive speed, or chaotic directional decision making could occur in complex migratory situations. Therefore, *TRAK2* mRNA localisation acts a brake mechanism to refine cell migration speed via mitochondria redistribution.

In conclusion, this work demonstrates how mRNA localisation is a critical regulator of organelle distribution and cell motile ability. Interestingly, dysregulated mitochondria dynamics and mRNA processing are key features of neurodegenerative disease, yet how these characteristics are linked is not well understood (Quintanilla et al., 2020; E. T. Wang et al., 2016; Yang et al., 2021). Therefore, the results presented within may represent a key stepping-stone in the future advancement of our understanding of mRNA localisation in both health and disease.

### 3.5 Materials and Methods

#### 3.5.1 Cell Culture, Transfections, and Cell-Derived Matrix Production.

HUVEC (PromoCell) and hCMEC/d3 (Poller et al., 2008) were cultured on 0.1% gelatin coated T75 flasks (Corning) in endothelial cell basal medium 2 (EBM-2, Promocell) with an additional supplement pack (5% FCS, EGF (5ng/ml), VEGF (0.5ng/ml), FGF2 (10ng/ml), long R3 insulin growth factor-1 (20ng/ml), hydrocortisone (0.2µg/ml), and ascorbic acid (1µg/ml)). 50mg/ml gentamycin (Sigma) and 250µg/ml amphotericin (Sigma) were also added to the culture media. All HUVEC experiments were conducted with cells between passage 3-6. Mouse Balb/c brain endothelioma cells (b.End5, ATCC) and Telomerase-Immortalised Fibroblasts (TIF) were cultured in Dulbeccos Modified Eagle Medium (DMEM, Sigma) supplemented with 10%FCS and 10U/ml Penicillin-Streptomycin. All cells were split prior to reaching 90% confluency and their media was changed every two days.

For MS2 transfections,  $1 \times 10^5$  b.End5 cells were cultured in 35mm round glass-bottom dishes (Greiner CellView) and transfected with the following: 0.5µg pcDNA3.1-Lyn-Cherry, 1µg pCS2-MCP-GFPnls, 1µg different versions of pcDNA3.1-*HBB*-24xMS2SL-3'UTR. Lipofectamine 3000 (Thermo) was used following manufacturer's instructions. Cells were incubated for 48hrs before microscopic analysis.

Gene knockdown was achieved using ON-TARGETplus non-targeting or gene-specific SMARTpool siRNAs (Horizon). 0.3µM siRNA was diluted in 200µl Opti-MEM containing 1.5% v/v GeneFECTOR (Venn Nova). This mix was then added to a well of a 6-well plate containing 1ml Opti-MEM and the sample was incubated at 37°C for 3 hours. Opti-MEM was then replaced with endothelial growth media and samples were allowed to recover for 48-72 hours.

Cell-Derived Matrixes were produced according to previously described protocols (Cukierman et al., 2001; Franco-Barraza et al., 2016). Briefly, 0.2% gelatin-coated (Sigma) cell culture dishes or coverslips were fixed with 1% Glutaraldehyde (Sigma), before quenching with 1M Glycine (Sigma) and equilibration with DMEM. TIFs were seeded at full confluency and grown for 8 days with 25µg/ml Ascorbic Acid (Sigma), changing the media every 2-3 days. TIFs were then denuded with 20 mM NH<sub>4</sub>OH, 0.5% Triton X-100 in PBS. Finally, samples were treated with 10µg/ml DNase I (Roche) before seeding of endothelial cells.

### 3.5.2 Generation of CRISPR-Cas9 mutant cell lines.

crRNAs were designed to target sequences immediately surrounding the minimal localisation elements in the *TRAK2* and *KIF1C* 3'UTRs using the online IDT Alt-R CRISPR-Cas9 design tool to minimise off-target effects (Table 3.1). IDT Alt-R CRISPR-Cas9 protocol was followed mostly according to manufacturer's instructions. Briefly, 200µM each crRNA was hybridised to 200µM tracrRNA by heating to 95°C in a thermal cycler and allowing to cool to room temperature. RNP complexes were formed by mixing 120pmol crRNA:tracrRNA duplex with 104pmol Alt-R Cas9 in PBS and incubating at room temperature for 20 minutes. RNP complexes for generating *wt* cell lines contain no crRNA:tracrRNA duplexes.

RNP complexes were added to  $5 \times 10^5$  hCMEC/d3 cells along with 2µg pMAX-GFP plasmid (Lonza) and transfection was carried out using a Nucleofector 2b (Lonza) according to manufacturer's instructions. Cells were then cultured for 72hrs before individual GFP-expressing clones were sorted into wells of a 96-well plate using a FACS Aria Fusion cell sorter (BD Biosciences). Clonal populations were screened for genomic lesions using gene-specific primers to amplify regions in the 3'UTRs by PCR (Table 3.1). Two *wt*, four  $\Delta$ *TRAK2* and four  $\Delta$ *KIF1C* were created and used in combination for each experiment.

### 3.5.3 smFISH and Immunofluorescence

Endothelial cells on coverslips and cell-derived matrix were fixed in methanol-free 4% formaldehyde and permeabilised in 70% ethanol. Stellaris single molecule fluorescence *in situ* hybridisation (smFISH) gene-specific probes sets (Table 3.2), conjugated to Quasar 570/670 fluorophores, were designed using an online tool (Biosearchtech), and validated by siRNA knockdown. Predesigned *GAPDH* reference probe sets are purchased directly. smFISH probe hybridisation was carried out as described previously. Briefly, samples were washed in wash buffer (2X SSC, 10% formamide) before incubation overnight at 37°C with smFISH probe sets diluted in hybridisation buffer (2X SSC, 10% formamide, 10% w/v Dextran Sulphate). Samples were then washed twice in wash buffer at 37°C for 30 minutes.

In samples co-stained for mRNA and protein, immunofluorescence was carried out following smFISH. Samples were washed with PBS before blocking with blocking buffer (PBS, 0.2% Tween-20, 5% Goat Serum) for 30 mins. Primary antibodies were diluted in blocking buffer and incubated with samples for 1hr at room temperature. Samples were then washed with blocking buffer before incubation with secondary antibodies for 1hr at room temperature. Samples were mounted using Prolong Gold (Thermo Fisher Scientific).



### 3.5.4 Antibodies

Primary and secondary antibodies were used at the following concentrations: 1:200 rabbit COXIV (immunofluorescence, Thermo Fisher Scientific, MA5-15078), 1:2000 rabbit KIF1C (western blot, Abcam, ab72238), 1:500 rabbit TRAK1 (western blot, Proteintech, 13987-1-AP), 1:1000 rabbit TRAK2 (western blot, Proteintech, 13770-1), 1:3000 HRP-conjugated goat anti-rabbit (Cell Signalling Technology), 1:500 goat anti-rabbit AlexaFluor 488 (Thermo Fisher Scientific).

### 3.5.5 Plasmid Construction

All plasmids for *in vitro* MS2 experiments were generated as described previously (Costa et al., 2020). Briefly, 3'UTR sequences were amplified by PCR using sequence-specific primers (Table 3.1) from human genomic DNA using MyTaq Red Mix (Bioline) according to manufacturer's instructions. Site-directed mutagenesis was used to create precise deletions in 3'UTRs. Primers for SDM were designed using Agilent QuickChange II design software. Phusion (NEB) was then used with the following reactions conditions: denaturation 95°C for 30s, annealing 55°C for 1m30s, extension 72°C for 6m for 18 cycles. Reactions were then treated with DpnI (NEB) for a minimum of 1hr at 37°C. 3'UTR sequences were then cloned into a pcDNA3.1-*HBB*-24xMS2SL-MCS expression vector using the NheI and XhoI/ApaI restriction sites in the multiple cloning site (Costa et al., 2020).

All plasmid maps and details are available upon request.

### 3.5.6 Microscopy

All fluorescent microscopy data was obtained using an Olympus IX83 inverted microscope using Lumencor LED excitation, a 100x/ 1.40 UplanSApo objective and a Sedat QUAD filter set (Chroma 89000). The images were collected using a R6 (Qimaging) CCD camera with a Z optical spacing of 0.2µm. Raw images were then deconvolved using the Huygens Pro software (SVI) and maximum intensity projections of these deconvolved images are shown in the results.

Cell motility tracking data in 3D was obtained using an Eclipse Ti inverted microscope (Nikon) using a 10x/ 0.45 Plan Fluor (Ph1<sup>DLL</sup>) objective, and a pE-300 LED (CoolLED) fluorescent light source. Imaging software NIS Elements AR.46.00.0. Point visiting was used in combination with laser-base autofocus to allow multiple positions to be imaged within the

same time-course, and cells were maintained at 37°C and 5% CO<sub>2</sub>. The images were collected using a Retiga R6 (Q-Imaging) camera.

### **3.5.7 Western Blotting**

Whole cell protein was extracted using RIPA buffer (25 mM Tris-HCl pH 7.6, 150 mM NaCl, 1% NP-40, 1% sodium deoxycholate and 0.1% SDS) containing 1:100 Protease Inhibitor Cocktail. Protein concentration was quantified using Pierce BCA Protein Assay Kit (Thermo Fisher Scientific) before denaturation with Laemmli Buffer (250 mM Tris-HCl pH 6.8, 2% SDS, 10% glycerol, 0.0025% bromophenol blue, 2.5%  $\beta$ -mercaptoethanol) at 95°C for 5 min. Proteins were separated using 10% Mini-PROTEAN TGX precast protein gels (Bio-Rad). Trans-Blot Turbo transfer system (Bio-Rad) was used to transfer proteins to PVDF membranes using manufacturers guidelines. Membranes were then blocked for 1hr at room temperature in 2.5% BSA (Sigma) in TBS containing 0.1% Tween-20. Primary antibodies were diluted in blocking buffer and incubated overnight at 4°C. Membranes were then washes with TBS containing 0.1% Tween-20 before incubation with secondary antibodies diluted in blocking buffer for 1hr at room temperature, followed by more washes. Pierce ECL Western Blotting substrate (Thermo Fisher Scientific) was used to develop chemiluminescent signal, which was then detected digitally using a ChemiDoc MP Imager (Bio-Rad).

### **3.5.8 Image Analysis**

mRNA spot counts were obtained using ImageJ plugin FindFoci (Herbert et al., 2014). mRNA polarisation measurement was obtained for background-subtracted smFISH images using either the previously described Polarisation and Dispersion Index (Park et al., 2012) or Distal mRNA Index. The Distal mRNA Index was developed here to analyse cells migrating in 3D with a unipolar morphology. Briefly, the XY coordinates of the centre of mass of the mRNA fluorescence was calculated using the Analyse menu in ImageJ. The Euclidean distance between these coordinates and the nearest edge of the nucleus was calculated. This distance was then represented as a percentage of the length of the protrusive front of the cell, from the edge of the nucleus to the leading edge.

Mitochondria distribution plots were generated by drawing a segmented line from the edge of the nucleus to the leading edge of cells in ImageJ, adjusting the width of the line to encompass the full width of the cell, and creating a line profile of the fluorescence intensity. Individual pixel fluorescence values along the protrusion were then normalised against the

total protrusion mitochondria fluorescence. Normalised pixel fluorescence values were then scaled from 0-1, before summing of the values within defined bins from 0-0.01, 0.01-0.02, etc... to create 100 bins of equal width along the length of the protrusion. The mean mitochondria fluorescence of each bin (Y axis) was then plotted against protrusion length (X axis). Shaded area in graphs shows the SEM. A 3<sup>rd</sup> order polynomial was then fitted to create a model for how mitochondria fluorescence changes with position along the protrusion.

Cell motility tracking in 3D was performed manually using the MTrackJ plugin for ImageJ. Randomly selected cells were tracked through each frame of the timelapse movies. Imaging in cases was performed for 24 hours with 15 minute intervals. Quantification was achieved using the Chemotaxis and Migration Tool (Ibidi).

### **3.5.9 Statistics**

All data is presented as mean  $\pm$  standard deviation, unless stated otherwise. Accepted levels of significance were \*P < 0.05, \*\*P < 0.01, \*\*\*P < 0.001, \*\*\*\*P < 0.0001. All graphs were produced, and all statistical tests were computed in Graphpad Prism Software. Normality of all data sets was tested using D'Agostino-Pearson tests to determine the use of parametric or non-parametric tests. The exact statistical test and exact *n* is stated in the figure legends.

### 3.6 References

- Andreassi, C., & Riccio, A. (2009). To localize or not to localize: mRNA fate is in 3'UTR ends. *Trends in Cell Biology*, *19*(9), 465–474.  
<https://doi.org/10.1016/J.TCB.2009.06.001>
- Arora, A., Gutierrez, R. C., Eletto, D., Becker, R., Brown, M., Moor, A. E., Russ, H. A., & Taliaferro, J. M. (2021). High-throughput identification of RNA localization elements reveals a regulatory role for A/G rich sequences. *BioRxiv*, 2021.10.20.465152.  
<https://doi.org/10.1101/2021.10.20.465152>
- Astrof, S., & Hynes, R. O. (2009). Fibronectins in Vascular Morphogenesis. *Angiogenesis*, *12*(2), 165. <https://doi.org/10.1007/S10456-009-9136-6>
- Baumann, S., Komissarov, A., Gili, M., Ruprecht, V., Wieser, S., & Maurer, S. P. (2020). A reconstituted mammalian APC-kinesin complex selectively transports defined packages of axonal mRNAs. *Science Advances*, *6*(11), eaaz1588.  
<https://doi.org/10.1126/sciadv.aaz1588>
- Bertrand, E., Chartrand, P., Schaefer, M., Shenoy, S. M., Singer, R. H., & Long, R. M. (1998). Localization of ASH1 mRNA Particles in Living Yeast. *Molecular Cell*, *2*(4), 437–445. [https://doi.org/10.1016/S1097-2765\(00\)80143-4](https://doi.org/10.1016/S1097-2765(00)80143-4)
- Caswell, P. T., & Zech, T. (2018). Actin-Based Cell Protrusion in a 3D Matrix. *Trends in Cell Biology*, *28*, 823–834. <https://doi.org/10.1016/j.tcb.2018.06.003>
- Chabanon, H., Mickleburgh, I., & Hesketh, J. (2004). Zipcodes and postage stamps: mRNA localisation signals and their trans-acting binding proteins. *Briefings in Functional Genomics & Proteomics*, *3*(3), 240–256. <https://doi.org/10.1093/bfpg/3.3.240>
- Chrisafis, G., Wang, T., Moissoglou, K., Gasparski, A. N., Ng, Y., Weigert, R., Lockett, S. J., & Mili, S. (2020). Collective cancer cell invasion requires RNA accumulation at the invasive front. *Proceedings of the National Academy of Sciences*, *117*(44), 27423–27434. <https://doi.org/10.1073/PNAS.2010872117>
- Costa, G., Bradbury, J. J., Tarannum, N., & Herbert, S. P. (2020). RAB13 mRNA compartmentalisation spatially orients tissue morphogenesis. *The EMBO Journal*, *39*(21), e106003. <https://doi.org/10.15252/EMBJ.2020106003>
- Costa, G., Harrington, K. I., Lovegrove, H. E., Page, D. J., Chakravartula, S., Bentley, K., & Herbert, S. P. (2016). Asymmetric division coordinates collective cell migration in angiogenesis. *Nature Cell Biology* *2016 18:12*, *18*(12), 1292–1301.  
<https://doi.org/10.1038/ncb3443>
- Cukierman, E., Pankov, R., Stevens, D. R., & Yamada, K. M. (2001). Taking Cell-Matrix Adhesions to the Third Dimension. *Science*, *294*(5547), 1708–1712.  
<https://doi.org/10.1126/SCIENCE.1064829>
- Cunniff, B., McKenzie, A. J., Heintz, N. H., & Howe, A. K. (2016). AMPK activity regulates trafficking of mitochondria to the leading edge during cell migration and matrix invasion. *Molecular Biology of the Cell*, *27*(17), 2662.  
<https://doi.org/10.1091/MBC.E16-05-0286>

- Fenton, A. R., Jongens, T. A., & Holzbaur, E. L. F. (2021). Mitochondrial adaptor TRAK2 activates and functionally links opposing kinesin and dynein motors. *Nature Communications* 2021 12:1, 12(1), 1–15. <https://doi.org/10.1038/s41467-021-24862-7>
- Franco-Barraza, J., Beacham, D. A., Amatangelo, M. D., & Cukierman, E. (2016). Preparation of extracellular matrices produced by cultured and primary fibroblasts. *Current Protocols in Cell Biology*, 71, 10.9.1. <https://doi.org/10.1002/CPCB.2>
- Furnish, M., & Caino, M. C. (2020). Altered mitochondrial trafficking as a novel mechanism of cancer metastasis. *Cancer Reports*, 3(1). <https://doi.org/10.1002/CNR2.1157>
- George, E. L., Baldwin, H. S., & Hynes, R. O. (1997). Fibronectins Are Essential for Heart and Blood Vessel Morphogenesis But Are Dispensable for Initial Specification of Precursor Cells. *Blood*, 90(8), 3073–3081. <https://doi.org/10.1182/BLOOD.V90.8.3073>
- Glater, E. E., Megeath, L. J., Stowers, R. S., & Schwarz, T. L. (2006). Axonal transport of mitochondria requires milton to recruit kinesin heavy chain and is light chain independent. *Journal of Cell Biology*, 173(4), 545–557. <https://doi.org/10.1083/JCB.200601067>
- Grabham, P. W., Seale, G. E., Bennecib, M., Goldberg, D. J., & Vallee, R. B. (2007). Cytoplasmic Dynein and LIS1 Are Required for Microtubule Advance during Growth Cone Remodeling and Fast Axonal Outgrowth. *Journal of Neuroscience*, 27(21), 5823–5834. <https://doi.org/10.1523/JNEUROSCI.1135-07.2007>
- Herbert, A. D., Carr, A. M., & Hoffmann, E. (2014). FindFoci: A Focus Detection Algorithm with Automated Parameter Training That Closely Matches Human Assignments, Reduces Human Inconsistencies and Increases Speed of Analysis. *PLOS ONE*, 9(12), e114749. <https://doi.org/10.1371/JOURNAL.PONE.0114749>
- Iyer, S. P. N., Akimoto, Y., & Hart, G. W. (2003). Identification and Cloning of a Novel Family of Coiled-coil Domain Proteins That Interact with O-GlcNAc Transferase \*. *Journal of Biological Chemistry*, 278(7), 5399–5409. <https://doi.org/10.1074/JBC.M209384200>
- Jakobsen, K. R., Sørensen, E., Brøndum, K. K., Daugaard, T. F., Thomsen, R., & Nielsen, A. L. (2013). Direct RNA sequencing mediated identification of mRNA localized in protrusions of human MDA-MB-231 metastatic breast cancer cells. *Journal of Molecular Signaling*, 8(1), 9. <https://doi.org/10.1186/1750-2187-8-9>
- Katz, Z. B., Wells, A. L., Park, H. Y., Wu, B., Shenoy, S. M., & Singer, R. H. (2012).  $\beta$ -actin mRNA compartmentalization enhances focal adhesion stability and directs cell migration. *Genes and Development*, 26(17), 1885–1890. <https://doi.org/10.1101/gad.190413.112>
- Kim, N. Y., Lee, S., Yu, J., Kim, N., Won, S. S., Park, H., & Heo, W. do. (2020). Optogenetic control of mRNA localization and translation in live cells. *Nature Cell Biology* 2020 22:3, 22(3), 341–352. <https://doi.org/10.1038/s41556-020-0468-1>
- Kislauskis, E. H., Zhu, X., & Singer, R. H. (1994). Sequences responsible for intracellular localization of beta-actin messenger RNA also affect cell phenotype. *The Journal of Cell Biology*, 127(2), 441–451. <http://www.ncbi.nlm.nih.gov/pubmed/7929587>

- Kislauskis, E. H., Zhu, X., & Singer, R. H. (1997). beta-Actin messenger RNA localization and protein synthesis augment cell motility. *The Journal of Cell Biology*, *136*(6), 1263–1270. <https://doi.org/10.1083/JCB.136.6.1263>
- Lawrence, J. B., & Singer, R. H. (1986). Intracellular localization of messenger RNAs for cytoskeletal proteins. *Cell*, *45*(3), 407–415. <http://www.ncbi.nlm.nih.gov/pubmed/3698103>
- Lécuyer, E., Yoshida, H., Parthasarathy, N., Alm, C., Babak, T., Cerovina, T., Hughes, T. R., Tomancak, P., & Krause, H. M. (2007). Global Analysis of mRNA Localization Reveals a Prominent Role in Organizing Cellular Architecture and Function. *Cell*, *131*(1), 174–187. <https://doi.org/10.1016/j.cell.2007.08.003>
- López-Doménech, G., Covill-Cooke, C., Ivankovic, D., Halff, E. F., Sheehan, D. F., Norkett, R., Birsá, N., & Kittler, J. T. (2018). Miro proteins coordinate microtubule- and actin-dependent mitochondrial transport and distribution. *The EMBO Journal*, *37*(3), 321–336. <https://doi.org/10.15252/emboj.201696380>
- López-Doménech, G., Higgs, N. F., Vaccaro, V., Roš, H., Arancibia-Cárcamo, I. L., MacAskill, A. F., & Kittler, J. T. (2016). Loss of Dendritic Complexity Precedes Neurodegeneration in a Mouse Model with Disrupted Mitochondrial Distribution in Mature Dendrites. *Cell Reports*, *17*(2), 317–327. <https://doi.org/10.1016/J.CELREP.2016.09.004>
- MacAskill, A. F., Brickley, K., Stephenson, F. A., & Kittler, J. T. (2009). GTPase dependent recruitment of Grif-1 by Miro1 regulates mitochondrial trafficking in hippocampal neurons. *Molecular and Cellular Neuroscience*, *40*(3), 301–312. <https://doi.org/10.1016/j.mcn.2008.10.016>
- MacAskill, A. F., & Kittler, J. T. (2010). Control of mitochondrial transport and localization in neurons. *Trends in Cell Biology*, *20*(2), 102–112. <https://doi.org/10.1016/J.TCB.2009.11.002>
- Mayr, C. (2018). What Are 3' UTRs Doing? *Cold Spring Harbor Perspectives in Biology*, *11*(10), a034728. <https://doi.org/10.1101/CSHPERSPECT.A034728>
- Medioni, C., Mowry, K., & Besse, F. (2012). Principles and roles of mRNA localization in animal development. *Development (Cambridge, England)*, *139*(18), 3263. <https://doi.org/10.1242/DEV.078626>
- Mili, S., Moissoglu, K., & Macara, I. G. (2008). Genome-wide screen reveals APC-associated RNAs enriched in cell protrusions. *Nature*, *453*(7191), 115–119. <https://doi.org/10.1038/nature06888>
- Moissoglu, K., Stueland, M., Gasparski, A. N., Wang, T., Jenkins, L. M., Hastings, M. L., & Mili, S. (2020). RNA localization and co-translational interactions control RAB13 GTPase function and cell migration. *The EMBO Journal*, *39*(21), e104958. <https://doi.org/10.15252/EMBJ.2020104958>
- Onodera, Y., Nam, J. M., Horikawa, M., Shirato, H., & Sabe, H. (2018). Arf6-driven cell invasion is intrinsically linked to TRAK1-mediated mitochondrial anterograde

- trafficking to avoid oxidative catastrophe. *Nature Communications*, 9(1), 1–16. <https://doi.org/10.1038/s41467-018-05087-7>
- Park, H. Y., Trcek, T., Wells, A. L., Chao, J. A., & Singer, R. H. (2012). An Unbiased Analysis Method to Quantify mRNA Localization Reveals Its Correlation with Cell Motility. *Cell Reports*, 1(2), 179–184. <https://doi.org/10.1016/j.celrep.2011.12.009>
- Pekkurnaz, G., Trinidad, J. C., Wang, X., Kong, D., & Schwarz, T. L. (2014). Glucose Regulates Mitochondrial Motility via Milton Modification by O-GlcNAc Transferase. *Cell*, 158(1), 54–68. <https://doi.org/10.1016/J.CELL.2014.06.007>
- Petrie, R. J., Gavara, N., Chadwick, R. S., & Yamada, K. M. (2012). Nonpolarized signaling reveals two distinct modes of 3D cell migration. *Journal of Cell Biology*, 197(3), 439–455. <https://doi.org/10.1083/JCB.201201124>
- Pichon, X., Moissoglu, K., Coleno, E., Wang, T., Imbert, A., Robert, M.-C., Peter, M., Chouaib, R., Walter, T., Mueller, F., Zibara, K., Bertrand, E., & Mili, S. (2021). The kinesin KIF1C transports APC-dependent mRNAs to cell protrusions. *RNA*, rna.078576.120. <https://doi.org/10.1261/RNA.078576.120>
- Poller, B., Gutmann, H., Krähenbühl, S., Weksler, B., Romero, I., Couraud, P. O., Tuffin, G., Drewe, J., & Huwyler, J. (2008). The human brain endothelial cell line hCMEC/D3 as a human blood-brain barrier model for drug transport studies. *Journal of Neurochemistry*, 107(5), 1358–1368. <https://doi.org/10.1111/J.1471-4159.2008.05730.X>
- Quintanilla, R. A., Tapia-Monsalves, C., Vergara, E. H., Pérez, M. J., & Aranguiz, A. (2020). Truncated Tau Induces Mitochondrial Transport Failure Through the Impairment of TRAK2 Protein and Bioenergetics Decline in Neuronal Cells. *Frontiers in Cellular Neuroscience*, 14, 175. <https://doi.org/10.3389/fncel.2020.00175>
- Ridley, A. J., Schwartz, M. A., Burridge, K., Firtel, R. A., Ginsberg, M. H., Borisy, G., Parsons, J. T., & Horwitz, A. R. (2003). Cell Migration: Integrating Signals from Front to Back. In *Science* (Vol. 302, Issue 5651, pp. 1704–1709). American Association for the Advancement of Science. <https://doi.org/10.1126/science.1092053>
- Ross, A. F., Oleynikov, Y., Kislauskis, E. H., Taneja, K. L., & Singer, R. H. (1997). *Characterization of a  $\square$ -Actin mRNA Zipcode-Binding Protein*. 17(4), 2158–2165. <http://mcb.asm.org/content/17/4/2158.full.pdf>
- Samacoits, A., Chouaib, R., Safieddine, A., Traboulsi, A.-M., Ouyang, W., Zimmer, C., Peter, M., Bertrand, E., Walter, T., & Mueller, F. (2018). A computational framework to study sub-cellular RNA localization. *Nature Communications* 2018 9:1, 9(1), 1–10. <https://doi.org/10.1038/s41467-018-06868-w>
- Schuler, M.-H., Lewandowska, A., Caprio, G. di, Skillern, W., Upadhyayula, S., Kirchhausen, T., Shaw, J. M., & Cunniff, B. (2017). Miro1-mediated mitochondrial positioning shapes intracellular energy gradients required for cell migration. *Molecular Biology of the Cell*, 28(16), 2159. <https://doi.org/10.1091/MBE16-10-0741>
- Shankar, J., Messenberg, A., Chan, J., Underhill, T. M., Foster, L. J., & Nabi, I. R. (2010). Pseudopodial Actin Dynamics Control Epithelial-Mesenchymal Transition in Metastatic

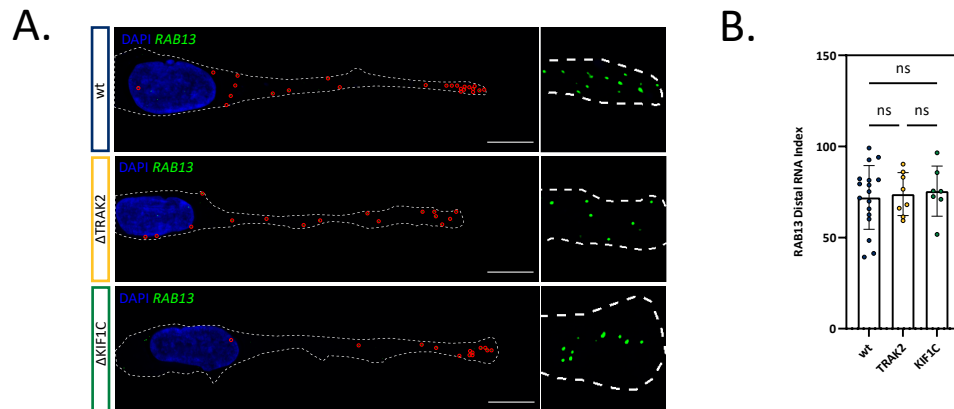
- Cancer Cells. *Cancer Research*, 70(9), 3780–3790. <https://doi.org/10.1158/0008-5472.CAN-09-4439>
- Shepard, K. A., Gerber, A. P., Jambhekar, A., Takizawa, P. A., Brown, P. O., Herschlag, D., DeRisi, J. L., & Vale, R. D. (2003). Widespread cytoplasmic mRNA transport in yeast: Identification of 22 bud-localized transcripts using DNA microarray analysis. *Proceedings of the National Academy of Sciences of the United States of America*, 100(20), 11429–11434. <https://doi.org/10.1073/pnas.2033246100>
- Shestakova, E. A., Singer, R. H., & Condeelis, J. (2001). The physiological significance of beta -actin mRNA localization in determining cell polarity and directional motility. *Proceedings of the National Academy of Sciences of the United States of America*, 98(13), 7045–7050. <https://doi.org/10.1073/pnas.121146098>
- Shestakova, E. A., Wyckoff, J., Jones, J., Singer, R. H., & Condeelis, J. (1999). Correlation of  $\beta$ -Actin Messenger RNA Localization with Metastatic Potential in Rat Adenocarcinoma Cell Lines. *CANCER RESEARCH*, 59, 1202–1205. <http://cancerres.aacrjournals.org/content/canres/59/6/1202.full.pdf>
- Stowers, R. S., Megeath, L. J., Górska-Andrzejak, J., Meinertzhagen, I. A., & Schwarz, T. L. (2002). Axonal Transport of Mitochondria to Synapses Depends on Milton, a Novel Drosophila Protein. *Neuron*, 36(6), 1063–1077. [https://doi.org/10.1016/S0896-6273\(02\)01094-2](https://doi.org/10.1016/S0896-6273(02)01094-2)
- Stuart, H. C., Jia, Z., Messenberg, A., Joshi, B., Underhill, T. M., Moukhles, H., & Nabi, I. R. (2008). Localized Rho GTPase activation regulates RNA dynamics and compartmentalization in tumor cell protrusions. *Journal of Biological Chemistry*, 283(50), 34785–34795. <https://doi.org/10.1074/jbc.M804014200>
- van Spronsen, M., Mikhaylova, M., Lipka, J., Schlager, M. A., van den Heuvel, D. J., Kuijpers, M., Wulf, P. S., Keijzer, N., Demmers, J., Kapitein, L. C., Jaarsma, D., Gerritsen, H. C., Akhmanova, A., & Hoogenraad, C. C. (2013). Article TRAK/Milton Motor-Adaptor Proteins Steer Mitochondrial Trafficking to Axons and Dendrites. *Neuron*, 77, 485–502. <https://doi.org/10.1016/j.neuron.2012.11.027>
- Wang, E. T., Taliaferro, J. M., Lee, J. A., Sudhakaran, I. P., Rossoll, W., Gross, C., Moss, K. R., & Bassell, G. J. (2016). Dysregulation of mRNA Localization and Translation in Genetic Disease. *The Journal of Neuroscience*, 36(45), 11418. <https://doi.org/10.1523/JNEUROSCI.2352-16.2016>
- Wang, T., Hamilla, S., Cam, M., Aranda-Espinoza, H., & Mili, S. (2017). Extracellular matrix stiffness and cell contractility control RNA localization to promote cell migration. *Nature Communications*, 8(1). <https://doi.org/10.1038/s41467-017-00884-y>
- Yamada, K. M., & Sixt, M. (2019). Mechanisms of 3D cell migration. *Nature Reviews Molecular Cell Biology* 20:12, 20(12), 738–752. <https://doi.org/10.1038/s41580-019-0172-9>
- Yang, D., Ying, J., Wang, X., Zhao, T., Yoon, S., Fang, Y., Zheng, Q., Liu, X., Yu, W., & Hua, F. (2021). Mitochondrial Dynamics: A Key Role in Neurodegeneration and a



Potential Target for Neurodegenerative Disease. *Frontiers in Neuroscience*, 15, 359.  
<https://doi.org/10.3389/FNINS.2021.654785/BIBTEX>

Zappulo, A., van den Bruck, D., Ciolli Mattioli, C., Franke, V., Imami, K., McShane, E., Moreno-Estelles, M., Calviello, L., Filipchuk, A., Peguero-Sanchez, E., Müller, T., Woehler, A., Birchmeier, C., Merino, E., Rajewsky, N., Ohler, U., Mazzoni, E. O., Selbach, M., Akalin, A., & Chekulaeva, M. (2017). RNA localization is a key determinant of neurite-enriched proteome. *Nature Communications*, 8(1), 1–13.  
<https://doi.org/10.1038/s41467-017-00690-6>

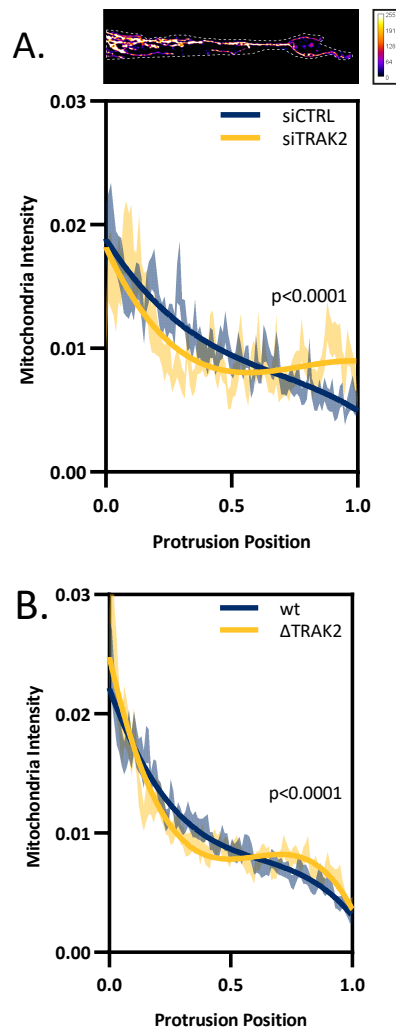
Zovein, A. C., Luque, A., Turlo, K. A., Hofmann, J. J., Yee, K. M., Becker, M. S., Fassler, R., Mellman, I., Lane, T. F., & Iruela-Arispe, M. L. (2010).  $\beta$ 1 Integrin Establishes Endothelial Cell Polarity and Arteriolar Lumen Formation via a Par3-Dependent Mechanism. *Developmental Cell*, 18(1), 39–51.  
<https://doi.org/10.1016/J.DEVCEL.2009.12.006>



**Supplementary Figure 1: Genomic localisation element excision specifically alters host RNA distribution.**

- A. smFISH detection of *RAB13* RNA in *wt*,  $\Delta$ TRAK2, and  $\Delta$ KIF1C cells.
- B. Distal RNA Index quantification of *RAB13* RNA polarisation ( $n \geq 7$  cells, one-way ANOVA with Šídák's multiple comparisons test).

Data Information: Red circles highlight single smFISH RNA spots. Error bars = SD; Scale bars = 10 $\mu$ m; Ns = Not Significant, \*P < 0.05, \*\*P < 0.01, \*\*\*P < 0.001, \*\*\*\*P < 0.0001.



**Supplementary Figure 2: TRAK2 RNA depolarisation causes altered mitochondria distribution.**

- A. Above: Heat map of representative endothelial cell treated with MitoTracker.  
Below: Line plot of mitochondria fluorescence intensity in siCTRL and siTRAK2 cells from the edge of the nucleus to the tip of the leading edge ( $n \geq 21$  cells, 3<sup>rd</sup> order polynomial curve fit, extra-sum-of-squares F-test).
- B. Line plot of mitochondria fluorescence intensity in *wt* and  $\Delta$ TRAK2 cells from the edge of the nucleus to the tip of the leading edge ( $n \geq 31$  cells, 3<sup>rd</sup> order polynomial curve fit, extra-sum-of-squares F-test).

Data Information: Error bars = SEM; Solid line = 3<sup>rd</sup> order polynomial; \*\*\*\*P < 0.0001.

Table 3.1 Oligonucleotide sequences.	
<b>CRISPr/Cas9</b>	
Name	Sequences (5' – 3')
5' crRNA <i>KIF1C</i> 3' UTR	CAGAAGTGCTGGGCAGGGA
3' crRNA <i>KIF1C</i> 3' UTR	GTGGGAGAGGACTGAGAGTG
5' crRNA <i>TRAK2</i> 3' UTR	AGAAAAGGAATGTTGCACAA
3' crRNA <i>TRAK2</i> 3' UTR	GGAGGAATGGAAATAAAATT
<b>Genotyping</b>	
Name	Sequences (5' – 3')
<i>KIF1C</i> 3' UTR F	TGCTAGGAGAAGGGAAGACG
<i>KIF1C</i> 3' UTR R	AAGGAAGAGACAGGAGGGTG
<i>TRAK2</i> 3' UTR F	TGAAACATGTGGTCTGGTCTG
<i>TRAK2</i> 3' UTR R	TCCCTCTGAACACTCATGGC
<b>Cloning</b>	
Name	Sequences (5' – 3')
NheI 1nt <i>KIF1C</i> 3'UTR F	GGAA <u>AGCTAGC</u> GTCCCACATCCTGGGCAGA
XhoI 572nt <i>KIF1C</i> 3'UTR R	GGAA <u>CTCGAG</u> ACCCAAAACAAACAGGCCAC
NheI 87nt <i>KIF1C</i> 3'UTR F	GGAA <u>GCTAGC</u> GGGCAGGGAGGCCAGGAGA
XhoI 358nt <i>KIF1C</i> 3'UTR R	GGAA <u>CTCGAG</u> TCTCAGTCTCTCCACTTTC
NheI 115nt <i>KIF1C</i> 3'UTR F	GGAA <u>GCTAGC</u> AGGTCCGAGTAGGTGATAG
XhoI 328nt <i>KIF1C</i> 3'UTR R	GGAA <u>CTCGAG</u> GAAAAGAAAGTCAAACACT
XhoI 281nt <i>KIF1C</i> 3'UTR R	GGAA <u>CTCGAG</u> ACCCATAGCAGCGTTTGTGG
NheI 67nt <i>KIF1C</i> 3'UTR F	GGAA <u>GCTAGC</u> CTGCTTCCCCAGAAGTGCTG
XhoI 378nt <i>KIF1C</i> 3'UTR R	GGAA <u>CTCGAG</u> CTGGGGAGAAGTTCCTCAC
NheI 1nt <i>TRAK2</i> 3'UTR F	GGAA <u>GCTAGC</u> GGTTCAGCAGTTAACTGACC
XhoI 3336nt <i>TRAK2</i> 3'UTR R	GGAA <u>CTCGAG</u> TGAAAATTCAGCTACTCATG
XhoI 1280nt <i>TRAK2</i> 3'UTR R	GGAA <u>CTCGAG</u> ATCTAACCCAGAGCCTCAC
del114-142 <i>TRAK2</i> R	GGGCTCATCCCAATTTATCACACCCTTGTGCAACAT
del114-142 <i>TRAK2</i> F	ATGTTGCACAAGGGTTGTGATAAAAATTGGGATGAGCCC
del374-402 <i>TRAK2</i> F	AAGCATAAAGCAGAGAGAACCCAGTTTTATTGCTTATAGAAAGC
del374-402 <i>TRAK2</i> R	GCTTTCATAAAGCAATAAACTGGGGTTCTCTCTGCTTTATGCTT
T7 <i>RASSF3</i> 1-1343bp F	taatacgactcactatagggAGCGGGGCTCCCTGCC
<i>RASSF3</i> 1-1343bp R	ACTCACAGTCAAGTTGCCCT
T7 <i>NET1</i> 830-2063bp F	taatacgactcactatagggGTGTAGCATTTCAGGGTAAAGAC
<i>NET1</i> 830-2063bp R	TATTTCTGAAGAACATTCATT
T7 <i>KIF1C</i> 1-572bp F	taatacgactcactatagggGTCCCACATCCTGGGCAGA
<i>KIF1C</i> 1-572bp R	ACCCAAAACAAACAGGCCAC
T7 <i>TRAK2</i> 1-1280bp F	taatacgactcactatagggGGTTCAGCAGTTAACTGACC
<i>TRAK2</i> 1-1280bp R	ATCTAACCCAGAGCCTCAC
T7 <i>NET1</i> 1-956 F	taatacgactcactatagggGAGAAGGCTCTGTGTGTTAAC
<i>NET1</i> 1-956 R	CCAATCACCTTCCCTCTTGC
T7 <i>RASSF3</i> 1343-2655 F	taatacgactcactatagggAGGGCAACTTGACTGTGAGT
<i>RASSF3</i> 1343-2655 R	AACTAATAACTTCAATTTT
<b>Notes:</b> underlined uppercase - restriction site; lower case - T7 promoter sequence.	

Table 3.2 List of smFISH probes.

mRNA	Probe sequence (5' - 3')	mRNA	Probe sequence (5' - 3')	mRNA	Probe sequence (5' - 3')	mRNA	Probe sequence (5' - 3')
<i>ACTB</i>	gctcgagccataaaaggcaa	<i>KIF1C</i>	tctctatcacctactcgg	<i>RAB13</i>	caggccaggaagaagtttc	<i>TRAK2</i>	cacacaattggggaagccaa
<i>ACTB</i>	cgatatacatcatccatggtg	<i>KIF1C</i>	ttggtttgctctcggcaac	<i>RAB13</i>	tggacgggtggcaaacagag	<i>TRAK2</i>	ctttggacagctcagctgg
<i>ACTB</i>	cacgatggagggaagacgg	<i>KIF1C</i>	cttctactctctctcca	<i>RAB13</i>	cagcaactgaagaggtggt	<i>TRAK2</i>	gcactctcatggtattaca
<i>ACTB</i>	acatagggaatcctctgacc	<i>KIF1C</i>	cagcgtttggtggacacac	<i>RAB13</i>	atgatcagacaagtctgcc	<i>TRAK2</i>	gtcaaatgacatccgtgaca
<i>ACTB</i>	ggtactcagggtgaggatg	<i>KIF1C</i>	gtcaaacactggctacgca	<i>RAB13</i>	gtttgtgaagtgtcctctg	<i>TRAK2</i>	aaatgattgtgcacatgg
<i>ACTB</i>	cagatttttccatctctc	<i>KIF1C</i>	acttatgatcctacatgc	<i>RAB13</i>	ttccgatggtggagatgtaa	<i>TRAK2</i>	ggaatccatcaagccattc
<i>ACTB</i>	acacgcagctcattgtgaaa	<i>KIF1C</i>	ccaaatagcaggaggccc	<i>RAB13</i>	ccacagtcgggatctgaaa	<i>TRAK2</i>	gctttggtatgaaacagatg
<i>ACTB</i>	acatgatctgggtcatcttc	<i>KIF1C</i>	cagccaaacaccagctgctc	<i>RAB13</i>	ccagactgtgattgatct	<i>TRAK2</i>	ctttctgctttggtgaga
<i>ACTB</i>	ggatagcacagcctgtagatg	<i>KIF1C</i>	tattaaaggcccacatcc	<i>RAB13</i>	attgtcttgaaccgctcttg	<i>TRAK2</i>	attctgggattgactcatgc
<i>ACTB</i>	catcacgatgcccagtggtac	<i>KIF1C</i>	aagctcccgtgttctctc	<i>RAB13</i>	ttccagctagtagcagtag	<i>TRAK2</i>	ttcacctgtgtggtgatgaa
<i>ACTB</i>	tcgtagatgggcacagtggtg	<i>KIF1C</i>	aaagatcgggctgcgcacc	<i>RAB13</i>	atactaggataatcccctg	<i>TRAK2</i>	gagtctctgtgattgctatt
<i>ACTB</i>	tcttcatgaggtgagctcagtc	<i>KIF1C</i>	cttctgtgctttgctcaca	<i>RAB13</i>	gatttctcatccgtgatctc	<i>TRAK2</i>	cattggagcagacatcagtg
<i>ACTB</i>	taatgtcacgcacgatttcc	<i>KIF1C</i>	aaagcattgacaggtgctgcg	<i>RAB13</i>	ccagttctgaaatattctega	<i>TRAK2</i>	agctcaactcaggagagatc
<i>ACTB</i>	atctcttctcagcctcag	<i>KIF1C</i>	atctgtcagcaacagccag	<i>RAB13</i>	catctctctgagctctttc	<i>TRAK2</i>	ggaagtttctctagacaga
<i>ACTB</i>	caggagaggagctggaacgag	<i>KIF1C</i>	gtaccoccaaaatcctctc	<i>RAB13</i>	ctccatgtcacattgttcc	<i>TRAK2</i>	agtgctctctttgacctat
<i>ACTB</i>	tcattccaatggtgatgac	<i>KIF1C</i>	gacttaagcagaactcct	<i>RAB13</i>	aaatcggattccatgctctc	<i>TRAK2</i>	agtcagctctgattttcat
<i>ACTB</i>	gaaggtagttctggtgagc	<i>KIF1C</i>	gcttggagaccttcaag	<i>RAB13</i>	ctggatttagcactagtcttc	<i>TRAK2</i>	aacggaaagctctctcagca
<i>ACTB</i>	cgtcacactctatgatggag	<i>KIF1C</i>	aggtaaagcagatgatcct	<i>RAB13</i>	aaaagcctcatccacattca	<i>TRAK2</i>	ctgtctgtcctagaatcat
<i>ACTB</i>	tacagctctttgcgtagctc	<i>KIF1C</i>	gcaggttaacacaacagga	<i>RAB13</i>	ctctcactgagcaagatg	<i>TRAK2</i>	gtaagttttgctcatctct
<i>ACTB</i>	caatgccagggtacatggtg	<i>KIF1C</i>	aacaatgatgtagcctgcc	<i>RAB13</i>	agttttcaggtcagctactgg	<i>TRAK2</i>	ggagatgtgaaacatgctgc
<i>ACTB</i>	atcttcattgtctggtgctc	<i>KIF1C</i>	gctcnaagccagaacatta	<i>RAB13</i>	actgtgtggtgttctcttg	<i>TRAK2</i>	cagatcacgacctctctctg
<i>ACTB</i>	ctcaggaggacatgatct	<i>KIF1C</i>	tggcatagtcaaggctcgc	<i>RAB13</i>	aggcaagaaaggctcctcag	<i>TRAK2</i>	tgctcaattcagcagcagc
<i>ACTB</i>	cgatccacacggagtaactg	<i>KIF1C</i>	acctgcacaaatcctggcaa	<i>RAB13</i>	tactatgtgacctccaag	<i>TRAK2</i>	taactgttcccttttaagag
<i>ACTB</i>	tcatactcctgcttgetgat	<i>KIF1C</i>	gcagtcctgtagtacaatc	<i>RAB13</i>	aaccaggttaaggctggaag	<i>TRAK2</i>	ggattgctgtcctcagata
<i>ACTB</i>	atttgcggtggacgatggag	<i>KIF1C</i>	ccagagctctgccaagccaa	<i>RAB13</i>	tttacattatgtttgccct	<i>TRAK2</i>	tcaaaagcgttcccacattg
<i>ACTB</i>	aagtcatagtccgctagaa	<i>KIF1C</i>	aagcagtagctcagagctt	<i>RAB13</i>	ggaccctaaaacctgatcta	<i>TRAK2</i>	atgctcagctgattaactt
<i>ACTB</i>	gtcaagaagggtgtaacgc	<i>KIF1C</i>	ctatggttttggctggaga	<i>RAB13</i>	gagcaaatccctagtgtag	<i>TRAK2</i>	actcatcttctctcatagc
<i>ACTB</i>	ttttctgcgaagttaggtt	<i>KIF1C</i>	aacctaactgttccctcgc	<i>RAB13</i>	agaccatgacaagtgcagaga	<i>TRAK2</i>	ctcagaagcaatggagagc
<i>ACTB</i>	cattgtgaacttgggggat	<i>KIF1C</i>	aaaggcaggagcatcaggg	<i>RAB13</i>	tgcaaatggtgaccttaat	<i>TRAK2</i>	cagctggaatcagtttcaat
<i>ACTB</i>	gtgcaatcaaatcctcgcgc	<i>KIF1C</i>	ggcagtcagaggtgtcaaa			<i>TRAK2</i>	tcattgaaccgaagaggtgt
<i>ACTB</i>	cctgtaaacacgcatctcat	<i>KIF1C</i>	ctgtcaacagctgtgaa			<i>TRAK2</i>	gcaaccctgagataagctca
<i>ACTB</i>	cttttagatggcaaggagac	<i>KIF1C</i>	tacattccagatctgagt			<i>TRAK2</i>	ttttctgagcatttccaa
<i>ACTB</i>	tctcttagagagaagtggg	<i>KIF1C</i>	cactgttgcacaaacctcc			<i>TRAK2</i>	catattctcttccaggt
<i>ACTB</i>	gtggacttggagagagactg	<i>KIF1C</i>	tctatcatttctgctca			<i>TRAK2</i>	gacaagccttgatcgaaga
<i>ACTB</i>	aaagcaatgetatcacctcc	<i>KIF1C</i>	gcattctcggtaacactca			<i>TRAK2</i>	aggtaacagtttctgtctt
<i>ACTB</i>	catacatctcaagtggggg	<i>KIF1C</i>	ttttctatctcaaacccc			<i>TRAK2</i>	agctgtgttccctttcttc
<i>ACTB</i>	actccagggagaccacaaag	<i>KIF1C</i>	tctaagtaaaagttgccca			<i>TRAK2</i>	ttctttaaacacagctgctga
<i>ACTB</i>	gtctcaagctggtgacagg	<i>KIF1C</i>	cttgatggcctagaggggt			<i>TRAK2</i>	tctgagcattgtttcacaga
<i>ACTB</i>	gggtgcaactttattcaac	<i>KIF1C</i>	gaggtgatggtgagctctg			<i>TRAK2</i>	gaaacagctcaactcttc
		<i>KIF1C</i>	aaggccccatgattctaa			<i>TRAK2</i>	agaggaagctctcttgggt
						<i>TRAK2</i>	aggctcaactgtgacaaa
						<i>TRAK2</i>	atgtctttaaagttgtgct
						<i>TRAK2</i>	catcttggaaagcttcagg
						<i>TRAK2</i>	ctgtcttgaactctgctgag
						<i>TRAK2</i>	aacattctgacactccat
						<i>TRAK2</i>	gggccagactactacgaag
						<i>TRAK2</i>	cccagtaaaagctccatag
						<i>TRAK2</i>	caatctcagctgcaaaagat

# **Microtubule-dependent localisation of mRNAs encoding CCN Family proteins to peri-Golgi sites.**

Joshua J. Bradbury<sup>1</sup> and Shane P. Herbert<sup>1,\*</sup>

1. Faculty of Biology, Medicine and Health, University of Manchester, Manchester, UK.

\* = Corresponding Authors.

Intended Journal – Journal of Biological Chemistry.

## **Contribution**

JJB and SPH conceptualised the study. JJB conducted the experimental work and data analysis. JJB designed the figures and wrote the manuscript.

## 4.1 Abstract

CCN Family proteins are crucial secreted regulators of angiogenesis, performing multifaceted roles in endothelial cell adhesion, migration, and proliferation. The molecular regulation of protein secretion has come under the spotlight in recent times, as classical signal recognition particle-mediated entry to the secretory pathway appears to be more complex than previously thought. Yet, the contribution of messenger mRNA targeting as a mechanism influencing classic co-translational secretory pathway entry is relatively unexplored. Here, we investigate the localisation of mRNAs encoding secreted CCN family members, which we previously revealed to display a highly polarised distribution in endothelial cells (Costa et al., 2020). Using single-molecule imaging, we reveal here that CCN Family member mRNAs are accumulated in a polarised proximal cell region that is biased juxta-nuclearly to one side of the cell's longest axis. Importantly, using mRNA and protein co-detection, we found that that CCN Family mRNAs are specifically enriched near, but not physically attached to, the Golgi Apparatus. Finally, a striking co-distribution of single CCN Family mRNAs was observed with microtubule fibres, and microtubule depolymerisation disrupted the mRNA localisation. Therefore, CCN Family mRNAs uniquely occupy a peri-Golgi locale, and they may reach this destination via microtubule active transport. This unique localisation could in turn modulate CCN protein translation rate, or enable post-translational modification of newly-translated CCN protein, and therefore control secreted CCN protein activity. Hence, this study defines a new subcellular mRNA destination which may confer important molecular information to secreted proteins. Ultimately, precise control over secretion of CCN proteins via mRNA localisation could plausibly modulate key aspects of endothelial cell behaviour during angiogenesis.

## 4.2 Introduction

Messenger mRNA localisation is a widespread and vital phenomenon (Medioni et al., 2012). In eukaryotic cells, mRNAs are localised to virtually every known subcellular location. These can include specific zones of cytoplasm, or organelles including the endoplasmic reticulum (ER), centrosomes, mitochondria, and peroxisomes (Das et al., 2021). In recent times, high resolution sequencing and spatial transcriptomics have provided a broad outlook of the diversity of mRNA localisation patterns exhibited by cells (K. H. Chen et al., 2015; Eng et al., 2019). However, detailed characterisation of these patterns in relation to other subcellular

structures, the mechanism of how localised mRNAs reach these destinations, and the function that the mRNA localisation pattern confers on the resulting protein is only known for a handful of mRNAs (Herbert & Costa, 2019).

Some mRNAs are actively targeted to their destination via *cis*-acting localisation elements in their 3'UTRs. These elements are bound by *trans*-acting mRNA binding proteins (RBPs) which link the mRNA to molecular motors for transport via the cytoskeleton, and can also thought to maintain mRNAs in a translationally-repressed state (Buxbaum et al., 2014; Chabanon et al., 2004). However, this paradigm does not usually apply to mRNAs that encode proteins destined for the secretory system. Proteins destined for the classical secretory pathway are targeted to the ER via specialised forms of mRNA localisation. The components that drive this process have been studied for decades and are well understood (Gilmore et al., 1982; Walter & Blobel, 1981). Briefly, ER targeting begins when an N-terminal signal sequence emerges from the ribosome during translation in the cytoplasm. Translation is then paused, and the signal sequence is bound by a conserved ribonucleoprotein complex called the signal recognition particle (SRP). SRP-mediated targeting therefore occurs co-translationally. The ribosome-nascent chain (RNC) complex is then thought to be targeted by the SRP to the surface of the ER, where the SRP interacts with cognate SRP receptor. The RNC is then delivered to the Sec61p machinery, which facilitates translocation of the RNC complex to the ER lumen and entry to the secretory pathway (reviewed in Akopian et al., 2013). In addition to this canonical protein entry pathway, two other pathways have evolved that import proteins posttranslationally. The GET/TRC pathway specifically enables the insertion of tail-anchored membrane proteins (Colombo et al., 2016; Johnson et al., 2013). The SND pathway displays some functional redundancy with both the SRP and GET/TRC pathways, since it appears to support the translocation of protein species with diverse targeting sequences, although some preference is shown to targeting sequences with low hydrophobicity (Aviram et al., 2016; Tirincci et al., 2021). These three pathways therefore work together to ensure that that diverse secretory protein species can enter the ER.

The scale and ubiquity of transcripts that must enter the secretory system creates problems of organisation. 10-20% of the transcriptome (or even more in specialised cells) is thought to pass through the secretory system (Uhlén et al., 2015). In that case, targeting of the correct RNC complexes to the ER must be tightly coordinated. To complicate matters, signal peptides exhibit a wide variety of biochemical characteristics, sizes, and shapes (Saraogi &



Shan, 2011; Zheng & Gierasch, 1996). The dilemma for SRP is therefore that it must be sufficiently flexible to accommodate highly divergent signal peptides, but sufficiently specific to only target the correct mRNA complexes to the ER. Furthermore, the relative contribution of either mRNA targeting via 3'UTR localisation elements or SRP-mediated cotranslational targeting has not been fully tested. This is important when considering that such a wide variety of protein classes appear to be translated at the ER, including a large number of non-secretory proteins that do not contain signal peptides (Jan et al., 2014; Reid & Nicchitta, 2012). Finally, the spatiotemporal control of protein entry to the secretory pathway in subcellular space is also poorly understood. It is not known whether any RNC complex can enter the ER at any location, or whether spatial compartments of the ER carry out specific secretory functions. The potential for this phenomenon is especially relevant in highly polarised or large cells where protein activity domains must be constrained to specific regions. Together, this evidence show that regulation of the site of protein entry to the secretory pathway is complex, and intricate protein-specific pathways are likely to exist. Hence, further research is required to understand the exact mechanisms by which specific proteins enter the secretory pathway.

Here, we have investigated the localisation of mRNAs encoding members of the CCN family during angiogenesis. The CCN family are non-homologous matricellular secreted proteins consisting of 6 members including *CYR61*, *CTGF*, *NOV*, *WISP1*, *WISP2*, and *WISP3* (also named *CCNI-6*). The most well characterised are *CYR61* and *CTGF*, which display pleiotropic functions in skeletal development, fibrosis, cancer, inflammation, and angiogenesis (Brigstock, 2002). CCN multi-functionality is conveyed via the mosaic structure of the proteins, with each consisting of four modular domains including insulin-like growth factor binding protein (IGFBP), von Willebrand factor type C, thrombospondin type 1, and cysteine knot repeats (C. C. Chen & Lau, 2009; N. Chen et al., 2000; Gao & Brigstock, 2004; Leu et al., 2002). Combinatorial binding of different CCN domains to different protein partners enables CCN proteins to act as molecular scaffolds, mediating interaction between cells and the extracellular matrix (Grzeszkiewicz et al., 2002). In doing so, CCN family members regulate key cell behaviours like adhesion, proliferation, and migration (Kubota & Takigawa, 2007). Modulation of adhesion is primarily achieved through activation of integrin  $\alpha V\beta 3$  (Babic et al., 1999) and  $\alpha V\beta 1$  (Leu et al., 2002). Growth factor signalling can also be altered by CCN proteins through direct binding to TGF- $\beta$ , BMP4, FGF, and VEGF, and

therefore modulation of the ability of these growth factors to bind to their cognate receptors (Abreu et al., 2002; Inoki et al., 2002; Kolesnikova & Lau, 1998). Interestingly, expression of CCN members is also regulated by VEGF, bFGF, TGF $\beta$ , and the Hippo pathway (Astone et al., 2018; Shimo et al., 1998; Suzuma et al., 2000). This indicates that complex feedback pathways exist in the regulation of CCN family expression and activity. Perhaps the most well-characterised cellular functions of *CYR61* and *CTGF* are in angiogenesis. *CYR61* knockout mice are embryonic lethal due to angiogenic defects in the placental vasculature thought to be mediated by local impairment of VEGF activity (Mo et al., 2002). In contrast *CTGF* knockout mice are not embryonic lethal but die at birth due to defects of angiogenic infiltration of bones (Ivkovic et al., 2003). This evidence demonstrates the vital role that CCN family members play in the regulation of vascular development. Whilst the cellular functions and upstream regulators of CCN family members are well known, the molecular regulation of their secretion is poorly understood.

We have recently characterised the cell-type diversity of mRNA localisation in migratory endothelial cells (G. Costa et al., 2020). We identified a collection of mRNAs including the CCN family members *CYR61* and *CTGF* that display a unique and conserved perinuclear distribution. Here, we interrogate this localisation further. We first reveal that *CTGF* and *CYR61* transcripts display highly polarised, juxtannuclear asymmetry along the cell's longest axis. Considering the CCN family are secreted proteins, we then compared the relative localisation of *CYR61* mRNA to various secretory pathway components, and observed accumulation adjacent to the *cis*-Golgi. The specificity of this localisation was then compared to other highly expressed mRNAs encoding secretory proteins, to show that peri-Golgi distribution is a unique feature of CCN family mRNAs. Physical interaction of *CYR61* mRNAs with the *cis*-Golgi was not detected, since Golgi collapse did not alter the mRNA localisation. Finally, the mechanism by which *CYR61* mRNAs reach their Golgi-adjacent destination was tested. Individual *CYR61* mRNA molecules were observed to partially overlap with microtubule filaments, and microtubule depolymerisation severely disrupted the mRNA localisation. Together, this evidence suggests that CCN family mRNAs display a unique distribution pattern that distinguishes them from other secretory proteins, and they may reach this unique locale via microtubule transport. This work therefore adds weight to recent evidence that protein entry to the secretory system is a more complex process than previously thought.

## 4.3 Results

### 4.3.1 *CYR61*, *CTGF*, and *EDNI* display mRNA polarisation along cell long axis.

In our previous work we conducted a screen for mRNA asymmetries in migratory endothelial cells (Costa et al., 2020). By comparing our data to other published datasets, we were able to characterise the cell-type diversity of mRNA localisation. Interestingly, we found that mRNA spatial patterns were confined to specific clusters, including an observed perinuclear localisation of cluster *k7* mRNAs, which contrasted with the distinct localisation patterns of mRNAs from other clusters. The conserved nature of the perinuclear localisation pattern of the *k7* mRNAs led us to speculate that they encode proteins with related functions. Strikingly, we noticed that this cluster included the two most well-characterised members of the CCN family, *CTGF* and *CYR61*, which are known as important regulators of endothelial cell biology. Moreover, another key secreted regulator of endothelial cell behaviour, *EDNI*, was also present in this cluster, and displayed similar perinuclear localisation. The critical importance of these proteins for angiogenesis and their unique mRNA spatial distributions motivated us to characterise their localisation further.

In our previous work, we observed that *CYR61*, *CTGF*, and *EDNI* display a concentrated perinuclear localisation when cells are migrating in 2D on glass, and hence when quantified have significantly lower polarisation indexes than a control, diffusely distributed *GAPDH* (G. Costa et al., 2020). This localisation was markedly different to that displayed by other groups of polarised mRNAs, especially the highly polarised and peripherally-located *k5* transcripts such as *RAB13* and *TRAK2* (G. Costa et al., 2020). The proximally-accumulated localisation of the *k7* mRNAs in endothelial cells grown on a flat substrate was initially surprising to us, since this group was significantly and consistently enriched in the protrusions of endothelial cells during 3D Transwell migration (G. Costa et al., 2020). However, since different extracellular environments can promote different modes of migration (Yamada & Sixt, 2019), we hypothesised that *k7* mRNA polarisation may be more subtle during 2D migration. We therefore aimed to find a suitable quantification method to test for more subtle forms of mRNA polarisation.

Quantification methods for analysing mRNA localisation patterns have mostly been developed to describe mRNAs that are highly enriched in peripheral and distal cell processes (Park et al., 2012; Stueland et al., 2019). Since *CYR61*, *CTGF*, and *EDNI* are all uniquely located in central cell regions during 2D migration, we wanted to test whether these mRNA

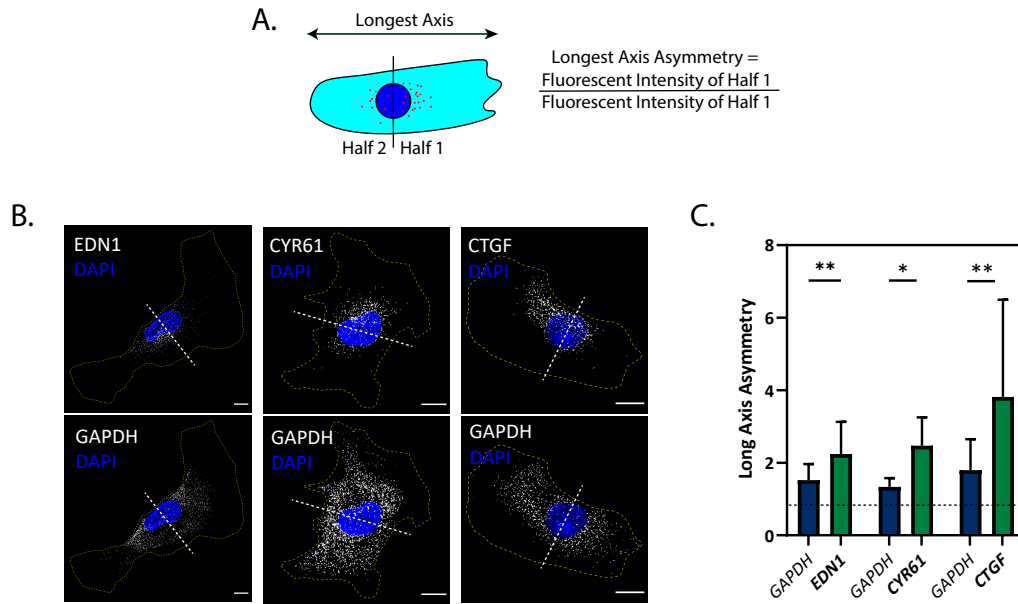


**Figure 4.1: *CYR61*, *CTGF*, and *EDN1* display RNA polarisation along cell long axis.**

- A. Illustration of method for quantification cell long axis RNA polarisation.
- B. smFISH co-detection of *CYR61*, *CTGF*, and *EDN1* RNAs with *GAPDH* in endothelial cells.
- C. Polarisation of *CYR61*, *CTGF*, and *EDN1* RNAs co-detected in endothelial cells ( $n \geq 6$  cells; \* $P < 0.05$ , \*\* $P < 0.01$ , Wilcoxon test).

Data Information: Scale bars =  $10\mu\text{m}$ ; Error Bars = SD; white dotted line indicates perpendicular line to cell long axis, along which cells were divided in two for analysis.

display intrinsic polarity to the leading side of the nucleus, which may explain their identification as polarised mRNAs by mRNA-seq. As an unbiased detection method to test for whole cell mRNA asymmetry, we visually identified the cells longest axis and divided the cell in two perpendicular to this axis through the centre of the nucleus to create two subcellular areas (Fig. 4.1a). We then measured the fluorescence intensity of *CYR61*, *CTGF*, and *EDNI* in these two areas and calculated a ratio by dividing the area with the highest fluorescence intensity by the lowest. We found that *CYR61*, *CTGF*, and *EDNI* display greater mRNA asymmetry along the cells longest axis than diffusely distributed control mRNA *GAPDH* (Fig. 4.1b, c). This suggests that despite their perinuclear accumulated distribution, this group of mRNAs are naturally polarised to one side of the cell.

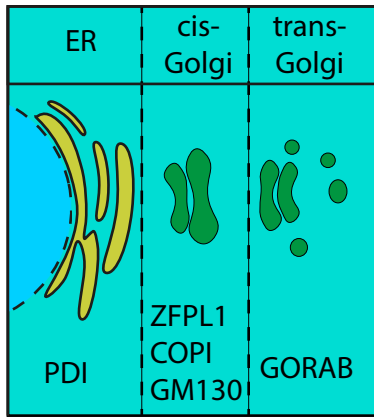
#### **4.3.2 Comparing *CYR61* localisation to secretory pathway components.**

During cell migration and wound healing, the centrosome and Golgi apparatus reorient towards the leading edge and membrane trafficking becomes polarised to the front of the cell (Dubois et al., 2017; Kupfer et al., 1982; Martin et al., 2018; Xing et al., 2016). This is thought to be essential for a number of reasons including for the local deposition of extracellular and membrane proteins to the leading edge (Schmoranzer et al., 2003). Since *CYR61*, *CTGF*, and *EDNI* encode important secreted proteins, we hypothesised that they might be polarised to orient with the secretory pathway. We therefore wanted to refine our understanding of their asymmetric mRNA distribution by comparing their localisation to various components of the secretory pathway. We chose antibody markers of secretory pathway components including the ER, the *cis*-Golgi, and the *trans*-Golgi, and co-stained for these with *CYR61* in migratory endothelial cells. We chose a general ER marker Protein Disulphide Isomerase (PDI), a *cis*-Golgi and ER-Golgi Intermediate Compartment marker COPII, the specific *cis*-Golgi markers ZFPL1 and GM130, and a *trans*-Golgi marker Rab6-interacting Golgin (GORAB) (Fig. 4.2a). The ER in this cell type appears to occupy most of the cell, hence no specific polarised association of *CYR61* could be seen. Surprisingly, we did observe accumulations of mRNA close to and overlapping the *cis*-Golgi, but less so with the *trans*-Golgi (Fig. 4.2b; arrows). This qualitative, comparative assessment inspired us to apply quantitative measures to understand the proximal Golgi localisation of *CYR61* further.

#### **4.3.3 *CYR61* mRNA is enriched adjacent to the *cis*-Golgi.**

We decided to compare the Golgi-adjacent localisation of *CYR61* to control mRNAs *LAMB1* and *COL4A1*. These mRNAs were chosen because they also encode secreted proteins, and

A. Secretory Pathway



B.

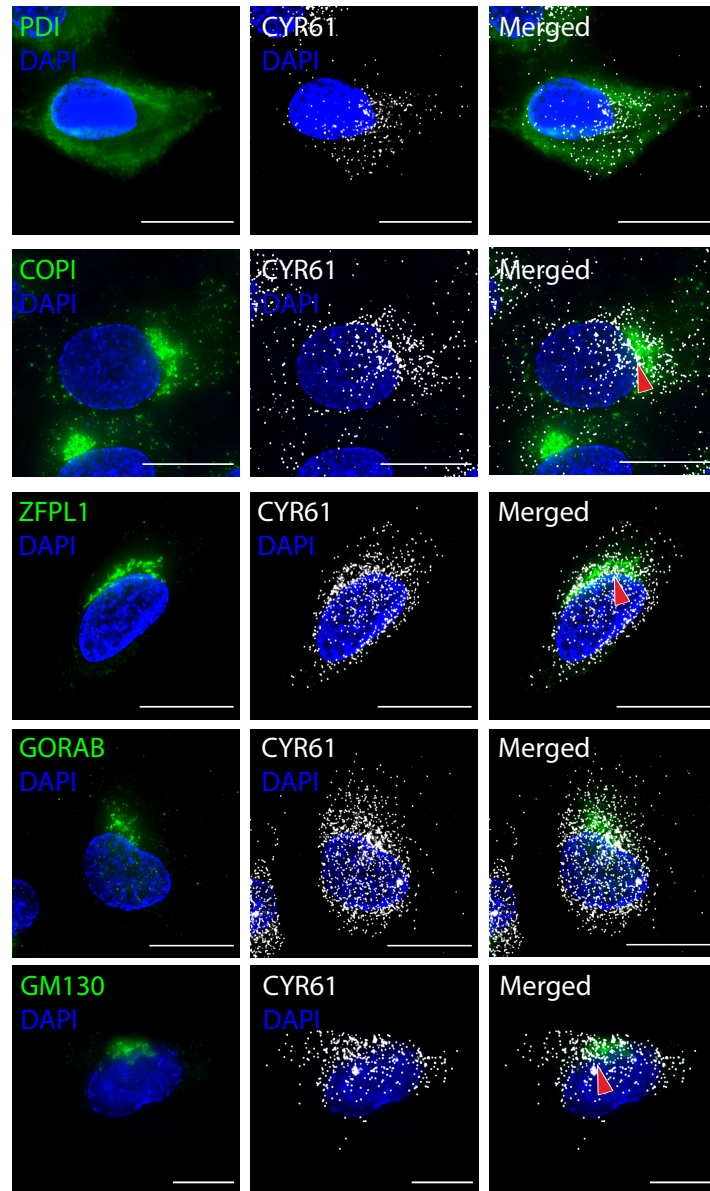


**Figure 4.2: Comparison of *CYR61* RNA distribution with secretory pathway organelles.**

A. Illustration of secretory pathway organelles and selected marker antibodies used for investigation.

B. smFISH and immunofluorescence co-detection of *CYR61* RNA and secretory pathway organelles in HUVECs.

Data Information: Scale bars = 10 $\mu$ m; red arrowhead shows potential *CYR61* RNA accumulations in close proximity to the *cis*-Golgi.

they are expressed at similar levels in endothelial cells (G. Costa et al., 2020). However, they are strongly cell body enriched during Transwell migration, hence should exhibit distinct mRNA localisation in endothelial cells (data from G. Costa et al., 2020; Fig. 4.3a). We therefore aimed to test whether the observed Golgi-adjacent localisation of *CYR61* is a specific phenomenon experienced only by *CYR61*, *CTGF*, and *EDN1* mRNAs, by co-staining for *CYR61* mRNA with *LAMB1*, *COL4A1*, and the *cis*-Golgi marker GM130 (Fig. 4.3b). We then measured the Golgi-adjacent localisation of *CYR61* and compared it to *LAMB1* and *COL4A1*. To do this, we defined the *cis*-Golgi as a region of interest and calculated the percentage of total mRNA fluorescence found within the bounds of the *cis*-Golgi stacks compared to the whole cell. Although we did not specifically test whether the control mRNAs are expressed to the same level as *CYR61*, we found that a significantly larger percentage of total *CYR61* mRNA was overlapping the *cis*-Golgi than *LAMB1* and *COL4A1*. This suggests that a portion of *CYR61* transcripts are found in a peri-Golgi position, thus distinguishing the distribution of *CYR61* from other highly expressed secretory protein mRNAs (Fig. 4.3c, d).

#### **4.3.4 *CYR61* mRNA is not physically attached to the Golgi.**

Targeting of mRNAs encoding proteins that function within membrane-bound organelles to their site of function is a well-established phenomenon (reviewed in Weis et al., 2013). For example, peroxisomal protein mRNAs and mitochondria protein mRNAs are known to be targeted to their respective functional destinations (Gadir et al., 2011; Zipor et al., 2009). Despite *CYR61* transcript supposedly requiring entry to the ER before progression to the Golgi, their distribution in close apposition with the Golgi, prompted us to first test whether they interact directly with the Golgi surface. To do this we treated migratory endothelial cells with Brefeldin A, which inhibits vesicle transport between the ER and Golgi, and hence causes Golgi collapse (Fig. 4.4a). We then stained for *CYR61* mRNA and quantified the localisation using two different measures. Firstly, we returned to our long axis analysis of mRNA distribution described previously and found no significant difference after Brefeldin A treatment (Fig. 4.4b). We also used the dispersion index, which measures how diffuse or accumulated an mRNA is, and found no significant difference after Brefeldin A treatment (Fig. 4.4c) (Park et al., 2012). As a positive control for Brefeldin A effectiveness, we also calculated the Long Axis Asymmetry and Dispersion Index of GM130 signal. Although Brefeldin A treatment did not cause a significant alteration in Golgi Long Axis Asymmetry (Fig. 4.4d), we did observe an increase in the Golgi Dispersion Index (Fig. 4.4e), showing

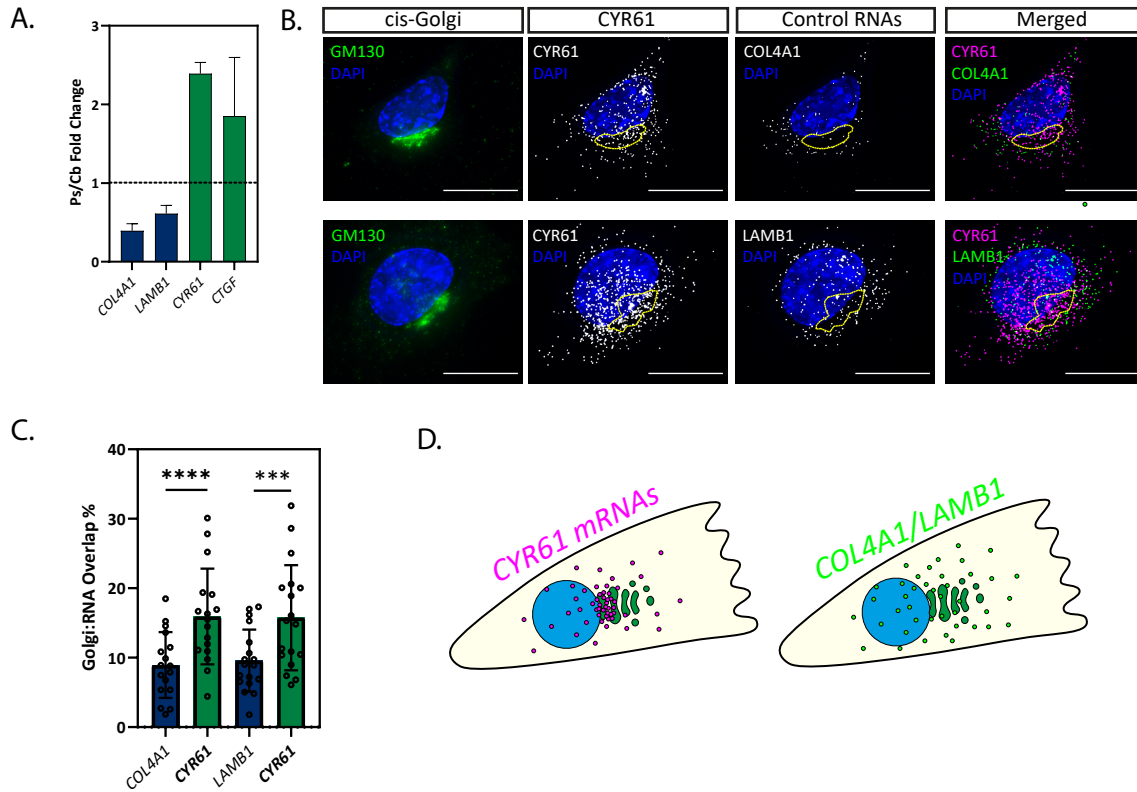


**Figure 4.3: *CYR61* RNA displays unique peri-Golgi localisation.**

- A. Fold Change (Protrusion/Cell Body) enrichment values for *k7* RNAs and secreted protein RNAs used subsequently as controls.
- B. smFISH and immunofluorescence co-detection of *CYR61* RNA, *COL4A1/LAMB1* RNA, and GM130 in HUVECs
- C. Analysis of the proportion of RNA fluorescence intensity observed overlapping the Golgi ( $n \geq 17$  cells; \*\*\* $P < 0.001$ , \*\*\*\* $P < 0.0001$ ; paired *t*-test).
- D. Illustration depicting the distinct peri-Golgi localisation of *CYR61* RNA when compared to *COL4A1/LAMB1* control RNAs.

Data Information: Scale bars = 10µm; Error Bars = SD; green dotted line shows perimeter of GM130 *cis*-Golgi immunofluorescence staining.



that Brefeldin A treatment did indeed cause Golgi collapse. Together, this evidence suggests that despite loss of Golgi structure *CYR61* transcripts appear to maintain their distribution, displaying a perinuclear accumulation biased to one side of the nucleus. Hence, *CYR61* transcripts do not appear to be physically attached to the Golgi, suggesting that the transcripts are not actively localised to the surface of the Golgi membranes.

#### **4.3.5 *CYR61* mRNA localisation is dependent on microtubules.**

Localised mRNAs are often transported to their destination by molecular motors that move transcripts along the cytoskeletal network. Both actin and microtubule networks have been shown to be essential for targeting of different mRNAs, and anterograde and retrograde movements can be required depending on the specific destination (Gagnon & Mowry, 2011). The microtubule network in migrating cells is anchored at the centrosome, which is located during cell migration in close apposition to the Golgi (Garcin & Straube, 2019). The Golgi itself also has some microtubule organising capabilities (Hao et al., 2020; Wu et al., 2016). Hence, the minus-ends of microtubules are clustered perinuclearly at the centrosome and Golgi. Having observed *CYR61* mRNA accumulations in this approximate location, we therefore wanted to test whether microtubule transport may play a role in the localisation mechanism. We co-stained for *CYR61* mRNA with immunofluorescence for alpha tubulin ( $\alpha$ TUB) (Fig. 4.5a). Strikingly, we observed co-distribution of many *CYR61* transcripts along microtubule fibres (Fig. 4.5a, inset with blue arrows). We then tested the potential function of this microtubule association by disrupting microtubules with colchicine. Microtubule depolymerisation severely disrupted *CYR61* transcript distribution (Fig. 4.5b). Interestingly, we observed a greater proportion of *CYR61* transcripts overlapping the nucleus (Fig. 4.5c), perhaps suggesting that mRNAs are not able to be transported away from the nucleus when microtubules are not present. We also observed, a significant increase in the dispersion index of *CYR61*, showing that the accumulated perinuclear localisation is lost when microtubules are disrupted (Fig. 4.5c). Together, this evidence suggests that the microtubule network is required to maintain *CYR61* mRNA distribution in endothelial cells.

#### **4.4 Discussion**

During cell migration, cells must periodically modulate the secretion rate of particular proteins. This is generally thought to be enabled by changing the transcription or translation rate. Cells also target secretion to particular subcellular zones. In migratory cells, secretion at the leading edge is particularly important (Prigozhina & Waterman-Storer, 2004). The

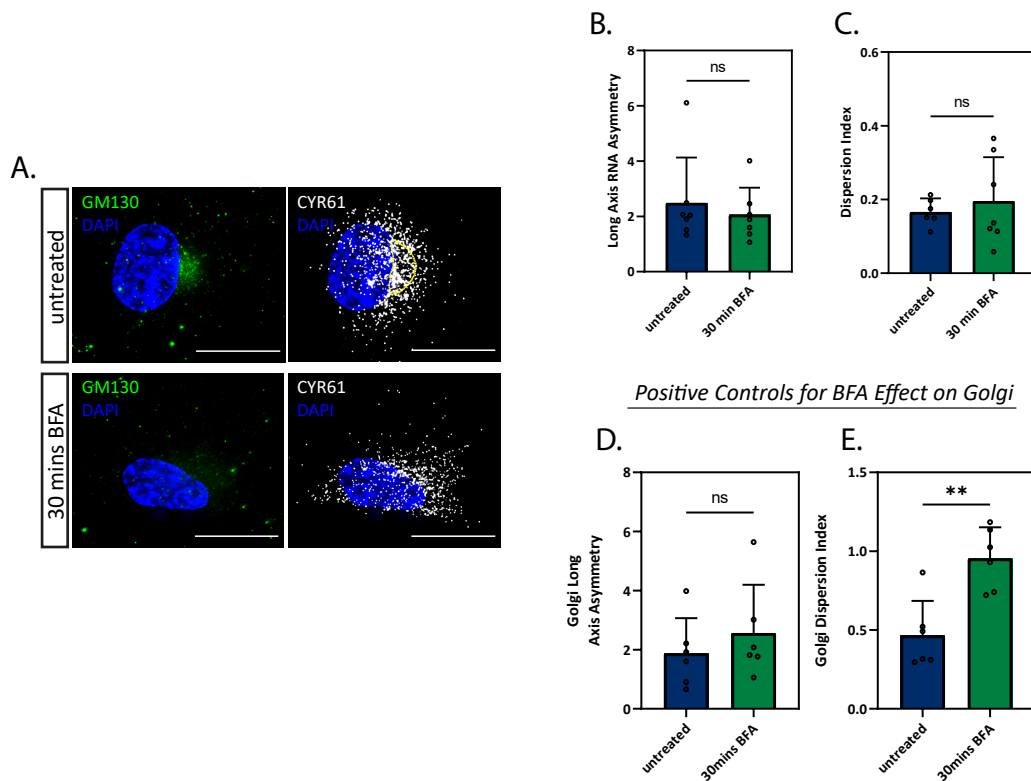


**Figure 4.4: *CYR61* mRNA is not physically connected to the Golgi.**

- smFISH and immunofluorescence co-detection of *CYR61* RNA and GM130 in HUVECs treated/untreated with Brefeldin A.
- Polarisation of *CYR61* RNA along the cells longest axis in endothelial cells treated/untreated with Brefeldin A (n = 7 cells; ns = not significant; unpaired t-test).
- Dispersion Index of *CYR61* RNA treated/untreated with Brefeldin A (n = 7 cells; ns = not significant; unpaired t-test).
- Polarisation of GM130 immunofluorescence along the cells longest axis in endothelial cells treated/untreated with Brefeldin A (n = 6 cells; ns = not significant; unpaired t-test).
- Dispersion Index of GM130 immunofluorescence treated/untreated with Brefeldin A (n = 6 cells; ns = not significant; unpaired t-test).

Data Information: Scale bars = 10 $\mu$ m; Error Bars = SD; green dotted line shows perimeter of GM130 cis-Golgi immunofluorescence staining.

direction of protein secretion must therefore be altered as the cell navigates and the leading edge position changes. Therefore, the dynamics of secretion must be fine-tuned with great spatiotemporal precision during cell migration. Interestingly, the role that mRNA localisation, and hence protein entry to the secretory system, may play in the spatiotemporal regulation of secretion is completely unexplored.

We have shown that CCN family mRNAs display a unique localisation pattern, enriched near to but not physically attached to the Golgi. This suggests that CCN family mRNAs may occupy a previously uncharacterised subcellular region surrounding the Golgi. Microtubule depolymerisation severely disrupted this localisation. Since the Golgi is located near to microtubule minus-ends, retrograde microtubule transport may play a role in targeting CCN family mRNAs to their destination. Together this evidence indicates that CCN family protein secretion may be regulated by targeting of mRNAs to a peri-Golgi zone, where specific properties may be applied to the protein during translation.

#### **4.4.1 Entry to the secretory pathway via specialised ER compartments**

Unconventional secretion routes via the endosomal system, plasma membrane pores, or Golgi-bypass are known to exist for specific proteins (Nickel & Rabouille, 2008). However, we expect a significant proportion of CCN proteins to pass through the classical secretory pathway, since immunofluorescence in previous reports shows CCN proteins present throughout the Golgi stacks (Chen et al., 2001; Tall et al., 2010). Therefore, since CCN proteins must pass through the ER lumen, and exit via COPII-coated vesicles to enter the Golgi apparatus, we expect localised CCN family mRNAs to be interacting primarily with the ER. This is also backed-up by the fact that Golgi collapse does not appear to alter the mRNA localisation. Moreover, CCN family members are reported to have N-terminal hydrophobic signal peptides, so they can be expected to be bound by SRP and enter the secretory pathway by Sec61 translocation to the ER. However, SRP is not the sole regulator of secretory protein targeting to the ER, since loss of SRP is not lethal in yeast or mammalian cells (Mutka & Walter, 2001; Ren et al., 2004). Alternative pathways to enable protein entry to the secretory pathway must therefore exist. Further evidence for this comes from the fact that a substantial fraction of the secretome in yeast is targeted to the ER by SRP-independent mechanisms. These methods rely on Hsp40 chaperones to translocate proteins to the ER, and are thought to have evolved to allow for efficient translocation of proteins of variable size or structure (Ast et al., 2013). SRP is also thought to be present at quite low concentrations in cells, relative to

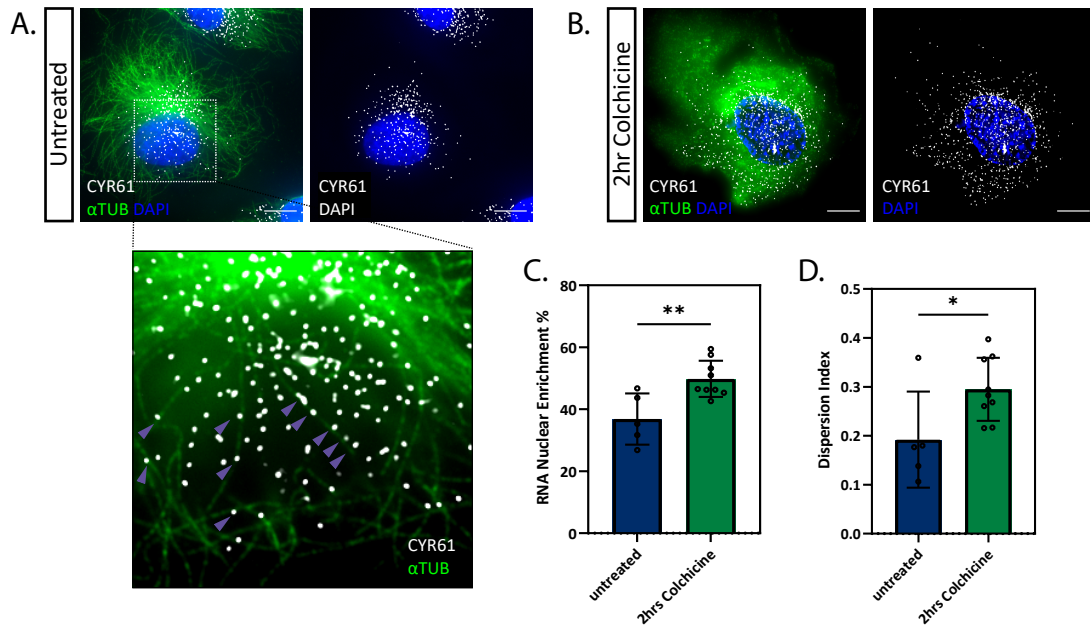


**Figure 4.5: *CYR61* mRNA co-distributes with microtubules.**

- smFISH and immunofluorescence co-detection of *CYR61* mRNA with  $\alpha$ -Tubulin in HUVECs. Inset box shows *CYR61* RNA co-distributing with microtubule fibres.
- smFISH and immunofluorescence co-detection of *CYR61* mRNA with  $\alpha$ -Tubulin in HUVECs after treatment with colchicine.
- Proportion of *CYR61* observed overlapping the nucleus in colchicine untreated/treated endothelial cells ( $n \geq 5$  cells; \*\* $P < 0.01$ ; unpaired t-test).
- Dispersion Index of *CYR61* in colchicine untreated/treated endothelial cells ( $n \geq 5$  cells; \* $P < 0.05$ ; unpaired t-test).

Data Information: Scale bars = 10 $\mu$ m; Error Bars = SD; blue arrowheads so co-distributing *CYR61* mRNA spots with microtubules.

the vast number of ribosome-nascent chain complexes (Chartron et al., 2016). How the SRP efficiently targets proteins co-translationally is therefore still something of a mystery (Costa et al., 2018). This is compounded by the fact that recent evidence suggests *cis*-acting sequences may also play a role in targeting secretory protein mRNAs to the ER and enhancing protein secretion (Cohen-Zontag et al., 2019). Therefore, heterogeneous pathways for targeting mRNA or proteins to the ER exist, and how these pathways are coordinated on an mRNA-specific basis is not yet known. Hence, targeting of CCN mRNAs to the peri-Golgi zone identified here, via microtubule transport, may serve to enable efficient protein entry to the secretory pathway, perhaps by acting synergistically with SRP-mediated translocation, or with unknown alternative translocation mechanisms.

The presence of specialised subunits of ER has been hypothesised for some time. In particularly large cells like neurons, which extend processes at great distance from the cell body, the use of specialised secretory routes is essential to enable delivery of secretory proteins to the correct cellular location. The major components of the secretory pathway including the bulk of the ER and Golgi are situated in neuronal cell bodies, but a significant proportion are also present in axons and dendrites (Mikhaylova et al., 2016; Öztürk et al., 2020). These secretory outposts situated at large distances from the cell body contribute to neuron function by synthesising proteins locally (Farías et al., 2015; Valenzuela et al., 2014; Wang et al., 2020). Interestingly, despite the ER network being continuous throughout the cytoplasm, ER in dendrites is known to exhibit distinct properties to ER in the cell body. Dendritic ER has a more complex structure with more anastomosing tubules, and this causes proteins to diffuse slower in dendritic ER than cell body ER (Cui-Wang et al., 2012). These complex ER regions correspond with regions of protein export from the ER to the Golgi. Hence, local compartments of ER exist in neurons to enable specialised trafficking of certain proteins. It remains to be seen whether functionally-distinct secretory pathway components exist in specific spatial compartments in migratory cells as well as in neurons. We hypothesise that CCN family mRNAs may occupy a previously undescribed specific secretory locale, perhaps a specialised local ER compartment, surrounding the Golgi, and this region may confer specific translatory properties to proteins translated within.

#### **4.4.2 mRNA localisation can direct secretory protein translation and function in *Drosophila*.**

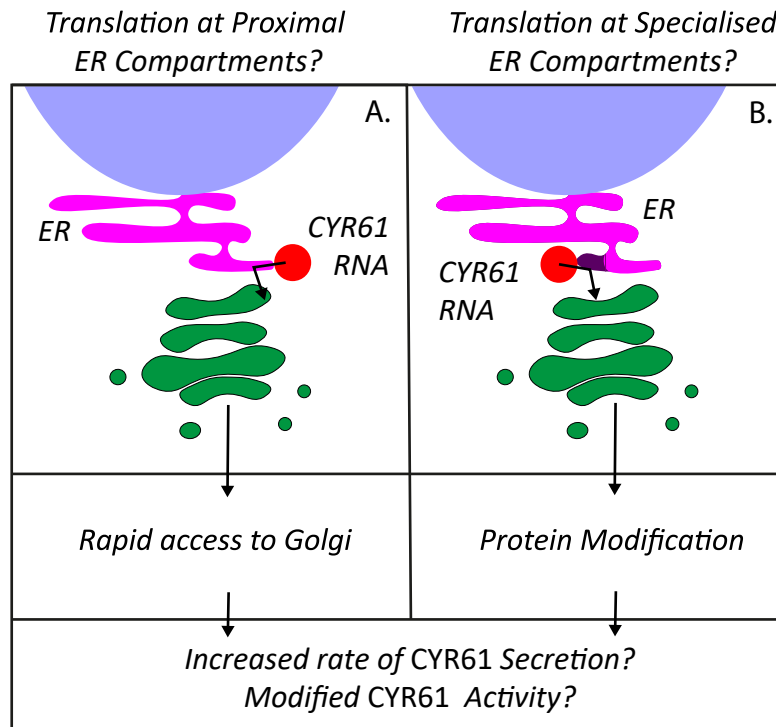


**Figure 4.6: Potential molecular functions of *CYR61* RNA peri-Golgi localisation.**

- A. *CYR61* RNAs could be localised to regions of the ER that are proximal to the Golgi. Translation at this site could minimise transport time of translated proteins through the ER lumen, and minimise transport time of COPI coated vesicles from the ER to the Golgi. An increased rate of secretion could therefore be facilitated by reducing the processing time of proteins through the secretory pathway.
- B. *CYR61* RNAs could be localised to specialised compartments of the ER. Translation at these compartments could confer unique biochemical properties to newly-translated proteins, which could influence their activity.

A growing number of secretory protein mRNAs are known to exhibit polarised or asymmetric distributions in various organisms. Perhaps the most well characterised are *gurken* and *wingless*. *gurken* is actively targeted to the dorsal/anterior corner of the developing *Drosophila* oocyte (Kugler & Lasko, 2009). *gurken* encodes a TGF $\alpha$  family member that is secreted specifically in the dorsal/anterior corner of the oocyte, where it stimulates the surrounding follicle cells to adopt dorsal fate (Roth & Edwards, 2003). The *Drosophila* oocyte has a unique secretory pathway architecture, consisting of many individual Golgi units each in contact with a region of transitional ER (the ER exit site rich region where translated protein finally leave the ER). These individual secretory modules are called tER-Golgi units. Importantly, *gurken* mRNA localisation biases translation to specific tER-Golgi units located in the dorsal/anterior corner of the oocyte. Hence, mRNA localisation to regulate encoded protein translation at specific ER compartments is an observed phenomenon in the *Drosophila* oocyte (Herpers & Rabouille, 2004).

The localisation of *wingless* in the *Drosophila* ectoderm represents an alternative example where localisation of secretory protein mRNAs is important for the secretion of the resulting protein. *wingless* transcripts are enriched apically in *Drosophila* epithelial tissues by a *cis*-acting sequence in their 3'UTRs (dos Santos et al., 2008). When *wingless* mRNA is mislocalised, it can still be efficiently translated, but the protein is not secreted to the apical zone correctly (Simmonds et al., 2001). This suggests that only *wingless* protein produced from apically-located *wingless* mRNA is able to access the secretory pathway. These two examples of *gurken* and *wingless* illustrate that mRNAs encoding secreted proteins can exhibit specific localisation patterns that enable the correct translation, processing, and secretion of the protein. It remains to be seen whether such specialised secretory zones exist in mammalian cells, but we hypothesise that the peri-Golgi locale occupied by the *CYR61* mRNAs could plausibly be an example of such a zone. Further experimental work is required to test this.

#### **4.4.3 Why localise CCN family mRNAs?**

We hypothesise that the observed localisation of CCN family mRNAs in the peri-Golgi zone may regulate protein entry to the secretory system by two possible methods (summarised in Fig. 4.7). Firstly, mRNA localisation may bias protein translation at ER zones proximal to the Golgi, thereby increasing the speed at which proteins can pass from the ER to the Golgi. ER-Golgi transport of proteins is achieved by the budding of COPII coated vesicles from ER exit

sites (ERES) to the Golgi (Barlowe et al., 1994). Interestingly, ERES are predominantly located in a similar location to CCN family mRNAs, proximal to the Golgi (Kurokawa & Nakano, 2019). The *cis*-Golgi is also known to make contact with ERES and collect cargo without vesicle budding taking place (Kurokawa et al., 2014). This evidence suggests that promoting the translation of secreted proteins in regions proximal to ERES and the *cis*-Golgi could allow for faster secretion, because diffusion of the protein through the ER lumen and transport of COPII coated vesicles from distal ER sites to the surface of the Golgi could be avoided. So, the first potential advantage of CCN family localisation is that proximity to the Golgi may enhance secretion rate. The second possibility is that the peri-Golgi zone may also confer distinct molecular properties to proteins translated within. For example, recent evidence suggests that translation of transmembrane proteins in specific ER-proximal zones can enable cofactor interaction (Ma & Mayr, 2018). This zone is defined by the presence of an mRNA-binding protein called TIS11B that forms a 3D gel-like structure surrounding the ER. CD47 mRNAs containing AU-rich elements in their 3'UTRs are bound by TIS11B and enriched in this zone, where translation enables higher protein expression than translation in other parts of the cytoplasm. Increased binding of translated CD47 to effector protein called SET is also observed (Ma & Mayr, 2018). Hence, translation of secreted proteins in biochemically distinct subcellular compartments can inform protein expression via modulation of co-factor interaction.

One particularly poorly understood area of research is how protein secretion can be targeted to specific regions in subcellular space. In neurons the requirement for this phenomenon is clear, since distal processes of neurons display clear subfunctionalisation, with some receptor proteins only present in particular regions. Yet in migratory cells, which display similar divisions of labour between front and rear, the requirement for spatially restricted secretion to specific extracellular regions is not well studied. However, directed secretion of growth factors via exosomes to the leading edge is known to be essential for fibroblast migration (Prigozhina & Waterman-Storer, 2004). It is thought that growth factors could then act in a hyper-localised autocrine manner, as signalling may be partially restricted to the leading edge, resulting in promotion of adhesion formation and leading edge stability (Sung et al., 2015). CCN family proteins are also vitally important in the modulation of cell adhesion and growth factor signalling. It is interesting to speculate that the localisation of CCN family mRNAs presented here could help to direct CCN proteins to their functional destination by



orienting secretion to the leading edge. The peri-Golgi localisation hints at this possibility since the Golgi is known to be positioned at the front of cells during cell migration.

In summary, we have found that CCN family mRNAs specifically occupy a peri-Golgi subcellular compartment, and this localisation is dependent on microtubules. How this localisation contributes to CCN protein functionality, and therefore CCN function in endothelial cell biology during health and disease, is yet to be discovered. Moreover, this work shows that mRNAs encoding particular classes of secretory protein can occupy specific subcellular locales, hinting that mRNA localisation to additional, as yet undiscovered destinations, may be a broad regulatory mechanism controlling activity of a wide range of secreted proteins.

## 4.5 Materials and Methods

### 4.5.1 Cell Culture.

HUVEC (PromoCell) were cultured on 0.1% gelatin coated T75 flasks (Corning) in endothelial cell basal medium 2 (EBM-2, Promocell) with an additional supplement pack (5% FCS, EGF (5ng/ml), VEGF (0.5ng/ml), FGF2 (10ng/ml), long R3 insulin growth factor-1 (20ng/ml), hydrocortisone (0.2µg/ml), and ascorbic acid (1µg/ml)). 50mg/ml gentamycin (Sigma) and 250µg/ml amphotericin (Sigma) were also added to the culture media. All HUVEC experiments were conducted with cells between passage 3-6. All cells were split prior to reaching 90% confluency and their media was changed every two days.

### 4.5.2 smFISH and Immunofluorescence

Endothelial cells on coverslips were fixed in methanol-free 4% formaldehyde and permeabilised in 70% ethanol. Stellaris single molecule fluorescence *in situ* hybridisation (smFISH) gene-specific probes sets (Table 4.1), conjugated to Quasar 570/670 fluorophores, were designed using an online tool (Biosearchtech). Predesigned *GAPDH* reference probe sets are purchased directly. smFISH probe hybridisation was carried out as described previously. Briefly, samples were washed in wash buffer (2X SSC, 10% formamide) before incubation overnight at 37°C with smFISH probe sets diluted in hybridisation buffer (2X SSC, 10% formamide, 10% w/v Dextran Sulphate). Samples were then washed twice in wash buffer at 37°C for 30 minutes.

In samples co-stained for mRNA and protein, immunofluorescence was carried out following smFISH. Samples were washed with PBS before blocking with blocking buffer (PBS, 0.2% Tween-20, 5% Goat Serum) for 30 mins. Primary antibodies were diluted in blocking buffer and incubated with samples for 1hr at room temperature. Samples were then washed with blocking buffer before incubation with secondary antibodies for 1hr at room temperature. Samples were mounted using Prolong Gold (Thermo Fisher Scientific).

### 4.5.3 Antibodies

Primary and secondary antibodies were used at the following concentrations: 1:200 mouse COPI (CM1A10) (Palmer et al., 1993); 1:200 sheep ZFPL1 (Chiu et al., 2008); 1:200 rabbit PDI (C81H6, Cell Signalling Technologies); 1:200 rabbit GORAB (Witkos et al., 2019); mouse anti-αTUB 1:500 (TAT-1, ECACC 00020911); 1:500 goat anti-rabbit/mouse AlexaFluor 488 (Thermo Fisher Scientific).

#### **4.5.4 Microscopy**

All fluorescent microscopy data was obtained using an Olympus IX83 inverted microscope using Lumencor LED excitation, a 100x/ 1.40 UplanSApo objective and a Sedat QUAD filter set (Chroma 89000). The images were collected using a R6 (Qimaging) CCD camera with a Z optical spacing of 0.2 $\mu$ m. Raw images were then deconvolved using the Huygens Pro software (SVI) and maximum intensity projections of these deconvolved images are shown in the results.

#### **4.5.5 Image Analysis**

Dispersion indexes were calculated as previously described (Park et al., 2012).

Longest axis asymmetry distribution was calculated as follows. The longest axis of individual cells was obtained visually or by measuring cell length using the draw line function in ImageJ. Cells were then divided in two perpendicular to the longest axis, through the centre of the nucleus. Regions of interest were then calculate incorporating each of these two areas. The integrated density of mRNA fluorescence was then calculated using the measure function of ImageJ. The area that had the largest integrated density was then divided by the smallest, to create a value for mRNA fluorescence asymmetry along the cell longest axis.

Nuclear mRNA enrichment was calculated by creating a region of interest of the nucleus, and a region of interest of the whole cell perimeter, and calculating the percentage of total cell mRNA integrated density fluorescence that was found within the bounds of the nucleus. Similarly, to calculate Golgi:mRNA overlap, regions of interest were drawn around the perimeter of the GM130 immunofluorescence staining, and around the perimeter of the whole cell. The percentage of total cell mRNA integrated density fluorescence that was found within the bounds of the Golgi was then calculated and represented in the graphs shown.

#### **4.5.6 Inhibitor Treatment**

Brefeldin A (Sigma) was added to culture medium at 2.5 $\mu$ g/ml for 30 mins to cause collapse of the Golgi. Microtubule depolymerisation was achieved through Colchicine (Sigma) treatment at 50nM for 2 hours.

## 4.5 References

- Ast, T., Cohen, G., & Schuldiner, M. (2013). A network of cytosolic factors targets SRP-independent proteins to the endoplasmic reticulum. *Cell*, *152*(5), 1134–1145. <https://doi.org/10.1016/J.CELL.2013.02.003/ATTACHMENT/356F1F1D-09CE-49DF-8892-255F210B4778/MMC5.XLS>
- Aviram, N., Ast, T., costa, E. A., Arakel, E., chuartzman, S. G., Jan, calvin H., Haßdenteufel, S., dudek, J., Jung, martin, Schorr, S., Zimmermann, R., Schwappach, blanche, Weissman, J. S., & Schuldiner, maya. (2016). The SND proteins constitute an alternative targeting route to the endoplasmic reticulum. *Nature*, *540*. <https://doi.org/10.1038/nature20169>
- Barlowe, C., Orci, L., Yeung, T., Hosobuchi, M., Hamamoto, S., Salama, N., Rexach, M. F., Ravazzola, M., Amherdt, M., & Schekman, R. (1994). COPII: A membrane coat formed by Sec proteins that drive vesicle budding from the endoplasmic reticulum. *Cell*, *77*(6), 895–907. [https://doi.org/10.1016/0092-8674\(94\)90138-4](https://doi.org/10.1016/0092-8674(94)90138-4)
- Chartron, J. W., Hunt, K. C. L., & Frydman, J. (2016). Cotranslational signal-independent SRP preloading during membrane targeting. *Nature 2016 536:7615*, *536*(7615), 224–228. <https://doi.org/10.1038/nature19309>
- Chen, Y., Segarini, P., Raoufi, F., Bradham, D., & Leask, A. (2001). Connective Tissue Growth Factor Is Secreted through the Golgi and Is Degraded in the Endosome. *Experimental Cell Research*, *271*(1), 109–117. <https://doi.org/10.1006/EXCR.2001.5364>
- Chiu, C. F., Ghanekar, Y., Frost, L., Diao, A., Morrison, D., McKenzie, E., & Lowe, M. (2008). ZFPL1, a novel ring finger protein required for cis-Golgi integrity and efficient ER-to-Golgi transport. *The EMBO Journal*, *27*(7), 934–947. <https://doi.org/10.1038/EMBOJ.2008.40>
- Cohen-Zontag, O., Baez, C., Lim, L. Q. J., Olender, T., Schirman, D., Dahary, D., Pilpel, Y., & Gerst, J. E. (2019). A secretion-enhancing cis regulatory targeting element (SECRETE) involved in mRNA localization and protein synthesis. *PLOS Genetics*, *15*(7), e1008248. <https://doi.org/10.1371/JOURNAL.PGEN.1008248>
- Colombo, S. F., Cardani, S., Maroli, A., Vitiello, A., Soffientini, P., Crespi, A., Bram, R. F., Benfante, R., & Borgese, N. (2016). Tail-anchored protein insertion in mammals

- function and reciprocal interactions of the two subunits of the trc40receptor. *Journal of Biological Chemistry*, 291(29), 15292–15306.  
<https://doi.org/10.1074/JBC.M115.707752>
- Costa, E. A., Subramanian, K., Nunnari, J., & Weissman, J. S. (2018). *Defining the physiological role of SRP in protein-targeting efficiency and specificity*.  
<https://doi.org/10.1126/science.aar3607>
- Costa, G., Bradbury, J. J., Tarannum, N., & Herbert, S. P. (2020). RAB13 mRNA compartmentalisation spatially orients tissue morphogenesis. *The EMBO Journal*, 39(21), e106003. <https://doi.org/10.15252/EMBJ.2020106003>
- Cui-Wang, T., Hanus, C., Cui, T., Helton, T., Bourne, J., Watson, D., Harris, K. M., & Ehlers, M. D. (2012). *Local Zones of Endoplasmic Reticulum Complexity Confine Cargo in Neuronal Dendrites*. <https://doi.org/10.1016/j.cell.2011.11.056>
- dos Santos, G., Simmonds, A. J., & Krause, H. M. (2008). A stem-loop structure in the wingless transcript defines a consensus motif for apical RNA transport. *Development (Cambridge, England)*, 135(1), 133–143. <https://doi.org/10.1242/dev.014068>
- Dubois, F., Alpha, K., & Turner, C. E. (2017). Paxillin regulates cell polarization and anterograde vesicle trafficking during cell migration. *Molecular Biology of the Cell*, 28(26), 3815–3831. <https://doi.org/10.1091/MBC.E17-08-0488/ASSET/IMAGES/LARGE/3815FIG8.TIF.GZ.JPEG>
- Farías, G. G., Guardia, C. M., Britt, D. J., Guo, X., & Bonifacino, J. S. (2015). Sorting of Dendritic and Axonal Vesicles at the Pre-axonal Exclusion Zone. *Cell Reports*, 13(6), 1221–1232. <https://doi.org/10.1016/J.CELREP.2015.09.074>
- Gadir, N., Haim-Vilmovsky, L., Kraut-Cohen, J., & Gerst, J. E. (2011). Localization of mRNAs coding for mitochondrial proteins in the yeast *Saccharomyces cerevisiae*. *RNA*, 17(8), 1551–1565. <https://doi.org/10.1261/RNA.2621111>
- Gagnon, J. A., & Mowry, K. L. (2011). Molecular Motors: Directing Traffic during RNA Localization. *Critical Reviews in Biochemistry and Molecular Biology*, 46(3), 229. <https://doi.org/10.3109/10409238.2011.572861>
- Garcin, C., & Straube, A. (2019). Microtubules in cell migration. *Essays in Biochemistry*, 63(5), 509. <https://doi.org/10.1042/EBC20190016>

- Hao, H., Niu, J., Xue, B., Su, Q. P., Liu, M., Yang, J., Qin, J., Zhao, S., Wu, C., & Sun, Y. (2020). Golgi-associated microtubules are fast cargo tracks and required for persistent cell migration. *EMBO Reports*, *21*(3), e48385. <https://doi.org/10.15252/EMBR.201948385>
- Herbert, S. P., & Costa, G. (2019). Sending messages in moving cells: mRNA localization and the regulation of cell migration. In *Essays in Biochemistry* (Vol. 63, Issue 5, pp. 595–606). Portland Press Ltd. <https://doi.org/10.1042/EBC20190009>
- Herpers, B., & Rabouille, C. (2004). mRNA Localization and ER-based Protein Sorting Mechanisms Dictate the Use of Transitional Endoplasmic Reticulum-Golgi Units Involved in Gurken Transport in Drosophila Oocytes. *Molecular Biology of the Cell*, *15*, 5306–5317. <https://doi.org/10.1091/mbc.E04>
- Jan, C. H., Williams, C. C., & Weissman, J. S. (2014). Principles of ER cotranslational translocation revealed by proximity-specific ribosome profiling. *Science*, *346*(6210). [https://doi.org/10.1126/SCIENCE.1257521/SUPPL\\_FILE/REVISION1\\_MS1257521TABLES6.TXT](https://doi.org/10.1126/SCIENCE.1257521/SUPPL_FILE/REVISION1_MS1257521TABLES6.TXT)
- Johnson, N., Powis, K., & High, S. (2013). Post-translational translocation into the endoplasmic reticulum. *Biochimica et Biophysica Acta (BBA) - Molecular Cell Research*, *1833*(11), 2403–2409. <https://doi.org/10.1016/J.BBAMCR.2012.12.008>
- Kugler, J.-M., & Lasko, P. (2009). *Localization, anchoring and translational control of oskar, gurken, bicoid and nanos mRNA during Drosophila oogenesis*. <https://doi.org/10.4161/fly.3.1.7751>
- Kupfer, A., Louvard, D., & Singer, S. J. (1982). Polarization of the Golgi apparatus and the microtubule-organizing center in cultured fibroblasts at the edge of an experimental wound. *Proceedings of the National Academy of Sciences of the United States of America*, *79*(8), 2603–2607. <http://www.ncbi.nlm.nih.gov/pubmed/7045867>
- Kurokawa, K., & Nakano, A. (2019). The ER exit sites are specialized ER zones for the transport of cargo proteins from the ER to the Golgi apparatus. *The Journal of Biochemistry*, *165*(2), 109–114. <https://doi.org/10.1093/JB/MVY080>

- Kurokawa, K., Okamoto, M., & Nakano, A. (2014). Contact of cis-Golgi with ER exit sites executes cargo capture and delivery from the ER. *Nature Communications*.  
<https://doi.org/10.1038/ncomms4653>
- Ma, W., & Mayr, C. (2018). A Membraneless Organelle Associated with the Endoplasmic Reticulum Enables 3'UTR-Mediated Protein-Protein Interactions. *Cell*, *175*(6), 1492-1506.e19. <https://doi.org/10.1016/J.CELL.2018.10.007/ATTACHMENT/F5E54EA8-36AD-422A-87B7-6A2E21BA4340/MMC2.PDF>
- Martin, M., Veloso, A., Wu, J., Katrukha, E. A., & Akhmanova, A. (2018). Control of endothelial cell polarity and sprouting angiogenesis by noncentrosomal microtubules. *ELife*, *7*. <https://doi.org/10.7554/ELIFE.33864>
- Mikhaylova, M., Bera, S., Kobler, O., Frischknecht, R., & Kreutz, M. R. (2016). A Dendritic Golgi Satellite between ERGIC and Retromer. *Cell Reports*, *14*(2), 189–199.  
<https://doi.org/10.1016/J.CELREP.2015.12.024>
- Mutka, S. C., & Walter, P. (2001). Multifaceted Physiological Response Allows Yeast to Adapt to the Loss of the Signal Recognition Particle-dependent Protein-targeting Pathway. *Molecular Biology of the Cell*, *12*(3), 577–588.  
<https://doi.org/10.1091/mbc.12.3.577>
- Nickel, W., & Rabouille, C. (2008). Mechanisms of regulated unconventional protein secretion. *Nature Reviews Molecular Cell Biology* *2009* *10*:2, *10*(2), 148–155.  
<https://doi.org/10.1038/nrm2617>
- Öztürk, Z., O’Kane, C. J., & Pérez-Moreno, J. J. (2020). Axonal Endoplasmic Reticulum Dynamics and Its Roles in Neurodegeneration. *Frontiers in Neuroscience*, *14*, 48.  
<https://doi.org/10.3389/FNINS.2020.00048/BIBTEX>
- Palmer, D. J., Helms, J. B., Beckers, C. J. M., Orci, L., & Rothman, J. E. (1993). Binding of coatomer to Golgi membranes requires ADP-ribosylation factor. *Journal of Biological Chemistry*, *268*(16), 12083–12089. [https://doi.org/10.1016/S0021-9258\(19\)50311-8](https://doi.org/10.1016/S0021-9258(19)50311-8)
- Park, H. Y., Trcek, T., Wells, A. L., Chao, J. A., & Singer, R. H. (2012). An Unbiased Analysis Method to Quantify mRNA Localization Reveals Its Correlation with Cell Motility. *Cell Reports*, *1*(2), 179–184. <https://doi.org/10.1016/j.celrep.2011.12.009>

- Prigozhina, N. L., & Waterman-Storer, C. M. (2004). Protein Kinase D-Mediated Anterograde Membrane Trafficking Is Required for Fibroblast Motility. *Current Biology*, 14(2), 88–98.  
<https://doi.org/10.1016/J.CUB.2004.01.003/ATTACHMENT/203F37C2-2700-4B1E-969E-C19C087777EA/MMC5.MOV>
- Reid, D. W., & Nicchitta, C. v. (2012). Primary role for endoplasmic reticulum-bound ribosomes in cellular translation identified by ribosome profiling. *The Journal of Biological Chemistry*, 287(8), 5518–5527. <https://doi.org/10.1074/JBC.M111.312280>
- Ren, Y. G., Wagner, K. W., Knee, D. A., Aza-Blanc, P., Nasoff, M., & Deveraux, Q. L. (2004). Differential regulation of the TRAIL death receptors DR4 and DR5 by the signal recognition particle. *Molecular Biology of the Cell*, 15(11), 5064–5074.  
<https://doi.org/10.1091/MBC.E04-03-0184/ASSET/IMAGES/LARGE/ZMK0110428840007.JPEG>
- Roth, S., & Edwards, R. G. (2003). The origin of dorsoventral polarity in *Drosophila*. *Philosophical Transactions of the Royal Society of London. Series B: Biological Sciences*, 358(1436), 1317–1329. <https://doi.org/10.1098/RSTB.2003.1325>
- Schmoranzer, J., Kreitzer, G., & Simon, S. M. (2003). Migrating fibroblasts perform polarized, microtubule-dependent exocytosis towards the leading edge. *Journal of Cell Science*, 116(22), 4513–4519. <https://doi.org/10.1242/JCS.00748>
- Simmonds, A. J., dosSantos, G., Livne-Bar, I., & Krause, H. M. (2001). Apical localization of wingless transcripts is required for wingless signaling. *Cell*, 105(2), 197–207.  
<http://www.ncbi.nlm.nih.gov/pubmed/11336670>
- Stueland, M., Wang, T., Park, H. Y., & Mili, S. (2019). RDI Calculator: An Analysis Tool to Assess RNA Distributions in Cells. *Scientific Reports*, 9(1).  
<https://doi.org/10.1038/S41598-019-44783-2>
- Sung, B. H., Ketova, T., Hoshino, D., Zijlstra, A., & Weaver, A. M. (2015). Directional cell movement through tissues is controlled by exosome secretion. *Nature Communications* 2015 6:1, 6(1), 1–14. <https://doi.org/10.1038/ncomms8164>
- Tall, E. G., Bernstein, A. M., Oliver, N., Gray, J. L., & Masur, S. K. (2010). TGF- $\beta$ -Stimulated CTGF Production Enhanced by Collagen and Associated with Biogenesis of



a Novel 31-kDa CTGF Form in Human Corneal Fibroblasts. *Investigative Ophthalmology & Visual Science*, 51(10), 5002–5011. <https://doi.org/10.1167/IOVS.09-5110>

- Tirincsi, A., Sicking, M., Hadzibeganovic, D., Haßdenteufel, S., & Lang, S. (2021). The Molecular Biodiversity of Protein Targeting and Protein Transport Related to the Endoplasmic Reticulum. *International Journal of Molecular Sciences* 2022, Vol. 23, Page 143, 23(1), 143. <https://doi.org/10.3390/IJMS23010143>
- Valenzuela, J. I., Jaureguiberry-Bravo, M., Salas, D. A., Ramírez, O. A., Cornejo, V. H., Lu, H. E., Blanpied, T. A., & Couve, A. (2014). Transport along the dendritic endoplasmic reticulum mediates the trafficking of GABAB receptors. *Journal of Cell Science*, 127(15), 3382–3395. <https://doi.org/10.1242/JCS.151092>
- Wang, J., Fourriere, L., & Gleeson, P. A. (2020). Local Secretory Trafficking Pathways in Neurons and the Role of Dendritic Golgi Outposts in Different Cell Models. *Frontiers in Molecular Neuroscience*, 13. <https://doi.org/10.3389/FNMOL.2020.597391>
- Weis, B. L., Schleiff, E., & Zerges, W. (2013). Protein targeting to subcellular organelles via mRNA localization. *Biochimica et Biophysica Acta (BBA) - Molecular Cell Research*, 1833(2), 260–273. <https://doi.org/10.1016/J.BBAMCR.2012.04.004>
- Witkos, T. M., Chan, W. L., Joensuu, M., Rhiel, M., Pallister, E., Thomas-Oates, J., Mould, A. P., Mironov, A. A., Biot, C., Guerardel, Y., Morelle, W., Ungar, D., Wieland, F. T., Jokitalo, E., Tassabehji, M., Kornak, U., & Lowe, M. (2019). GORAB scaffolds COPI at the trans-Golgi for efficient enzyme recycling and correct protein glycosylation. *Nature Communications*, 10(1). <https://doi.org/10.1038/S41467-018-08044-6>
- Wu, J., de Heus, C., Liu, Q., Bouchet, B. P., Noordstra, I., Jiang, K., Hua, S., Martin, M., Yang, C., Grigoriev, I., Katrukha, E. A., Altelaar, A. F. M., Hoogenraad, C. C., Qi, R. Z., Klumperman, J., & Akhmanova, A. (2016). Molecular Pathway of Microtubule Organization at the Golgi Apparatus. *Developmental Cell*, 39(1), 44–60. <https://doi.org/10.1016/J.DEVCEL.2016.08.009/ATTACHMENT/02EF4A46-FAEE-4F66-B4F4-53B6C1589231/MMC8.MP4>
- Xing, M., Peterman, M. C., Davis, R. L., Oegema, K., Shiau, A. K., & Field, S. J. (2016). GOLPH3 drives cell migration by promoting Golgi reorientation and directional

trafficking to the leading edge. *Molecular Biology of the Cell*, 27(24), 3828–3840.  
<https://doi.org/10.1091/MBC.E16-01-0005/MC-E16-01-0005-S11.MOV>

Yamada, K. M., & Sixt, M. (2019). Mechanisms of 3D cell migration. *Nature Reviews Molecular Cell Biology* 2019 20:12, 20(12), 738–752. <https://doi.org/10.1038/s41580-019-0172-9>

Zipor, G., Haim-Vilmovsky, L., Gelin-Licht, R., Gadir, N., Brocard, C., & Gerst, J. E. (2009). Localization of mRNAs coding for peroxisomal proteins in the yeast, *Saccharomyces cerevisiae*. *Proceedings of the National Academy of Sciences*, 106(47), 19848–19853. <https://doi.org/10.1073/PNAS.0910754106>

Table 4.1 smFISH probes.

mRNA	Probe sequence (5' - 3')	mRNA	Probe sequence (5' - 3')	mRNA	Probe sequence (5' - 3')	mRNA	Probe sequence (5' - 3')	mRNA	Probe sequence (5' - 3')
CTGF	cggggaaggtgtgtgtg	CYR61	acgaagacccaacaagctg	EDN1	catacggacaacogtctcg	LAMB1	cagggagtgagaagagcgc	COLA1	gacagctagctcgggaag
CTGF	ggagccgaagtgcagaata	CYR61	agaagggtgacgactaaggc	EDN1	caagctctctggacctag	LAMB1	ctctgcacagggctaagaaa	COLA1	ctccatggcagctcacattg
CTGF	tacaccgtaccccaagat	CYR61	ctgactgagctctgcagatc	EDN1	gcccttggggaagtaaat	LAMB1	caagtggctgacatcacgt	COLA1	accatgacacctgttac
CTGF	taactgcactctctggaa	CYR61	gttatattcacaggctctgc	EDN1	gcactatcttcacgctctg	LAMB1	ggctctcatgataaggatct	COLA1	ttttgtccaggtagctctg
CTGF	tggcgacgacgctccatg	CYR61	acagttggctggaaacttt	EDN1	tgtcttttgcagctacac	LAMB1	tcaatgagatggctctcagg	COLA1	aggaattccgggaagctctg
CTGF	caaacgctctccagctgg	CYR61	ccatcaatacatgtgcaactg	EDN1	ttctttctgctggcnaaa	LAMB1	gcggfctggagcaaatgtg	COLA1	ttccaggaaccaagcaag
CTGF	gcttaatacatgttgatc	CYR61	agttgggagagatagttct	EDN1	ttccataatgtcttcaag	LAMB1	tcaagttgccacaaacttt	COLA1	aagtctctcactggatcac
CTGF	gagcgtgtcattgtaaac	CYR61	gtaactttgacacgacgagg	EDN1	atacatttccccaagctt	LAMB1	agttacattttccacacct	COLA1	aaactctctcactttcaaa
CTGF	ttaatgtctctccagctc	CYR61	atactactctctcagacac	EDN1	tcagactctgtgtcttag	LAMB1	gaattctgctccaatcca	COLA1	taaatcggagccccaaca
CTGF	agtagcgatgcacttttgc	CYR61	cacctcgagcgatcgaatc	EDN1	tgatattgacgctgtttctg	LAMB1	caaatggacatgctgttct	COLA1	catcttgccttttcaactg
CTGF	tgcacccaagaagctcaaac	CYR61	atfcattgtttctctcaac	EDN1	cttcaagctgggatacatg	LAMB1	gaagatctctacacacccc	COLA1	cttttggctctgaaact
CTGF	tagctcgtatgctctcatg	CYR61	ctgectttcaactgcaat	EDN1	tcacaataagctctctggag	LAMB1	catcgacttttcatgggg	COLA1	ttgagcttctctgactc
CTGF	tcggtaataactccaca gaa	CYR61	aaaaacagggagccgctca	EDN1	gaagctctgccaactgtg	LAMB1	gtgaggcttcaatgtcaga	COLA1	cgaagctctctttcttga
CTGF	tcagggcactgaactccac	CYR61	ttgtatagatgcaggctc	EDN1	gagcctgtgcttcagacag	LAMB1	acgaataatcacctctctt	COLA1	aaatcaggctcacttttt
CTGF	atgtttctctcagctc	CYR61	acattctggccttgaag	EDN1	aggctggagatgcagagtc	LAMB1	ctgtactctgctcctaaag	COLA1	tttctcaccatttctcg
CTGF	agggcaagctctgatgaac	CYR61	acacatgaagttgttgaaca	EDN1	tcaggaaccagcagaggatg	LAMB1	cccaagaatgacgtttcac	COLA1	ttccacggaaacaggac
CTGF	ttccgggacagttgtaagt	CYR61	ccacagcttcttgacactg	EDN1	tgttttgaacggcagctg	LAMB1	cttggatccagaaggttat	COLA1	ctgtcctataacattcca
CTGF	gtacatctctctgtagtaca	CYR61	aaactgtgtgagataccag	EDN1	aaactcctaacctcttgg	LAMB1	aagcaatctctcgaaccac	COLA1	tagctctggaaacttttg
CTGF	taagtctctcactctctg	CYR61	ggcactcaggggtgctattg	EDN1	catcccagatgaaaga	LAMB1	cttctcattgaatccatc	COLA1	ggcagagatgaccaggaaa
CTGF	attgggtgggaatctttcc	CYR61	aatccgggtttttcaaca	EDN1	aggacactctgcgaaac	LAMB1	tttaagcctctgtgtatg	COLA1	ctcagctccacaattctat
CTGF	tttgatcagtcacaatgtt	CYR61	gtacactggctctccaag	EDN1	ggctgactgacacaaaaca	LAMB1	ggtagaatccatcagagatg	COLA1	ccaatctgctataaatcc
CTGF	gtttgggtttgatacact	CYR61	caattctgccccttttccag	EDN1	tttcccgaatgtgccag	LAMB1	agcagctctcaagtaaat	COLA1	ctctcttttgactcttt
CTGF	ccactgcaagcttcaaat	CYR61	cgggggaattctgtcttg	EDN1	atctttgtggaacttggga	LAMB1	acagccatgcaagtgaca	COLA1	tttgagcccaagctgaaat
CTGF	ggtctgctactaattagtag	CYR61	tcacagtaagtaaacctga	EDN1	caatttgcactcttga	LAMB1	tgtgacagctcacacac	COLA1	ctctctcaactctacaga
CTGF	caactgctcctaaagccaac	CYR61	cggtattcttcaactcaa	EDN1	gtttgctttgtggtgtgt	LAMB1	agtaaaacggcttgcactgc	COLA1	agcagacactctctggag
CTGF	gatactaaactttctctg	CYR61	cgaggaaccgcaactctg	EDN1	atatcctgattatgtagt	LAMB1	cacacgtacatgftcaag	COLA1	cttctcttgcacaagt
CTGF	agcagccatattactctgat	CYR61	atctcagctctctgtctg	EDN1	tgggaaactcttccgaga	LAMB1	aattccctcatttggagagc	COLA1	ggccctgtaaaaggacaat
CTGF	tcctctcaattacacttca	CYR61	gaaaatgctccccacttct	EDN1	ctcagagctagagattagt	LAMB1	accaaatgattctcactgc	COLA1	ctggaatcaactgctgc
CTGF	ggtcagtgagcagctaaaa	CYR61	ctggatcatcatgactgttct	EDN1	tgtctgacattagacaga	LAMB1	gaatttccagagagattg	COLA1	gtaagccgtcaaacctttg
CTGF	gagaaatgcaatcctagctg	CYR61	caagttgtagtgcatttga	EDN1	tcagagctagatgattacca	LAMB1	ctgtctggaatcacagaga	COLA1	caagtaagctcaaatatcc
CTGF	ttgactcgtctctgtagtg	CYR61	agggaaacgctgcttactg	EDN1	gaacagggaactctctgatt	LAMB1	atccatcaaatcattgctt	COLA1	aaactttgctcccgtag
CTGF	gctgttctgactaa ggaac	CYR61	atgctcattgaacagctgta	EDN1	tcataaacacccctatacca	LAMB1	aaggtcagctcactgctc	COLA1	aggaatccgggaagactg
CTGF	tcagaatgctcagagctgagt	CYR61	aaaccaggtgacattttag	EDN1	atccaactcttcaatgagc	LAMB1	gcaactgttttaaggctc	COLA1	ctccatgtctccaggaag
CTGF	ttctgaacagctgctattg	CYR61	cttctccctgtttgctag	EDN1	ctctgccccaaagatattta	LAMB1	ctgactccaatcagctgag	COLA1	ttctctctttattccagg
CTGF	tcacgtcaatgcagagat	CYR61	ctccatgattctgattctga			LAMB1	aagtagtaaccaggttccac	COLA1	tcagggaatccggggaaac
CTGF	tacagcaaaactcactgcc	CYR61	ctttcacaatgagctccat			LAMB1	catagagtagctgatccagg	COLA1	ctccctggaaactggaaac
CTGF	ggtgttcagaaattgagctt	CYR61	tcctcaagaatgagcaagge			LAMB1	aatcccgctctgatatatt	COLA1	cttatacctttcaagccag
CTGF	acaagcttcaactctactc	CYR61	ctggcaagttcgaataacc			LAMB1	gctctgagcgaattaggatg		
CTGF	gtatccaaatctcatttga	CYR61	cttttacgactgtagaacc			LAMB1	catcatcggggatggtatta		
CTGF	ttgacggactgctcattctat	CYR61	agctttaaactgtccaacta			LAMB1	ccgagaagagcagacatate		
CTGF	tcocctttgcaaacactgc	CYR61	ccctcaggaaggtggaat			LAMB1	tagtttgcctctctcaaa		
CTGF	ctagaatcagcctgccaaag	CYR61	acagacactcatggagctgc			LAMB1	ctatcagagagctgtactg		
CTGF	aagtgagctaccacatttc	CYR61	tttagagtgcaatgactctc			LAMB1	agaatcagcagctgtgtag		
CTGF	ataaagccattgttctcatt	CYR61	aacactgatttctgttgc			LAMB1	ggtgaaatgctcagtgatt		
CTGF	gctatagatgctactcagt	CYR61	taccgaatggcatacactca			LAMB1	ggatctctgaaaggttcc		
CTGF	actgtccgaaaaacagctcat	CYR61	gaactttctactgaaggt			LAMB1	ctgcaaacatctgtcactgc		
						LAMB1	ctgtgttaacaggcgagaaa		
						LAMB1	caggaaactaacgaacct		

## **Chapter 5 – APPENDIX.**

### **The molecular mechanism of polarised mRNA localisation in endothelial cells.**

All of the experimental work in Chapter 5 was conducted by myself, with the exception of the qPCR experiment in Fig. 5.4a, and part of the dataset presented in Fig. 5.4b, which were conducted by Guilherme Costa and presented here with his permission.

## 5.1 Introduction.

This appendix serves to supplement the results presented in Chapter 2 and Chapter 3. In chapter 2 we identified a novel group of mRNAs that display similarly polarised localisation patterns in endothelial cells. We then characterised the 3'UTR sequences that drive their localisation. Surprisingly, we identified a common G-rich motif repeated throughout the 3'UTRs of the polarised *k5* mRNAs, which we then showed to be necessary to drive their localisation. This finding raised the possibility that the *k5* mRNAs share localisation sequences because they share transport machinery. To investigate this, we asked three questions:

1. Are polarised mRNAs transported/translated together as part of the same granule?
2. Is the use of G-rich motifs specific to the *k5* mRNAs?
3. Which trans-acting factors play a role?

Each of these questions will now be introduced.

### 5.1.2 Are polarised mRNAs transported together as part of the same granule?

If the polarised *k5* mRNAs we identified in Chapter 2 are transported via the same transport machinery, it is possible that they are transported as heterogeneous mRNA granules containing multiple different polarised mRNAs to their destination. One could imagine that this may be a more efficient method to achieve mRNA polarisation, rather than multiple individual transport events. mRNA granules have gained prominence recently for their role as molecular factories for mRNA processes like degradation, silencing, and translation (Moujaber & Stochaj, 2018). Some evidence obtained through live imaging of endogenous mRNAs in dendrites suggests multiple *ACTB* transcripts can be found in motile higher order structures. Importantly, these structures can merge when coming into contact with one another which is a key characteristic of a phase-separated granule (Donlin-Asp et al., 2021). This indicates that multiple *ACTB* transcripts can be transported within granules in dendrites. This is backed up by multiplexed imaging in both live and fixed cells showing that heterogeneous mRNA granules can also exist, with around 70% of dendrite mRNA granules contain more than one transcript of either *CaMKII $\alpha$* , *ARC*, or *NRGN* (Gao et al., 2008; Tübing et al., 2010). In the context of cell migration, some evidence suggests that polarised mRNAs can form heterogeneous clusters at protrusion tips, but these experiments were not conducted with single-molecule sensitivity (Moissoglu et al., 2019). Therefore, further investigation of the existence of polarised mRNA transport granules is necessary, visualising

endogenous mRNA with more refined imaging resolution, and particularly in the context of cell migration.

### **5.1.3 Is the use of G-rich motifs specific to the *k5* mRNAs?**

G-rich sequences are highly represented throughout 3'UTRs where they can perform varied mRNA processing roles. In Chapter 2, we showed that G-rich sequences are present in mRNAs from clusters other than the highly polarised *k5*, although at a much lower rate (Chapter 2, Fig. 2c). Moreover, evidence suggests that the G-richness of 3'UTRs does not correlate with the protrusion-enrichment of the polarised mRNA (Arora et al., 2021). If similar G-rich sequences are ubiquitous, it suggests that achieving specificity of mRNA polarisation may be a challenge. Interestingly, in parallel studies to Chapter 2, we identified some additional polarised mRNAs that shed light on these problems, and these will be discussed here.

### **5.1.4 Which trans-acting factors drive mRNA polarisation?**

mRNA binding proteins (RBPs) are the driving force of mRNA localisation. They play a critical role by binding to both the localisation sequences of mRNA, and to molecular motors. In this way, RBPs form a molecular bridge from the mRNA to the cytoskeleton to enable mRNA transport. The importance of RBPs is illustrated by the fact that mutations in such RBPs as FUS and FMRP are strongly linked to pathogenic mRNA mislocalisation in neurodegenerative diseases (Fiesel & Kahle, 2011; E. T. Wang et al., 2016). Moreover, misexpression of ZBP1, the RBP responsible for localisation of *ACTB* transcripts, is a hallmark of cancer progression (Gu et al., 2012; Hamilton et al., 2013; Nwokafor et al., 2016). Therefore, identification of RBPs is of paramount importance for understanding of the mechanisms of mRNA localisation in health and disease.

Characterisation of the RBPs responsible for driving the localisation of the *k5* mRNAs has been carried out in other studies, and a number of different RBPs have been implicated. The *k5* mRNAs have all been categorised as dependent on the multi-functional tumour suppressor protein Adenomatous Polyposis Coli (APC) for their transport to protrusions (T. Wang et al., 2017). *RAB13* has been suggested to co-localise with APC at the tips of growing deetyrosinated microtubules (Mili et al., 2008), and APC itself has both motor-binding and mRNA-binding domains, suggesting that it may link APC-dependent mRNAs to the cytoskeleton for transport (Preitner et al., 2014). Interestingly, KIF1C has also been implicated in the localisation of its own mRNA and the other members of the *k5* group

(Pichon et al., 2021). In Pichon et al., all *k5* mRNAs were found to associate with KIF1C, and knockdown of KIF1C expression severely abrogated *k5* mRNA polarisation. KIF1C was also shown to bind to APC, suggesting that both may be necessary to enable mRNA transport. Exactly how the roles of KIF1C and APC are coordinated in controlling mRNA localisation are not yet understood. Recently, the transport of *k5* mRNAs in dendrites has also been investigated with contradictory results to those just mentioned (Arora et al., 2021). Interestingly, knockdown of APC in neurons significantly increased the polarisation of exogenous *TRAK2* and *NET1* in dendrites. Therefore, it seems the role that APC may play in *k5* localisation may be cell-type dependent. Here, we aimed to test whether APC plays a role in endothelial cell mRNA polarisation, and then to identify other important RBPs.

## 5.2 Results

### 5.2.1 Polarised mRNAs colocalise with each other.

The *k5* mRNAs have uniquely conserved protrusion-enrichment across different cell types and display similar spatially-defined patterns. However, the relationship between different *k5* members remains to be tested. For example, it is not known whether *k5* mRNAs can occupy the same cellular protrusions, or whether they are targeted to different protrusions concurrently. Moreover, if they are targeted to the same protrusions, then the finer structural detail of their localisation remains to be understood. For example, it is not known whether polarised *k5* mRNAs exist as single copies in space, or whether multi-mRNA granules can form. Therefore, comparing the localisation of individual *k5* members to other *k5* members could provide great insight into the regulation of their localisation or translation.

Here, we compared the localisation of *RAB13* mRNA in a pairwise manner to the other *k5* cluster members using smFISH (Fig. 5.1a). First, we calculated average smFISH spot size by plotting a spot size histogram (Fig. 5.1b). Then we computed the Euclidean distance between all mRNA spots and filtered the data to identify colocalised spots. To do this, we used the radius of a single spot as the cut-off to categorise mRNAs as co-distributed (Fig. 5.1c). Interestingly, we found that around 5-10% of transcripts co-distributed with *RAB13* (Fig. 5.1d). This suggests that polarised mRNAs are capable of forming multi-mRNA higher order complexes. We then tested where in the cell these localisation events, occurred, by calculating the Euclidean distance from the centre of the nucleus to the colocalised spot coordinates, and presenting this as a percentage of the distance between the centre of the

A.

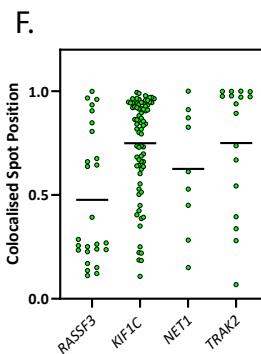
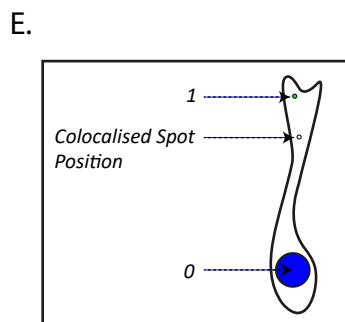
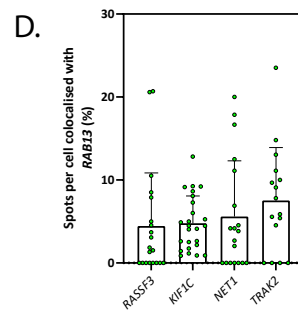
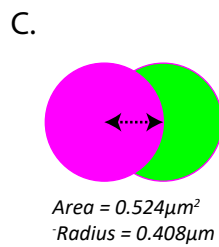
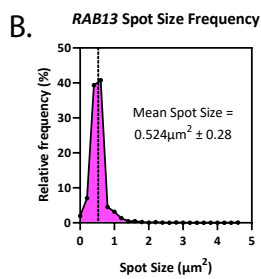
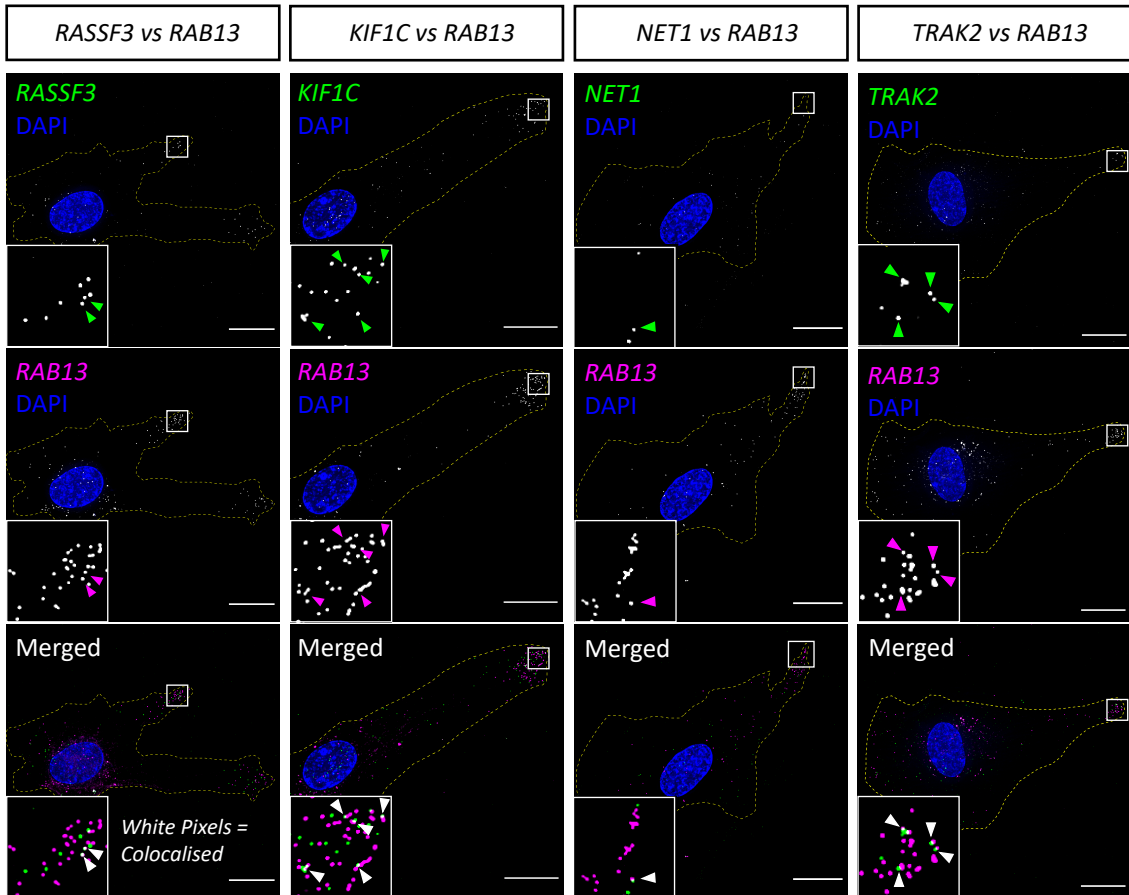




**Figure 5.1: Polarised RNAs colocalise with each other.**

- A. smFISH co-detection of *RAB13* RNA with other polarised *k5* RNAs in HUVECs. Arrowheads point to colocalised RNA spots.
- B. Histogram of *RAB13* RNA spot size frequency. Dotted black line shows mean spot size.
- C. Illustration of method to identify colocalised spots, via classifying colocalisation events as instances where spots are less than one spots radius away from one another.
- D. Percentage of total *k5* RNA spots that colocalise with *RAB13* RNA spots ( $n \geq 15$  cells).
- E. Illustration of method to test spatial distribution of colocalised spots, by showing colocalised spot position in relation to the most distal spot from the cell nucleus.
- F. Colocalised spot position in reference to the length of cellular protrusions ( $n \geq 8$  cells).

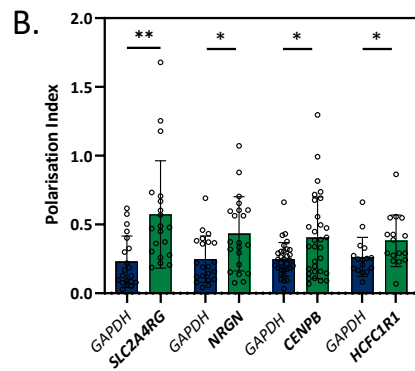
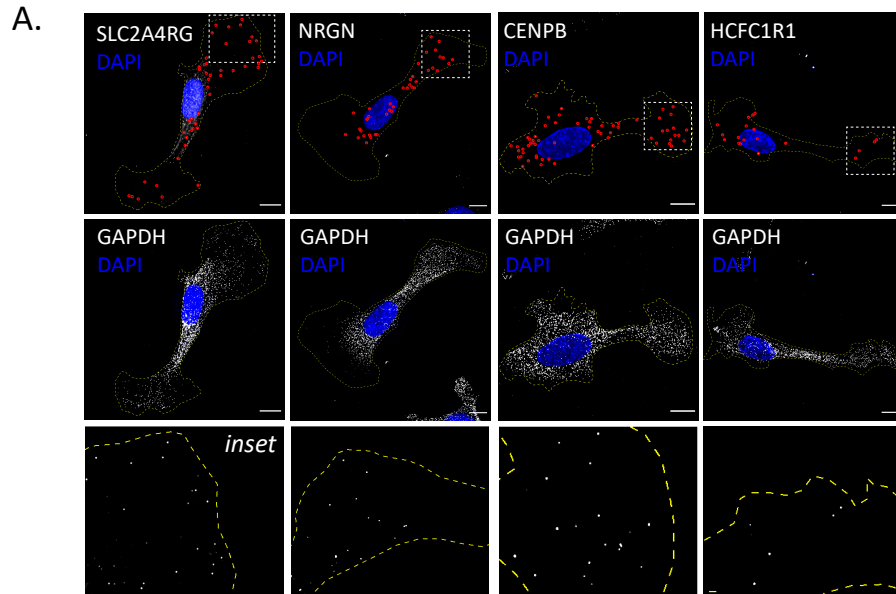
Data Information: Scale Bars = 10 $\mu$ m; Error Bars = SD; arrowheads point to colocalised spots.

nucleus and the most distal mRNA spot. In doing so, we found that whilst colocalised spots could occur at any position in the cell, they seemed to be slightly biased to the distal reaches of the protrusion (Fig. 5.1e, f). Hence, polarised mRNAs can exist in close proximity, perhaps as part of the same mRNA granule with other polarised mRNAs, and this seems to occur mostly in cellular protrusions.

### **5.2.2 The use of G-rich motifs is context specific as only *k5* 3'UTRs drive mRNA polarisation.**

During the validation of the clustering data presented in Chapter 2, we screened many different mRNAs for localisation patterns using smFISH. In doing so, we identified a group of mRNAs that display polarised localisation patterns (*HCFC1R1*, *SLC2A4RG*, *CENPB*, and *NRGN*) (Fig. 5.2a). These mRNAs were all significantly more polarised than control mRNA *GAPDH* (Fig. 5.2b). We noticed that each of these mRNAs had important characteristics that could help to reveal new information about the diversity of mRNA polarisation mechanisms, and the role that G-rich sequences play in driving mRNA localisation (Fig. 5.2c). For example, during the clustering process presented in Chapter 2, we were forced to exclude mRNAs that were not expressed in other cell types. Hence, we excluded endothelial-specific polarised mRNAs such as *SLC2A4RG* and *NRGN*. Also, we found that *CENPB* and *HCFC1R1* were present in *k1* and *k2*, respectively (Fig. 5.2c). This therefore shows that significant heterogeneity in mRNA polarisation is present within clusters, since we showed in Chapter 2 that other *k2* mRNA members are often diffusely distributed throughout the cell, whereas *CENPB* and *HCFC1R1* display more distal localisations. Moreover, although these additional mRNAs were found to have higher polarisation indexes than *GAPDH* (Fig. 5.2b), their polarisation was not as acute as that observed for the *k5* mRNAs (see Chapter 2). This evidence therefore highlights the specific, conserved nature of the localisation patterns of the highly polarised *k5*, and the perinuclear-located *k7* mRNAs.

We next wanted to test whether our newly-identified group of polarised mRNAs use the same mechanism for localisation as the *k5* mRNAs. Indeed, the presence of several G-rich motifs in the *CENPB* and *HCFC1R1* 3'UTRs prompted us to do this (Fig. 5.2c). We therefore returned to the MS2-MCP system, which we used to visualise exogenous mRNA with GFP in Chapter 2 and 3 (Fig. 5.3a). We then tested the potential of the 3'UTRs of the newly-identified polarised mRNAs to drive mRNA polarisation to protrusions. Interestingly, we found that the 3'UTRs of these mRNAs did not have localising potential, which contrasted



C.

Gene Name	Ps/Cb Enrichment				k cluster	3'UTR Length (bp)	Number of G-Motifs
	HUVEC	NIH/3T3	MDA-MB231	iNeurons			
<i>SLC2A4RG</i>	1.62	N/A	0.16	N/A	N/A	1060	0
<i>NRGN</i>	1.71	N/A	0.69	1.01	N/A	830	0
<i>CENPB</i>	1.64	4.79	0.87	1.35	1	833	1
<i>HCFC1R1</i>	1.95	1.68	0.59	1.72	2	238	2

**Figure 5.2: Identification of additional polarised RNAs.**

- A. smFISH co-detection of *SLC2A4RG*, *NRGN*, *CENPB*, and *HCFC1R1* RNA with *GAPDH* RNA in HUVECs.
- B. Polarisation index of RNAs detected in HUVECs ( $n \geq 15$  cells; \* $P < 0.05$ , \*\* $P < 0.01$ , paired  $t$ -test).
- C. Table with properties of identified polarised RNAs. Protrusion/Cell Body (Ps/CB) Fold Change Enrichment values and  $k$  cluster information from Costa *et al.*, 2020.

Data Information: Scale Bars = 10 $\mu$ m; Error Bars = SD.

with the 3'UTR of *RAB13* (Fig. 3b, c). The 3'UTRs of *SLC2A4RG* and *NRGN* also did not drive mRNA polarisation. This evidence suggests that the localising potential of 3'UTR G-rich motifs discovered in Chapter 2 is restricted to the *k5* mRNAs, and that other polarised mRNAs must use alternative mechanisms to achieve their polarised distribution.

### 5.2.3 Characterisation of RBPs necessary for *k5* localisation

APC has been reported previously to drive the localisation of *k5* polarised mRNAs (Mili et al., 2008). Therefore, we first tested the contribution that APC makes to mRNA polarisation in endothelial cells by siRNA knockdown (Fig. 5.4a). Similar to recent work in neurons (Arora et al., 2021), we found that reduced APC expression did not abrogate *RAB13* polarisation, suggesting that other protein factors may be the driving force, at least in our system (Fig. 5.4b, c). In order to identify these unknown factors, we designed an mRNA-RBP pull-down scheme to characterise the proteins that binds to G-rich sequence motifs. In these experiments, we synthesised *in vitro* biotinylated 3'UTR sequences that either contained or did not contain G-rich motifs. We then incubated these mRNAs with endothelial cell protein extract, before retrieving the mRNAs using a streptavidin magnetic pull-down. Proteins bound to the mRNAs were then identified using mass spectrometry (Fig. 5.4d). Interestingly, we noticed hnRNPA2 preferentially bound to mRNAs that contain G-rich sequences (Fig. 5.4e). hnRNPA2 immediately stood out to us as a potential important regulator because of its well established roles in various mRNA processing events including mRNA targeting in neurons (Fig. 5.4f) (Ainger et al., 1997; Gao et al., 2008). However, siRNA knockdown of hnRNPA2 did not affect the polarisation of *RAB13* mRNA (Fig. 4g, h), and this was corroborated by recent work in neurons (Arora et al., 2021). Therefore, this work illustrates the challenges associated with identification of necessary RBPs and highlights the need for further research to elucidate the molecular mechanism that drives *k5* mRNA transport.

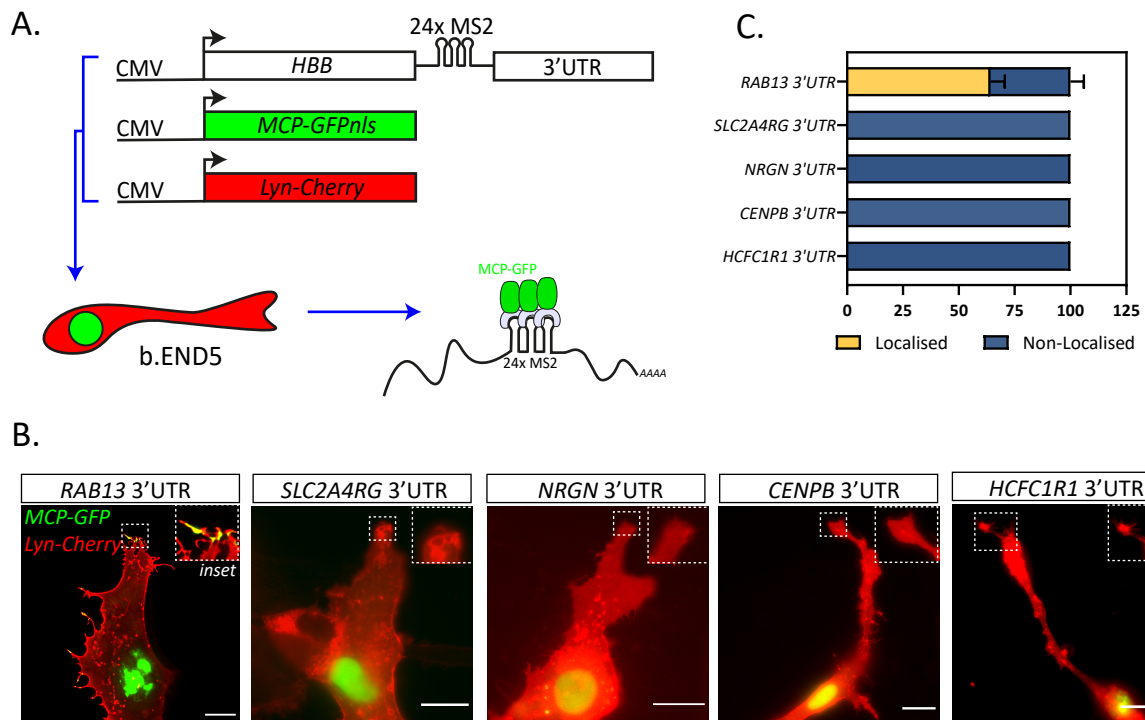


**Figure 5.3: Additional polarised RNA 3'UTRs do not contain localisation sequences.**

- A. Illustration of MS2-MCP system method for testing the localising capacity of RNA 3'UTRs. Endothelial cells were transfected plasmids for CMV promoter-driven expression of 24xMS2 tagged 3'UTRs, and MCP-GFPnls, allowing visualisation of RNA localisation.
- B. Representative bEND5 cells co-expressing lyn-Cherry, MCP-GFPnls, and 24xMS2-3'UTR. 3'UTRs from the respective RNAs were tested for RNA localising capacity.
- C. Percentage of bEND5 cells with MCP-GFPnls in protrusions when transfected with different 24xMS2-tagged 3'UTRs (n ≥ 3 experiments).

Data Information: Scale Bars = 10µm; Error Bars = SD.

### 5.3 Discussion

In this chapter we have turned our attention to investigation of the molecular mechanism that drives mRNA polarisation. In doing so, we have revealed novel insights into: i. how polarised mRNAs are organised into multi-mRNA structures, ii. the context-specific requirement for G-rich motifs, and iii. the role that RBPs play in driving mRNA localisation.

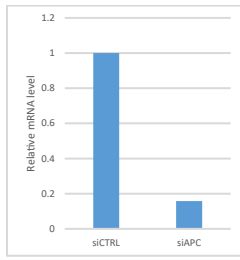
#### 5.3.1 K5 mRNAs are found in close proximity to each other.

mRNA granules containing many different mRNAs and proteins exist to compartmentalise mRNA processing events within subcellular space. Spatially restricting particular pathways to a granule is thought to be advantageous because the efficiency of interaction between multiple factors can be increased. This can be achieved by promoting the proximity between necessary interactors, or through the generation of a specific biochemical environment in the granule (Moujaber & Stochaj, 2018).

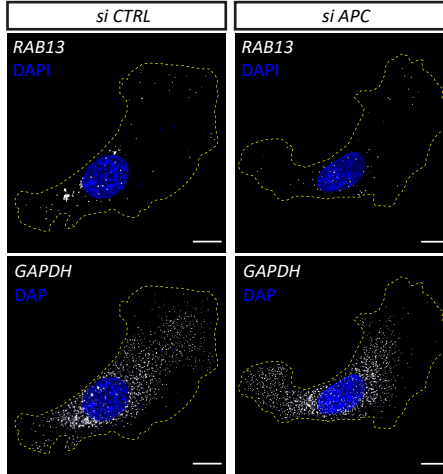
We aimed here to characterise the organisation of polarised mRNAs by single-molecule imaging of endogenous transcripts. We found that 5-10% of polarised mRNA spots directly colocalised with *RAB13*, and that most of these instances of colocalisation occur in the protrusions. However, colocalisation events did also occur in more proximal zones. We hypothesise that these low frequency proximal colocalisation events could correspond to multiple mRNAs undergoing co-transport to the protrusion. mRNA co-transport is a relatively well-established phenomenon in neurons, where it is thought to increase the efficiency of transport, since multiple mRNAs can be deposited at the destination at the same time, reducing the need for multiple individual transport events (Donlin-Asp et al., 2021). In migratory cells live imaging studies using exogenous mRNA have shown that mRNA expressed from reporter constructs is mostly transported as single molecules (Moissoglu et al., 2019). However, live imaging of endogenous mRNA in migratory cells is yet to be carried out. In the future, these experiments will be essential to investigate further the conclusions drawn here using fixed cells.

It is interesting to speculate that the co-distributing mRNAs in distal protrusions are undergoing some kind of translational regulation. Interestingly, the formation of multi-mRNA complexes in migratory protrusions has been suggested to only take place when those mRNAs are translationally repressed (Moissoglu et al., 2019). This is reminiscent of P-bodies and stress granules, two types of mRNA granule where the higher order structure renders the mRNA inaccessible to the translation machinery and hence translation is repressed (Luo et

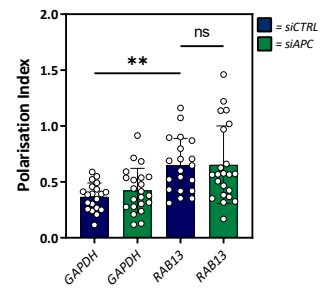
A.



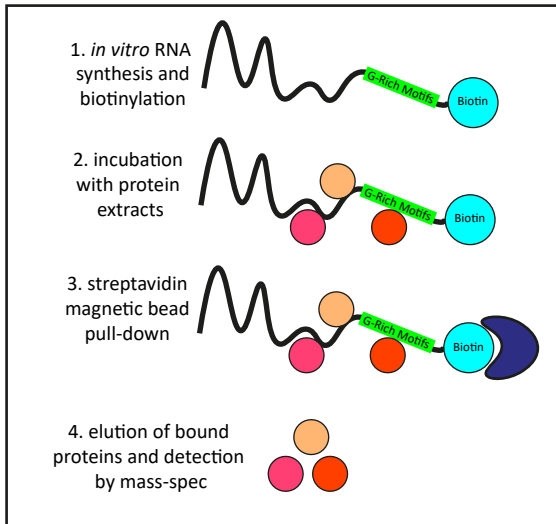
B.



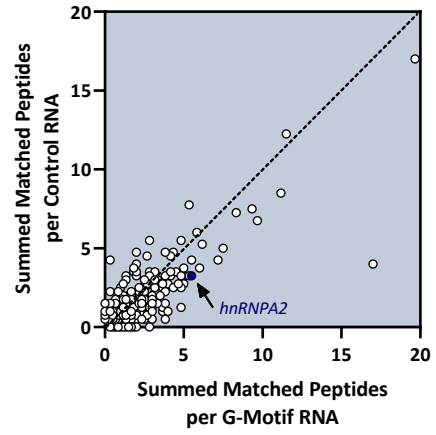
C.



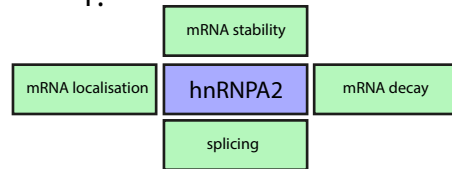
D.



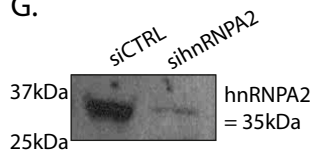
E.



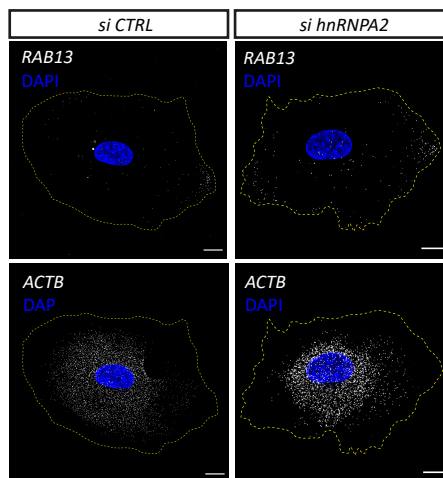
F.



G.



H.



I.

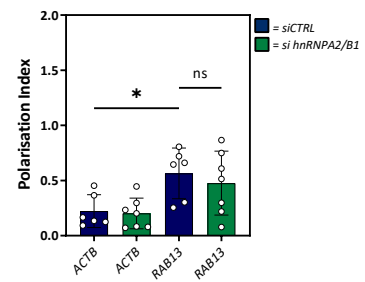




**Figure 5.4: Characterising RNA-Binding Proteins involved in polarised RNA transport.**

- A. qPCR analysis of *APC* expression level in HUVECs treated with siRNAs for *APC* (n = 1 experiment).
- B. smFISH co-detection of *RAB13* and *GAPDH* RNA in siCTRL and siAPC cells.
- C. Polarisation index of *RAB13* and *GAPDH* RNA in siCTRL and siAPC cells (n ≥ 20 cells; ns = not significant, \*P < 0.05, \*\*P < 0.01; one-way ANOVA with Šídák's multiple comparisons test).
- D. Scheme for identification of G-motif RBP interactors by *in vitro* RNA-RBP pull-down and mass spectrometry.
- E. Matched peptides identified by mass spectrometry interacting with G-rich containing, vs G-rich absent, RNA sequences.
- F. Illustration of crucial RNA processing functions performed by hnRNPA2.
- G. Representative Western Blotting of siCTRL and sihnRNPA2 cells.
- H. smFISH co-detection of *RAB13* RNA and *ACTB* (used here as a diffusely distributed control) in siCTRL and sihnRNPA2 HUVECs.
- I. Polarisation Index of *RAB13* and *ACTB* RNA in siCTRL and sihnRNPA2 HUVECs (n ≥ 7 cells; ns = not significant, \*P < 0.05; one-way ANOVA with Šídák's multiple comparisons test).

Data Information: Scale Bars = 10µm; Error Bars = SD.

al., 2018). Interestingly, the coalescence of polarised mRNAs into multi-mRNA structures occurs only when migratory protrusions are retracted (Moissoglu et al., 2019). This shows that cell physiological events can dictate the assembly/disassembly of mRNA complexes and suggests that our fixed cell approach may only be capturing a snapshot of the mRNA granule dynamics. To conclude, perhaps the *k5* mRNAs are participating in two types of mRNA granule. In distal protrusions, granule formation could suggest translational co-regulation. In more proximal zones, granule formation could suggest ongoing co-transport. In the future, live imaging of endogenous mRNA will be necessary to test these hypotheses.

### **5.3.2 G-rich motifs specifically drive polarisation of the *k5* mRNAs, and other polarised mRNAs must use alternative mechanisms.**

The identification of additional polarised mRNAs to those presented in Chapter 2 has helped to reveal important information about the diversity of polarised mRNAs and the mechanism by which they are transported. We have found that *SLC2A4RG* is specifically polarised in endothelial cells, suggesting that it performs a vital role in endothelial cell biology, although the molecular function of SLC2A4RG protein has not yet been well investigated. We also found that *NRGN* is polarised in endothelial cells. *NRGN* has previously been reported to be enriched in dendrites via its 3'UTR, which contains an hnRNPA2-dependent localisation element (Gao et al., 2008). We were therefore interested to find that the *NRGN* 3'UTR has no localising capacity in endothelial cells, suggesting that cell-type specific differences in the mechanism that drives polarisation of mRNAs may exist. Finally, we found unexpected mRNA polarisation diversity across the clusters identified in Chapter 2, as *CENPB* and *HCFC1R1* (*K1*, *K2* respectively) were enriched in endothelial protrusions. However, despite the presence of G-rich motifs in their 3'UTRs, these sequences did not drive localisation. This suggests that the presence of G-motifs alone is not enough to enable mRNA localisation, and that the surrounding sequence/structural context may also be important. Perhaps also the number of motifs, or the exact sequence composition of the motifs may also play a role. The additional polarised mRNAs described here may possibly use alternative localisation sequences, which could perhaps be located in the 5'UTR or coding sequence.

### **5.3.3 Neither APC nor hnRNPA2 drive *RAB13* localisation in endothelial cells.**

Here, I have presented evidence that suggests that neither APC or hnRNPA2 are required for the localisation of polarised mRNA in endothelial cells. However, some caveats do apply. Full depletion of APC and hnRNPA2 were not confirmed by western blot, suggesting that

perhaps some functional protein may persist. Similar experiments have also been conducted in neurons recently, with interesting conclusions. Both APC and hnRNPA2 knockdown resulted in increased polarisation of reporter mRNA (Arora et al., 2021). This work perhaps suggests cell-type specific mechanisms of localisation of mRNAs may occur. Importantly, this study identified a novel trans-acting factor as necessary for the localisation of *TRAK2* and *NET1* in neurons, namely the RBP, UNK. Interestingly, we did not identify UNK in our *in vitro* mRNA pull-down experiments, which likely indicates slight experimental differences, perhaps due to the use of protein extracts from different cell types. Future work should aim to address whether UNK plays a role in endogenous *k5* localisation in migratory cells.

The exact molecular function of APC in the localisation of polarised mRNAs therefore remains elusive. APC is known to bind to *k5* mRNAs, and APC knockdown reduces *k5* polarisation during Transwell migration (Mili et al., 2008; T. Wang et al., 2017). However, knockdown of APC expression is yet to produce a concomitant reduction in mRNA polarisation when mRNAs are imaged in cells during 2D migration on flat substrates. This could be due to the context dependency of particular migration assays. To test this in the future more physiological forms of migration should be used in combination with more thorough analysis of mRNA distribution. A deeper interrogation of mRNA distribution during 3D or matrix migration when APC or other RBPs are knocked down could allow more subtle mRNA distribution phenotypes to be observed. To conclude, although the experiments here have not identified the necessary RBP responsible for driving polarised mRNA distribution, they have shed light on the function of APC and hnRNPA2 in mRNA localisation in endothelial cells, and shown that further work is necessary to fully reveal the molecular mechanism that enables polarised mRNA transport.

## **5.4 Materials and Methods**

### **5.4.1 Cell Culture**

HUVEC (PromoCell) were cultured on 0.1% gelatin coated T75 flasks (Corning) in endothelial cell basal medium 2 (EBM-2, Promocell) with an additional supplement pack (5% FCS, EGF (5ng/ml), VEGF (0.5ng/ml), FGF2 (10ng/ml), long R3 insulin growth factor-1 (20ng/ml), hydrocortisone (0.2µg/ml), and ascorbic acid (1µg/ml)). 50mg/ml gentamycin (Sigma) and 250µg/ml amphotericin (Sigma) were also added to the culture media. All HUVEC experiments were conducted with cells between passage 3-6. All cells were split prior to reaching 90% confluency and their media was changed every two days.

### **5.4.2 siRNA Knockdown**

Gene knockdown was achieved using ON-TARGETplus non-targeting or gene-specific SMARTpool siRNAs (Horizon). 0.3µM siRNA was diluted in 200µl Opti-MEM containing 1.5% v/v GeneFECTOR (Venn Nova). This mix was then added to a well of a 6-well plate containing 1ml Opti-MEM and the sample was incubated at 37°C for 3 hours. Opti-MEM was then replaced with endothelial growth media and samples were allowed to recover for 48-72 hours.

### **5.4.3 qPCR**

qPCR analysis of *APC* expression was performed using 1–2 µl cDNA, 0.25 µM gene-specific primers, and 1× Power SYBR Green Master Mix (Thermo Fisher Scientific) in a StepOne Real-Time PCR System (Applied Biosystems). GAPDH expression was used to normalise gene expression levels, and the relative mRNA levels were analysed with the  $2^{-\Delta\Delta CT}$  method.

### **5.4.4 Western Blot**

Whole cell protein was extracted using RIPA buffer (25 mM Tris–HCl pH 7.6, 150 mM NaCl, 1% NP-40, 1% sodium deoxycholate and 0.1% SDS) containing 1:100 Protease Inhibitor Cocktail. Protein concentration was quantified using Pierce BCA Protein Assay Kit (Thermo Fisher Scientific) before denaturation with Laemmli Buffer (250 mM Tris–HCl pH 6.8, 2% SDS, 10% glycerol, 0.0025% bromophenol blue, 2.5% β-mercaptoethanol) at 95°C for 5 min. Proteins were separated using 10% Mini-PROTEAN TGX precast protein gels (Bio-Rad). Trans-Blot Turbo transfer system (Bio-Rad) was used to transfer proteins to PVDF membranes using manufacturers guidelines. Membranes were then blocked for 1hr at

room temperature in 2.5% BSA (Sigma) in TBS containing 0.1% Tween-20. Primary antibodies were diluted in blocking buffer and incubated overnight at 4°C. Membranes were then washed with TBS containing 0.1% Tween-20 before incubation with secondary antibodies diluted in blocking buffer for 1hr at room temperature, followed by more washes. Pierce ECL Western Blotting substrate (Thermo Fisher Scientific) was used to develop chemiluminescent signal, which was then detected digitally using a ChemiDoc MP Imager (Bio-Rad).

The following primary and secondary antibodies were used for western blotting at the indicated concentrations: 1:500 mouse hnRNPA2/B1 (Santa Cruz EF-67:sc-53531), 1:3000 HRP-conjugated goat anti-mouse (Cell Signalling Technology).

#### **5.4.5 smFISH**

HUVECs on coverslips were fixed in methanol-free 4% formaldehyde and permeabilised in 70% ethanol. Stellaris smFISH gene-specific probes sets (Table 5.1), conjugated to Quasar 570/670 fluorophores, were designed using an online tool (Biosearchtech). GAPDH pre-designed reference probe sets were purchased directly. smFISH probe hybridisation was carried out as described previously. Briefly, samples were washed in wash buffer (2X SSC, 10% formamide) before incubation overnight at 37°C with smFISH probe sets diluted in hybridisation buffer (2X SSC, 10% formamide, 10% w/v Dextran Sulphate). Samples were then washed twice in wash buffer at 37°C for 30 minutes.

#### **5.4.6 mRNA-Protein Pull Down**

Bait mRNA was transcribed *in vitro* from PCR generated DNA fragments using either T7 mMESSAGE mMACHINE or MegaShortScript reverse transcription kits following manufacturer's guidelines (Thermo Fisher Scientific). mRNA cleanup following synthesis was carried out using MEGAClear Cleanup Kit (Thermo Fisher Scientific). 50pmol mRNA was then labelled with desthobiotin using Pierce mRNA 3'End Desthobiotinylation Kit (Thermo Fisher Scientific). Briefly, mRNA samples were denatured in 25% DMSO for 5 minutes at 85°C, before following manufacturers guidelines and incubating labelling reaction at 16°C for 2 hours. Finally, each labelled mRNA sample was then mixed with 100µg whole HUVEC lysates for 4 hours in the presence of 100mM NaCl before isolation of mRNA-Binding Proteins using Pierce Magnetic mRNA Pull-Down Kit (Thermo Fisher Scientific). Peptides were separated and analysed using a Q Exactive HF Orbitrap LC-MS/MS System. (Thermo Fisher Scientific). Finally, proteins were identified using Mascot software.

#### 5.4.7 MS2-MCP System

MS2 experiments were conducted as previously described (Costa et al., 2020). Briefly, b.End5 cells were transfected with the following plasmids: pcDNA3-lyn-Cherry, PCS2-MCP-GFPnls, and pcDNA3-HBB-MS2-3'UTR. Corresponding 3'UTR sequences from *RAB13*, *SLC2A4RG*, *CENPB*, *NRGN*, and *HCFC1R1* were amplified using gene-specific primers (Table 5.2) and cloned into pcDNA3-HBB-MS2-3'UTR using the NheI and XhoI restriction sites.

## 5.5 References

- Ainger, K., Avossa, D., Diana, A. S., Barry, C., Barbarese, E., & Carson, J. H. (1997). Transport and localization elements in myelin basic protein mRNA. *Journal of Cell Biology*, *138*(5), 1077–1087. <https://doi.org/10.1083/jcb.138.5.1077>
- Arora, A., Gutierrez, R. C., Eletto, D., Becker, R., Brown, M., Moor, A. E., Russ, H. A., & Taliaferro, J. M. (2021). High-throughput identification of RNA localization elements reveals a regulatory role for A/G rich sequences. *BioRxiv*, 2021.10.20.465152. <https://doi.org/10.1101/2021.10.20.465152>
- Costa, G., Bradbury, J. J., Tarannum, N., & Herbert, S. P. (2020). RAB13 mRNA compartmentalisation spatially orients tissue morphogenesis. *The EMBO Journal*, *39*(21), e106003. <https://doi.org/10.15252/EMBJ.2020106003>
- Donlin-Asp, P. G., Polisseni, C., Klimek, R., Heckel, A., & Schuman, E. M. (2021). Differential regulation of local mRNA dynamics and translation following long-term potentiation and depression. *Proceedings of the National Academy of Sciences*, *118*(13), 2017578118. <https://doi.org/10.1073/PNAS.2017578118>
- Fiesel, F. C., & Kahle, P. J. (2011). TDP-43 and FUS/TLS: Cellular functions and implications for neurodegeneration. In *FEBS Journal* (Vol. 278, Issue 19, pp. 3550–3568). <https://doi.org/10.1111/j.1742-4658.2011.08258.x>
- Gao, Y., Tatavarty, V., Korza, G., Levin, M. K., & Carson, J. H. (2008). Multiplexed dendritic targeting of  $\alpha$  calcium calmodulin-dependent protein kinase II, neurogranin, and activity-regulated cytoskeleton-associated protein RNAs by the A2 pathway. *Molecular Biology of the Cell*, *19*(5), 2311–2327. <https://doi.org/10.1091/mbc.E07-09-0914>
- Gu, W., Katz, Z., Wu, B., Park, H. Y., Li, D., Lin, S., Wells, A. L., & Singer, R. H. (2012). Regulation of local expression of cell adhesion and motility-related mRNAs in breast cancer cells by IMP1/ZBP1. *Journal of Cell Science*, *125*(1), 81–91. <https://doi.org/10.1242/jcs.086132>
- Hamilton, K. E., Noubissi, F. K., Katti, P. S., Hahn, C. M., Davey, S. R., Lundsmith, E. T., Klein-Szanto, A. J., Rhim, A. D., Spiegelman, V. S., & Rustgi, A. K. (2013). IMP1 promotes tumor growth, dissemination and a tumor-initiating cell phenotype in colorectal cancer cell xenografts. *Carcinogenesis*, *34*(11), 2647. <https://doi.org/10.1093/CARCIN/BGT217>
- Luo, Y., Na, Z., & Slavoff, S. A. (2018). P-Bodies: Composition, Properties, and Functions. *Biochemistry*, *57*(17), 2424–2431. <https://doi.org/10.1021/ACS.BIOCHEM.7B01162>
- Mili, S., Moissoglu, K., & Macara, I. G. (2008). Genome-wide screen reveals APC-associated RNAs enriched in cell protrusions. *Nature*, *453*(7191), 115–119. <https://doi.org/10.1038/nature06888>
- Moissoglu, K., Yasuda, K., Wang, T., Chrisafis, G., & Mili, S. (2019). Translational regulation of protrusion-localized RNAs involves silencing and clustering after transport. *ELife*, *8*. <https://doi.org/10.7554/eLife.44752>

- Moujaber, O., & Stochaj, U. (2018). *Cytoplasmic RNA Granules in Somatic Maintenance*. <https://doi.org/10.1159/000488759>
- Nwokafor, C. U., Sellers, R. S., & Singer, R. H. (2016). IMP1, an mRNA binding protein that reduces the metastatic potential of breast cancer in a mouse model. *Oncotarget*, *7*(45), 72662–72671. <https://doi.org/10.18632/oncotarget.12083>
- Pichon, X., Moissoglu, K., Coleno, E., Wang, T., Imbert, A., Robert, M.-C., Peter, M., Chouaib, R., Walter, T., Mueller, F., Zibara, K., Bertrand, E., & Mili, S. (2021). The kinesin KIF1C transports APC-dependent mRNAs to cell protrusions. *RNA*, *rna.078576.120*. <https://doi.org/10.1261/RNA.078576.120>
- Preitner, N., Quan, J., Nowakowski, D. W., Hancock, M. L., Shi, J., Tcherkezian, J., Young-Pearse, T. L., & Flanagan, J. G. (2014). APC is an RNA-binding protein, and its interactome provides a link to neural development and microtubule assembly. *Cell*, *158*(2), 368–382. <https://doi.org/10.1016/j.cell.2014.05.042>
- Tübing, F., Vendra, G., Mikl, M., Macchi, P., Thomas, S., & Kiebler, M. A. (2010). Dendritically Localized Transcripts Are Sorted into Distinct Ribonucleoprotein Particles That Display Fast Directional Motility along Dendrites of Hippocampal Neurons. *Journal of Neuroscience*, *30*(11), 4160–4170. <https://doi.org/10.1523/JNEUROSCI.3537-09.2010>
- Wang, E. T., Taliaferro, J. M., Lee, J. A., Sudhakaran, I. P., Rossoll, W., Gross, C., Moss, K. R., & Bassell, G. J. (2016). Dysregulation of mRNA Localization and Translation in Genetic Disease. *The Journal of Neuroscience*, *36*(45), 11418. <https://doi.org/10.1523/JNEUROSCI.2352-16.2016>
- Wang, T., Hamilla, S., Cam, M., Aranda-Espinoza, H., & Mili, S. (2017). Extracellular matrix stiffness and cell contractility control RNA localization to promote cell migration. *Nature Communications*, *8*(1). <https://doi.org/10.1038/s41467-017-00884-y>



**Table 5.1 smFISH probes.**

mRNA	Probe sequence (5' - 3')	mRNA	Probe sequence (5' - 3')	mRNA	Probe sequence (5' - 3')	mRNA	Probe sequence (5' - 3')
<i>CENPB</i>	cgagacaaagcgctcgcg	<i>HCFC1R1</i>	tagggttcgggacggtac	<i>SLC2A4RG</i>	gagggctgactctcaggac	<i>NRGN</i>	ggcggggagaagtggag
<i>CENPB</i>	tgacttctcccgaacgctc	<i>HCFC1R1</i>	ggfggacaccactctcta	<i>SLC2A4RG</i>	gaactccaagcccgcgaag	<i>NRGN</i>	gggaagccaatcaggagc
<i>CENPB</i>	ggacggcgggatgtgaag	<i>HCFC1R1</i>	tatccggcttaagggggc	<i>SLC2A4RG</i>	caggcttgaaggcagcg	<i>NRGN</i>	ctccctcgcgaatgtaa
<i>CENPB</i>	ttgttctcaggatcgtgc	<i>HCFC1R1</i>	tggcggaaaggcaggettg	<i>SLC2A4RG</i>	cagaaggagagggtggtg	<i>NRGN</i>	aacagcagctctgctc
<i>CENPB</i>	gagacagctgtgtgctct	<i>HCFC1R1</i>	cacagccgcgaggttctg	<i>SLC2A4RG</i>	ctgggctgaaggctcaac	<i>NRGN</i>	tcctctgggggacgaag
<i>CENPB</i>	cgatgagcaagccctcgag	<i>HCFC1R1</i>	ccaagagaggatgggcgt	<i>SLC2A4RG</i>	gacggagaggactggtcac	<i>NRGN</i>	cagtcctcgtgtctg
<i>CENPB</i>	ttctccttgaggatgatgc	<i>HCFC1R1</i>	gaggagtctctgaggcg	<i>SLC2A4RG</i>	cccaaacagaaagtggct	<i>NRGN</i>	gagcaggcttctcgtg
<i>CENPB</i>	ttggaggcgggtaagtgt	<i>HCFC1R1</i>	gtggatctgggacacag	<i>SLC2A4RG</i>	cttcttttctcagggtg	<i>NRGN</i>	tagaatgtcgtctccg
<i>CENPB</i>	ctgaacacgtctcgcgagg	<i>HCFC1R1</i>	ttgggtttggggctcctg	<i>SLC2A4RG</i>	cactggaacatgacctggg	<i>NRGN</i>	ggatcgtccagcgggatg
<i>CENPB</i>	catagactggtctcgtgg	<i>HCFC1R1</i>	caaggctcgtcagcagat	<i>SLC2A4RG</i>	cggatgtctctcgtcatc	<i>NRGN</i>	ctgattttggcggcgc
<i>CENPB</i>	ctggtcggcaggaagtgc	<i>HCFC1R1</i>	ctcggagaggggagctgg	<i>SLC2A4RG</i>	tcacatcactctgctcag	<i>NRGN</i>	atgtggccccgaaactc
<i>CENPB</i>	cattgcccagatgagcagc	<i>HCFC1R1</i>	tgtgctcatgggacacag	<i>SLC2A4RG</i>	ctctgtgtagtagaagtcc	<i>NRGN</i>	ctccgctcttactct
<i>CENPB</i>	cttgaggtggcgggtgag	<i>HCFC1R1</i>	gaaactgctgcgcagag	<i>SLC2A4RG</i>	agcgtgtccacaccaat	<i>NRGN</i>	catctctctcgggaact
<i>CENPB</i>	ctcaagtactggccagg	<i>HCFC1R1</i>	tggccatgttctctcag	<i>SLC2A4RG</i>	tggggacactggagtacg	<i>NRGN</i>	tctctcgtcgaagg
<i>CENPB</i>	gagactctcagccattcg	<i>HCFC1R1</i>	ggctgagttgagagaagt	<i>SLC2A4RG</i>	gaaggcagcggcatggag	<i>NRGN</i>	tcacaacacgcagggga
<i>CENPB</i>	aagaaggccagctgcacat	<i>HCFC1R1</i>	gtaggggtggtcattgtg	<i>SLC2A4RG</i>	ttagcaacggtctcagga	<i>NRGN</i>	aaaggccagcagctcagc
<i>CENPB</i>	catggccttgagcagcatg	<i>HCFC1R1</i>	aaggtcatggggggctg	<i>SLC2A4RG</i>	gacacggctactgtgacag	<i>NRGN</i>	aggccaatgggacat
<i>CENPB</i>	cggcagccacaagtgcag	<i>HCFC1R1</i>	agagcaaggctcctgag	<i>SLC2A4RG</i>	tccgatctggagacaag	<i>NRGN</i>	attggagcgcagtggtt
<i>CENPB</i>	tatgtccgaaggctccact	<i>HCFC1R1</i>	tagcgcagagaagcagc	<i>SLC2A4RG</i>	atacacttccggcactc	<i>NRGN</i>	agaggtggcgagaagca
<i>CENPB</i>	caaagccagcctcacgaaa	<i>HCFC1R1</i>	cagggatgaggtccag	<i>SLC2A4RG</i>	ttagtccaggaaccgctgg	<i>NRGN</i>	aaagcgcactgagcctgc
<i>CENPB</i>	aaagtgggtacagccacc	<i>HCFC1R1</i>	cagcctcagcagcaggag	<i>SLC2A4RG</i>	atgttctgaacgagccgg	<i>NRGN</i>	gagtgctctgggtgacg
<i>CENPB</i>	aaagtaagccatgcccctc	<i>HCFC1R1</i>	ttcagggtaggggggac	<i>SLC2A4RG</i>	gggaggagaaggtggtag	<i>NRGN</i>	cttttagctcgcacaga
<i>CENPB</i>	caggtacctctgaccatg	<i>HCFC1R1</i>	cattatgtcccagctgg	<i>SLC2A4RG</i>	tcagctggtgaaagccag	<i>NRGN</i>	ggagtggcagcagatgt
<i>CENPB</i>	gtcatcaatggggaaggag	<i>HCFC1R1</i>	gtcccaccagcactcagag	<i>SLC2A4RG</i>	cccccacaagtaaaagcag	<i>NRGN</i>	cccggatccaagtcttg
<i>CENPB</i>	gaggatgtgctctgcacg	<i>HCFC1R1</i>	cgctgctctctctgttg	<i>SLC2A4RG</i>	agaggcactttgagtggtg	<i>NRGN</i>	aacaacctcttcccttc
<i>CENPB</i>	aaccagatcgtgtccaag	<i>HCFC1R1</i>	aggaacctgtccctttg	<i>SLC2A4RG</i>	gtgtggtttggctttagtg	<i>NRGN</i>	caaggctcgtccgaaacc
<i>CENPB</i>	gtggttctctggtcaca	<i>HCFC1R1</i>	gctactctcagcagagag	<i>SLC2A4RG</i>	cttgggctaaggggacag	<i>NRGN</i>	gaacttcttccggtcag
<i>CENPB</i>	tgactcagctttgatgtcc	<i>HCFC1R1</i>	gaaggtctgtgtcccag	<i>SLC2A4RG</i>	aaatctacggccgacagg	<i>NRGN</i>	acaggcaggtgtgggata
<i>CENPB</i>	aatctaggtgggggcaca	<i>HCFC1R1</i>	ctcagtgctctctgttga	<i>SLC2A4RG</i>	aaagctgggcccataacac	<i>NRGN</i>	cgctcggctttgcataa
<i>CENPB</i>	actctggctccatgcacag	<i>HCFC1R1</i>	catcccagaactccgttg	<i>SLC2A4RG</i>	ctcaaaagtcatcgggact	<i>NRGN</i>	aagactcctcactcagag
<i>CENPB</i>	caggaccaggggaagcatt	<i>HCFC1R1</i>	cagttctctgggggtg	<i>SLC2A4RG</i>	gagttaaagtcgagtggtg	<i>NRGN</i>	tcagaaaccttgcgcca
<i>CENPB</i>	aagcaggcagtgagcctga	<i>HCFC1R1</i>	tcctttgctcagaactct	<i>SLC2A4RG</i>	tggtaaaaacagccccagg	<i>NRGN</i>	tgttcaattccaacca
<i>CENPB</i>	gtgtgtagcaccggacag			<i>SLC2A4RG</i>	agacgtgagacacctgagc	<i>NRGN</i>	acattggacattcctct
<i>CENPB</i>	ctgtggttagtccactgag			<i>SLC2A4RG</i>	ttatttctctctcgcct		
<i>CENPB</i>	agaggggagagcactctc						
<i>CENPB</i>	cacaaagacctgacgtgg						
<i>CENPB</i>	cttcccagaatggctttgg						
<i>CENPB</i>	aactgtgcttcaaggcg						
<i>CENPB</i>	cttggttacttccacggtg						
<i>CENPB</i>	actggaaaggagcagctg						
<i>CENPB</i>	aggggagtgacagattta						
<i>CENPB</i>	ttaaaacgttcacccccac						

**Table 5.2 Oligonucleotide sequences.**

Cloning	
Name	Sequences (5' - 3')
NheI <i>CENPB</i> 3'UTR F	GGAAGCTAGCGTCACTGGACCTAGCTGTGC
XhoI <i>CENPB</i> 3'UTR R	GGAACCTCGAGTTGGCTGTTAAAACGTTTAC
NheI <i>HCFC1R1</i> 3'UTR F	GGAAGCTAGCGTCTGGTGGACAGTGCCCC
XhoI <i>HCFC1R1</i> 3'UTR R	GGAACCTCGAGTCTGAGCAAAGGAAGGCTT
NheI <i>NRGN</i> 3'UTR F	GGAAGCTAGCGCCAGAAGTGGACATTTTCA
XhoI <i>NRGN</i> 3'UTR R	GGAACCTCGAGTGAACACTTGGACATTCCTC
NheI <i>SLC2A4RG</i> 3'UTR F	GGAAGCTAGCGTCCGGCTCGTTCAAGAAC
XhoI <i>SLC2A4RG</i> 3'UTR R	GGAACCTCGAGTTCTGAAAAACCTCAAATCTT

## 6. DISCUSSION

### 6.1 Summary

Whilst mRNA localisation has been appreciated as an important factor in migrating cells for some time, precise understanding of where, how, and why mRNAs are localised has been lacking. The work presented in this thesis represents a major step forward in our understanding of these questions. Firstly, we have characterised two subcellular zones that harbour specific groups mRNAs; highly polarised *k5* mRNAs in endothelial protrusions, and peri-Golgi associated *k7* mRNAs. In identification of the *k5* group of highly polarised mRNAs, we have revealed that mRNA polarisation is conserved across multiple cell types, and these five mRNAs display highly similar subcellular distributions. We then provided new insights into the mechanism that drives their localisation, by identifying common G-rich 3'UTR sequences as necessary localisation elements. This evidence suggested to us that polarised mRNAs may use shared transport machinery to reach their destination, and in support of this hypothesis we found that *k5* mRNAs can co-distribute with one another. We then characterised the mRNA-binding proteins that bind to G-rich motifs in an attempt to identify parts of the transport machinery. Lastly, we revealed the molecular function of *RAB13* and *TRAK2* mRNA polarisation in physiological endothelial cell migration and *in vivo* angiogenesis. These findings are summarised in Figure 6.

### 6.2 Identification of common localisation elements

Here, we have identified a necessary G-rich sequence motif repeated throughout the 3'UTRs of polarised mRNAs which is necessary for driving their localisation. Common localisation elements have been reported in the past to drive the localisation of a group of polarised mRNAs including *ARC*, *NRGN*, *CaMKiia*, *BDNF*, and *TAU* to neuronal dendrites. These mRNA 3'UTRs contain a common stem loop structure which is bound by RBP hnRNPA2 to enable transport (Ainger et al., 1997; Gao et al., 2008; Raju et al., 2011). Similarly, *gurken* and *the I factor* are also reported to harbour a common stem loop sequence that drives their localisation to the same location in *Drosophila* oocytes (van de Bor et al., 2005). However, identification of common localisation elements has been challenging in the context of cell migration. One of the reasons for this may be that a refined understanding of the exact localisation of particular mRNAs has been elusive, until the work presented in Chapter 2 of this thesis. Importantly, it is possible that the workflow described here could be used in the future for identification of novel localised mRNAs and the sequences that drive their

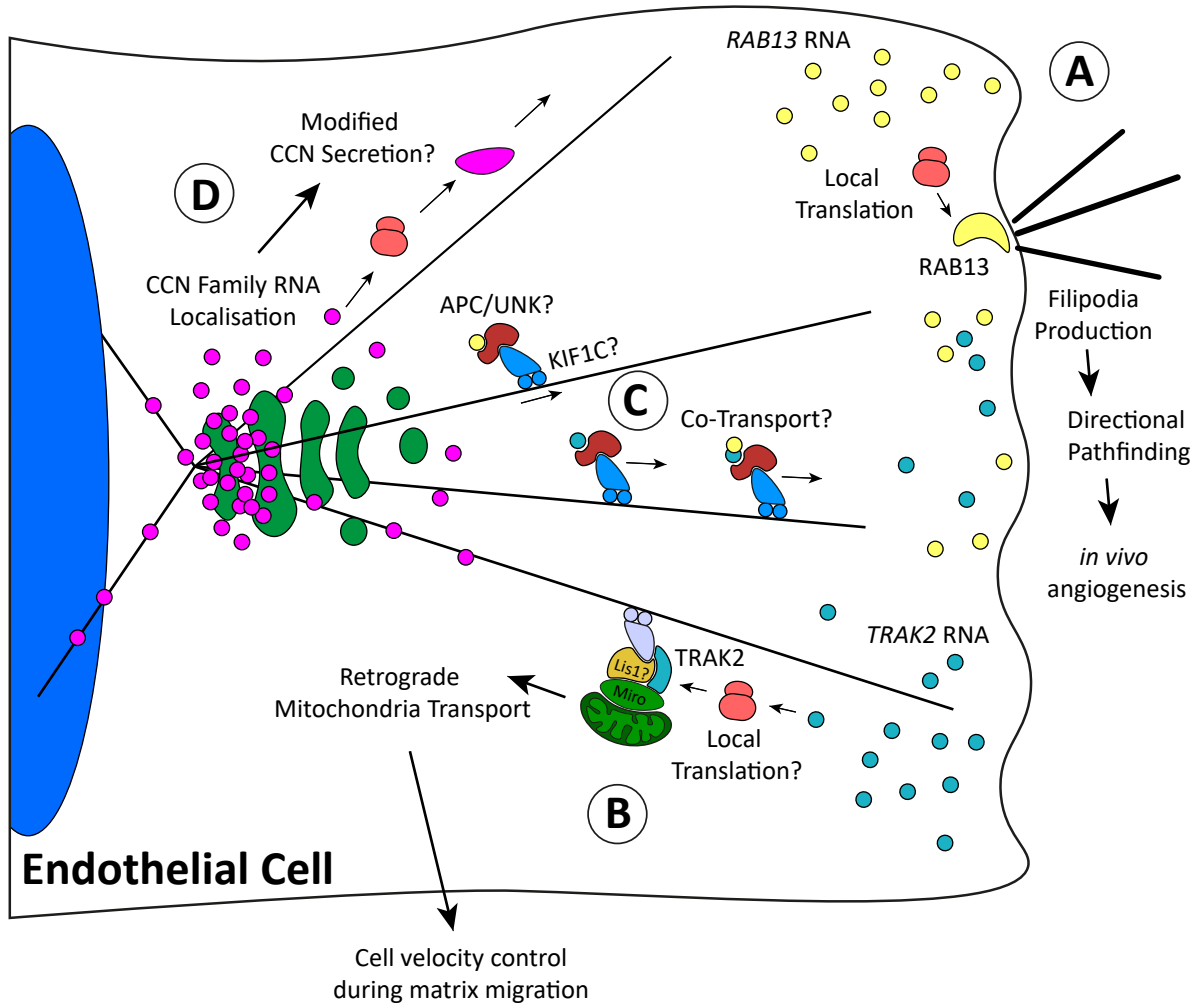


**Figure 6. Defining the role of RNA localisation in cell migration.**

A). *RAB13* transcripts are targeted to protrusions where their local translation defines a zone of filopodia production. This process is essential for enabling directional pathfinding of motile endothelial cells during *in vivo* angiogenesis.

B). The enrichment of *TRAK2* mRNA in the leading edge determines the subcellular spatial range that mitochondria can occupy and acts as a cellular brake on motile speed.

C). The molecular mechanism, and RNA-binding proteins, that drive polarised RNA localisation still require further investigation. However, polarised RNAs can co-distribute with one another, indicating the potential for co-transport in RNA granules.

D). CCN family RNAs adopt a unique subcellular distribution surrounding the Golgi Apparatus, and this localisation is dependent on the microtubule network. It remains to be seen how this localisation modifies CCN family protein production, secretion, and hence angiogenesis.

localisation. This workflow could include: *i*). Characterisation of broad localisation patterns by mRNA sequencing coupled to cell fractionation. Potential applications could include *in vivo* laser-microdissected tissue samples, or purified organelle fractions of particular cell types. *ii*). Datasets could be compared to existing published mRNA sequencing data to reveal the diversity or specificity of mRNA localisation patterns between cell types *iii*). Enriched mRNA candidates could be validated by endogenous mRNA visualisation, to understand the finer detail of the mRNA distribution, perhaps in combination with immunofluorescence of other subcellular landmarks. *iv*). Then, motif enrichment analysis could be used to identify overrepresented sequence motifs that are shared between multiple mRNAs in the same subcellular location, or indeed motifs repeated within a single candidate mRNA 3'UTR. *v*). Motif function can be tested using the MS2-MCP reporter system described here.

A similar workflow to this has recently been used to identify important localised mRNAs in oligodendrocytes (Yergert et al., 2021). Oligodendrocytes localise mRNAs to long protrusions called myelin sheaths that wrap around and insulate surrounding axons. Localised mRNAs were first identified here by sequencing and mRNA imaging, then overrepresented sequence motifs were found by enrichment analysis. They then showed that these motifs were necessary and sufficient for mRNA transport to myelin sheaths. This shows how the workflow described in this report can be applied to other mRNAs and other biological systems for the identification of important sequence motifs. Indeed, in the future this workflow should be applied to identify necessary motifs that drive the peri-Golgi localisation of the *k7* mRNAs described here.

### **6.3 Necessary and sufficient localisation elements.**

Work in the past has focussed on finding “minimal localisation elements”. These sequences are defined as the smallest sequence that is both necessary and sufficient to drive mRNA localisation. Identifying sufficiency is particularly challenging, because small yet necessary sequence elements can be repeated and dispersed throughout the 3'UTR. These small motifs often contribute more than the sum of their parts to the localisation process, because they can perform crucial organisational roles within the mRNA secondary structure. RBPs are mostly thought to interact with particular structural configurations rather than specific sequence elements. Therefore, nucleotide sequences are quite often less important than overall secondary structure (Martin & Ephrussi, 2009). We hypothesise that the necessary G-motifs identified here are likely to play a structural role, since the number and distribution varies

widely between mRNAs. Both *KIF1C* and *RAB13* require tightly clustered groups of multiple G-motifs, yet only a single 29bp motif is necessary for *TRAK2* localisation. We focussed on identifying minimal necessary, rather than minimal sufficient motifs because this then provided a route into investigating the primary aim of this work: testing the functions of localised mRNAs. However, in the future it will perhaps be important to characterise the exact minimal sufficient localisation sequences. This could help with identification of RBPs that drive localisation, because a more specific sequence could be used to screen for binding partners. Therefore, whilst this work has provided important information on necessary motif sequences, in the future a more detailed characterisation of sufficient sequences may be required.

#### **6.4 Molecular functions of localised mRNAs**

Decades of research has provided detailed understanding of the molecular function of localised *ACTB* during cell migration (Hüttelmaier et al., 2005; Katz et al., 2012; Shestakova et al., 2001). Despite this, until recently we have not known whether mRNA localisation to migratory protrusions is unique to *ACTB*, or conversely whether *ACTB* represents a paradigm for many different mRNAs. The work presented here shows that additional mRNAs are localised to the protrusions of migratory cells, where they perform diverse functions. Hence, mRNA localisation is an eminent, vital phenomenon during cell migration.

The work presented here identified two novel functions of localised mRNAs. Firstly, we found that *RAB13* localisation defines a zone of filopodia production in the leading edge of migrating cells, and that mislocalisation of *RAB13* then forces the production of filopodia in more proximal regions. Then, we found that *TRAK2* mRNA localisation regulates the subcellular range that mitochondria can occupy in migratory protrusions, and that *TRAK2* mislocalisation causes inappropriate accumulation of mitochondria in the leading edge. Hence, it seems that mRNA localisation to migratory protrusions is required to restrict or promote protein activity within that subcellular region, and that abrogation of this localisation allows translated proteins to be active in inappropriate regions. mRNA localisation therefore serves to spatiotemporally regulate protein activity, and subsequently ensure that particular cellular functions occur only in specific regions. In doing so, mRNA localisation enables migratory cells to become polarised by promoting subfunctionalisation of the leading edge.

To conclude, this work has greatly expanded the cohort of known functions of localised mRNAs and revealed that mRNA localisation is not a niche mechanism used for regulation of

protein function by *ACTB* alone. Indeed, following this work, the diversity of roles of localised mRNAs in migratory protrusions now includes cytoskeletal organisation, membrane remodelling, and organelle distribution.

Despite these findings, some key experiments should still be undertaken to validate the observations. For example, the exact components of the TRAK2-mediated mitochondria transport complex are not completely defined, and the role that mRNA localisation contributes to the building of this complex has not been explored. Testing of the molecular interaction between TRAK2 protein produced from localised versus non-localised mRNA with LIS1 and MIRO should be carried out. Confirmation of the observed mitochondria distribution phenotype could also be achieved by knockdown of these components, thus testing whether *TRAK2* mRNA mislocalisation phenocopies total loss of mitochondria minus end directed movement. Finally, the link between mitochondria distribution and cell motility should be interrogated further by carrying out mitochondria functional assessment in *wt* and  $\Delta$ TRAK2 cells, to test whether increased mitochondria activity is observed in protrusions of  $\Delta$ TRAK2 cells.

## **6.5 Cellular functions of localised mRNAs.**

Evidence of broader localised mRNA functionality in migratory cell physiology has been mostly limited to studies focussed on *ACTB*. These experiments have shown that *ACTB* localisation to migratory protrusions is essential to enable fibroblast directional pathfinding (Shestakova et al., 2001). Here, we developed a CRISPR-Cas9 method to excise necessary endogenous localisation elements from 3'UTRs, abrogating mRNA localisation, and hence used this to understand the role that localisation of *RAB13* and *TRAK2* mRNA localisation plays in cell migration. We have applied these tools to endothelial cells and assayed phenotypic consequences during physiological modes of migration *in vitro* and *in vivo*. Importantly, the experiments shown here are the first to report a role for mRNA localisation in cell migration during *in vivo* vertebrate tissue development.

## **6.6 Angiogenesis as a model to understand the role of mRNA localisation in cell migration**

Here, we opted to use endothelial cell migration as a model to test the function of mRNA localisation during *in vivo* cell migration. Previously, most research has used *in vitro* fibroblast or cancer cell migration (Mardakheh et al., 2015; Shestakova et al., 2001; Wang et al., 2017). We believe endothelial cell migration to be a suitable model for testing the

principles of mRNA localisation for a number of reasons. Firstly, endothelial cell migration is a vital and ubiquitous feature of multicellular life, since it enables angiogenesis.

Angiogenesis is the process used by organisms to build new blood vessels (Herbert & R Stainier, 2011). It occurs by the sprouting and branching of new blood vessels from existing ones. Early in development, the blood vessel network must be established via angiogenesis prior to other organs so that oxygen and nutrients can be supplied. Later in life, angiogenesis is reactivated to restore blood supply to damaged tissues, and angiogenesis is co-opted by tumours during cancer pathogenesis. Therefore, understanding more about the importance of mRNA localisation in this process is particularly important. Secondly, well-established *in vitro* and *in vivo* models of angiogenesis exist for investigation of endothelial migration. We have used a variety of these here. The zebrafish intersegmental vessel model used to assay the effects of *RAB13* mRNA mislocalisation in Chapter 2 is gaining prominence. One reason for this is that cells migrate during intersegmental vessel morphogenesis in a highly stereotyped manner, so assaying phenotypic consequences of mRNA mislocalisation is relatively simple (Childs et al., 2002). Importantly, zebrafish embryos also possess a number of characteristics that make them particularly amenable to experimental manipulation including their high fecundity, well-established genetic manipulation tools, and high imaging resolution due to embryo transparency (Chávez et al., 2016). However, for investigation of human genes, a number of *in vitro* systems also exist that recapitulate many of the aspects of *in vivo* endothelial migration such as the co-culture and cell-derived matrix systems used here (Cukierman et al., 2001; Franco-Barraza et al., 2016; Hetheridge et al., 2011). For these reasons, we believe endothelial cell migration and angiogenesis provides a suitable physiological scenario for investigation of the principles of mRNA localisation.

## **7 Future Work**

### **7.1 Molecular functions of many localised mRNAs remain unknown**

Whilst the work presented here has provided new insights into the molecular roles that localised mRNAs can play, there still remains a lot that we do not know. For example, the molecular roles of other *k5* mRNAs *NET1*, *KIF1C*, and *RASSF3* are yet to be characterised. Recent work has shown that *NET1* mRNA localisation is essential to enable cancer cell invasion, although precise detail about why it is essential is lacking (Chrisafis et al., 2020). Since we have characterised the necessary regions of the 3'UTRs that drive their localisation

(Chapter 2), the next step would be to endogenously impair their localisation using the CRISPR-Cas9 method we have described. In contrast, the sequences that drive the polarised localisation of the additional polarised mRNAs *SLC2A4RG*, *CENPB*, *NRGN*, and *HCFC1R1* presented in the Appendix chapter remain uncharacterised, although we have shown they are not present in their 3'UTRs. Future work should aim to identify the necessary sequences potentially in the 5'UTR or coding sequences, perhaps using the motif enrichment method described here, and impair their localisation in order to assay function. One challenge associated with understanding the roles of these mRNAs is that the proteins they encode are not very well characterised during cell migration. This would make assaying phenotypic consequences of mRNA localisation impairment particularly difficult. In contrast, the essential molecular functions of CCN family proteins in angiogenesis are well known. Hence, testing the function of the peri-Golgi localisation of the CCN mRNAs here, via identification of the molecular determinants of their localisation and subsequent impairment of their localisation, could reveal important information about how mRNA localisation may contribute to protein secretion. This work is important to reveal the total diversity of roles that localised mRNAs play during cell migration.

## **7.2 Molecular determinants of polarised mRNA localisation remain unknown**

The work presented here has revealed key insights into the molecular transport mechanism of polarised mRNAs, yet much more remains to be uncovered. Firstly, we showed that polarised mRNAs can colocalise with one another, and that this interaction can occur throughout the cell but is slightly biased towards migratory protrusions. This finding is indicative of coordinated mRNA regulation, but it remains to be seen exactly what kind of regulation. For example, it could be that polarised mRNAs are packaged into multi-mRNA complexes to undergo either co-transport or translational co-regulation. In order to test these possibilities, it is essential that the dynamics of endogenous mRNAs are characterised further. Here, we are only capturing a snapshot of the mRNA life in our fixed samples. Live imaging of endogenous mRNA dynamics has only been achieved for a handful of mRNAs in mammalian cells, and most of these instances have been in neurons (Das et al., 2018; Park et al., 2014). For example, recent advances in molecular beacon technologies, which are fluorescently-labelled antisense oligonucleotide sequences, have enabled tracking of endogenous *ACTB* transcripts in dendrites and growth cones (Donlin-Asp et al., 2021; Turner-Bridger et al., 2018). Tracking how individual mRNAs move in live migrating cells could provide a wealth of information on their regulation. It could reveal whether polarised mRNAs coalesce into



multi-mRNA granules, whether these granules display the properties of phase-separated condensates, and the trafficking dynamics of these granules through the cytoplasm. Moreover, when combined with chemical manipulation of translation, the role that mRNA granule formation plays in translational regulation could also be tested. Finally, mRNA dynamics could also be correlated with cell morphological changes to understand how cell physiology and mRNA polarisation are coordinated. Therefore, in the future it will be essential to visualise live polarised mRNA dynamics to reveal new information about polarised mRNA transport and translational regulation.

mRNA-binding proteins (RBPs) are the gatekeepers of mRNA regulation. Here, we attempted to identify important RBPs for the localisation of polarised mRNAs.

Unfortunately, we were only able to report negative results from these experiments, although some insights were produced. Namely, there now appears to be a question mark over the exact role that APC, the predominant RBP implicated in regulation of these localised mRNAs in previous studies, plays in regulating *k5* cluster mRNA localisation (Mili et al., 2008; Wang et al., 2017), since we found that APC knockdown did not affect *RAB13* polarisation.

Interestingly, another recent study has found that APC knockdown in fact increased mRNA polarisation to neurites (Arora et al., 2021). Clearly, further research is required to exactly elucidate whether APC is the driving factor for localisation of these polarised mRNAs, and this should be coordinated with research to calculate the relative contribution of other recently identified trans-acting factors. For example, KIF1C has been shown to participate in mRNA transport and also bind to APC (Pichon et al., 2021). KIF1C is a kinesin-3 family motor protein, but APC has been shown in *in vitro* reconstitution assays to also make motile complexes with a kinesin 3 family motor KIF3A (Baumann et al., 2020). It may be that APC performs a scaffolding role in mRNA transport complexes, perhaps linking mRNAs to motors for transport. However, our mRNA pull-down assays have not identified APC as binding to 3'UTR G-rich sequences, and neither have other studies (Arora et al., 2021). It is possible that APC only performs a cell-type specific role in fibroblasts, but the conserved nature of the polarised *k5* mRNAs suggests that this is unlikely. Alternatively, APC may only associate with mRNA once it has already reached the protrusions and mediate some form of mRNA anchoring. Anchoring of mRNAs in place at their functional destination is an established phenomenon in the localisation of other mRNAs including *ASH1* in yeast bud tips and *ACTB* in migratory protrusions, where anchoring provides a stable platform for translation machinery (Beach et al., 1999; Liu et al., 2002). In this case, it would explain why

our study does not show any decrease in mRNA polarisation when APC expression is knocked down, since polarised mRNAs might still reach their destination. More detailed characterisation of APC function in mRNA polarisation is therefore required, and a “master regulator” RBP in control of mRNA polarisation remains to be found.

In the future, more precise protein identification methods should be used to assay the proteins that interact with polarised mRNAs. For example, *ACTB* transcripts were recently tagged with biotin ligase, which is an enzyme that labels surrounding proteins with biotin. These biotin-labelled proteins were then isolated by streptavidin pull-down and identified with mass spectrometry (Mukherjee et al., 2019). This resulted in the identification of novel *ACTB* regulator FUBP3, and knockdown of FUBP3 was then found to reduce *ACTB* mRNA polarisation to the leading edge in fibroblasts. In the future, tools such as these could be applied to identify the total protein interaction network of the polarised mRNAs described here.

### **7.3 Role of the extracellular environment in controlling mRNA localisation**

One key missing aspect from our understanding is the role that the extracellular environment plays in instructing mRNA localisation. Here, we have used physiologically relevant models of cell migration that incorporate information from the extracellular environment to help us understand the situational requirement for localised mRNA *in vivo*. Importantly, we have observed that cell migration in physiological conditions when extracellular matrix is present induces an altered mode of endothelial migration. This change is also associated with increasingly stereotyped and acute mRNA polarisation, compared to cells migrating in 2D on flat substrates. It could be that changes in cell morphology cause the changes in mRNA polarisation, or conversely that mRNA polarisation is the driving factor behind the morphological changes. In the future, live imaging of mRNA movements could be coupled to imaging of protrusion dynamics to explain this causality dilemma.

Whilst it is clear the extracellular environment greatly influences mRNA localisation patterns, the instrumental elements within the extracellular environment have not been characterised. It is likely that, as is the case for most cell biological phenomena, a combination of mechanical and biochemical cues work together to regulate mRNA localisation. Evidence for the importance of the mechanical environment comes from the fact that matrix stiffness influences the degree of mRNA polarisation, and that these alterations are mediated by actomyosin contractility in protrusions (Wang et al., 2017). In agreement

with this, integrin engagement has long been suggested to direct the localisation of both mRNAs and ribosomes to active focal adhesions (Chicurel et al., 1998). It's therefore likely that cell adhesions to extracellular matrix components can directly influence the degree of mRNA polarisation. One possible instructive matrix factor appears to be laminin, since a dense, stiff region of laminin is found to be enriched at the leading front of invasive cancer cells. Importantly, blocking the sensing of laminin using an antibody has been shown to impair mRNA localisation (Chrisafis et al., 2020). Hence, the mechanical environment is a crucial factor in the regulation of mRNA polarisation.

One relatively unexplored avenue of research is the role that growth factor signalling may play. Specific local signals including Brain-Derived Neurotrophic Factor (BDNF), Neurotrophin-3 and Netrin-1 are known to stimulate the directed localisation of *ACTB* transcripts to growth cones and neurites (Baj et al., 2016; Leung et al., 2018; Yao et al., 2006; Zhang et al., 2001). However, in the context of cell migration, the role that specific signalling molecules play has never been tested. Despite the critical importance of growth factors like VEGF to endothelial cell migration during angiogenesis, the possibility that mRNA localisation could act as a critical downstream effector of physiological responses has been surprisingly overlooked. One method by which this could work is that growth factor receptor activation in protrusions could stimulate downstream processes that result in modulation of mRNA binding protein activity, which could in turn affect mRNA localisation. A key advantage of this is that it would allow migratory cells to bypass slow transcriptional changes and respond rapidly, and in a spatially-precise manner, by increasing local transcript concentration and presumably local protein concentration in a specific locale in the region of the cell where the signal was received. This is known to occur in neurons, where specific dendrite stimulation is known to cause *ACTB* transcripts to stop movement in close proximity to the stimulated dendrite, thereby increasing mRNA enrichment in that zone (Bauer et al., 2019; Yoon et al., 2016). Similarly, *ACTB* mRNA polarisation increases in migratory cells upon stimulation with lysophosphatidic acid (Latham et al., 1994). In the future it could be important to understand whether specific growth factors also promote the localisation of the polarised mRNAs identified in our work. Moreover, it is possible that specific growth factor combinations received by migratory cells could produce a specific mRNA localisation signature. It may be that this context-dependency means that the total cohort of protrusion-localised mRNAs are yet to be discovered.

#### **7.4 Translation of polarised mRNAs**

For mRNA localisation to produce a spatially-restricted increase in local protein concentration, local protein synthesis must take place at the final mRNA destination. Understanding of where in subcellular space local translation can take place has been improved in recent times by the development of novel imaging tools to visualise translation. One of these, based on the proximity ligation assay, we have used in Chapter 2 to show that *RAB13* is translated in migratory protrusions (Tom Dieck et al., 2015). One key advantage of this system is that it allows visualisation of endogenous protein translation. Nevertheless, this work has also been built on recently by the development of Suntag tools that allow single-molecule live imaging of translation from exogenous constructs (Tanenbaum et al., 2014). Using these tools, translation rate of *RAB13* was found to be increased at extending protrusions and reduced at retracting protrusions (Moissoglu et al., 2019). These studies therefore revealed that *RAB13* translation is dynamically regulated in accordance with changes to cell physiology. One aspect we have not covered in this report is how *TRAK2* local translation is regulated. It remains to be seen whether *TRAK2* is translated primarily in the distal reaches of protrusions, or conversely whether it is translated throughout the cell. The use of the Suntag system would help to answer this question. Most evidence from other polarised mRNAs including *RAB13* suggests that mRNA position does not usually correlate with translated protein position, and that proteins produced from localised mRNAs can be found distributed throughout cells (Moissoglu et al., 2020). Indeed, GFP-tagged *TRAK2* protein has been observed to co-distribute with all mitochondria, not just mitochondria in the most distal protrusions (López-Doménech et al., 2018). Hence, it can be assumed that *TRAK2* functionality is likely to be necessary for the transport of mitochondria throughout the cell. It could be that functional *TRAK2* in proximal regions is produced from proximal mRNAs, perhaps by translation during the mRNA journey from nucleus to protrusion. Indeed, since *TRAK2* mislocalisation did not result in a reduction in overall *TRAK2* protein levels, it seems that translation of *TRAK2* mRNAs does not preferentially occur in the protrusions and can occur throughout the whole cell. In the future, more experiments using advanced visualisation tools for translation described here will be necessary to answer these questions.

## **8. Conclusion**

The work presented in this thesis makes major contributions to our understanding of the role of mRNA localisation in cell migration by revealing important information about:

1. The diversity of mRNA localisation patterns exhibited in migrating cells.
2. The mechanism by which localised mRNAs reach their subcellular destination.
3. The physiological role that localised mRNAs play in endothelial cell migration and angiogenesis.

## 9. References

- Ainger, K., Avossa, D., Diana, A. S., Barry, C., Barbarese, E., & Carson, J. H. (1997). Transport and localization elements in myelin basic protein mRNA. *Journal of Cell Biology*, *138*(5), 1077–1087. <https://doi.org/10.1083/jcb.138.5.1077>
- Alami, N. H., Smith, R. B., Carrasco, M. A., Williams, L. A., Winborn, C. S., Han, S. S. W., Kiskinis, E., Winborn, B., Freibaum, B. D., Kanagaraj, A., Clare, A. J., Badders, N. M., Bilican, B., Chaum, E., Chandran, S., Shaw, C. E., Eggen, K. C., Maniatis, T., & Taylor, J. P. (2014). Axonal transport of TDP-43 mRNA granules in neurons is impaired by ALS-causing mutations. *Neuron*, *81*(3), 536. <https://doi.org/10.1016/J.NEURON.2013.12.018>
- Amrute-Nayak, M., & Bullock, S. L. (2012). Single-molecule assays reveal that RNA localization signals regulate dynein–dynactin copy number on individual transcript cargoes. *Nature Cell Biology* 2012 *14*:4, *14*(4), 416–423. <https://doi.org/10.1038/ncb2446>
- An, J. J., Gharami, K., Liao, G.-Y., Woo, N. H., Lau, A. G., Vanevski, F., Torre, E. R., Jones, K. R., Feng, Y., Lu, B., & Xu, B. (2008). Distinct Role of Long 3' UTR BDNF mRNA in Spine Morphology and Synaptic Plasticity in Hippocampal Neurons. *Cell*, *134*(1), 175–187. <https://doi.org/10.1016/j.cell.2008.05.045>
- Aoki, K., & Taketo, M. M. (2007). Adenomatous polyposis coli (APC): A multi-functional tumor suppressor gene. In *Journal of Cell Science* (Vol. 120, Issue 19, pp. 3327–3335). The Company of Biologists Ltd. <https://doi.org/10.1242/jcs.03485>
- Arn, E. A., Cha, B. J., Theurkauf, W. E., & Macdonald, P. M. (2003). Recognition of a bicoid mRNA localization signal by a protein complex containing Swallow, Nod, and RNA binding proteins. *Developmental Cell*, *4*(1), 41–51. [https://doi.org/10.1016/S1534-5807\(02\)00397-0](https://doi.org/10.1016/S1534-5807(02)00397-0)
- Arnautova, I., George, J., Kleinman, H. K., & Benton, G. (2009). The endothelial cell tube formation assay on basement membrane turns 20: State of the science and the art. *Angiogenesis*, *12*(3), 267–274. <https://doi.org/10.1007/S10456-009-9146-4>
- Arora, A., Gutierrez, R. C., Eletto, D., Becker, R., Brown, M., Moor, A. E., Russ, H. A., & Taliaferro, J. M. (2021). High-throughput identification of RNA localization elements reveals a regulatory role for A/G rich sequences. *BioRxiv*, 2021.10.20.465152. <https://doi.org/10.1101/2021.10.20.465152>

Babu, M. M., van der Lee, R., de Groot, N. S., & Gsponer, J. (2011). Intrinsically disordered proteins: Regulation and disease. In *Current Opinion in Structural Biology* (Vol. 21, Issue 3, pp. 432–440). <https://doi.org/10.1016/j.sbi.2011.03.011>

Bagni, C., Mannucci, L., Dotti, C. G., & Amaldi, F. (2000). *Chemical Stimulation of Synaptosomes Modulates-Ca<sup>2+</sup>/Calmodulin-Dependent Protein Kinase II mRNA Association to Polysomes*. <http://www.jneurosci.org/cgi/content/full/4207>

Baj, G., Leone, E., Chao, M. v., & Tongiorgi, E. (2011). Spatial segregation of BDNF transcripts enables BDNF to differentially shape distinct dendritic compartments. *Proceedings of the National Academy of Sciences of the United States of America*, *108*(40), 16813–16818. <https://doi.org/10.1073/pnas.1014168108>

Baj, G., Pinhero, V., Vaghi, V., & Tongiorgi, E. (2016). Signaling pathways controlling activity-dependent local translation of BDNF and their localization in dendritic arbors. *Journal of Cell Science*, *129*(14), 2852–2864. <https://doi.org/10.1242/JCS.177626>

Bathina, S., & Das, U. N. (2015). Brain-derived neurotrophic factor and its clinical implications. *Archives of Medical Science : AMS*, *11*(6), 1164. <https://doi.org/10.5114/AOMS.2015.56342>

Batish, M., Bogaard, P. van den, Kramer, F. R., & Tyagi, S. (2012). Neuronal mRNAs travel singly into dendrites. *Proceedings of the National Academy of Sciences*, *109*(12), 4645–4650. <https://doi.org/10.1073/PNAS.1111226109>

Bauer, K. E., Segura, I., Gaspar, I., Scheuss, V., Illig, C., Ammer, G., Hutten, S., Basyuk, E., Fernández-Moya, S. M., Ehses, J., Bertrand, E., & Kiebler, M. A. (2019). Live cell imaging reveals 3'-UTR dependent mRNA sorting to synapses. *Nature Communications* *2019 10:1*, *10*(1), 1–13. <https://doi.org/10.1038/s41467-019-11123-x>

Baumann, S., Komissarov, A., Gili, M., Ruprecht, V., Wieser, S., & Maurer, S. P. (2020). A reconstituted mammalian APC-kinesin complex selectively transports defined packages of axonal mRNAs. *Science Advances*, *6*(11), eaaz1588. <https://doi.org/10.1126/sciadv.aaz1588>

Baumann, S., Ko'nig, J., Koepke, J., & Feldbru'gge, M. (2014). Endosomal transport of septin mRNA and protein indicates local translation on endosomes and is required for correct septin filamentation. *EMBO Reports*, *15*(1), 94–102. <https://doi.org/10.1002/EMBR.201338037>

- Baumann, S., Pohlmann, T., Jungbluth, M., Brachmann, A., & Feldbrügge, M. (2012). Kinesin-3 and dynein mediate microtubule-dependent co-transport of mrnps and endosomes. *Journal of Cell Science*, 125(11), 2740–2752. <https://doi.org/10.1242/JCS.101212/263032/AM/KINESIN-3-AND-DYNEIN-MEDIATE-MICROTUBULE-DEPENDENT>
- Beach, D. L., Salmon, E. D., & Bloom, K. (1999). Localization and anchoring of mRNA in budding yeast. *Current Biology*, 9(11), 569–578. [https://doi.org/10.1016/S0960-9822\(99\)80260-7](https://doi.org/10.1016/S0960-9822(99)80260-7)
- Bertrand, E., Chartrand, P., Schaefer, M., Shenoy, S. M., Singer, R. H., & Long, R. M. (1998). Localization of ASH1 mRNA Particles in Living Yeast. *Molecular Cell*, 2(4), 437–445. [https://doi.org/10.1016/S1097-2765\(00\)80143-4](https://doi.org/10.1016/S1097-2765(00)80143-4)
- Bodian, D. (1965). A SUGGESTIVE RELATIONSHIP OF NERVE CELL RNA WITH SPECIFIC SYNAPTIC SITES. *Proceedings of the National Academy of Sciences of the United States of America*, 53(2), 418. <https://doi.org/10.1073/PNAS.53.2.418>
- Bohl, F., Kruse, C., Frank, A., Ferring, D., & Jansen, R. P. (2000). She2p, a novel RNA-binding protein tethers ASH1 mRNA to the Myo4p myosin motor via She3p. *The EMBO Journal*, 19(20), 5514–5524. <https://doi.org/10.1093/emboj/19.20.5514>
- BOYDEN, S. (1962). The chemotactic effect of mixtures of antibody and antigen on polymorphonuclear leucocytes. *The Journal of Experimental Medicine*, 115(3), 453–466. <https://doi.org/10.1084/jem.115.3.453>
- Bubunenko, M., Kress, T. L., Vempati, U. D., Mowry, K. L., & King, M. lou. (2002). A consensus RNA signal that directs germ layer determinants to the vegetal cortex of *Xenopus* oocytes. *Developmental Biology*, 248(1), 82–92. <https://doi.org/10.1006/dbio.2002.0719>
- Buckley, P. T., Lee, M. T., Sul, J. Y., Miyashiro, K. Y., Bell, T. J., Fisher, S. A., Kim, J., & Eberwine, J. (2011). Cytoplasmic intron sequence-retaining transcripts can be dendritically targeted via ID element retrotransposons. *Neuron*, 69(5), 877–884. <https://doi.org/10.1016/J.NEURON.2011.02.028>
- Buxbaum, A. R., Haimovich, G., & Singer, R. H. (2014). In the right place at the right time: visualizing and understanding mRNA localization. *Nature Publishing Group*. <https://doi.org/10.1038/nrm3918>



- Chabanon, H., Mickleburgh, I., & Hesketh, J. (2004). Zipcodes and postage stamps: mRNA localisation signals and their trans-acting binding proteins. *Briefings in Functional Genomics & Proteomics*, 3(3), 240–256. <https://doi.org/10.1093/bfgp/3.3.240>
- Chao, J. A., Patskovsky, Y., Patel, V., Levy, M., Almo, S. C., & Singer, R. H. (2010). ZBP1 recognition of beta-actin zipcode induces RNA looping. *Genes & Development*, 24(2), 148–158. <https://doi.org/10.1101/gad.1862910>
- Chatterjee, K., Nostramo, R. T., Wan, Y., & Hopper, A. K. (2018). tRNA dynamics between the nucleus, cytoplasm and mitochondrial surface: Location, location, location. *Biochimica et Biophysica Acta*, 1861(4), 373. <https://doi.org/10.1016/J.BBAGRM.2017.11.007>
- Chaudhuri, A., Das, S., & Das, B. (2020). Localization elements and zip codes in the intracellular transport and localization of messenger RNAs in *Saccharomyces cerevisiae*. *Wiley Interdisciplinary Reviews: RNA*, 11(4), e1591. <https://doi.org/10.1002/WRNA.1591>
- Chávez, M. N., Aedo, G., Fierro, F. A., Allende, M. L., & Egaña, J. T. (2016). Zebrafish as an Emerging Model Organism to Study Angiogenesis in Development and Regeneration. *Frontiers in Physiology*, 7(MAR), 56. <https://doi.org/10.3389/FPHYS.2016.00056>
- Chekulaeva, M., Hentze, M. W., & Ephrussi, A. (2006). Bruno Acts as a Dual Repressor of oskar Translation, Promoting mRNA Oligomerization and Formation of Silencing Particles. *Cell*, 124(3), 521–533. <https://doi.org/10.1016/J.CELL.2006.01.031>
- Chicurel, M. E., Singer, R. H., Meyer, C. J., & Ingber, D. E. (1998). Integrin binding and mechanical tension induce movement of mRNA and ribosomes to focal adhesions. *Nature* 1998 392:6677, 392(6677), 730–733. <https://doi.org/10.1038/33719>
- Childs, S., Chen, J.-N., Garrity, D. M., & Fishman, M. C. (2002). Patterning of angiogenesis in the zebrafish embryo. *Development*, 129(4), 973–982. <https://doi.org/10.1242/DEV.129.4.973>
- Chrisafis, G., Wang, T., Moissoglou, K., Gasparski, A. N., Ng, Y., Weigert, R., Lockett, S. J., & Mili, S. (2020). Collective cancer cell invasion requires RNA accumulation at the invasive front. *Proceedings of the National Academy of Sciences*, 117(44), 27423–27434. <https://doi.org/10.1073/PNAS.2010872117>

- Cioni, J. M., Koppers, M., & Holt, C. E. (2018). Molecular control of local translation in axon development and maintenance. In *Current Opinion in Neurobiology* (Vol. 51, pp. 86–94). Elsevier Ltd. <https://doi.org/10.1016/j.conb.2018.02.025>
- Cioni, J. M., Lin, J. Q., Holtermann, A. v., Koppers, M., Jakobs, M. A. H., Azizi, A., Turner-Bridger, B., Shigeoka, T., Franze, K., Harris, W. A., & Holt, C. E. (2019). Late Endosomes Act as mRNA Translation Platforms and Sustain Mitochondria in Axons. *Cell*, *176*(1–2), 56–72.e15. <https://doi.org/10.1016/J.CELL.2018.11.030>
- Condeelis, J., & Singer, R. H. (2005). How and why does  $\beta$ -actin mRNA target? *Biology of the Cell*, *97*(1), 97–110. <https://doi.org/10.1042/bc20040063>
- Cukierman, E., Pankov, R., Stevens, D. R., & Yamada, K. M. (2001). Taking Cell-Matrix Adhesions to the Third Dimension. *Science*, *294*(5547), 1708–1712. <https://doi.org/10.1126/SCIENCE.1064829>
- Cumberworth, A., Lamour, G., Babu, M. M., & Gsponer, J. (2013). Promiscuity as a functional trait: Intrinsically disordered regions as central players of interactomes. In *Biochemical Journal* (Vol. 454, Issue 3, pp. 361–369). Portland Press. <https://doi.org/10.1042/BJ20130545>
- Das, S., Moon, H. C., Singer, R. H., & Park, H. Y. (2018). A transgenic mouse for imaging activity-dependent dynamics of endogenous arc mRNA in live neurons. *Science Advances*, *4*(6). <https://doi.org/10.1126/SCIADV.AAR3448>
- de Hoog, C. L., Foster, L. J., & Mann, M. (2004). RNA and RNA binding proteins participate in early stages of cell spreading through spreading initiation centers. *Cell*, *117*(5), 649–662. [https://doi.org/10.1016/S0092-8674\(04\)00456-8](https://doi.org/10.1016/S0092-8674(04)00456-8)
- Deka, J., Herter, P., Sprenger-Haußels, M., Koosch, S., Franz, D., Müller, K. M., Kuhnen, C., Hoffmann, I., & Müller, O. (1999). The APC protein binds to A/T rich DNA sequences. *Oncogene*, *18*(41), 5654–5661. <https://doi.org/10.1038/sj.onc.1202944>
- Deng, Y., Singer, R. H., & Gu, W. (2008). Translation of ASH1 mRNA is repressed by Puf6p–Fun12p/eIF5B interaction and released by CK2 phosphorylation. *Genes & Development*, *22*(8), 1037. <https://doi.org/10.1101/GAD.1611308>
- Dermit, M., Dodel, M., Lee, F. C. Y., Azman, M. S., Schwenzer, H., Jones, J. L., Blagden, S. P., Ule, J., & Mardakheh, F. K. (2020). Subcellular mRNA Localization Regulates Ribosome

Biogenesis in Migrating Cells. *Developmental Cell*, 55(3), 298-313.e10.

<https://doi.org/10.1016/J.DEVCEL.2020.10.006>

Deshler, J. O., Highett, M. I., & Schnapp, B. J. (1997). Localization of *Xenopus* Vg1 mRNA by Vera protein and the endoplasmic reticulum. *Science*, 276(5315), 1128–1131.

<https://doi.org/10.1126/science.276.5315.1128>

Dever, T. E., Dinman, J. D., & Green, R. (2018). Translation Elongation and Recoding in Eukaryotes. *Cold Spring Harbor Perspectives in Biology*, 10(8), a032649.

<https://doi.org/10.1101/CSHPERSPECT.A032649>

Dieck, S. tom, Kochen, L., Hanus, C., Bartnik, I., Nassim-Assir, B., Merk, K., Mosler, T., Garg, S., Bunse, S., Tirrell, D. A., & Schuman, E. M. (2015). Direct visualization of identified and newly synthesized proteins in situ. *Nature Methods*, 12(5), 411.

<https://doi.org/10.1038/NMETH.3319>

Ding, D., Parkhurst, S. M., Halsell, S. R., & Lipshitz, H. D. (1993). Dynamic Hsp83 RNA localization during *Drosophila* oogenesis and embryogenesis. *Molecular and Cellular Biology*, 13(6), 3773–3781. <http://www.ncbi.nlm.nih.gov/pubmed/7684502>

Donlin-Asp, P. G., Polisseni, C., Klimek, R., Heckel, A., & Schuman, E. M. (2021). Differential regulation of local mRNA dynamics and translation following long-term potentiation and depression. *Proceedings of the National Academy of Sciences*, 118(13), 2017578118. <https://doi.org/10.1073/PNAS.2017578118>

Engel, K. L., Arora, A., Goering, R., Lo, H. Y. G., & Taliaferro, J. M. (2020). Mechanisms and consequences of subcellular RNA localization across diverse cell types. *Traffic*, 21(6), 404–418. <https://doi.org/10.1111/TRA.12730/>

Etienne-Manneville, S. (2004). Cdc42 - The centre of polarity. In *Journal of Cell Science* (Vol. 117, Issue 8, pp. 1291–1300). The Company of Biologists Ltd.

<https://doi.org/10.1242/jcs.01115>

Farina, K. L., Httelmaier, S., Musunuru, K., Darnell, R., & Singer, R. H. (2003). Two ZBP1 KH domains facilitate  $\beta$ -actin mRNA localization, granule formation, and cytoskeletal attachment. *Journal of Cell Biology*, 160(1), 77–87. <https://doi.org/10.1083/jcb.200206003>

- Forrest, K. M., & Gavis, E. R. (2003). Live imaging of endogenous RNA reveals a diffusion and entrapment mechanism for nanos mRNA localization in *Drosophila*. *Current Biology* : *CB*, *13*(14), 1159–1168. <http://www.ncbi.nlm.nih.gov/pubmed/12867026>
- Franco, C. A., Jones, M. L., Bernabeu, M. O., Geudens, I., Mathivet, T., Rosa, A., Lopes, F. M., Lima, A. P., Ragab, A., Collins, R. T., Phng, L.-K., Coveney, P. v, & Gerhardt, H. (2015). Dynamic endothelial cell rearrangements drive developmental vessel regression. *PLoS Biology*, *13*(4), e1002125. <https://doi.org/10.1371/journal.pbio.1002125>
- Franco-Barraza, J., Beacham, D. A., Amatangelo, M. D., & Cukierman, E. (2016a). Preparation of extracellular matrices produced by cultured and primary fibroblasts. *Current Protocols in Cell Biology*, *71*, 10.9.1. <https://doi.org/10.1002/CPCB.2>
- Franco-Barraza, J., Beacham, D. A., Amatangelo, M. D., & Cukierman, E. (2016b). Preparation of extracellular matrices produced by cultured and primary fibroblasts. *Current Protocols in Cell Biology*, *71*, 10.9.1. <https://doi.org/10.1002/CPCB.2>
- Fusco, D., Accornero, N., Lavoie, B., Shenoy, S. M., Blanchard, J. M., Singer, R. H., & Bertrand, E. (2003). Single mRNA molecules demonstrate probabilistic movement in living mammalian cells. *Current Biology*, *13*(2), 161–167. [https://doi.org/10.1016/S0960-9822\(02\)01436-7](https://doi.org/10.1016/S0960-9822(02)01436-7)
- Gagnon, J. A., & Mowry, K. L. (2011). Molecular Motors: Directing Traffic during RNA Localization. *Critical Reviews in Biochemistry and Molecular Biology*, *46*(3), 229. <https://doi.org/10.3109/10409238.2011.572861>
- Gao, Y., Tataavarty, V., Korza, G., Levin, M. K., & Carson, J. H. (2008). Multiplexed dendritic targeting of  $\alpha$  calcium calmodulin-dependent protein kinase II, neurogranin, and activity-regulated cytoskeleton-associated protein RNAs by the A2 pathway. *Molecular Biology of the Cell*, *19*(5), 2311–2327. <https://doi.org/10.1091/mbc.E07-09-0914>
- Gautreau, D., Cote, C. A., & Mowry, K. L. (1997). Two copies of a subelement from the Vg1 RNA localization sequence are sufficient to direct vegetal localization in *Xenopus* oocytes. *Development*, *124*(24), 5013–5020.
- Gelin-Licht, R., Paliwal, S., Conlon, P., Levchenko, A., & Gerst, J. E. (2012). Scp160-Dependent mRNA Trafficking Mediates Pheromone Gradient Sensing and Chemotropism in Yeast. *Cell Reports*, *1*(5), 483–494. <https://doi.org/10.1016/J.CELREP.2012.03.004>

- Gerhardt, H., Golding, M., Fruttiger, M., Ruhrberg, C., Lundkvist, A., Abramsson, A., Jeltsch, M., Mitchell, C., Alitalo, K., Shima, D., & Betsholtz, C. (2003). VEGF guides angiogenic sprouting utilizing endothelial tip cell filopodia. *Journal of Cell Biology*, *161*(6), 1163–1177. <https://doi.org/10.1083/JCB.200302047>
- Ghosh, S., Marchand, V., Gáspár, I., & Ephrussi, A. (2012). Control of RNP motility and localization by a splicing-dependent structure in oskar mRNA. *Nature Structural and Molecular Biology*, *19*(4), 441–449. <https://doi.org/10.1038/nsmb.2257>
- Glock, C., Biever, A., Tushev, G., Nassim-Assir, B., Kao, A., Bartnik, I., Dieck, S. tom, & Schuman, E. M. (2021). The translome of neuronal cell bodies, dendrites, and axons. *Proceedings of the National Academy of Sciences*, *118*(43), e2113929118. <https://doi.org/10.1073/PNAS.2113929118>
- Goering, R., Hudish, L. I., Guzman, B. B., Raj, N., Bassell, G. J., Russ, H. A., Dominguez, D., & Taliaferro, J. M. (2020). FMRP promotes RNA localization to neuronal projections through interactions between its RGG domain and g-quadruplex RNA sequences. *ELife*, *9*, 1–31. <https://doi.org/10.7554/ELIFE.52621>
- Gold, V. A., Chroscicki, P., Bragoszewski, P., & Chacinska, A. (2017). Visualization of cytosolic ribosomes on the surface of mitochondria by electron cryo-tomography. *EMBO Reports*, *18*(10), 1786–1800. <https://doi.org/10.15252/EMBR.201744261>
- Goldstein, B., & Macara, I. G. (2007). The PAR Proteins: Fundamental Players in Animal Cell Polarization. *Developmental Cell*, *13*(5), 609. <https://doi.org/10.1016/J.DEVCEL.2007.10.007>
- Gopal, P. P., Nirschl, J. J., Klinman, E., Holzbaaur, E. L. F., & Designed, E. L. F. H. (2017). *Amyotrophic lateral sclerosis-linked mutations increase the viscosity of liquid-like TDP-43 RNP granules in neurons*. <https://doi.org/10.1073/pnas.1614462114>
- Gu, W., Deng, Y., Zenklusen, D., & Singer, R. H. (2004). A new yeast PUF family protein, Puf6p, represses ASH1 mRNA translation and is required for its localization. *Genes & Development*, *18*(12), 1452–1465. <https://doi.org/10.1101/GAD.1189004>
- Gu, W., Katz, Z., Wu, B., Park, H. Y., Li, D., Lin, S., Wells, A. L., & Singer, R. H. (2012). Regulation of local expression of cell adhesion and motility-related mRNAs in breast cancer

cells by IMP1/ZBP1. *Journal of Cell Science*, 125(1), 81–91.

<https://doi.org/10.1242/jcs.086132>

Gumy, L. F., Yeo, G. S. H., Tung, Y.-C. L., Zivraj, K. H., Willis, D., Coppola, G., Lam, B. Y. H., Twiss, J. L., Holt, C. E., & Fawcett, J. W. (2011). Transcriptome analysis of embryonic and adult sensory axons reveals changes in mRNA repertoire localization. *RNA*, 17(1), 85. <https://doi.org/10.1261/RNA.2386111>

Guo, Q., Shi, X., & Wang, X. (2021). RNA and liquid-liquid phase separation. *Non-Coding RNA Research*, 6(2), 92–99. <https://doi.org/10.1016/J.NCRNA.2021.04.003>

Hachet, O., & Ephrussi, A. (2001). Drosophila Y14 shuttles to the posterior of the oocyte and is required for oskar mRNA transport. *Current Biology*, 11(21), 1666–1674.

[https://doi.org/10.1016/S0960-9822\(01\)00508-5](https://doi.org/10.1016/S0960-9822(01)00508-5)

Hachet, O., & Ephrussi, A. (2004). Splicing of oskar RNA in the nucleus is coupled to its cytoplasmic localization. *Nature* 2004 428:6986, 428(6986), 959–963.

<https://doi.org/10.1038/nature02521>

Hafner, A.-S., Donlin-Asp, P. G., Leitch, B., Herzog, E., & Schuman, E. M. (2019). Local protein synthesis is a ubiquitous feature of neuronal pre- and postsynaptic compartments. *Science*, 364(6441). <https://doi.org/10.1126/SCIENCE.AAU3644>

Hellen, C. U. T. (2018). Translation Termination and Ribosome Recycling in Eukaryotes. *Cold Spring Harbor Perspectives in Biology*, 10(10), a032656.

<https://doi.org/10.1101/CSHPERSPECT.A032656>

Herbert, S. P., & Costa, G. (2019). Sending messages in moving cells: mRNA localization and the regulation of cell migration. In *Essays in Biochemistry* (Vol. 63, Issue 5, pp. 595–606). Portland Press Ltd. <https://doi.org/10.1042/EBC20190009>

Herbert, S. P., & R Stainier, D. Y. (2011). *Molecular control of endothelial cell behaviour during blood vessel morphogenesis*. <https://doi.org/10.1038/nrm3176>

Hershey, J. W. B., Sonenberg, N., & Mathews, M. B. (2019). Principles of Translational Control. *Cold Spring Harbor Perspectives in Biology*, 11(9), a032607.

<https://doi.org/10.1101/CSHPERSPECT.A032607>

- Hetheridge, C., Mavria, G., & Mellor, H. (2011). Uses of the in vitro endothelial–fibroblast organotypic co-culture assay in angiogenesis research. *Biochemical Society Transactions*, 39(6), 1597–1600. <https://doi.org/10.1042/BST20110738>
- Hoek, K. S., Kidd, G. J., Carson, J. H., & Smith, R. (1998). hnRNP A2 Selectively Binds the Cytoplasmic Transport Sequence of Myelin Basic Protein mRNA †. *Biochemistry*, 37(19), 7021–7029. <https://doi.org/10.1021/bi9800247>
- Holt, C. E., & Schuman, E. M. (2013). The central dogma decentralized: new perspectives on RNA function and local translation in neurons. *Neuron*, 80(3), 648–657. <https://doi.org/10.1016/j.neuron.2013.10.036>
- Hoock, T. C., Newcomb, P. M., & Herman, I. M. (1991). Beta actin and its mRNA are localized at the plasma membrane and the regions of moving cytoplasm during the cellular response to injury. *The Journal of Cell Biology*, 112(4), 653–664. <http://www.ncbi.nlm.nih.gov/pubmed/1993736>
- Huber, K. M., Kayser, M. S., & Bear, M. F. (2000). Role for Rapid Dendritic Protein Synthesis in Hippocampal mGluR-Dependent Long-Term Depression. *Science*, 288(5469), 1254–1256. <https://doi.org/10.1126/SCIENCE.288.5469.1254>
- Hurov, J. B., Watkins, J. L., & Piwnica-Worms, H. (2004). Atypical PKC phosphorylates PAR-1 kinases to regulate localization and activity. *Current Biology*, 14(8), 736–741. <https://doi.org/10.1016/J.CUB.2004.04.007/ATTACHMENT/9ED83956-E1D0-49C1-9A9B-985DF91618D7/MMC1.PDF>
- Hüttelmaier, S., Zenklusen, D., Lederer, M., Dichtenberg, J., Lorenz, M., Meng, X., Bassell, G. J., Condeelis, J., & Singer, R. H. (2005). Spatial regulation of  $\beta$ -actin translation by Src-dependent phosphorylation of ZBP1. *Nature*, 438(7067), 512–515. <https://doi.org/10.1038/nature04115>
- Huynh, J. R., Munro, T. P., Smith-Litière, K., Lepesant, J. A., & St Johnston, D. (2004). The *Drosophila* hnRNPA/B homolog, Hrp48, is specifically required for a distinct step in *osk* mRNA localization. *Developmental Cell*, 6(5), 625–635. [https://doi.org/10.1016/S1534-5807\(04\)00130-3](https://doi.org/10.1016/S1534-5807(04)00130-3)
- Irie, K., Tadauchi, T., Takizawa, P. A., Vale, R. D., Matsumoto, K., & Herskowitz, I. (2002). The Khd1 protein, which has three KH RNA-binding motifs, is required for proper

localization of ASH1 mRNA in yeast. *The EMBO Journal*, 21(5), 1158.

<https://doi.org/10.1093/EMBOJ/21.5.1158>

Izumi, Y., Hirose, T., Tamai, Y., Hirai, S. I., Nagashima, Y., Fujimoto, T., Tabuse, Y., Kempfues, K. J., & Ohno, S. (1998). An Atypical PKC Directly Associates and Colocalizes at the Epithelial Tight Junction with ASIP, a Mammalian Homologue of *Caenorhabditis elegans* Polarity Protein PAR-3. *The Journal of Cell Biology*, 143(1), 95.

<https://doi.org/10.1083/JCB.143.1.95>

Jain, R. A., & Gavis, E. R. (2008). The *Drosophila* hnRNP M homolog Rumpelstiltskin regulates nanos mRNA localization. *Development*, 135(5), 973–982.

<https://doi.org/10.1242/dev.015438>

Jakobsen, K. R., Sørensen, E., Brøndum, K. K., Daugaard, T. F., Thomsen, R., & Nielsen, A. L. (2013). Direct RNA sequencing mediated identification of mRNA localized in protrusions of human MDA-MB-231 metastatic breast cancer cells. *Journal of Molecular Signaling*, 8(1), 9. <https://doi.org/10.1186/1750-2187-8-9>

Jambhekar, A., & Derisi, J. L. (2007). Cis-acting determinants of asymmetric, cytoplasmic RNA transport. In *RNA* (Vol. 13, Issue 5, pp. 625–642). RNA.

<https://doi.org/10.1261/rna.262607>

Jankowski, S., Pohlmann, T., Baumann, S., Müntjes, K., Devan, S. K., Zander, S., & Feldbrügge, M. (2019). The multi PAM2 protein Upa2 functions as novel core component of endosomal mRNA transport. *EMBO Reports*, 20(9), e47381.

<https://doi.org/10.15252/EMBR.201847381>

Johnstone, O., & Lasko, P. (2001). Translational Regulation and RNA Localization in *Drosophila* Oocytes and Embryos. *Annual Review of Genetics*, 35(1), 365–406.

<https://doi.org/10.1146/annurev.genet.35.102401.090756>

Jung, H., Gkogkas, C. G., Sonenberg, N., & Holt, C. E. (2014). Remote control of gene function by local translation. In *Cell* (Vol. 157, Issue 1, pp. 26–40). Cell Press.

<https://doi.org/10.1016/j.cell.2014.03.005>

Kamei, M., Brian Saunders, W., Bayless, K. J., Dye, L., Davis, G. E., & Weinstein, B. M. (2006). Endothelial tubes assemble from intracellular vacuoles in vivo. *Nature* 2006

442:7101, 442(7101), 453–456. <https://doi.org/10.1038/nature04923>



- Kang, H., & Schuman, E. M. (1996). A Requirement for Local Protein Synthesis in Neurotrophin-Induced Hippocampal Synaptic Plasticity. *Science*, 273(5280), 1402–1406. <https://doi.org/10.1126/SCIENCE.273.5280.1402>
- Katz, Z. B., Wells, A. L., Park, H. Y., Wu, B., Shenoy, S. M., & Singer, R. H. (2012).  $\beta$ -actin mRNA compartmentalization enhances focal adhesion stability and directs cell migration. *Genes and Development*, 26(17), 1885–1890. <https://doi.org/10.1101/gad.190413.112>
- Kedersha, N., & Anderson, P. (2007). Mammalian Stress Granules and Processing Bodies. *Methods in Enzymology*, 431, 61–81. [https://doi.org/10.1016/S0076-6879\(07\)31005-7](https://doi.org/10.1016/S0076-6879(07)31005-7)
- Kim, G., Pai, C. I., Sato, K., Person, M. D., Nakamura, A., & Macdonald, P. M. (2015). Region-Specific Activation of oskar mRNA Translation by Inhibition of Bruno-Mediated Repression. *PLOS Genetics*, 11(2), e1004992. <https://doi.org/10.1371/JOURNAL.PGEN.1004992>
- Kim, N. Y., Lee, S., Yu, J., Kim, N., Won, S. S., Park, H., & Heo, W. do. (2020). Optogenetic control of mRNA localization and translation in live cells. *Nature Cell Biology* 2020 22:3, 22(3), 341–352. <https://doi.org/10.1038/s41556-020-0468-1>
- Kim, S., & Martin, K. C. (2015). Neuron-wide RNA transport combines with netrin-mediated local translation to spatially regulate the synaptic proteome. *ELife*, 2015(4). <https://doi.org/10.7554/ELIFE.04158>
- Kim-Ha, J., Kerr, K., & Macdonald, P. M. (1995). Translational regulation of oskar mRNA by Bruno, an ovarian RNA-binding protein, is essential. In *Cell* (Vol. 81, Issue 3, pp. 403–412). Elsevier. [https://doi.org/10.1016/0092-8674\(95\)90393-3](https://doi.org/10.1016/0092-8674(95)90393-3)
- Kim-Ha, J., Smith, J. L., & Macdonald, P. M. (1991). oskar mRNA is localized to the posterior pole of the Drosophila oocyte. *Cell*, 66(1), 23–35. [https://doi.org/10.1016/0092-8674\(91\)90136-M](https://doi.org/10.1016/0092-8674(91)90136-M)
- Kislauskis, E. H., Zhu, X., & Singer, R. H. (1994). Sequences responsible for intracellular localization of beta-actin messenger RNA also affect cell phenotype. *The Journal of Cell Biology*, 127(2), 441–451. <http://www.ncbi.nlm.nih.gov/pubmed/7929587>
- Kislauskis, E. H., Zhu, X., & Singer, R. H. (1997). beta-Actin messenger RNA localization and protein synthesis augment cell motility. *The Journal of Cell Biology*, 136(6), 1263–1270. <https://doi.org/10.1083/JCB.136.6.1263>

Kramer, E. B., & Hopper, A. K. (2013). Retrograde transfer RNA nuclear import provides a new level of tRNA quality control in *Saccharomyces cerevisiae*. *Proceedings of the National Academy of Sciences of the United States of America*, *110*(52), 21042–21047.

[https://doi.org/10.1073/PNAS.1316579110/SUPPL\\_FILE/PNAS.201316579SI.PDF](https://doi.org/10.1073/PNAS.1316579110/SUPPL_FILE/PNAS.201316579SI.PDF)

Kroboth, K., Newton, I. P., Kita, K., Dikovskaya, D., Zumbunn, J., Waterman-Storer, C. M., & Näthke, I. S. (2007). Lack of adenomatous polyposis coli protein correlates with a decrease in cell migration and overall changes in microtubule stability. *Molecular Biology of the Cell*, *18*(3), 910–918. <https://doi.org/10.1091/mbc.E06-03-0179>

Kruse, C., Jaedicke, A., Beaudouin, J., Böhl, F., Ferring, D., Güttler, T., Ellenberg, J., & Jansen, R.-P. (2002). Ribonucleoprotein-dependent localization of the yeast class V myosin Myo4p. *The Journal of Cell Biology*, *159*(6), 971. <https://doi.org/10.1083/JCB.200207101>

Kundel, M., Jones, K. J., Shin, C. Y., & Wells, D. G. (2009). Cytoplasmic Polyadenylation Element-Binding Protein Regulates Neurotrophin-3-Dependent  $\beta$ -Catenin mRNA Translation in Developing Hippocampal Neurons. *Journal of Neuroscience*, *29*(43), 13630–13639.

<https://doi.org/10.1523/JNEUROSCI.2910-08.2009>

Kupfer, A., Louvard, D., & Singer, S. J. (1982). Polarization of the Golgi apparatus and the microtubule-organizing center in cultured fibroblasts at the edge of an experimental wound. *Proceedings of the National Academy of Sciences of the United States of America*, *79*(8), 2603–2607. <http://www.ncbi.nlm.nih.gov/pubmed/7045867>

Lange, S., Katayama, Y., Schmid, M., Burkacky, O., Bräuchle, C., Lamb, D. C., & Jansen, R.-P. (2008). Simultaneous Transport of Different Localized mRNA Species Revealed by Live-Cell Imaging. *Traffic*, *9*(8), 1256–1267. <https://doi.org/10.1111/J.1600-0854.2008.00763.X>

Latham, V. M. J., Kislauskis, E. H., Singer, R. H., & Ross, A. F. (1994). Beta-actin mRNA localization is regulated by signal transduction mechanisms. *The Journal of Cell Biology*, *126*(5), 1211–1219. <https://doi.org/10.1083/jcb.126.5.1211>

Latham, V. M., Yu, E. H. S., Tullio, A. N., Adelstein, R. S., & Singer, R. H. (2001). A Rho-dependent signaling pathway operating through myosin localizes  $\beta$ -actin mRNA in fibroblasts. *Current Biology*, *11*(13), 1010–1016. [https://doi.org/10.1016/S0960-9822\(01\)00291-3](https://doi.org/10.1016/S0960-9822(01)00291-3)

- Lawrence, J. B., & Singer, R. H. (1986). Intracellular localization of messenger RNAs for cytoskeletal proteins. *Cell*, *45*(3), 407–415. <http://www.ncbi.nlm.nih.gov/pubmed/3698103>
- Lécuyer, E., Yoshida, H., Parthasarathy, N., Alm, C., Babak, T., Cerovina, T., Hughes, T. R., Tomancak, P., & Krause, H. M. (2007). Global Analysis of mRNA Localization Reveals a Prominent Role in Organizing Cellular Architecture and Function. *Cell*, *131*(1), 174–187. <https://doi.org/10.1016/j.cell.2007.08.003>
- Leung, K.-M., Lu, B., Wong, H. H.-W., Lin, J. Q., Turner-Bridger, B., & Holt, C. E. (2018). Cue-Polarized Transport of  $\beta$ -actin mRNA Depends on 3'UTR and Microtubules in Live Growth Cones. *Frontiers in Cellular Neuroscience*, *12*, 300. <https://doi.org/10.3389/fncel.2018.00300>
- Lewis, R. A., Kress, T. L., Cote, C. A., Gautreau, D., Rokop, M. E., & Mowry, K. L. (2004). Conserved and clustered RNA recognition sequences are a critical feature of signals directing RNA localization in *Xenopus* oocytes. *Mechanisms of Development*, *121*(1), 101–109. <https://doi.org/10.1016/j.mod.2003.09.009>
- Li, R., & Gundersen, G. G. (2008). Beyond polymer polarity: How the cytoskeleton builds a polarized cell. In *Nature Reviews Molecular Cell Biology* (Vol. 9, Issue 11, pp. 860–873). Nature Publishing Group. <https://doi.org/10.1038/nrm2522>
- Liao, G., Simone, B., & Liu, G. (2011). Mis-localization of Arp2 mRNA impairs persistence of directional cell migration. *Experimental Cell Research*, *317*(6), 812–822. <https://doi.org/10.1016/j.yexcr.2010.12.002>
- Liao, Y. C., Fernandopulle, M. S., Wang, G., Choi, H., Hao, L., Drerup, C. M., Patel, R., Qamar, S., Nixon-Abell, J., Shen, Y., Meadows, W., Vendruscolo, M., Knowles, T. P. J., Nelson, M., Czekalska, M. A., Musteikyte, G., Gachechiladze, M. A., Stephens, C. A., Pasolli, H. A., ... Ward, M. E. (2019). RNA Granules Hitchhike on Lysosomes for Long-Distance Transport, Using Annexin A11 as a Molecular Tether. *Cell*, *179*(1), 147–164.e20. <https://doi.org/10.1016/J.CELL.2019.08.050>
- Liu, G., Grant, W. M., Persky, D., Latham, V. M., Singer, R. H., & Condeelis, J. (2002a). Interactions of Elongation Factor 1<sub>γ</sub> with F-Actin and  $\alpha$ -Actin mRNA: Implications for Anchoring mRNA in Cell Protrusions. *Molecular Biology of the Cell*, *13*, 579–592. <https://doi.org/10.1091/mbc.01>

Liu, G., Grant, W. M., Persky, D., Latham, V. M., Singer, R. H., & Condeelis, J. (2002b). Interactions of elongation factor 1 $\alpha$  with F-actin and  $\beta$ -actin mRNA: Implications for anchoring mRNA in cell protrusions. *Molecular Biology of the Cell*, *13*(2), 579–592. <https://doi.org/10.1091/MBC.01-03-0140/ASSET/IMAGES/LARGE/MK0221740012.JPEG>

Long, R. M., Gu, W., Lorimer, E., Singer, R. H., & Chartrand, P. (2000). She2p is a novel RNA-binding protein that recruits the Myo4p-She3p complex to ASH1 mRNA. *The EMBO Journal*, *19*(23), 6592–6601. <https://doi.org/10.1093/emboj/19.23.6592>

Long, R. M., Gu, W., Meng, X., Gonsalvez, G., Singer, R. H., & Chartrand, P. (2001). An Exclusively Nuclear RNA-Binding Protein Affects Asymmetric Localization of ASH1 mRNA and Ash1p in Yeast. *Journal of Cell Biology*, *153*(2), 307–318. <https://doi.org/10.1083/JCB.153.2.307>

Long, R. M., Singer, R. H., Meng, X., Gonzalez, I., Nasmyth, K., & Jansen, R. P. (1997). Mating type switching in yeast controlled by asymmetric localization of ASH1 mRNA. *Science (New York, N.Y.)*, *277*(5324), 383–387. <http://www.ncbi.nlm.nih.gov/pubmed/9219698>

López-Doménech, G., Covill-Cooke, C., Ivankovic, D., Halff, E. F., Sheehan, D. F., Norkett, R., Birsa, N., & Kittler, J. T. (2018). Miro proteins coordinate microtubule- and actin-dependent mitochondrial transport and distribution. *The EMBO Journal*, *37*(3), 321–336. <https://doi.org/10.15252/emboj.201696380>

Ludwik, K. A., von Kuegelgen, N., & Chekulaeva, M. (2019). Genome-wide analysis of RNA and protein localization and local translation in mESC-derived neurons. *Methods*, *162–163*, 31–41. <https://doi.org/10.1016/J.YMETH.2019.02.002>

Lugano, R., Ramachandran, M., & Dimberg, A. (2019). Tumor angiogenesis: causes, consequences, challenges and opportunities. *Cellular and Molecular Life Sciences* *2019* 77:9, *77*(9), 1745–1770. <https://doi.org/10.1007/S00018-019-03351-7>

Lyles, V., Zhao, Y., & Martin, K. C. (2006). Synapse Formation and mRNA Localization in Cultured Aplysia Neurons. *Neuron*, *49*(3), 349–356. <https://doi.org/10.1016/J.NEURON.2005.12.029>

Macdonald, P. M., & Kerr, K. (1997). Redundant RNA recognition events in bicoid mRNA localization. *RNA (New York, N.Y.)*, 3(12), 1413–1420.

<http://www.ncbi.nlm.nih.gov/pubmed/9404892>

Mackenzie, I. R., Nicholson, A. M., Sarkar, M., Messing, J., Purice, M. D., Pottier, C., Annu, K., Baker, M., Perkerson, R. B., Kurti, A., Matchett, B. J., Mittag, T., Temirov, J., Hsiung, G. Y. R., Krieger, C., Murray, M. E., Kato, M., Fryer, J. D., Petrucelli, L., ... Rademakers, R. (2017). TIA1 Mutations in Amyotrophic Lateral Sclerosis and Frontotemporal Dementia Promote Phase Separation and Alter Stress Granule Dynamics. *Neuron*, 95(4), 808-816.e9.

<https://doi.org/10.1016/J.NEURON.2017.07.025>

Maizels, Y., Oberman, F., Miloslavski, R., Ginzach, N., Berman, M., & Yisraeli, J. K. (2015). Localization of cofilin mRNA to the leading edge of migrating cells promotes directed cell migration. *Journal of Cell Science*, 128(10), 1922–1933.

<https://doi.org/10.1242/jcs.163972>

Mardakheh, F. K., Paul, A., Kü, S., Mccarthy, A., Yuan, Y., & Correspondence, C. J. M. (2015). Global Analysis of mRNA, Translation, and Protein Localization: Local Translation Is a Key Regulator of Cell Protrusions. *Developmental Cell*, 35, 344–357.

<https://doi.org/10.1016/j.devcel.2015.10.005>

Martin, K. C., & Ephrussi, A. (2009). mRNA Localization: Gene Expression in the Spatial Dimension. *Cell*, 136(4), 719–730. <https://doi.org/10.1016/j.cell.2009.01.044>

Mayford, M., Bach, M. E., Huang, Y. Y., Wang, L., Hawkins, R. D., & Kandel, E. R. (1996). Control of memory formation through regulated expression of a CaMKII transgene. *Science*, 274(5293), 1678–1683. <https://doi.org/10.1126/science.274.5293.1678>

Mayford, M., Baranes, D., Podsypanina, K., & Kandel, E. R. (1996). The 3'-untranslated region of CaMKII alpha is a cis-acting signal for the localization and translation of mRNA in dendrites. *Proceedings of the National Academy of Sciences of the United States of America*, 93(23), 13250–13255. <http://www.ncbi.nlm.nih.gov/pubmed/8917577>

Mayor, R., & Etienne-Manneville, S. (2016). The front and rear of collective cell migration. *Nature Publishing Group*. <https://doi.org/10.1038/nrm.2015.14>

- Medioni, C., Mowry, K., & Besse, F. (2012). Principles and roles of mRNA localization in animal development. *Development (Cambridge, England)*, *139*(18), 3263.  
<https://doi.org/10.1242/DEV.078626>
- Meer, E. J., Wang, D. O., Kim, S., Barr, I., Guo, F., & Martin, K. C. (2012). Identification of a cis-acting element that localizes mRNA to synapses. *Proceedings of the National Academy of Sciences of the United States of America*, *109*(12), 4639–4644.  
<https://doi.org/10.1073/PNAS.1116269109/-/DCSUPPLEMENTAL>
- Merrick, W. C., & Pavitt, G. D. (2018). Protein Synthesis Initiation in Eukaryotic Cells. *Cold Spring Harbor Perspectives in Biology*, *10*(12), a033092.  
<https://doi.org/10.1101/CSHPERSPECT.A033092>
- Micklem, D. R., Dasgupta, R., Elliott, H., Gergely, F., Davidson, C., Brand, A., González-Reyes, A., & Johnston, D. (1997). The mago nashi gene is required for the polarisation of the oocyte and the formation of perpendicular axes in *Drosophila*. *Current Biology*, *7*(7), 468–478. [https://doi.org/10.1016/S0960-9822\(06\)00218-1](https://doi.org/10.1016/S0960-9822(06)00218-1)
- Mili, S., Moissoglu, K., & Macara, I. G. (2008). Genome-wide screen reveals APC-associated RNAs enriched in cell protrusions. *Nature*, *453*(7191), 115–119.  
<https://doi.org/10.1038/nature06888>
- Mimori-Kiyosue, Y., Shiina, N., & Tsukita, S. (2000). Adenomatous polyposis coli (APC) protein moves along microtubules and concentrates at their growing ends in epithelial cells. *Journal of Cell Biology*, *148*(3), 505–517. <https://doi.org/10.1083/jcb.148.3.505>
- Minde, D. P., Anvarian, Z., Rüdiger, S. G. D., & Maurice, M. M. (2011). Messing up disorder: How do missense mutations in the tumor suppressor protein APC lead to cancer? In *Molecular Cancer* (Vol. 10, Issue 1, p. 101). BioMed Central. <https://doi.org/10.1186/1476-4598-10-101>
- Mingle, L. A., Bonamy, G., Barroso, M., Liao, G., & Liu, G. (2009). LPA-induced mutually exclusive subcellular localization of active RhoA and Arp2 mRNA revealed by sequential FRET and FISH. *Histochemistry and Cell Biology*, *132*(1), 47–58.  
<https://doi.org/10.1007/S00418-009-0589-X/FIGURES/7>
- Mingle, L. A., Okuhama, N. N., Shi, J., Singer, R. H., Condeelis, J., & Liu, G. (2005a). Localization of all seven messenger RNAs for the actin-polymerization nucleator Arp2/3

- complex in the protrusions of fibroblasts. *Journal of Cell Science*, 118(11), 2425–2433.  
<https://doi.org/10.1242/jcs.02371>
- Mingle, L. A., Okuhama, N. N., Shi, J., Singer, R. H., Condeelis, J., & Liu, G. (2005b). Localization of all seven messenger RNAs for the actin-polymerization nucleator Arp2/3 complex in the protrusions of fibroblasts. *Journal of Cell Science*, 118(11), 2425–2433.  
<https://doi.org/10.1242/jcs.02371>
- Minis, A., Dahary, D., Manor, O., Leshkowitz, D., Pilpel, Y., & Yaron, A. (2014). Subcellular transcriptomics—Dissection of the mRNA composition in the axonal compartment of sensory neurons. *Developmental Neurobiology*, 74(3), 365–381.  
<https://doi.org/10.1002/DNEU.22140>
- Moissoglu, K., Stueland, M., Gasparski, A. N., Wang, T., Jenkins, L. M., Hastings, M. L., & Mili, S. (2020). RNA localization and co-translational interactions control RAB13 GTPase function and cell migration. *The EMBO Journal*, 39(21), e104958.  
<https://doi.org/10.15252/EMBJ.2020104958>
- Moissoglu, K., Yasuda, K., Wang, T., Chrisafis, G., & Mili, S. (2019). Translational regulation of protrusion-localized RNAs involves silencing and clustering after transport. *ELife*, 8. <https://doi.org/10.7554/eLife.44752>
- Moujaber, O., & Stochaj, U. (2018). *Cytoplasmic RNA Granules in Somatic Maintenance*.  
<https://doi.org/10.1159/000488759>
- Mowry, K. L., & Melton, D. A. (1992). Vegetal messenger RNA localization directed by a 340-nt RNA sequence element in *Xenopus* oocytes. *Science*, 255(5047), 991–994.  
<https://doi.org/10.1126/science.1546297>
- Mukherjee, J., Hermesh, O., Eliscovich, C., Nalpas, N., Franz-Wachtel, M., Maček, B., & Jansen, R.-P. (2019).  $\beta$ -Actin mRNA interactome mapping by proximity biotinylation. *Proceedings of the National Academy of Sciences*, 116(26), 12863–12872.  
<https://doi.org/10.1073/PNAS.1820737116>
- Müller, M., Heym, R. G., Mayer, A., Kramer, K., Schmid, M., Cramer, P., Urlaub, H., Jansen, R.-P., & Niessing, D. (2011). A Cytoplasmic Complex Mediates Specific mRNA Recognition and Localization in Yeast. *PLOS Biology*, 9(4), e1000611.  
<https://doi.org/10.1371/JOURNAL.PBIO.1000611>

- Murakami, T., Qamar, S., Lin, J. Q., Schierle, G. S. K., Rees, E., Miyashita, A., Costa, A. R., Dodd, R. B., Chan, F. T. S., Michel, C. H., Kronenberg-Versteeg, D., Li, Y., Yang, S.-P., Wakutani, Y., Meadows, W., Ferry, R. R., Dong, L., Tartaglia, G. G., Favrin, G., ... St George-Hyslop, P. (2015). ALS/FTD Mutation-Induced Phase Transition of FUS Liquid Droplets and Reversible Hydrogels into Irreversible Hydrogels Impairs RNP Granule Function. *Neuron*, 88(4), 678. <https://doi.org/10.1016/J.NEURON.2015.10.030>
- Murthy, A. C., Dignon, G. L., Kan, Y., Zerbe, G. H., Parekh, S. H., Mittal, J., & Fawzi, N. L. (2019). Molecular interactions underlying liquid–liquid phase separation of the FUS low-complexity domain. *Nature Structural & Molecular Biology* 2019 26:7, 26(7), 637–648. <https://doi.org/10.1038/s41594-019-0250-x>
- Nakamura, A., Sato, K., & Hanyu-Nakamura, K. (2004). Drosophila Cup Is an eIF4E Binding Protein that Associates with Bruno and Regulates oskar mRNA Translation in Oogenesis. *Developmental Cell*, 6(1), 69–78. [https://doi.org/10.1016/S1534-5807\(03\)00400-3](https://doi.org/10.1016/S1534-5807(03)00400-3)
- Nakatsu, M. N., Davis, J., & Hughes, C. C. W. (2007). Optimized Fibrin Gel Bead Assay for the Study of Angiogenesis. *Journal of Visualized Experiments : JoVE*, 3. <https://doi.org/10.3791/186>
- Näthke, I. S., Adams, C. L., Polakis, P., Sellin, J. H., & Nelson, W. J. (1996). The adenomatous polyposis coli tumor suppressor protein localizes to plasma membrane sites involved in active cell migration. *Journal of Cell Biology*, 134(1), 165–179. <https://doi.org/10.1083/jcb.134.1.165>
- Néant-Fery, M., Pérès, E., Nasrallah, C., Kessner, M., Gribaudo, S., Greer, C., Didier, A., Trembleau, A., & Caillé, I. (2012). A Role for Dendritic Translation of CaMKII $\alpha$  mRNA in Olfactory Plasticity. *PLOS ONE*, 7(6), e40133. <https://doi.org/10.1371/JOURNAL.PONE.0040133>
- Nicastro, G., Candel, A. M., Uhl, M., Backofen, R., Martin, S. R., Ramos Correspondence, A., Oregioni, A., Hollingworth, D., & Ramos, A. (2017). Mechanism of  $\beta$ -actin mRNA Recognition by ZBP1. *CellReports*, 18, 1187–1199. <https://doi.org/10.1016/j.celrep.2016.12.091>



Niedner, A., Edelmann, F. T., & Niessing, D. (2014). Of social molecules: The interactive assembly of ASH1 mRNA-transport complexes in yeast. *RNA Biology*, *11*(8), 998.

<https://doi.org/10.4161/RNA.29946>

Niedner, A., Müller, M., Moorthy, B. T., Jansen, R.-P., & Niessing, D. (2013). Role of Loc1p in assembly and reorganization of nuclear ASH1 messenger ribonucleoprotein particles in yeast. *Proceedings of the National Academy of Sciences*, *110*(52), E5049–E5058.

<https://doi.org/10.1073/PNAS.1315289111>

Noma, K., Goncharov, A., Ellisman, M. H., & Jin, Y. (2017). Microtubule-dependent ribosome localization in *C. elegans* neurons. *ELife*, *6*. <https://doi.org/10.7554/ELIFE.26376>

Orlando, K., & Guo, W. (2009). Membrane organization and dynamics in cell polarity. In *Cold Spring Harbor perspectives in biology* (Vol. 1, Issue 5). Cold Spring Harbor Laboratory Press. <https://doi.org/10.1101/cshperspect.a001321>

Ouwenga, R., Lake, A. M., Aryal, S., Lagunas, T., & Dougherty, J. D. (2018). The Differences in Local Translatome across Distinct Neuron Types Is Mediated by Both Baseline Cellular Differences and Post-transcriptional Mechanisms. *ENeuro*, *5*(6).

<https://doi.org/10.1523/ENEURO.0320-18.2018>

Paquin, N., Ménade, M., Poirier, G., Donato, D., Drouet, E., & Chartrand, P. (2007). Local Activation of Yeast ASH1 mRNA Translation through Phosphorylation of Khd1p by the Casein Kinase Yck1p. *Molecular Cell*, *26*(6), 795–809.

<https://doi.org/10.1016/J.MOLCEL.2007.05.016>

Park, H. Y., Lim, H., Yoon, Y. J., Follenzi, A., Nwokafor, C., Lopez-Jones, M., Meng, X., & Singer, R. H. (2014). Visualization of dynamics of single endogenous mRNA labeled in live mouse. *Science*, *343*(6169), 422–424. <https://doi.org/10.1126/SCIENCE.1239200>

Park, H. Y., Trcek, T., Wells, A. L., Chao, J. A., & Singer, R. H. (2012). An Unbiased Analysis Method to Quantify mRNA Localization Reveals Its Correlation with Cell Motility. *Cell Reports*, *1*(2), 179–184. <https://doi.org/10.1016/j.celrep.2011.12.009>

Patel, V. L., Mitra, S., Harris, R., Buxbaum, A. R., Lionnet, T., Brenowitz, M., Girvin, M., Levy, M., Almo, S. C., Singer, R. H., & Chao, J. A. (2012). Spatial arrangement of an RNA zipcode identifies mRNAs under post-transcriptional control. *Genes & Development*, *26*(1), 43–53. <https://doi.org/10.1101/GAD.177428.111>

- Pichon, X., Moissoglu, K., Coleno, E., Wang, T., Imbert, A., Robert, M.-C., Peter, M., Chouaib, R., Walter, T., Mueller, F., Zibara, K., Bertrand, E., & Mili, S. (2021). The kinesin KIF1C transports APC-dependent mRNAs to cell protrusions. *RNA*, rna.078576.120. <https://doi.org/10.1261/RNA.078576.120>
- Preitner, N., Quan, J., Nowakowski, D. W., Hancock, M. L., Shi, J., Tcherkezian, J., Young-Pearse, T. L., & Flanagan, J. G. (2014). APC is an RNA-binding protein, and its interactome provides a link to neural development and microtubule assembly. *Cell*, 158(2), 368–382. <https://doi.org/10.1016/j.cell.2014.05.042>
- Raftopoulou, M., & Hall, A. (2004). Cell migration: Rho GTPases lead the way. In *Developmental Biology* (Vol. 265, Issue 1, pp. 23–32). Academic Press Inc. <https://doi.org/10.1016/j.ydbio.2003.06.003>
- Raju, C. S., Fukuda, N., López-Iglesias, C., Göritz, C., Visa, N., & Percipalle, P. (2011). In neurons, activity-dependent association of dendritically transported mRNA transcripts with the transacting factor CBF-A is mediated by A2RE/RTS elements. *Molecular Biology of the Cell*, 22(11), 1864–1877. <https://doi.org/10.1091/MBC.E10-11-0904/ASSET/IMAGES/LARGE/1864FIG10.JPEG>
- Raman, R., Pinto, C. S., & Sonawane, M. (2018). Polarized Organization of the Cytoskeleton: Regulation by Cell Polarity Proteins. *Journal of Molecular Biology*, 430(19), 3565–3584. <https://doi.org/10.1016/J.JMB.2018.06.028>
- Ridley, A. J. (2015). Rho GTPase signalling in cell migration. In *Current Opinion in Cell Biology* (Vol. 36, pp. 103–112). Elsevier Ltd. <https://doi.org/10.1016/j.ceb.2015.08.005>
- Ridley, A. J., Schwartz, M. A., Burridge, K., Firtel, R. A., Ginsberg, M. H., Borisy, G., Parsons, J. T., & Horwitz, A. R. (2003). Cell Migration: Integrating Signals from Front to Back. In *Science* (Vol. 302, Issue 5651, pp. 1704–1709). American Association for the Advancement of Science. <https://doi.org/10.1126/science.1092053>
- Riggs, C. L., Kedersha, N., Ivanov, P., & Anderson, P. (2020). Mammalian stress granules and P bodies at a glance. *Journal of Cell Science*, 133(16). <https://doi.org/10.1242/JCS.242487/225735>

- Rodriguez-Boulan, E., & Macara, I. G. (2014). Organization and execution of the epithelial polarity programme. In *Nature Reviews Molecular Cell Biology* (Vol. 15, Issue 4, pp. 225–242). Nature Publishing Group. <https://doi.org/10.1038/nrm3775>
- Ross, A. F., Oleynikov, Y., Kislauskis, E. H., Taneja, K. L., & Singer, R. H. (1997). *Characterization of a  $\alpha$ -Actin mRNA Zipcode-Binding Protein*. *17*(4), 2158–2165. <http://mcb.asm.org/content/17/4/2158.full.pdf>
- Ryder, P. v., & Lerit, D. A. (2018). RNA localization regulates diverse and dynamic cellular processes. In *Traffic* (Vol. 19, Issue 7, pp. 496–502). Blackwell Munksgaard. <https://doi.org/10.1111/tra.12571>
- Saha, S., Mundia, M. M., Zhang, F., Demers, R. W., Korobova, F., Svitkina, T., Perieteanu, A. A., Dawson, J. F., & Kashina, A. (2010). Arginylation regulates intracellular actin polymer level by modulating actin properties and binding of capping and severing proteins. *Molecular Biology of the Cell*, *21*(8), 1350–1361. <https://doi.org/10.1091/mbc.E09-09-0829>
- Scarborough, E. A., Uchida, K., Vogel, M., Erlitzki, N., Iyer, M., Phyto, S. A., Bogush, A., Kehat, I., & Prosser, B. L. (2021). Microtubules orchestrate local translation to enable cardiac growth. *Nature Communications* *2021 12:1*, *12*(1), 1–13. <https://doi.org/10.1038/s41467-021-21685-4>
- Sebeo, J., Hsiao, K., Bozdagi, O., Dumitriu, D., Ge, Y., Zhou, Q., & Benson, D. L. (2009). Requirement for Protein Synthesis at Developing Synapses. *Journal of Neuroscience*, *29*(31), 9778–9793. <https://doi.org/10.1523/JNEUROSCI.2613-09.2009>
- Shankar, J., Messenberg, A., Chan, J., Underhill, T. M., Foster, L. J., & Nabi, I. R. (2010). Pseudopodial Actin Dynamics Control Epithelial-Mesenchymal Transition in Metastatic Cancer Cells. *Cancer Research*, *70*(9), 3780–3790. <https://doi.org/10.1158/0008-5472.CAN-09-4439>
- Shen, Z., St-Denis, A., & Chartrand, P. (2010). Cotranscriptional recruitment of She2p by RNA pol II elongation factor Spt4–Spt5/DSIF promotes mRNA localization to the yeast bud. *Genes & Development*, *24*(17), 1914. <https://doi.org/10.1101/GAD.1937510>
- Shepard, K. A., Gerber, A. P., Jambhekar, A., Takizawa, P. A., Brown, P. O., Herschlag, D., DeRisi, J. L., & Vale, R. D. (2003). Widespread cytoplasmic mRNA transport in yeast: Identification of 22 bud-localized transcripts using DNA microarray analysis. *Proceedings of*

*the National Academy of Sciences of the United States of America*, 100(20), 11429–11434.  
<https://doi.org/10.1073/pnas.2033246100>

Shestakova, E. A., Singer, R. H., & Condeelis, J. (2001). The physiological significance of beta -actin mRNA localization in determining cell polarity and directional motility. *Proceedings of the National Academy of Sciences of the United States of America*, 98(13), 7045–7050. <https://doi.org/10.1073/pnas.121146098>

Shestakova, E. A., Wyckoff, J., Jones, J., Singer, R. H., & Condeelis, J. (1999). Correlation of beta-actin messenger RNA localization with metastatic potential in rat adenocarcinoma cell lines. *Cancer Research*, 59(6), 1202–1205.  
<http://www.ncbi.nlm.nih.gov/pubmed/10096548>

Shi, Z., Fujii, K., Kovary, K. M., Genuth, N. R., Röst, H. L., Teruel, M. N., & Barna, M. (2017). Heterogeneous Ribosomes Preferentially Translate Distinct Subpools of mRNAs Genome-wide. *Molecular Cell*, 67(1), 71-83.e7. <https://doi.org/10.1016/j.molcel.2017.05.021>

Shin, Y., & Brangwynne, C. P. (2017). Liquid phase condensation in cell physiology and disease. *Science*, 357(6357).  
[https://doi.org/10.1126/SCIENCE.AAF4382/ASSET/4C225E85-34DB-4023-8EC0-EF3AEA7D56A9/ASSETS/GRAPHIC/357\\_AAF4382\\_FA.JPEG](https://doi.org/10.1126/SCIENCE.AAF4382/ASSET/4C225E85-34DB-4023-8EC0-EF3AEA7D56A9/ASSETS/GRAPHIC/357_AAF4382_FA.JPEG)

Simon, B., Masiewicz, P., Ephrussi, A., & Carlomagno, T. (2015). The structure of the SOLE element of oskar mRNA. *RNA*, 21(8), 1444–1453. <https://doi.org/10.1261/rna.049601.115>

Sladewski, T. E., Bookwalter, C. S., Hong, M.-S., & Trybus, K. M. (2013). Single-molecule reconstitution of mRNA transport by a class V myosin. *Nature Structural & Molecular Biology* 2013 20:8, 20(8), 952–957. <https://doi.org/10.1038/nsmb.2614>

Solomon, L. R., & Rubenstein, P. A. (1987). *Studies on the Role of Actin's N'-Methylhistidine Using Oligodeoxynucleotide-directed Site-specific Mutagenesis*. 262(23), 11382–11388.

Song, M. S., Moon, H. C., Jeon, J.-H., & Park, H. Y. (2018). Neuronal messenger ribonucleoprotein transport follows an aging Lévy walk. *Nature Communications* 2018 9:1, 9(1), 1–8. <https://doi.org/10.1038/s41467-017-02700-z>

- Song, T., Zheng, Y., Wang, Y., Katz, Z., Liu, X., Chen, S., Singer, R. H., & Gu, W. (2015). Specific interaction of KIF11 with ZBP1 regulates the transport of  $\beta$ -actin mRNA and cell motility. *Journal of Cell Science*, *128*(5), 1001–1010. <https://doi.org/10.1242/jcs.161679>
- St Johnston, D., Beuchle, D., & Nüsslein-Volhard, C. (1991). *stau*, a gene required to localize maternal RNAs in the *Drosophila* egg. *Cell*, *66*(1), 51–63. [https://doi.org/10.1016/0092-8674\(91\)90138-O](https://doi.org/10.1016/0092-8674(91)90138-O)
- Staton, C. A., Reed, M. W. R., & Brown, N. J. (2009). A critical analysis of current in vitro and in vivo angiogenesis assays. *International Journal of Experimental Pathology*, *90*(3), 195. <https://doi.org/10.1111/J.1365-2613.2008.00633.X>
- Stuart, H. C., Jia, Z., Messenberg, A., Joshi, B., Underhill, T. M., Moukhles, H., & Nabi, I. R. (2008). Localized Rho GTPase Activation Regulates RNA Dynamics and Compartmentalization in Tumor Cell Protrusions. *Journal of Biological Chemistry*, *283*(50), 34785–34795. <https://doi.org/10.1074/jbc.M804014200>
- Subramanian, M., Rage, F., Tabet, R., Flatter, E., Mandel, J.-L., & Moine, H. (2011). G-quadruplex RNA structure as a signal for neurite mRNA targeting. *Nature Publishing Group*, *12*. <https://doi.org/10.1038/embor.2011.76>
- Sutton, M. A., Ito, H. T., Cressy, P., Kempf, C., Woo, J. C., & Schuman, E. M. (2006). Miniature Neurotransmission Stabilizes Synaptic Function via Tonic Suppression of Local Dendritic Protein Synthesis. *Cell*, *125*(4), 785–799. <https://doi.org/10.1016/J.CELL.2006.03.040>
- Tadros, W., Goldman, A. L., Babak, T., Menzies, F., Vardy, L., Orr-Weaver, T., Hughes, T. R., Westwood, J. T., Smibert, C. A., & Lipshitz, H. D. (2007). SMAUG Is a Major Regulator of Maternal mRNA Destabilization in *Drosophila* and Its Translation Is Activated by the PAN GU Kinase. *Developmental Cell*, *12*(1), 143–155. <https://doi.org/10.1016/j.devcel.2006.10.005>
- Tanenbaum, M. E., Gilbert, L. A., Qi, L. S., Weissman, J. S., & Vale, R. D. (2014). A protein tagging system for signal amplification in gene expression and fluorescence imaging. *Cell*, *159*(3), 635. <https://doi.org/10.1016/J.CELL.2014.09.039>

- Taylor, A. M., Wu, J., Tai, H.-C., & Schuman, E. M. (2013). Axonal Translation of  $\beta$ -Catenin Regulates Synaptic Vesicle Dynamics. *Journal of Neuroscience*, *33*(13), 5584–5589. <https://doi.org/10.1523/JNEUROSCI.2944-12.2013>
- Tom Dieck, S., Kochen, L., Hanus, C., Heumüller, M., Bartnik, I., Nassim-Assir, B., Merk, K., Mosler, T., Garg, S., Bunse, S., Tirrell, D. A., & Schuman, E. M. (2015). Direct visualization of identified and newly synthesized proteins in situ. *Nature Methods*, *12*(5), 411. <https://doi.org/10.1038/NMETH.3319>
- Torvund-Jensen, J., Steengaard, J., Askebjerg, L. B., Kjaer-Sorensen, K., Laursen, L. S., Frances Raab-Graham, K., Irma Perrone-Bizzozero, N., & Albert Hoeffler, C. (2018). The 3'UTRs of Myelin Basic Protein mRNAs Regulate Transport, Local Translation and Sensitivity to Neuronal Activity in Zebrafish. *Zebrafish. Front. Mol. Neurosci*, *11*, 185. <https://doi.org/10.3389/fnmol.2018.00185>
- Tsang, B., Arsenault, J., Vernon, R. M., Lin, H., Sonenberg, N., Wang, L.-Y., Bah, A., & Forman-Kay, J. D. (2019). Phosphoregulated FMRP phase separation models activity-dependent translation through bidirectional control of mRNA granule formation. *Proceedings of the National Academy of Sciences*, *116*(10), 4218–4227. <https://doi.org/10.1073/PNAS.1814385116>
- Turner-Bridger, B., Jakobs, M., Muresan, L., Wong, H. H. W., Franze, K., Harris, W. A., & Holt, C. E. (2018). Single-molecule analysis of endogenous  $\beta$ -actin mRNA trafficking reveals a mechanism for compartmentalized mRNA localization in axons. *Proceedings of the National Academy of Sciences of the United States of America*, *115*(41), E9697–E9706. <https://doi.org/10.1073/PNAS.1806189115/-/DCSUPPLEMENTAL>
- van de Bor, V., Hartswood, E., Jones, C., Finnegan, D., & Davis, I. (2005). gurken and the I factor retrotransposon RNAs share common localization signals and machinery. *Developmental Cell*, *9*(1), 51–62. <https://doi.org/10.1016/J.DEVCEL.2005.04.012/ATTACHMENT/3FD44C64-668F-4C78-909C-B4E1CFD38894/MMC10.MOV>
- Wang, D. O., Kim, S. M., Zhao, Y., Hwang, H., Miura, S. K., Sossin, W. S., & Martin, K. C. (2009). Synapse- and Stimulus-Specific Local Translation During Long-Term Neuronal Plasticity. *Science*, *324*(5934), 1536–1540. <https://doi.org/10.1126/SCIENCE.1173205>

- Wang, T., Hamilla, S., Cam, M., Aranda-Espinoza, H., & Mili, S. (2017). Extracellular matrix stiffness and cell contractility control RNA localization to promote cell migration. *Nature Communications*, 8(1). <https://doi.org/10.1038/s41467-017-00884-y>
- Weatheritt, R. J., Gibson, T. J., & Babu, M. M. (2014). Asymmetric mRNA localization contributes to fidelity and sensitivity of spatially localized systems. *Nature Structural & Molecular Biology*, 21(9), 833–839. <https://doi.org/10.1038/nsmb.2876>
- Weis, B. L., Schleiff, E., & Zerges, W. (2013). Protein targeting to subcellular organelles via mRNA localization. *Biochimica et Biophysica Acta (BBA) - Molecular Cell Research*, 1833(2), 260–273. <https://doi.org/10.1016/J.BBAMCR.2012.04.004>
- Wen, Y., Eng, C. H., Schmoranzler, J., Cabrera-Poch, N., Morris, E. J. S., Chen, M., Wallar, B. J., Alberts, A. S., & Gundersen, G. G. (2004). EB1 and APC bind to mDia to stabilize microtubules downstream of Rho and promote cell migration. *Nature Cell Biology*, 6(9), 820–830. <https://doi.org/10.1038/ncb1160>
- Willett, M., Pollard, H. J., Vlasak, M., & Morley, S. J. (2010). Localization of ribosomes and translation initiation factors to talin/ $\beta$ 3-integrin-enriched adhesion complexes in spreading and migrating mammalian cells. *Biology of the Cell*, 102(5), 265–276. <https://doi.org/10.1042/BC20090141>
- Willis, D. E., van Niekerk, E. A., Sasaki, Y., Mesngon, M., Merianda, T. T., Williams, G. G., Kendall, M., Smith, D. S., Bassell, G. J., & Twiss, J. L. (2007). Extracellular stimuli specifically regulate localized levels of individual neuronal mRNAs. *Journal of Cell Biology*, 178(6), 965–980. <https://doi.org/10.1083/jcb.200703209>
- Yamada, K. M., Collins, J. W., Walma, D. A. C., Doyle, A. D., Morales, S. G., Lu, J., Matsumoto, K., Nazari, S. S., Sekiguchi, R., Shinsato, Y., & Wang, S. (2019). Extracellular matrix dynamics in cell migration, invasion and tissue morphogenesis. *International Journal of Experimental Pathology*, 100(3), 144–152. <https://doi.org/10.1111/IEP.12329>
- Yan, X., Hoek, T. A., Vale, R. D., & Tanenbaum, M. E. (2016). Dynamics of Translation of Single mRNA Molecules In Vivo. *Cell*, 165(4), 976. <https://doi.org/10.1016/J.CELL.2016.04.034>

- Yao, J., Sasaki, Y., Wen, Z., Bassell, G. J., & Zheng, J. Q. (2006). An essential role for  $\beta$ -actin mRNA localization and translation in  $\text{Ca}^{2+}$ -dependent growth cone guidance. *Nature Neuroscience*, 9(10), 1265–1273. <https://doi.org/10.1038/nn1773>
- Yasuda, K., Clatterbuck-Soper, S. F., Jackrel, M. E., Shorter, J., & Mili, S. (2017). FUS inclusions disrupt RNA localization by sequestering kinesin-1 and inhibiting microtubule detyrosination. *Journal of Cell Biology*. <https://doi.org/10.1083/jcb.201608022>
- Yasuda, K., Zhang, H., Loisel, D., Haystead, T., Macara, I. G., & Mili, S. (2013). The RNA-binding protein Fus directs translation of localized mRNAs in APC-RNP granules. *The Journal of Cell Biology*, 203(5), 737–746. <https://doi.org/10.1083/jcb.201306058>
- Yergert, K. M., Doll, C. A., O'Rourke, R., Hines, J. H., & Appel, B. (2021). Identification of 3' UTR motifs required for mRNA localization to myelin sheaths in vivo. *PLOS Biology*, 19(1), e3001053. <https://doi.org/10.1371/JOURNAL.PBIO.3001053>
- Yoon, Y. J., & Mowry, K. L. (2004). Xenopus Staufen is a component of a ribonucleoprotein complex containing Vg1 RNA and kinesin. *Development*, 131(13), 3035–3045. <https://doi.org/10.1242/dev.01170>
- Yoon, Y. J., Wu, B., Buxbaum, A. R., Das, S., Tsai, A., English, B. P., Grimm, J. B., Lavis, L. D., & Singer, R. H. (2016). Glutamate-induced RNA localization and translation in neurons. *Proceedings of the National Academy of Sciences*, 113(44), E6877–E6886. <https://doi.org/10.1073/PNAS.1614267113>
- Younts, T. J., Monday, H. R., Dudok, B., Klein, M. E., Jordan, B. A., Katona, I., & Castillo, P. E. (2016). Presynaptic Protein Synthesis Is Required for Long-Term Plasticity of GABA Release. *Neuron*, 92(2), 479–492. <https://doi.org/10.1016/J.NEURON.2016.09.040>
- Zalcman, G., Federman, N., & Romano, A. (2018). CaMKII Isoforms in Learning and Memory: Localization and Function. *Frontiers in Molecular Neuroscience*, 0, 445. <https://doi.org/10.3389/FNMOL.2018.00445>
- Zappulo, A., van den Bruck, D., Ciolli Mattioli, C., Franke, V., Imami, K., McShane, E., Moreno-Estelles, M., Calviello, L., Filipchuk, A., Peguero-Sanchez, E., Müller, T., Woehler, A., Birchmeier, C., Merino, E., Rajewsky, N., Ohler, U., Mazzoni, E. O., Selbach, M., Akalin, A., & Chekulaeva, M. (2017). RNA localization is a key determinant of neurite-



enriched proteome. *Nature Communications*, 8(1), 1–13. <https://doi.org/10.1038/s41467-017-00690-6>

Zhang, H. L., Eom, T., Oleynikov, Y., Shenoy, S. M., Liebelt, D. A., Dichtenberg, J. B., Singer, R. H., & Bassell, G. J. (2001). Neurotrophin-induced transport of a  $\beta$ -actin mRNP complex increases  $\beta$ -actin levels and stimulates growth cone motility. *Neuron*, 31(2), 261–275. <https://doi.org/10.1016/S0896-6273>